UNIVERSIDADE DO PORTO FACULDADE DE DESPORTO

CENTRO DE INVESTIGAÇÃO FORMAÇÃO INOVAÇÃO E INTERVENÇÃO EM DESPORTO CIFI2D

UNIVERSITY OF PORTO

Faculty of Sport

Centre of Research, Education,

Innovation and Intervention in Sport

Biomechanical analysis of backstroke start technique: updating knowledge and technological devices for starting performance assessment

Academic dissertation submitted with the purpose of obtaining a doctoral degree in Sports Sciences according to the Decree-Law 74/2006 from March 24th.

Supervisors:

Prof. Dr. João Paulo Vilas-Boas

Prof Dr. Mário Augusto Pires Vaz

Karla de Jesus

Porto, June 2015

de Jesus, K. (2015). Biomechanical analysis of backstroke start technique: updating knowledge and technological devices for starting performance assessment. Doctoral Thesis in Sport Sciences. Centre of Research, Education, Innovation and Intervention in Sport. Faculty of Sport, University of Porto.

KEY WORDS: SPORTS ENGINEERING, INSTRUMENTATION, BIOMECHANICS, SWIMMING, DORSAL START

Funding

This doctoral Thesis was supported by the Coordination for the Improvement of Higher Personnel, Ministry of Education of Brazil (0761/12-5/2012-2015) and by the Science and Technology Foundation (EXPL/DTP-DES/2481/2013- FCOMP-01-0124-FEDER-041981).

“A single sunbeam is enough to drive away many shadows.”

(Saint Francis of Assisi)

Dedications

To my family, to my ex-teachers, professors, coaches and swimmers, who encouraged me to fulfill this dream.

To my grandfathers (Elísio de Jesus and Adolpho Goll — *in memoriam*).

To my grandmothers (Leonor Rodrigues de Jesus and Amanda Goll Klanschmidt — *in memoriam*).

To my heart grandmothers (Braulina and Aurelia - *in memoriam)*.

Acknowledgments

To Jesus, Virgin Mary, Saint Leopold and Friar Miguel.

To my sister and brilliant working partner Kelly de Jesus, without her assistance and patience many things would not be possible to work so perfectly.

To my father Hélio de Jesus and mother Irene Goll de Jesus, everything was carefully planned and permanently powered, since the first advice.

To my family, especially my aunt Ondina Schuster, my godmother Gilciane Silva, my godfather Enio de Jesus, who were always supporting me and encouraging me with their best wishes.

To Prof. Dr. João Paulo Vilas-Boas, for his excellent guidance, caring, patience, and providing me courage to believe in such ambitious goals.

To Prof. Dr. Ricardo Jorge Fernandes for knowing the time and the right way to criticize and praise, strengthening compliance with the established goals.

To Prof. Dr. Hélio Roesler, Prof Dr. Mário Vaz, Prof. Luis Mourão, for guiding my research during the prototype development, data collections, and also sharing their expertise in relevant scientific papers (already accepted or submitted) in recognized journals.

To Engº Pedro Gonçalves of Laboratory of Biomechanics (FADEUP) and Engº Nuno Viriato of Institute of Mechanical Engineering and Industrial Management (INEGI) for his patience to help me with proper engineering software.

To Prof. Dr. Leandro Machado for helping me in determinant math issues.

To FADEUP staff, particularly, Mrs. Maria Domingues, Mr. Teixeira, Mr. Marinho and Mr. Rui Biscaia.

To my teacher Drª. Marinho for helping me improve my skills with the English language during this journey.

To Prof. Alexandre Igor Araripe Medeiros, who provided his help in several data collection sessions and have still sharing his statistics expertise in relevant scientific papers.

To Phornpot Chainok and Siwa Leewattananupong (my friends), who helped me during the endless data collection sessions.

To Bruno Graça (my brother-in-law and friend) and all swimmers (and their coaches and clubs), who participated twice or even three times in extensive data collection sessions.

This Doctoral Thesis is based on the following scientific papers, which are referred in the text by their Arabic and Roman numerals, respectively:

1. de Jesus, K., de Jesus, K., Fernandes, R.J., Vilas-Boas, J.P., Sanders, R. (2015). The Backstroke Swimming Start: State of the Art. **Journal of Human Kinetics***,* 10(42), 27-40. DOI: 10.2478/hukin-2014-0058.

2. de Jesus, K., de Jesus, K., Medeiros, A., Fernandes, R.J., Vilas-Boas, J.P., (2014). The backstroke starting variants performed under the current swimming rules and block configuration. **Journal of Swimming Research**, 22, 1-5.

3. de Jesus, K., Mourão, L., Roesler, H., Fernandes, R.J., Vaz, M., Vilas-Boas, J.P. (2015). Design and validation of a 3D-6DoF instrumented swimming starting block for backstroke start external kinetics assessment. Under patent request - INPI108229.

4. de Jesus, K., de Jesus, K., Abraldes, J.A., Mourão, L.M., B-Santos, M., Medeiros, A.I.A, Gonçalves, P., Chainok, P., Fernandes, R.J., Vaz, M.A.P., Vilas-Boas, J.P. (2015). Effects of diverse feet and hands positioning on backstroke start performance. Submitted for publication to **Sports Biomechanics**.

5. de Jesus, K., de Jesus, K., Medeiros, A., Gonçalves, P., Figueiredo, P., Fernandes, R., Vilas-Boas, J.P. (2015). Neuromuscular activity of upper and lower limbs during two backstroke swimming start variants. Submitted for publication to **Journal of Sports Science and Medicine**.

6. de Jesus, K., de Jesus, K., Abraldes, A., Medeiros, A., Fernandes, R.J., Vilas-Boas, J.P. (2015). Are the new starting block facilities beneficial for the backstroke start performance? Submitted for publication to **Journal of Sports Sciences**.

7. de Jesus, K., de Jesus, K., Duarte, D., Pires, D., Torres, M.C., Gonçalves, P., Mourão, L., Roesler, H., Vasconcelos, O., Fernandes, R.J., Vaz, M.A.P., Vilas-Boas, J.P. (2015). Lateral kinetic proficiency and asymmetry in backstroke swimming start. Submitted for publication to **Journal of Applied Biomechanics**.

8. de Jesus, K., Ayala, V. H., de Jesus, K., Coelho, L.S., Mourão, L., Abraldes, J.A., Fernandes, R.J., Vaz, M.A.P., Vilas-Boas, J.P. (2015). Modelling and predicting backstroke start performance using non-linear and linear methods. Submitted for publication to **International Journal of Sports Medicine**.

9. de Jesus, K., de Jesus, K., Mourão, L., Roesler, H., Fernandes, R.J., Vaz, M.A.P., Vilas-Boas, J.P., Machado, L.J. (2015). Effective swimmer's action during the backstroke start technique. Submitted for publication to **PLoS ONE**.

I. Mourão, L., de Jesus, K., de Jesus, K., Fernandes, R.J., Vaz, M.A.P., Vilas-Boas, J.P. (2014). External kinetics in individual and relay swimming starts: A review. In B. Mason (ed.), *Proceedings of the* **XII International Symposium for Biomechanics and Medicine in Swimming** (pp.179-184). Australian Institute of Sport. Canberra, Australia.

II. de Jesus, K., de Jesus, K., Figueiredo, P., Vilas-Boas, J.P., Fernandes, R.J., Machado, L. (2015). Reconstruction accuracy assessment of surface and underwater 3D motion analysis: a new approach. **Computational and Mathematical Methods in Medicine**, 2015:269264.

III. de Jesus, K., de Jesus, K., Morais, S.T., Ribeiro, J., Fernandes, R., Vilas-Boas, J.P. (2014). Should the gliding phase be included in the backstroke starting analysis? In B. Mason (ed.), *Proceedings of the* **XII International Symposium for Biomechanics and Medicine in Swimming** (pp.112-117). Australian Institute of Sport. Canberra, Australia.

IV. Mourão, L., de Jesus, K., Roesler, H., Machado, L.J., Fernandes, R.J., Vilas-Boas, J.P., Vaz, M.A. (2015). Effective swimmer's action during the grab start technique. **PLoS ONE**, 10(5): e0123001.

Table of Contents

Index of Figures

mathematical model of $\overrightarrow{R}_{Passive}$ (continuous line) pattern. The vertical and horizontal force components, in both cases, are represented. For clarity of representation the horizontal component has been multiplied by -1.

Figure 6. Angle to the horizontal for the mathematical model of rigid body free rotating fall. In both panels the blue and cyan lines for a model with 90 kg and the red and magenta for a model with 60 kg. The initial conditions are: solid lines: θ(0)=89.9º;ω(0)=0 $rad.s-1$; dashed lines: θ(0)=80º; ω(0)=0 $rad.s-1$; dotted lines: θ(0)=90º; ω(0)=-0.1 $rad.s-1$; dash-dotted lines: θ(0)=89.9º; ω(0)=-0.1 $rad.s-1$. In panel A the angles generated have the same initial origin time and in panel B have the same take-off instant. CVIII

Figure 7. Horizontal and vertical components of the force for the mathematical model of rigid body free rotating fall. In both panels the blue and cyan lines stand for a model with 90 kg and the red and magenta for a model with 60 kg. The initial conditions are: solid lines: θ(0)=89.9º;ω(0)=0 $rad \cdot s^{-1}$; dashed lines: θ(0)=80º; ω(0)=0 $rad \cdot s^{-1}$; dotted lines: θ(0)=90º; ω(0)=-0.1 $rad \cdot s^{-1}$; dash-dotted lines: θ(0)=89.9º; ω(0)=-0.1 $rad \cdot s^{-1}$. For clarity of representation, the horizontal component has been multiplied by -1. CIX

Figure 8. Angle to the horizontal produced by the swimmer, while in contact to block (continuous black line) and angle to the horizontal for the mathematical model of rigid body free rotating fall. The blue and cyan lines stand for a model with 90 kg and the red and magenta for a model with 60 kg. The initial conditions are: solid lines: θ(0)=89.9º;ω(0)=0 $rad \cdot s^{-1}$; dashed lines: θ(0)=80º; ω(0)=0 $rad \cdot s^{-1}$; dotted lines: θ(0)=90º; ω(0)=-0.1 $rad \cdot s^{-1}$; dash-dotted lines: θ(0)=89.9º; ω(0)=-0.1 $rad \cdot s^{-1}$. The angles generated have the same take-off instant. CX

Figure 9. Mean horizontal and vertical (dash-dotted line and continuous line, respectively) force-time curves for the grab start technique, expressed as a percentage of the time period between starting signal and the take-off instant: Raw mean forces (A), passive mean forces (B) and active mean forces (C). The vertical continuous bars denote the local standard variations for each force component. Force data are presented as a fraction of the swimmers' body weight (BW). For clarity of representation the horizontal component has been multiplied by -1. CXI

Index of Tables

Index of Equations

Equation 5. $$Y_r = \sqrt{\frac{1}{N}\sum_{i=1}^{N}(y_{ni} - y_i)^2}$$ LXXII

Equation 6. $$Z_r = \sqrt{\frac{1}{N}\sum_{i=1}^{N}(z_{ni} - z_i)^2}$$ LXXII

Equation 7. $$R = \sqrt{\frac{1}{N}\sum_{i=1}^{N}\left[(x_{ni} - x_i)^2 + (y_{ni} - y_i)^2 + (z_{ni} - z_i)^2\right]}$$ LXXII

Appendix IV

Equation 1. $$\overrightarrow{GRF}(\mathrm{t}) + \vec{W} = \mathrm{m} \cdot \vec{a}_{\mathrm{swimmer}}(\mathrm{t})$$ XCVI

Equation 2. $$\int_0^{\tau}\left(\overrightarrow{GRF}(\mathrm{t}) + \vec{W}\right) \cdot \mathrm{dt} = \Delta\vec{\mathrm{p}}$$ XCVI

Equation 3. $$\overrightarrow{GRF}(t) = \vec{R}_{Passive}(t)$$ XCVI

Equation 4. $$\overrightarrow{GRF}(t) = \vec{R}_{Passive}(t) + \vec{R}_{Active}(t)$$ XCVII

Equation 5. $$R_{Passive} = m \cdot g \cdot \sin\theta - m \cdot r_{CM} \cdot \omega^2$$ C

Equation 6. $$\begin{cases} \dfrac{d(\omega(t))}{dt} = -r_{CM} \cdot m \cdot g \cdot \dfrac{\cos(\theta(t))}{I_{zz}} \\ \dfrac{d(\theta(t))}{dt} = \omega(t) \end{cases}$$ CI

Equation 7. $$\begin{cases} R_{\mathrm{v\_passive}} = m \cdot (g \cdot sin\theta - r_{CM} \cdot \omega^2) \cdot sin\theta \\ R_{\mathrm{h\_passive}} = m \cdot (g \cdot sin\theta - r_{CM} \cdot \omega^2) \cdot cos\theta \end{cases}$$ CII

Equation 8. $$\begin{cases} \vec{r}_{\mathrm{CM}} = r_{CM} \cdot (cos\theta, sin\theta) \\ \vec{v}_{\mathrm{CM}} = r_{CM} \cdot \omega \cdot (sin\theta, -cos\theta) \end{cases}$$ CII

Equation 9.

$$\begin{cases} R_{h\_Passive\_i}(t_1) = \dfrac{m_{swimmer}}{m_{Model}} R_{h\_Passive\_Model}(t_1) \\ R_{v\_Passive\_i}(t_1) = \dfrac{m_{swimmer}}{m_{Model}} R_{v\_Passive\_Model}(t_1) \\ \theta_{Passive\_i}(t_1) = \operatorname{atan}\left(\dfrac{R_{v\_Passive\_i}(t_1)}{R_{h\_Passive\_i}(t_1)} \right) \end{cases} \quad \text{CIV}$$

Equation 10.

$$\begin{cases} R_{h\_Active}(t) = GRF_h(t) - R_{h\_Passive}(t) \\ R_{v\_Active}(t) = GRF_v(t) - R_{v\_Passive}(t) \end{cases} \quad \text{CIV}$$

Equation 11.

$$\begin{cases} L_1 \rightarrow L_2 = \sqrt[3]{\dfrac{m_2}{m_1}} L_1 \\ V_1 \rightarrow V_2 = \dfrac{m_2}{m_1} V_1 \\ I_1 \rightarrow I_2 = \left(\sqrt[3]{\dfrac{m_2}{m_1}} \right)^2 \dfrac{m_2}{m_1} I_1 \end{cases} \quad \text{CXIV}$$

Abstract

This thesis updated technologies and methods for a detailed backstroke start biomechanical analysis considering FINA rules. Two literature reviews and a frequency study were conducted to highlight gaps and limitations and the currently most used backstroke start variants, respectively. Those findings guided an instrumented starting block framing composed by four triaxial six degree of freedom extensometric waterproof force plates, an above and underwater structure, an independent handgrip and wedge pair, which were simulated and validated for specific external kinetics assessment of the new backstroke start. Three-dimensional kinematic methods (digital video and motion capture system) were tested and improved for backstroke start analysis covering movements from auditory signal until 15 m mark. The implementation of updated kinetic and kinematic methods added to surface electromyography in the study of current backstroke start variants revealed that: (i) positioning feet entirely emerged with hands on highest horizontal and vertical handgrip implied clear kinematic and kinetic differences (e.g. ~0.15 m higher vertical centre of mass coordinate at set positioning) compared to those with feet entirely immersed; however, with similar 15 m start time; (ii) integrated electromyography activity of six muscles (upper and lower limbs) was similar comparing variants with feet partially emerged and hands on highest horizontal and vertical handgrip (e.g. Tibialis Anterior at hands off phase, -0.26 [-1.07, 0.55]); (iii) the wedge influenced backstroke start kinematics when performed with vertical handgrip (e.g. greater take-off angle, -0.81 [-1.55, -0.07]), but without 5 m start time changes; (iv) external kinetics in both starting variants revealed preferred and non-preferred upper and lower limbs differences; (v) kinetic and kinematic data modeled and predicted accurately 5 m backstroke start time through neural network tools; and (vi) horizontal and vertical lower limb forces were mainly dependent upon swimmers' actions rather than on inertial effects.

Key words: Sports engineering, biomechanics, competitive swimming, dorsal start technique.

Resumo

Esta Tese atualizou tecnologias e métodos para análise biomecânica detalhada da partida de costas sob regulamento da FINA. Duas revisões da literatura e um estudo de frequência foram implementados e revelaram lacunas e limitações e as variantes atuais da partida de costas. Estes achados orientaram a construção de um bloco instrumentado composto por quatro plataformas de força triaxias com seis graus de liberdade subaquáticas e extensométricas, um bloco e uma estrutura subaquática, um par de agarres e suporte para os pés independentes, os quais foram simulados e validados para medidas cinéticas externas específicas da técnica de partida de costas. Métodos de cinemática tri-dimensional (vídeo digital e sistema de captura de movimento) foram testados e melhorados para análise da partida de costas cobrindo movimentos do sinal auditivo até os 15 m. A implementação de tais métodos cinéticos e cinemáticos adicionados a eletromiografia de superfície no estudo das variantes da partida de costas revelaram que: (i) pés completamente emersos e mãos posicionadas no agarre horizontal mais alto e vertical implicaram diferenças cinemáticas e cinéticas (ex. centro de massa na posição de partida ~0.15 m mais alto) comparado com os pés completamente imersos, mas com similar tempo aos 15 m; (ii) integral do sinal eletromiográfico de seis músculos (membros superiores e inferiores) foi similar comparando variantes realizadas com pés parcialmente emersos e mãos posicionadas no agarre horizontal mais alto e vertical (ex. Tibial Anterior na fase de saída das mãos, -0.26 [-1.07, 0.55]); (iii) o suporte para os pés influenciou a cinemática da partida de costas com agarre vertical (ex. maior ângulo de saída, -0.81 [-1.55, -0.07]), mas sem alterações do tempo aos 5 m; (iv) as variantes da partida revelaram diferenças cinéticas entre a proficiência de membros preferidos e não-preferidos superiores e inferiores; (v) dados cinéticos e cinemáticos modelaram e predisseram precisamente o tempo aos 5 m da partida de costas através das redes neurais; e (vi) forças horizontal e vertical dos membros inferiores foram principalmente dependentes das ações dos nadadores preferivelmente aos efeitos inerciais.

Palavras chave: Engenharia desportiva, biomecânica, natação pura desportiva, técnica de partida dorsal.

Résumé

Cette étude a mise en jour des technologies e des méthodes pour connaître une analyse biomécanique détaillée du départ de dos en suivant les règles de la FINA. On a conduit deux revues de la littérature et une étude de fréquence qui ont mise en évidence les lacunes et les limitations des variantes du départ de dos le plus utilisées actuellement. Ces résultats nous ont emmené á construire un plot de départ personnalisé composé par quatre plaques de force triaxial, avec six degrés de liberté, extensométriques et imperméables, une structure dessus et sous- l'eau, une poignée indépendante et un pair de plot de départ, qui ont été simulés et certifiés pour l' évaluation cinétique externe du nouveau départ de dos. Des méthodes cinématiques tridimensionnels (système digital de vidéo et un système de capture de mouvement) ont été testés et améliorés pour analyser le départ de dos en couvrant mouvements de signal auditif jusqu'au au point de 15 m. L'implémentation des méthodes cinétiques et cinématiques ajoutés à l'électromyographie de surface pour étudier les actuelles variantes de départ de dos a révélé que: (i) le positionnement des pieds entièrement émergés avec les mains placées sur la poignée le plus élevé horizontalement et verticalement implique des différences cinématiques et cinétiques distinctes (par exemple, ~ 0.15 m le centre de la masse dans la position verticale plus haute coordonné au position de «set») en rapport aux variantes en utilisant les pieds entièrement immergés, mais avec une incertitude sur les différences aux 15 m du temps de départ; (ii) l'activité électromyographique incorporée de six muscles (membres supérieurs et inférieurs) a été semblable en comparant les variantes de départ avec les pieds partiellement émergés et les mains sur la plus haute poignée horizontale et verticale (par exemple jambier antérieur à la phase hands-off, -0,26 [-1,07, 0,55]); (iii) Le plot de départ a influencé la cinématique de départ de dos lorsqu'il est effectué avec poignée verticale (par exemple plus d'angle de décollage-take-off, -0,81 [-1,55, -0,07]), mais sans le changement des 5m de temps de départ; (iv) la cinétique externe dans les deux variantes de départ a révélé des différences sur les préférences e les non-préférences des membres inférieurs et supérieures; (v) l' information cinétique et cinématique a modelée et

a prévu avec précision le temps de départ de 5 m à travers des réseaux de neurones; et (vi) les forces horizontaux et verticaux des membres inférieurs ont été subordonnés principalement aux actions des nageurs plutôt qu'aux effets d'inerti.

Mots clés: Sport ingénierie, biomécanique, la natation de compétition, la technique de début de dorsale.

List of Abbreviations

A/D	Analogue to digital
ANOVA	Analysis of variance
ANN	Artificial neural network
$\vec{a}_{swimmer}(t)$	Swimmers' acceleration
atan	Tangent arc
BEX	Scholarship abroad
BMS	Biomechanics and Medicine in Swimming
BSFI	Backstoke start with feet immersed
BW	Body weight
ºC	Celsius degrees
CAD	Computer aided design
cf.	confer
CI	Confidence interval
CM	Center of mass
CMflx	Centre of mass horizontal coordinate at 3rd distal phalanx water contact
CMfly	Centre of mass vertical coordinate at 3rd distal phalanx water contact
CMssx	Centre of mass horizontal coordinate at 1st frame
CMssy	Centre of mass vertical coordinate at 1st frame
COP	Center of pressure
Corp.	corporation
CV	Coefficient of variation
dB	Decibel
df	Degrees of freedom
DLT	Direct linear transformation
EA	Entry angle
e.g.	For example
EMG	Electromyography
ESCI	Exploratory software for confidence intervals
EXPL/DTL-DES	Exploratory research project
et al.	And others
$\vec{F}_{co}$	Centrifugal force
Fh	Horizontal force
FINA	Fédération Internationale de Natation

FR	Facility rules
FRmax	Maximum resultant force
$\vec{F}_s$	Static friction component
Fv	Vertical force
FAW	Feet above water level
FUW	Feet underwater
$\overrightarrow{GRF}$	Ground reaction force
GRF_h	Horizontal ground reaction force
GRF_v	Vertical ground reaction force
h	Hour
H	Homography matrix
Hz	Hertz
I	Inertia momenta
IBM	International Business Machine Corporation
ICC	Intraclass correlation coefficient
i.e.	Means
iEMG	Integrated electromyographic signal
IJUP	Young research at University of Porto
IMPFXLL	Lower limb horizontal impulse
IMPFYLL	Lower limb vertical impulse
IMPFXUL	Upper limb horizontal impulse
IMPFYUL	Upper limb vertical impulse
Inc.	incorporated
INPI	National Institute of Industrial Property
IQ	Interquartile range
ISB	International Society of Biomechanics
ISBS	International Society of Biomechanics in Sports
ISI	Institute for scientific information
IVVx	Horizontal hip Intracyclic velocity variation during underwater phase
(I_{zz})	Momento of inertia arround halluces
kg	Kilogram
LABIOMEP	Porto Biomechanics Laboratory
LED	Light emitting diode
LLimpx	Lower limbs horizontal impulse
LLimpy	Lower limbs vertical impulse
LM	Linear model
Ltd.	Limited

m	Meter
m	Swimmers' mass
m^2	Square meter
mm^3	Cubic milimeter
min	minute
MIVC	Maximal isometric voluntary contraction
mm	Milimeter
m_{Model}	Model's mass
MoCap	Motion capture
ms	Milisecond
N	Newton
NASA	National Aeronautics and Space Administration
NCAA	National Collegiate Athletic Association
OSB	Omega starting block
PC	Personal computer
PhD	Doctor of Philosophy
PPP	Provisional patent application
$Proj_{\vec{W}}$	Weight projection
PROSUP	Support Program for Graduate Private Education Institutions
P1LL	Lower limb horizontal force at auditory signal
P2LL	1st lower limb horizontal force peak before hands-off
P3LL	Intermediate lower limb horizontal force at hands-off
P4LL	2nd lower limb horizontal peak force before take-off
P1UL	Upper limb horizontal force at auditory signal
P2UL	Upper limb horizontal peak force before hands-off
r	Effect size
R^2	Coefficient of determination
$\vec{R}_{Active}$	Active ground reaction force
$\vec{r}_{\mathrm{CM}}$	Centre of mass positioning
R_{h_Active}	Horizontal active ground reaction force
$R_{\mathrm{h\_passive}}$	Horizontal passive ground reaction force
RMS	Root mean square
$\vec{R}_{Passive}$	Passive ground reaction force
R_{v_Active}	Vertical active ground reaction force

$R_{v\_passive}$	Vertical passive ground reaction force
QTM	Qualisys track manager
Q1	1st quartile
Q3	3rd quartile
R	Resultant root mean square error
rad	Radian
s	Second
Sc	Surface cameras
SD	Standard deviation
SF	Surface cameras
SFIM	Swimmer's full immersion
SMD	Standardized mean difference
SPSS	Statistical package for the social sciences
ST	Time between starting signal and swimmer's vertex reached 15 m mark
SW	Swimming rules
T2LL	Time at 1st lower limb horizontal peak force before hands-off
T3LL	Time at intermediate lower limb horizontal force at hands-off
T4LL	Time at 2nd lower limb horizontal peak force before take-off
T2UL	Time at upper limb peak horizontal force before hands-off
TOA	Take-off angle
με	Microstrain
ULimpx	Upper limbs horizontal impulse
ULimpy	Upper limbs vertical impulse
UPW KICK	Upward kick
UW	Underwater cameras
V	Volume
$\vec{v}_{CM}$	Center of mass velocity
vs.	Versus
$\vec{W}$	Swimmer's weight
X_i	Horizontal reconstructed coordinate
X_{ni}	Horizontal real coordinate
X_r	Root mean square resultant error at horizontal axis
y_i	Vertical reconstructed coordinate
y_{ni}	Vertical real coordinate

Y_r	Root mean square resultant error at vertical axis
yrs	Years
Z	Standard score
Z_i	Lateral reconstructed coordinate
Z_{ni}	Lateral real coordinate
Z_r	Root mean square resultant error at lateral axis
2D	Two-dimensional
3D	Three-dimensional
6DoF	Six degrees of freedom
θ_{Raw}	Raw theta estimator
1st DWN KICK	1st downward kicking
1st UP to DWN KICK	First part of the transition from 1st upward to 2nd downward kicking
2nd UP to DWN KICK	2nd part of transition from 1st upward to 2nd downward kicking
2nd DWN KICK	2nd downward kicking

Chapter 1 General Introduction

Swimmer's overall performance is most simply and accurately determined in the time that he (or she) takes to complete the distance of a given race, being this time commonly broken into the start, free swimming and turns partial times (Hay & Guimarães, 1983). As the Fédération Internationale de Natation (FINA) dictates that swimmers are allowed to be completely submerged for a distance of no more than 15 m after the start; thus, researchers have often adopted swimmers' vertex crossing this mark to define start phase final instant (e.g. Cossor & Mason, 2001). However, different set distances ranging from 1.52 to 25 m have also been used to determine start effectiveness (for more details see Galbraith et al., 2008), which can be determinant particularly in short distance events (Cossor & Mason, 2001). For instance, during the last 2015 Long-Course World Junior Swimming Championship, the difference between the 2nd and 3rd place in the men's 200 m freestyle was 0.26, but this difference was already 0.13 s considering the reaction time. Furthermore, it has been shown that better starters are often 0.5 s faster than their poorer counterparts over the 15 m length (Mason et al., 2012; Seifert et al., 2010). In competition, swimmers initiate the race from starting platforms in all events, except for backstroke (Figure 1), which begins with the swimmer in-water, holding onto the starting block and diving backwards.

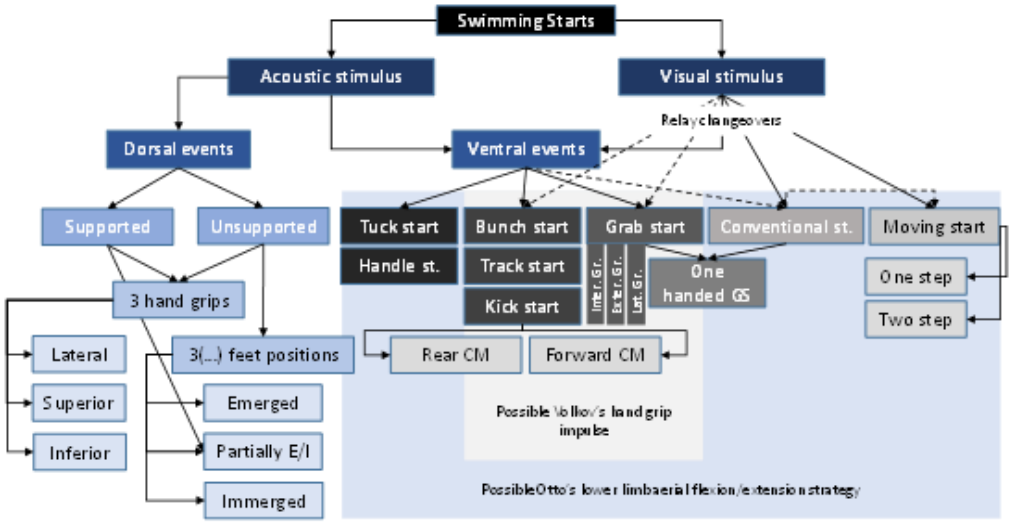

Figure 1. A synthesis of the different swimming start conditions and the different technical solutions most commonly used (adapted from Vilas-Boas & Fernandes, 2003).

In accordance with FINA backstroke start rules from earlier 1960s to 2005, swimmers were obliged to grasp the handgrips and place their feet entirely immersed on the wall. FINA backstroke start rules were modified by the National College Athletic Association (NCAA) from the early 1960 to 1990s and swimmers during NCAA competitions were authorized to curl their toes over the starting wall gutter. Swimmers who leaned on the pool gutter improved the backstroke start performance, since less resistant and longer flight were noticed due to vertical ground reaction force generated due to force applied on the wall (Stratten, 1970).

From 2005, FINA swimming rules started to change and swimmers were authorized to position their feet partially or entirely emerged. Following this authorization, it was noticed a great elite swimmers' acceptance to position feet entirely above water level (Nguyen et al., 2014), but findings comparing the start variant with feet parallel and entirely immersed and emerged using kinematics and kinetics remain contradictory in terms of the best start variant (de Jesus et al., 2013; Nguyen et al., 2014). Authors also had been interested in examining the decisive factors for better performance in each starting variant using linear modeling and noticed that greater horizontal center of mass positioning and take off-velocity were good predictors of start time when swimmers used feet entirely emerged (de Jesus et al., 2011; Nguyen et al., 2014) and underwater velocity explained high percentage of 5 m start time variance when feet was positioned entirely immersed (de Jesus et al., 2011).

In 2008 and 2013, FINA authorized meaningful changes in the starting block configuration for backstroke events, including different handgrips (i.e. two horizontal and one vertical) and a feet support (FR 2.7 and FR 2.10, respectively). These rule changes might be related in part to biomechanical advantages previously reported in studies conducted from 1960 to 1990s with NCAA rules (i.e. greater take-off angle, less resistant flight and shorter start time; e.g. Green et al., 1987). Indeed, positioning the body as high out of the water as possible, with reduced slippage chances, would provide less hydrodynamic drag during aerial trajectory, improving entry range, and consequently reducing start time

(Takeda et al., 2014). When swimmers position the center of mass out of the water and hold themselves on the wedge they might minimize the upper limbs sustaining role and achieve high vertical displacement. These ongoing modifications in FINA rules, driven by changes in swimming techniques and technologies, have increased the concern about research at different starts and respective variants (Tor et al., 2015a; Vantorre et al., 2014). Specifically in backstroke events, this interest has been observed through the number of studies published between the 1960s and 2005 (i.e. n = 12) compared to the period between 2005 to nowadays (i.e. n = 11). Nevertheless, none research had presented evidences about the current starting block configuration and its effect on the backstroke start biomechanics.

Curiously, men and women's 100 m backstroke short course World Record were broken in 2009 and 2014, respectively, suggesting that the starting block changes could have influenced start performance. In fact, it has been reported since the 1980s that at elite level, generally, it is not swimming speed that has won races but rather better technique in starts and turns (Larsen, 1981; Mason et al., 2012). In the light of above-mentioned observations, this Thesis aimed to update the backstroke start knowledge and technologies considering the current FINA starting (SW 6.1) and facility rules (FR 2.7 and FR 2.10). To fully achieve this purpose, thirteen studies were conducted, namely Chapter II to X and Appendix I to IV. Additionally, a General Discussion was elaborated upon the results obtained from those studies supported by the specialized literature (Chapter XI). The main Conclusions, Suggestions for Future Research and References are presented in Chapter XII, XIII and XIV (respectively).

A traditional literature review considering specific and relevant documents available about backstroke start studies was included in Chapter II, which would make clear the gaps and inconsistencies in the established body of knowledge (Pautasso, 2013). With the rapid technological developments within the backstroke start practice it would be timely to undertake such a review. As previous authors had already noticed that backstroke start research was scarce

compared to ventral start studies (e.g. Theut & Jensen, 2006), it was expected that many differences in literature would arise considering study's aims, sample size and competitive level, data collection and treatment methods and, consequently, conclusions. Furthermore, it was speculated that most of backstroke start studies would mainly apply similar ventral starts deterministic model variables for performance characterization (Guimarães & Hay, 1985). To date, only ventral start studies had been reviewed, being coherently established each start technique and corresponding variants used in competitions and their respective biomechanical assessment methodologies and findings (Vantorre et al., 2014; Vilas-Boas & Fernandes, 2003). Contrarily to ventral starts, even backstroke swimmers adopting different set positioning, the only evident differentiation leans on FINA and NCAA techniques. With Chapter II observations, it would be possible to conduct methodological improvements and formulate pertinent research questions for further studies considering the FINA backstroke start rule modifications.

Due to the current starting block configuration (Figure 2), it would be expectable that backstrokers would combine several feet and hands set positioning and, certainly, these facility rule changes (FR 2.7 and 2.10) would not be considered in literature together with swimming rules (SW 6.1) (Chapter II) due to the respective newness character. Generally, when a new technique, or variant is introduced into a sport, the first attempt to describe the change is by the coach, followed by the biomechanists that will review the involved mechanics to test the theory principles, propose future improvement directions or reject the change (Green et al., 1987). Therefore, it is pertinent to establish which start variants would be most commonly used (Chapter III), being a first objective attempting to standardize start variants during backstroke events, as also seen in ventral start techniques (e.g. Vantorre et al., 2014), and to identify further research issues. It was hypothesized that most of the elite male and female swimmers would perform starting variants with the feet positioned partially or entirely above the water level and hands grasping on the highest horizontal or vertical handgrip to

uplift the body as high as possible out of the water during the set positioning (Nguyen et al., 2014)..

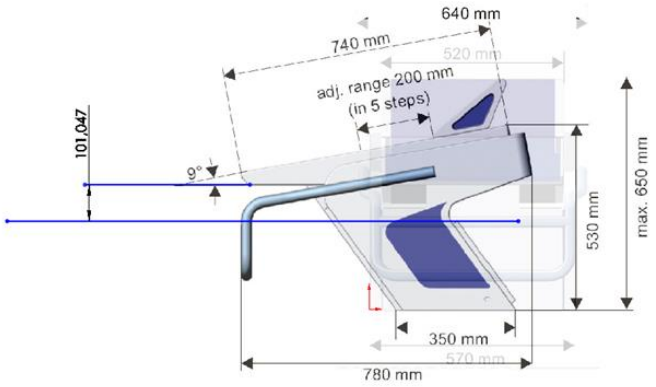

Figure 2. The international used starting block OSB11 (OSB11, Omega StartTime IV, Swiss Timing Ltd., Switzerland).

Following backstroke start variants qualitative characterization (Chapter III), it would be relevant to design a proper methodology that would enable a deep biomechanical analysis of each start variant. Previous studies have divided backstroke swimming start into several phases (i.e. hands-off, take-off, flight, entry, glide and undulatory underwater swimming; de Jesus et al., 2011; 2013; Hohmann et al., 2008), which have been considered interdependent (Vantorre et al., 2014). Despite previous predictive models have revealed that ~ 90% of start time variance is explained by average underwater horizontal velocity (de Jesus et al., 2011; Guimarães & Hay, 1985; Sanders, 2002), it depends upon preceding actions performed during the block and flight phases (Mason et al., 2007; Thow et al., 2012). Based on this reasoning, it was proposed to reinforce Chapter II findings through a new literature review that would increment understanding about the starting block instrumentation state of the art and most common parameters used to examine backstroke start kinetics (Appendix I). It was expected that researchers would focus mainly on the lower limb force analysis, since it is the primary source of the resultant impulse for propulsion (e.g. Guimarães & Hay, 1985). Chapter II and Appendix I findings would allow

improving previous instrumented start block design and capabilities to accurate and detailed assess current backstroke start kinetics.

Kinetic swimming starts analysis reveals how swimmers generate forces to propel themselves out of the wall in a proper steering positioning, and allows calculating decisive start performance parameters from upper and lower limbs (e.g. maximum force previously to the take-off; de Jesus et al., 2013; Hohmann et al., 2008; Nguyen et al., 2014). Therefore, based on Chapter II, Chapter III and Appendix I findings, it was proposed to develop and validate a proper-instrumented starting block, mimicking the internationally used Omega OSB11 block (Omega StartTime IV, Swiss Timing Ltd., Switzerland) (Figure 2), capable of estimating accurate kinetics from overall backstroke start variants (Chapter IV). To accomplish this task, some steps should be determined (as usually done in instrumentation studies, e.g. Wright et al., 2011): (i) instrumented starting block project development including anchorage structures, sensors and transducers; (ii) numerical simulations to test the structures and geometries adopted; and, (iii) device manufacturing, calibration and validation. Since backstroke swimming start should not be considered a symmetrical movement (Sanders et al., 2006) and knowing that ground reaction force asymmetries in bilateral jumping have already been reported (e.g. Yoshioka et al., 2010), technologies and methods developed should contemplate swimmers' laterality using three-dimensional (3D) perspective analysis.

Most of backstroke start studies seem to implement kinematics to describe the movement geometry using a bi-dimensional (2D) approach in the sagittal plane where the media-lateral movement could not be revealed (e.g. Wilson & Howard, 1983). Despite 2D analysis is less time-consuming and might also provide relevant data, it would be pertinent to use the 3D approach for supplying 2D insights since only the undulatory underwater movements has been considered a symmetrical skill in competitive swimming (Sanders et al., 2006). In fact, a certain asymmetry degree is common and can persist throughout life span in several bilateral sports (e.g. swimming technique; dos Santos et al., 2013), thus

it should be evaluated and controlled whenever possible through a full-body 3D analysis. To implement an accurate and reliable 3D kinematics approach during backstroke start, it would be necessary to design, frame and validate a new 3D calibration volume sufficiently large to cover backstroke start movements' space, as previously done in swimming technique analysis (e.g. Psycharakis et al., 2005), which was proposed in Appendix II. It would be hypothesized that the new calibration volume would provide accurate 3D reconstruction and measurements of backstroke start movements.

Previous backstroke start studies revealed that biomechanical advantages obtained during wall contact phases (e.g. horizontal lower limb impulse) should be maintained during flight, entry and underwater pathways (de Jesus et al., 2013; Takeda et al., 2014). However, most of studies have been focused on backstroke start movement analysis from acoustic signal until full body immersion (e.g. Takeda et al., 2014), because it reflects primarily the quality of the start activities on the block and it is not so much influenced by swimming actions below or at water level (Hohmann et al., 2008; McLean et al., 2000). However, beyond developing greater wall/block phase skills, researchers have mentioned that focusing on the underwater phase by finding the ideal trajectory will lead to improve start performance (Tor et al., 2015b). Thus, it was aimed to implement a 3D automatic tracking methodology for motion analysis, as previously used in swimming techniques (Kudo et al., 2010), capable to accurately verify how underwater backstroke start movements would be performed from the full immersion until 15 m mark (Appendix III). Moreover, the backstroke start phase's definition has not been clearly presented in previous reports in what concerns the underwater movements, contrarily to ventral techniques (e.g. Tor et al., 2015b; Vantorre et al., 2014), being the study proposed in Appendix III helpful in clarifying the underwater swimmers' action after backstroke start immersion. The automatic tracking motion analysis has been successfully used in land experimental settings, but was only adopted for underwater view and double media reconstruction of swimming techniques (Kudo et al., 2010; Olstad et al., 2014; Ribeiro et al., 2014). It would also be interesting to test this method in backstroke

start 3D reconstruction (differently than swimming technique due to high-velocity movements and greater water immersion resistance) from auditory signal to 15 m mark, minimizing larger digitization time-consuming process.

Following the proposed literature review (Chapter II), the start variants distribution analysis (Chapter III), and the methodological improvements (Chapter IV, Appendix II and III), it would be essential to quantitatively measure and in detail describe changes in backstroke start performance imposed by different combinations of hands and feet positioning (Chapter V). The implementation of previous methodological advances would allow to completely characterize the kinetics and kinematics of diverse start variants from the auditory signal to the 15 m mark. Despite Chapter III would reveal the backstroke start variants currently adopted in elite competitions, at least nine variants can be used by swimmers considering both, feet and hands combination, namely feet positioned parallel and entirely immersed and emerged and partially emerged (SW 6.1) and hands on lowest or highest horizontal and vertical handgrips. As for better results achievement, it would be necessary to provide swimmers with previous practice involving repetition and successive refinement for learning a new skill (Hanin et al., 2004; McLean et al., 2000), participants should be familiarized with backstroke start variants before experimental sessions using the proper developed technology, as previously done in experimental ventral start protocols (e.g. Barlow et al., 2014). It is hypothesized that swimmers adopting feet entirely and partially emerged and hands on highest horizontal or vertical handgrip would achieve higher center of mass set positioning, upper and lower limbs impulse, greater take-off and entry angles, longer and higher flight and reduced 15 m start time.

The kinetics and kinematics assessed in backstroke start allow understanding how swimmers generate and balance forces to propel themselves out of the starting block (Guimarães & Hay, 1985). However, as swimming start is highly dependent upon high-velocity coordinated maximal efforts, understanding muscular activity requirements would afford swimmers and coaches an insight

into the neuromuscular limits, capabilities and processes involved to complete task successfully (Ball & Scurr, 2013). The most common method of directly assessing neuromuscular contribution to any task is through electromyography (EMG), which has been applied in several swimming technique studies (for a more detailed review on the topic see Martens et al., 2015). This method is still considered time-consuming, demanding additional period for familiarization of specific normalization tests and experimental sessions. Therefore, it would be appropriated selecting the most often-used backstroke start variants for a detailed EMG analysis comparing selected muscles activities between and within variants (Chapter VI). It would be expected clear differences among variants at first start instants, since previous studies conducted in jumping (e.g. Van Soest et al., 1994) and swimming start (Hohmann et al., 2008) reported decrease in variability as the instant of take-off is approached. Moreover, comparing EMG among starting phases would clarify the role played by each muscle during backstroke start, as often done in other sports (e.g. throwing techniques, Escamilla and Andrews, 2009). It could be hypothesized that biarticular upper and lower limb muscles would contribute similarly throughout starting phases. For EMG findings support, it would be essential including kinetics and/or kinematics data.

For plenty understanding about FINA rule changes in backstroke start performance and technical parameters, it is essential to conduct a study considering the handgrips and new wedge configuration. It would be interesting to analyze the effects of the wedge when swimmers performing the most common used backstroke start variants depicted in Chapter III. The wedge can be positioned at five different heights (0.04 and 0.02 m above and below the water level and at the water level; FR 2.10), but as swimmers have rather adopted the feet entirely emerged for clear flight path and water immersion (Nguyen et al., 2014), it should be pertinent to analyze the effects of the wedge use on the highest positioning above water level (i.e. 0.04 m). In Chapter VII it was proposed to show how the new wedge could benefit backstroke swimmers and how they

would organize their lower limb joint actions to overcome task constraints and achieve mechanical goals.

A proximal-to-distal sequence has been reported as a successful strategy for lower limb joints extension, but, no study in backstroke start have described this coordinative profile. With the inclusion of the wedge, it would be expected changes in lower limb joints extension sequence since swimmers using the wedge could take longer wall contact phases time to improve vertical reaction impulse and could benefit from a greater ankle joint angular velocity. It could also be expectable to find biomechanical advantages in terms of performance (e.g. greater back arc angle), which was reported when backstrokers started using the swimming pool gutter (e.g. Rea and Soth, 1967). Since the starting phases are considered interdependent (Vantorre et al., 2014), benefits obtained using the wedge could be transferred throughout the flight, entry and underwater phases (de Jesus et al., 2013; Nguyen et al., 2014; Takeda et al., 2014).

The backstroke start is a high-force explosive movement such as jumping, throwing and kicking (Van Soest et al., 1994), where swimmers seem to depict a strong dynamic coordinated coupling between joints to achieve great impulse and proper targeting distance, as also recommended for ventral start techniques (Heusner, 1959; Vantorre et al., 2010). To achieve this goal, swimmers should perform low asymmetric force generation to avoid center of mass lateral deviation at take-off and flight phase, as previously mentioned for squat and countermovement jump (Yoshioka et al., 2010; 2011). However, since general hand/foot proficiency is lateralized even in bilateral practice, as swimming technique (dos Santos et al., 2013), it could be expected a certain asymmetry degree in reaction forces generation during the current backstroke start variants, which should be quantified (Chapter VIII). Researches conducted in previous bilateral practices (e.g. basketball) have shown that less lateralized individuals are most favored to advance in higher competitive levels (Stockel & Valter, 2014). In fact, it could be expected kinetic differences in backstroke start proficiency between preferred and non-preferred upper and lower limbs (Hart & Gabbard,

1997). Nevertheless, it should also be expected similar asymmetry responses between start variants because it has been reported that close-set positioning variants have been performed with similar motor strategies (Van Soest et al., 1994). Beyond studying eventual asymmetry changes between start variants, it should also be interesting to verify to what extend force unbalances would affect backstroke start performance. As theoretically, previous studies have reported that functional imbalance could deteriorate performance (Sanders et al., 2012), it could be expected that kinetics asymmetry would offset steering goal, increasing start time. These findings could help coaches improving resistance-training sessions and serving as one of objective criteria to select backstroke start variant.

After establishing the effects of the handgrips configuration and/or wedge use on backstroke start kinematics and kinetics (Chapter VII and Chapter VIII, respectively), it would be pertinent to test the accuracy of non-linear and linear models using variables that cover biomechanics from the acoustic signal until the swimmers' full immersion for backstroke start performance prediction. The studies in swimming starts have presented the most determinant biomechanical factors that contribute for start performance variance using linear regression models (e.g. Tor et al., 2015b). However, most relations in sport science are not linear, as each unit change in an independent variable will not always bring about similar change in the dependent variable (Zehr, 2005). In fact, when it comes to training science, especially in competitive sports, research questions are usually located in complex environments where a tight and comprehensive control of extraneous variables becomes impossible (Pfeiffer & Hohmann, 2012). Therefore, to a view of sports training as complex dynamic systems have implied in the abandonment of general, linear data analysis methods in favor of nonlinear ones (Edelmann-Nusser et al., 2002; Pfeiffer and Hohmann, 2012). In Chapter IX, it was proposed to investigate which method (artificial neural networks vs. linear) would model and predict backstroke start time more precisely when swimmers using current start variants (Chapters VII and VIII). It could be assumed that neural networks would produce more accurate predictions than

standard linear, as already mentioned (e.g. Hahn, 2007), having further potential for the application in backstroke start training.

Undoubtedly, ground reaction force patterns (also studied in Chapter IX) can be considered a crucial tool for swimming starts effectiveness assessment, providing information about how swimmers organize their movements to achieve starting goals (Bartlet, 2007). Therefore, it is assumed that in the absence of quantitative kinematics, coaches can certainly appeal for kinetics to design start-training improvements. However, overall starting kinetics should be interpreted dependent upon effective swimmers' muscular actions and body weight effects when considering fundamental mechanics. In the light of this assumption, it is pertinent to conduct a pilot study to develop an algorithm that would be able to split active from passive forces in raw swimmers' data. It would be necessary to implement this tool in commercial force plates data and using ventral grab start technique due to its similarity with a rigid body falling (Appendix IV). Following the algorithm development and implementation in the grab start technique, it was proposed to adopt this methodology in backstroke start kinetics data acquired from a new-instrumented starting block (Chapter IV). We expected that the new wedge would allow better feet contact, and consequently, horizontal and vertical reaction forces generation dependent upon swimmers' structure and effective muscular actions (Chapter X).

Chapter 2

The Backstroke Swimming Start: State of the Art.

Karla de Jesus[1], Kelly de Jesus[1], Ricardo Jorge Fernandes [1,2], João Paulo Vilas-Boas [1,2], Ross Sanders[3,4].

[1] Centre of Research, Education, Innovation and Intervention in Sport, Faculty of Sport, University of Porto, Porto, Portugal

[2] Porto Biomechanics Laboratory (LABIOMEP), Porto, Portugal

[3] Centre for Aquatics Research and Education, Institute for Sport, Physical Education, and Health Sciences, The University of Edinburgh, Edinburgh, UK.

[4] Exercise and Sport Science, Faculty of Health Sciences, The University of Sydney, Sydney, Australia.

Published on Journal of Human Kinetics (2014), 42, 27-40.

Abstract

As sprint swimming events can be decided by margins as small as .01 s, thus, an effective start is essential. This study reviews and discusses the 'state of the art' literature regarding backstroke start biomechanics from 23 documents. These included two swimming specific publications, eight peer-reviewed journal articles, three from the Biomechanics and Medicine in Swimming Congress series, eight from the International Society of Biomechanics in Sports Conference Proceedings, one from a Biomechanics Congress and one academic (PhD) thesis. The studies had diverse aims, including swimmers' proficiency levels and data collection settings. There was no single consensus for defining phase descriptions; and kinematics, kinetics and EMG approaches were implemented in laboratory settings. However, researchers face great challenges in improving methods of quantifying valid, reliable and accurate data between laboratory and competition conditions. For example, starting time was defined from the starting signal to distances as disparate as ~ 5 m to 22.86 m in several studies. Due to recent rule changes, some of the research outcomes now refer to obsolete backstroke start techniques, and only a few studies considered the actual international rules. This literature review indicated that further research is required, in both laboratory and competition settings focusing on the combined influences of the current rules and block configuration on backstroke starting performances.

Key words: biomechanics, dorsal starts, starting technique, starting variant, literature review.

Introduction

The total swimming race time is the sum of the starting, stroking and turning times (Guimarães & Hay, 1985). The start is the swimming race fastest part (Thow et al., 2012) and, if performed effectively, can influence race-finishing position (Arellano et al., 2003; Cossor & Mason, 2001; Girold et al., 2001; Thanopoulos et al., 2012). In fact, nearly all the small temporal differences in the short distance events (i.e., 50 m and 100 m) might be explained by the starting efficiency (Ikuta et al., 2001). For instance, at 15 m after the start, the second-place finisher of men's 100 m backstroke at Barcelona 2013 Swimming World Championships was 0.20 s slower than the eventual winner, and the final race time difference was 0.19 s. The importance of the start is emphasized further in that the time differences between individual international level swimmers at 15 m after the start can vary by 0.30 s in the same race (Vantorre et al., 2010).

Backstroke is the only competitive swimming technique in which the swimmer starts in the water. In accordance with the backstroke start rules at the Federation Internationale de Natation (FINA) from earlier 1960s to 2005, swimmers grasped the handgrips and placed their entirely immersed feet on the wall. Gripping one's toes on the pool gutter was not allowed. FINA backstroke start rules for feet positioning were modified by the National Collegiate Athletic Association (NCAA) from the early 1960s to 1990 to allow swimmers to curl their toes over the starting wall gutter. However, from 1991 to 2006 the feet positioning was restricted to underwater. This modification was made to prevent injuries in competitive swimming involving backstroke starts (Cornett et al., 2011). From 2005, FINA established that swimmers must position their hands on the starting grips and their feet totally or partially immersed or entirely out of the water without using the gutter (SW 6.1, FINA, 2005-2009). The alleged advantages of feet placed high on the wall to generate greater horizontal take-off velocity (de Jesus et al., 2011a, 2013; Nguyen et al., 2014), vertical peak force (Nguyen et al., 2014), and consequently faster start times (Nguyen et al., 2014), might be considered the main reason for the respective rule adaptation. After the 2008 Olympic Games,

the FINA approved a new designed starting block (OSB11, Corgémont, Switzerland), which included a back plate and three different backstroke start handgrips (i.e., two horizontal and one vertical) (FR 2.7, FINA 2009-2012). Recently, a non-slip wedge was authorised by FINA for feet placement during backstroke starts (FR 2.7, FINA, 2013-2017).

Despite the controversies between ruling authorities, and considerable swimming and facility backstroke start rule changes recently authorized by FINA, researchers have mainly attempted to analyse the ventral start biomechanics (e.g. Takeda et al., 2012). The greater quantity of ventral start studies is firstly justified by the greater quantity of events that begin from a starting block rather than in water (Theut & Jensen, 2006). Also, prior to recent rule changes, some controversies were possible with the dorsal, in-water start positions performed under the FINA rules (Vilas-Boas & Fernandes, 2003) and the difficulties concerning the underwater experimental set-up arrangements. Cornett et al. (2011) mentioned the non-existence of documented catastrophic injuries in competitive swimming backstroke starts as one reason for the scarce research. The backstroke start has been considered a more difficult and complex movement than the ventral techniques (de Jesus et al., 2011a, 2013; Nguyen et al., 2014; Takeda et al., 2014). It involves different skills to achieve the mechanical goals (de Jesus et al., 2011a, 2013; Maglischo, 2003; Nguyen et al., 2014; Takeda et al., 2014) and more scientific evidence is required.

The importance of swimming starts for enabling backstrokers to improve overall performances due to swimming rule changes and starting block modifications, makes it a valuable process to synthesize the scientific knowledge relating to backstroke starts. Literature reviews published regarding ventral start techniques were conducted by Vilas-Boas and Fernandes (2003) and Vantorre et al. (2014). This paper reviews the ‘state of the art’ regarding the biomechanics of backstroke starts. It underscores the gaps in and limitations of existing knowledge, and presents topics for future research to enable coaches and swimmers to better refine backstroke start training.

Material and Methods

Search strategy

The literature search was performed using PubMed, SportDiscus™, Scopus and ISI Web of Knowledge electronic databases, only for English written documents published before March 2014. Key words including “swimming”, “backstroke” and “start” were used to locate documents. Besides the electronic databases, the identified reference lists in the articles were also used to ensure, as far as practically possible, that all appropriate studies were considered for inclusion. Searches were carried out from the Proceedings of the Scientific Conferences of Biomechanics and Medicine in Swimming (BMS), the International Society of Biomechanics in Sports (ISBS), and the International Society of Biomechanics (ISB) from 1980 to 2013.

Inclusion and exclusion criteria

Included studies were experimental biomechanical approaches in the laboratory or during competitions with able-bodied swimmers. The documents that were available only as abstracts and duplicated studies from original investigations were excluded.

Results and Discussion

General Findings

Eighty-seven references were obtained from the preliminary search. Ultimately, 23 studies met the inclusion criteria: (i) two from swimming specific journals; (ii) eight peer-review journal articles; (iii) three from the proceedings of the BMS conferences; (iv) eight from proceedings of the ISBS conferences; (v) one from proceedings of an ISB Biomechanics Conference, and (vi) one doctoral thesis (Table 1).

Table 1 reveals a large variation in experimental designs that were used. Most of the studies analysed the different backstroke start variations performed under FINA rules (86.5%). Overall, studies included Olympic, International and National backstroke swimmers, who were able to master the aspects of the already tested backstroke starting techniques. The research settings included laboratory and competition analyses performed in the Commonwealth Games (Miller et al., 1984), Olympic Games (Arellano et al., 2001; Cossor & Mason, 2001; Chatard et al., 2003; Girold et al., 2001; Ikuta et al., 2001), Youth Olympics (Arellano et al., 2003), Age Group Swim Meeting (Cornett et al., 2011), and European Championships (Siljeg et al., 2011). The biomechanical settings in high calibre events might be more advantageous than the laboratorial conditions to obtain valid performance outcomes (Schwameder, 2008; Toubekis et al., 2013). Otherwise, the competition rules often hamper the use of biomechanical methodology, thereby narrowing the possibility of obtaining accurate and reliable data (Schwameder, 2008).

The above-mentioned factors, along with a limited number of existing studies, restrict quantitative assessments of the backstroke start variables. Therefore, a qualitative description was developed on relevant backstroke start evidence. This included the separate features of the starting phases, the biomechanical approaches used, and the start techniques and variations for which the main findings have been reported.

Backstroke starting phases

Aerial

The hands-off, take-off and flight are the most common aerial starting phases studied (Figure 1). However, the respective descriptions vary in the literature, with disparities that hamper communication among biomechanists, coaches and swimmers. In fact, breaking down a swim-start into its component parts can be challenging as each phase is not always clear cut (Vantorre et al., 2014). The hands-off and take-off phases are characterised by actions performed when

swimmers are in contact with the starting wall. The beginning of the hands-off phase is determined by the starting signal (Figure 1) (de Jesus et al., 2011a, 2013; Green, 1987; Hohmann et al., 2008; Miller et al., 1984) and the swimmer's first observable movement (Hohmann et al., 2008). Considering the take-off phase, authors determined the starting signal (Cossor & Mason, 2001; Hohmann et al., 2008; Miller et al., 1984; Nguyen et al., 2014; Stratten, 1970; Takeda et al., 2014), and the hands-off (de Jesus et al., 2010; 2011a; 2011b; 2013; Green, 1987; Hohmann et al., 2008) (Figure 1) as the instant of the beginning phase. This was also observed in ventral start studies (Takeda et al., 2012; Thanopoulos et al., 2012; Vantorre et al., 2010), where the hands-off was less analysed than the take-off in backstroke start studies.

The beginning of the flight phase was unanimously described as the instant of take-off by the feet (Cossor & Mason, 2001; de Jesus et al., 2011a, 2013; Green, 1987; Hohmann et al., 2008; Miller et al., 1984; Nguyen et al., 2014; Takeda et al., 2014) (Figure 1). However, authors differed regarding the conclusions for flight. These included: the instant that the head contacted the water (Cossor & Mason, 2001; Nguyen et al., 2014), the instant of the hip entry (Hohmann et al., 2008) and fingertip water contact (de Jesus et al., 2010; 2011a; 2013; Green, 1987; Miller et al., 1984; Takeda et al., 2014) (Figure 1). According to Maglischo (2003), the fingertip water contact is widely used to determine the end of the flight phase (Vantorre et al., 2014). The head and/or fingertip water contact could be a more appropriate reference point than the hip entry, since swimmers could immerse the hips before the hands/head contact the water (Takeda et al., 2014).

Aerial/In water and underwater phases

The entry and glide are the commonly studied aerial/in-water and underwater phases, respectively (Figure 1). As previously reported in ventral start studies, these phases have been less analyzed than the aerial phases, even though they contribute to reaching a considerable distance from the wall at the beginning of a

race (Vantorre et al., 2014). Further, contradictory definitions were found for some specific points of measurement.

Table 1. Descriptive analysis of the 22 included studies with the authors, main aim, swimmer's sample proficiency and data collection setting.

Author (s)	Main aim	Proficiency	Setting
Rea and Soth (1967)	Comparison of two NCAA variations	Olympic	Experimental
Stratten (1970)	Comparison of FINA and NCAA techniques	Recreational to Olympic	Experimental
Wilson and Howard (1983)	FINA backstroke start clusters	State to Olympic	Experimental
Miller et al. (1984)	Comparison of FINA technique	International	Competition
Green (1987)	Comparison of NCAA variations	National	Experimental
Green et al. (1987)	Comparison of NCAA variations	State	Experimental
Arellano et al. (2001)	Determinant swimming event factors	Olympic	Competition
Cossor and Mason (2001)	Correlation of FINA phases and starting time	Olympic	Competition
Girold et al. (2001)	Comparison among 200 m proficiency levels	Olympic	Competition
Ikuta et al. (2001)	Comparison between Japanese and other nations	Olympic	Competition
Arellano et al. (2003)	Correlation of FINA start and 100 m event time	International	Competition
Chatard et al. (2003)	Comparison among 200 m proficiency levels	Olympic	Competition
Theut and Jensen (2006)	Comparison of two FINA variations	Not clearly defined	Experimental
Hohmann et al. (2008)	FINA inter and intra-individual variability	International	Experimental
de Jesus et al. (2010)	Comparison of two FINA variations	National	Experimental
de Jesus et al. (2011a)	Performance prediction for two FINA variations	National	Experimental
de Jesus et al.(2011b)	Comparison of two FINA starting phases	National	Experimental
Siljeg et al. (2011)	Comparison of 100 m starting performance	International	Competition
Cornett et al. (2011)	Racing start safety analysis	Not clearly defined	Competition
de Jesus et al. (2012)	Comparison of two FINA variations	National	Experimental
de Jesus et al. (2013)	Comparison of two FINA variations	National	Experimental
Takeda et al. (2014)	Comparison between specialists and non-specialists	National	Experimental
Nguyen et al. (2014)	Comparison of two FINA variations	National	Experimental

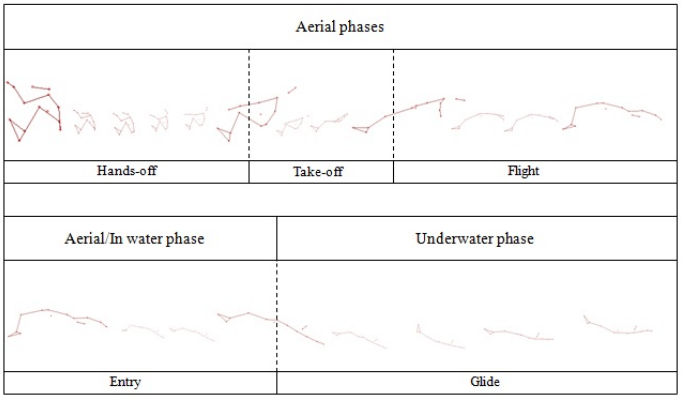

Figure 1. The most common starting phases and respective initial and final instants reported in the included studies, the starting signal, swimmer's hands-off, swimmer's feet take-off, swimmer's fingertip water contact, swimmer's full body immersion and beginning of lower limbs propulsive movements.

Table 2. The kinematic parameters studied at the overall starting and during the hands-off, take-off and flight phases.

Authors	Overall	Hands-off	Take-off	Flight
Rea and Soth (1967)	Temporal, velocity	/	/	/
Stratten (1970)	Temporal	/	Temporal	/
Wilson and Howard (1983)	/	Segmental length, angle	Segmental length, angle	Segmental length, angle
Miller et.al. (1984)	Temporal and distance	Temporal	Temporal, distance	Temporal
Green (1987)	Centre of mass displacement	Joint angles, centre of mass velocity, acceleration, angular velocity	Joint angles, centre of mass velocity, acceleration, angular velocity	Joint angles, centre of mass velocity, acceleration, angular velocity
Green et al. (1987)	Temporal	/	/	/
Arellano et al. (2001)	Temporal			
Cossor and Mason (2001)	Temporal	/	Temporal	Temporal, distance
Girold et al.(2001)	Temporal, velocity	/	/	/
Ikuta et al.(2001)	Temporal	/	/	/
Arellano et al.(2003)	Temporal, velocity	/	/	/
Chatard et al. (2003)	Velocity	/	/	/
Theut and Jensen (2006)	Velocity, distance	/	/	/
Hohmann et al.(2008)	Temporal	Temporal	Temporal, velocity	Temporal
de Jesus et al.(2010)	Temporal Angular displacement and velocity	Temporal, centre of mass displacement and velocity	Temporal, centre of mass displacement	Temporal, centre of mass displacement,
de Jesus et al. (2011a)	Temporal	Centre of mass positioning and velocity	Centre of mass displacement, velocity, angle	velocity
de Jesus et al. (2011b)	/	/	/	/
de Jesus et al. (2012)	/	/	/	/
Cornett et al. (2011)	/	/	/	/
Siljeg et al.(2011)	Temporal	/	/	/
de Jesus et al. (2013)	Temporal	Centre of mass position and velocity	Centre of mass velocity, angle	Centre of mass velocity, angle
Takeda et al., (2014)	Temporal	Height of toe, angular velocity	Temporal, Centre of mass velocity, joint angles, angular velocity	/
Nguyen et al. (2014)	Temporal	/	Temporal, displacement, velocity	/

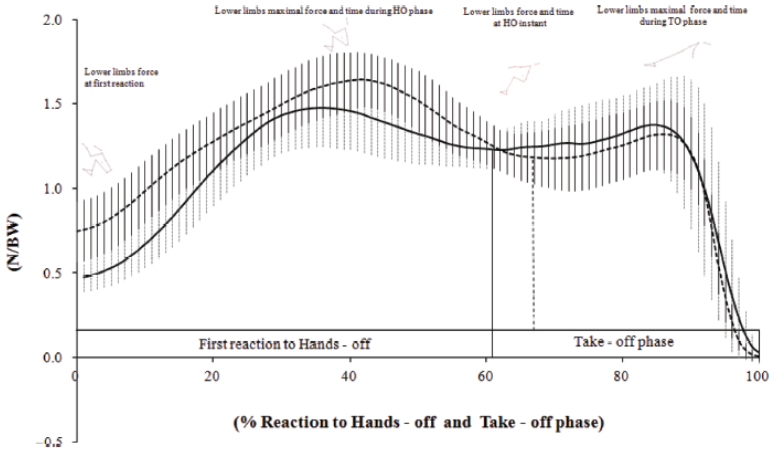

Figure 2. Mean lower limbs horizontal force-time curves for backstroke start with feet immerged (continuous line) and emerged (dashed line) (de Jesus et al., 2013).

Table 3. The set distance for the backstroke start variations performance assessment

Authors	Backstroke start variations (feet positioning)	Distance (m)	Start time (s)	Take-off Velocity ($m.s^{-1}$)
Rea and Soth (1967)	Entirely emerged, toes over the gutter	6.09	2.69	-
Rea and Soth (1967)	Entirely emerged, toes over the gutter, trunk leaned on block	6.09	2.51	-
Stratten (1970)	Entirely immersed	6.09	2.48	-
Stratten (1970)	Entirely emerged, toes curled over the pool gutter	6.09	2.26	-
Stratten (1970)	Entirely emerged, toes over the gutter, trunk leaned on block	6.09	2.49	-
Miller et al. (1984)	Entirely immersed	-	3.58	
Green et al. (1987)	Entirely emerged, toes over the gutter	22.86	16.62	4.70
Green et al. (1987)	Entirely emerged, toes over the gutter, parabolic flight trajectory	22.86	17.0	3.62
Arellano et al. (2003)	Entirely immersed	15	8.27	-
Hohmann et al. (2008)	Entirely immersed	7.5	3.29	3.45
de Jesus et al. (2010)	Entirely immersed	-	0.93	-
de Jesus et al. (2010)	Entirely emerged	-	0.98	-
Siljeg et al. (2011)	Entirely immersed	15	8.30	-
Siljeg et al. (2011)	-	15	7.72	-
de Jesus et al. (2013)	Entirely immersed	5	1.96	3.29
de Jesus et al. (2013)	Entirely emerged	5	2.11	3.80
Takeda et al. (2014)	Partially immersed	5	1.89	3.76
Nguyen et al. (2014)	Entirely immersed	5/ 15	1.86 / 7.59	3.51
Nguyen et al. (2014)	Entirely emerged	5/ 15	1.72 / 7.51	3.65

The beginning of the entry phase corresponds to the final instant of the flight; and, for which, definitions differ among authors (de Jesus et al., 2011a; Green, 1987; Hohmann et al., 2008). The end of the entry phase is defined as the maximum feet depth from the first downward underwater kicking by Hohmann et al. (2008) but the full body immersion by de Jesus et al. (2011a) and Green (1987). Full body immersion is considered to be the end of the entry phase in ventral start studies (Vantorre et al., 2010) (Figure 1).

Authors have defined the glide phase as beginning at the instant entry ends until the maximum feet depth of the second downward underwater kick is reached (Hohmann et al., 2008), the hands reach the 5 m mark (de Jesus et al., 2011a, 2013), and/or the instant before underwater kicking commences (Green, 1987). In competition, Miller et al. (1984) defined the glide phase as being from when the fingertips made first water contact, until the first hand which came out of the water at the end of the glide, re-enters the water. Cossor and Mason (2001) considered the entry, glide and undulatory underwater movements as one combined parameter.

In previous ventral start studies, authors divided the underwater phase into two parts: the glide (Guimarães & Hay, 1985; Thow et al., 2012; Vantorre et al., 2010) and the undulatory underwater swimming (Vantorre et al., 2010). This convention was adopted by de Jesus et al. (2012) for the backstroke start. The glide phase does not include lower limb propulsive movements (Guimarães & Hay, 1985; Thow et al., 2012; Vantorre et al., 2014) (Figure 1). Hence, future studies should examine if the underwater kicking observed by Hohmann et al. (2008) as soon as the feet entered the water, provides any advantage over a period of motionless gliding during the start.

Biomechanical approaches and parameters assessed

Kinematics

Despite some authors using immediate feedback devices such as stopwatches (Green et al., 1987; Stratten, 1970) and velocimeters (de Jesus et al., 2012), 82.6% of the studies assessed backstroke start kinematics using video-based techniques (Arellano et al., 2001; Arellano et al., 2003; Chatard et al., 2003; Cornett et al., 2011; Cossor & Mason, 2001; de Jesus et al., 2010; 2011a; 2013; Girold et al., 2001; Green, 1987; Hohmann et al., 2008; Ikuta et al., 2001; Miller et al., 1984; Nguyen et al., 2014; Rea & Soth, 1967; Siljeg et al., 2011; Takeda

et al., 2014; Theut & Jensen, 2006; Wilson & Howard, 1983). Only Green (1987) used a three-dimensional (3D) dual-media setting via cinematographic cameras.

Most studies used digital cameras to provide independent aerial, underwater or combined dual-media analysis. In competition settings, cameras were positioned 18 m above the swimming pool (Arellano et al., 2001; Cossor & Mason, 2001; Girold et al., 2001; Ikuta et al., 2001) and along the side of the pool, 15 m from the starting block wall (Arellano et al., 2003); or underwater at 6.5 m from the starting block wall (Cornett et al., 2011). Studies conducted under laboratory conditions, used aerial and underwater cameras positioned at 6.78 m (de Jesus et al., 2010; 2011a; 2013) and 7.5 m (Takeda et al., 2014), both from the primary swimmer's plane of motion, and 30 cm above- and below-water surface (de Jesus et al., 2010; 2011a; 2013). Takeda et al. (2014) also described the dual-media cameras as positioned above the poolside deck and 1 m below the water surface; while Theut and Jensen (2006) implemented the same above-water camera position but the underwater camera in the corner of the swimming pool. Hohmann et al. (2008) and Nguyen et al. (2014) did not provide further details about the dual-media camera positions.

Quantitative data processing from digital cameras usually requires a coordinate scale and prevents immediate results due to the need for manual digitizing (de Jesus et al., 2011a; 2013; Hohmann et al., 2008; Nguyen et al., 2014; Takeda et al., 2014; Theut & Jensen, 2006). Furthermore, the digitisation and reconstruction errors associated with this procedure require authors to measure the errors. However, only de Jesus et al. (2011a, 2013) and Takeda et al. (2014) displayed these values. In competition settings, challenges increase because the competition regulations make it difficult to use the most accurate biomechanical methodology (Schwameder, 2008), which requires researchers to use parts of the swimming pool to create a digitising scale (Miller et al., 1984). The automatic tracking motion analysis systems have been considered highly reliable for 3D underwater analysis (Kudo & Lee, 2010). However, further validation and

reliability testing is required to establish its viability for studying dual-media backstroke starts.

Most of the kinematics approaches mentioned in the backstroke start studies above provide biomechanical performance indicators instead of specifying how swimmers should organize body segments movements to optimize their performance. Performance indicators are less time-consuming for coaching feedback and hinder technique analysis method to be wide-used in backstroke start studies. Table 2 outlines the kinematic variables measured at the most common backstroke starting phases and for the overall start. In fact, 69.5% of the studies measured the starting time, which ranged from the signal to the first fingertip contact with the water (de Jesus et al., 2011a; 2013) and the time to 22.86 m (Green et al., 1987). Following Guimarães and Hay (1985), starting time has been often measured for ventral start studies (Vantorre et al., 2010), but, there is no clear consensus as to what distances are best for assessing the most effective start, yet.

Table 2 indicates that most backstroke start studies have measured only linear displacement and velocity parameters, despite swimming starts not being exclusively rectilinear motions (Bartlett, 2007). Authors have considered the swimmer as a rigid body to calculate the horizontal distance (Cornett et al., 2011; Cossor & Mason, 2001; Miller et al., 1984; Theut & Jensen, 2006) and the velocity during a backstroke start (Arellano et al., 2003; Chatard et al., 2003; Giroldi et al., 2001; Theut & Jensen, 2006). Although these variables provide important information in training and competition environments, the curvilinear motions in the backstroke start need to be quantified. Some authors have studied translational kinematic parameters of the center of mass or hip vectors during the overall backstroke start (Green, 1987) and during starting phases (de Jesus et al., 2010; 2011a; 2013; Green, 1987; Nguyen et al., 2014; Takeda et al., 2014), as have been conducted for ventral starts (Guimarães and Hay, 1985; Takeda et al., 2012).

As humans do not have rigid bodies and display combinations of rotational and linear motions (Bartlett, 2007), multi-segmental models have been used to analyse segmental positions (Nguyen et al., 2014; Takeda et al., 2014); and joint angles from upper (Green et al., 1987; Wilson & Howard, 1983) and lower limbs (de Jesus et al., 2010, 2011a; Green et al., 1987; Nguyen et al., 2014; Takeda et al., 2014; Wilson & Howard, 1983); and trunks (de Jesus et al., 2013; Wilson & Howard, 1983) at different starting phases (Table 2). The study of the coupling relationship between segments is required to provide insight into the optimal movement strategies underlying backstroke starts.

There is a paucity of evidence concerning the parameters in the aerial/in-water and underwater phases. In fact, research usually has highlighted the importance of assessing entry (Vantorre et al., 2010; Vantorre et al., 2014) and underwater phase kinematics (de Jesus et al., 2011a; Vantorre et al., 2010; Thow et al., 2012; Vantorre et al., 2014) for ventral starts. Only Green (1987) and de Jesus et al. (2011a) have calculated the centre of mass displacement and velocity, during the entry and glide phases; and the time and frequency of some undulatory underwater swimming cycles of the backstroke start (de Jesus et al., 2012). In competitions, authors have measured the combined time from the entry until the swimmer's head resurfaced (Cossor & Mason, 2001) and the beginning of the first arm stroking cycle (Miller et al., 1984).

Kinetics

Despite several studies having used kinematics, few studies of backstroke starts have included kinetic data. Kinetics requires higher costs than image based systems and presents technical difficulties when attaching the kinetic devices to the starting block and pool wall. However, de Jesus et al. (2010, 2011a, 2013) successfully lowered, then elevated pool water levels so as to position a strain gauge force plate at two heights on the pool wall. Also, they instrumented the handgrips with a strain gauge load cell, which was sequentially repositioned to remain at the same distance above the water surface. The dynamics between the lower limbs and the pool wall were studied using a 3D piezoelectric force plate

(Hohmann et al., 2008; Nguyen et al., 2014). The strain gauges are more commonly used due to their lower costs and highly accurate static and transient load measurement capabilities than via a 3D piezoelectric force plate.

The instrumentation of starting blocks for analysing backstroke starts has helped to verify how the respective movements are generated (de Jesus et al., 2013; Hohmann et al., 2008; Nguyen et al., 2014). The horizontal force exerted by swimmers' lower limbs on the pool wall is the main research topic of backstroke start kinetics (de Jesus et al., 2013; Hohmann et al., 2008; Nguyen et al., 2014). The horizontal swimmers' lower limbs force-time curve profiles (Figure 2) registered during backstroke start performances were similar among these three studies reporting two distinguished peak forces. Researchers stated that swimmers should optimize the force-time distribution during the take-off phase (de Jesus et al., 2011a, 2013; Guimarães & Hay, 1985; Hohmann et al., 2008; Nguyen et al., 2014; Vantorre et al., 2014). To obtain further insight into the mechanics of the backstroke start, de Jesus et al. (2011a, 2013) analyzed the horizontal forces exerted on the handgrips and noted that the role played by the upper limbs was to drive the center of mass above the water surface.

Despite the understanding about the horizontal force profile generated by backstroke swimmers to propel themselves off the wall (de Jesus et al., 2011a, 2013), coaches also recommended that swimmers endeavor to accelerate the center of mass upwards to clear the water surface because the air presents less resistance than water (de Jesus et al., 2013; Nguyen et al., 2014; Takeda et al., 2014). In fact, the external kinetics involved in backstroke starts should be analyzed and interpreted, to consider the magnitude and timing of horizontal and vertical propulsive force vectors applied by the swimmer's muscular actions to the handgrips and pool wall. Hohmann et al. (2008) and Nguyen et al. (2014) have assessed 3D resultant forces on swimmers' lower limbs; but only Nguyen et al. (2014) measured the vertical force component. These authors found that altering feet positions at the start resulted in a significant change in peak horizontal and vertical forces. In 2013, FINA approved the use of a new starting

platform to prevent the backstroke swimmers sliding down the wall at the start; previously a reasonably common mishap, with disastrous results for the competitor. Therefore, future research analyses are required to ascertain and confirm any advantages that could result from the increased vertical forces backstroke swimmers might achieve and could be translated into a faster racing start.

The instrumented starting blocks used in the previous research referred to the above are few and are now obsolete following the recent FINA facility rule changes approved in 2008 and 2013. The new hand and foot grips now available for backstroke starts have not been instrumented and used in research studies to date. Hence, sport biomechanists and engineers are urged to develop a 3D kinetic system in the new block configuration. Then, one could identify independently how the right and left, upper and lower, limbs contribute to propelling backstroke swimmers during the start.

Beyond the linear kinetics, Green (1987) and Takeda et al. (2014) used angular kinetics principles to study the resistance of the swimmers' bodies and separated segments to change angular motion during backstroke starts. In previous ventral start studies, swimmers were advised to generate enough angular momentum to make a clean entry into the water (Vantorre et al., 2010). Despite the unique and valid attempt to assess the swimmers' reluctance to generate angular motion during backstroke start, a number of kinetic and kinematic variables also are required to explain how much rotation is occurring in the sequential starting phases. Takeda et al. (2012) and Takeda et al. (2014) suggested that a combination of kinetic and kinematic measurements are needed for greater clarification of important swimming start components.

Electromyography (EMG)

As for kinetics, specific EMG studies of swimming starts are few. To measure the muscle activity of backstroke swimmers during the start, a cable EMG system with surface electrodes was used by Hohmann et al. (2008) and de Jesus et al.

(2011a; 2011b). This approach requires methodological adaptations to record accurate measurements (Clarys & Cabri, 1993) such as immobilization of cables and water proofing electrodes. De Jesus et al. (2011a, 2011b) used a complete swimming suit for electrode insulation and cable immobilization. The full body-swimming suit appeared to be suitable for immobilizing cables but these had to exit via holes in the suit resulting in potential places for leaks. Further, the use of full body swimming suits is no longer allowed in competition. Insulation to cover electrodes was provided by adhesive bandages (de Jesus et al., 2011a, 2011b; Hohmann et al., 2008). Knowledge of specific muscle activity is an important factor in understanding neuromuscular coordination and effective force production during the different phases of the backstroke start. Overcoming these challenges would greatly assist in determining the most effective techniques and optimize training drills.

The average and integrated EMGs, as amplitude signals, were calculated by Hohmann et al. (2008) and de Jesus et al. (2011a; 2011b), respectively; to provide trunk, and upper and lower limb muscle activation. Muscle intensity data are only one element of motor activity; and the sequential pattern in which the muscles are engaged in a complex backstroke start movement is a more important element (Clarys & Cabri, 1993). In fact, the EMG also provides information on timing of muscle activities in human movements (Bartlett, 2007); nevertheless, only Hohmann et al. (2008) have been concerned about the muscle activation sequence during the backstroke start. According to these authors the backstroke start is initiated by the Deltoideus Anterior that had been very active fixing the body in a high set starting position. Despite this initial undertaking, Hohmann's research group did not provide detailed descriptions of the criteria used to determine the muscles involvement along a continuum from strongly active to an inactive state. The lack of standard methodologies to define the EMG activity makes comparisons between studies difficult.

By studying the sequencing of muscle activation, one can focus on several factors relating to skill; including the timing and overlap of agonist and antagonist activity

(Bartlett, 2007). The agonist and antagonist activation in backstroke starts has not been studied yet, due to the swim start acyclic pattern. Nevertheless, Hohmann et al. (2008) mentioned that joint stabilization occurred during flight and entry phases to overcome the high water resistance. Therefore, simultaneous activation of muscles surrounding joints should be investigated during the backstroke start (Clarys & Cabri, 1993).

Seven muscles were commonly studied (de Jesus et al., 2011a, 2011b; Hohmann et al., 2008) namely, the Biceps Brachii, Triceps Brachii, Deltoideus Anterior, Erector Spinae Longissimus, Rectus Femoris, Gluteus Maximus and Gastrocnemius Medialis. Authors confirmed the crucial function of the lower limbs to generate the impulse during the take-off phase; however, they disagreed about the main muscle activities of the upper limbs. Studying the above-mentioned bi-articular muscles (de Jesus et al., 2011a, 2011b; Hohmann et al., 2008) has highlighted the need to clarify how the mechanical functions vary, depending on the different backstroke start variations and phases (e.g. hip flexor and knee extensor moments for the Rectus Femoris). As backstrokers are required to coordinate multiple muscles and joints to propel themselves rigorously out of the pool wall, more studies should couple EMG, kinetic and kinematic approaches to dictate how better backstroke start performance can be achieved.

Synchronization methods

The selected studies used a voice command (Stratten, 1970), starting pistol (Rea & Soth, 1967; Miller et al., 1984; Wilson & Howard, 1983), or the official competition timing systems for backstroke start synchronisation (Arellano et al., 2001; Arellano et al., 2003; Chatard et al., 2003; Cornett et al., 2011; Cossor & Mason, 2001; de Jesus et al., 2011a, 2011b, 2013; de Jesus et al., 2012; Girold et al., 2001; Green, 1987; Green et al., 1987; Hohmann et al., 2008; Ikuta et al., 2001; Nguyen et al., 2014; Siljeg et al., 2011; Takeda et al., 2014; Theut & Jensen, 2006).

The competition timing systems were used to simultaneously produce the starting signal and export a light to the video images (Arellano et al., 2001; Arellano et al., 2003; Chatard et al., 2003; Cornett et al., 2011; Cossor & Mason, 2001; de Jesus et al., 2011a; 2013; Hohmann et al., 2008; Ikuta et al., 2001; Nguyen et al., 2014; Siljeg, 2011; Takeda et al., 2014; Theut & Jensen, 2006); and a trigger pulse for the kinetics (de Jesus et al., 2011a; 2013; Hohmann et al., 2008; Nguyen et al., 2014) and EMG synchronization (de Jesus et al., 2011a; 2011b).

Alternative synchronization methods have been implemented as the use of force instants to record the swimmer's handgrip release (de Jesus et al., 2011a, 2013) and feet take-off (de Jesus et al., 2012) for the starting signal definition. Considering that a small temporal and spatial misalignment between different biomechanical devices can lead to large errors in the variables assessed, future studies should use a common system with consistent low trigger delay.

The backstroke start techniques, variations and main research findings

The main objective of swim-start research has been to identify the most effective start technique in terms of performance (Vantorre et al., 2014). From the selected studies, 65% have established comparisons using backstroke start techniques and variations (Table 1). Researchers have used different distances to assess the effectiveness of each one (Table 3).

Considering the backstroke start studies conducted with variations performed under the NCAA rules, both had used the 6.09 m distance to assess start time. According to Stratten (1970) the most efficient variation was performed when the swimmer's trunk was positioned upright just in front of the block, and hands holding the horizontal hand-grips; and, the respective mean start time seems to be shorter than the one presented by Rea and Soth (1967). This finding could be explained by the sample sizes and proficiency levels. Rea and Soth (1967) studied one specialist in backstroke start who performed with the trunk inclined forward over the top of the starting block and hands holding a bar mounted over the block. Stratten (1970) included 13 swimmers of different proficiency levels

who completed a training period for familiarization purposes. Yet, it is quite likely that previous experience with a technique may have an impact on start variables and performance (Vantorre et al., 2014). The feet positioned over the pool gutter allowed swimmers to clear the water from the starting position to the beginning of entry by generating greater vertical reaction force; and considered a crucial aspect for better backstroke start performances (de Jesus et al., 2013; Nguyen et al., 2014; Takeda et al., 2014). These statements corroborate other findings where the starts that were performed with shorter horizontal take-off velocities, implied greater aerial trajectory and shorter start time than the variation with a flatter profile (Green et al., 1987) (Table 3).

Most research considered backstroke starts performed under FINA old rules and measured the starting effectiveness using distances from 5 to 15 m (Table 3). Miller et al. (1984) and Arellano et al. (2003) assessed mean start times; although, only the latter specified the set distance. Siljeg et al. (2011) measured the 15 m start time considering the pre and post period of FINA rule changes for feet positioning (FINA 2005-2009, SW. 6.1), which explains the maximum 0.55 s mean difference from the Arellano et al. (2003) findings. Indeed, Nguyen et al. (2014) noted that since the FINA rule changed for feet positioning, many backstrokers have obtained advantages from altering their starting technique to place the feet completely out of the water. To achieve a great start-time performance at 7.5 m, elite backstrokers displayed considerable intra- and inter-variability of the upper limbs trajectory during the flight phase (Hohmann et al., 2008; Wilson & Howard, 1983). The upper limb pathways over the center of mass and close to the body allow the trunk to follow a greater parabolic flight than using a lateral path (Bartlett, 2007; Green, 1987; Maglischo, 2003). According to de Jesus et al. (2013), Nguyen et al. (2014) and Takeda et al. (2014), a greater parabolic flight path assists in minimizing drag and optimizing propulsion underwater. Since a clear water entry depends on preceding actions performed during the wall and flight phases (Thow et al., 2012), Theut and Jensen (2006) identified the effects of the feet submerged and positioned parallel to each other or staggered (i.e., one above the other) on backstroke start horizontal distance

and average velocity. Anecdotal evidence suggested that the feet staggered position prevented swimmers from slipping down the wall; nevertheless, findings did not confirm that difference between variations (Theut & Jensen, 2006). The backstroke start ledge (FINA FR. 2.7, 2013-2017) is pointed out to avoid the slippage; however, further studies are needed to describe in detail how technique must be changed to improve backstroke start performance.

Backstroke starts are performed now under the current FINA rule (adopted in 2005) and only de Jesus et al. (2010; 2011a; 2011b; 2013) and Nguyen et al. (2014) compared the variations with the feet parallel, and entirely submerged and out-of-water. Considering the 5 m start time (Table 3) for both variations, shorter values seem to be displayed by the latter research group, which is mainly explained by the swimmers' greater proficiency level. The variation with feet entirely submerged seems to register lower horizontal take-off mean values in both studies; and the values presented by de Jesus et al. (2013) seem lower than those of Nguyen et al. (2014). Although this finding was not significant, the trend might be explained by the use of a fixed point to indicate the swimmer's center of mass. Takeda et al. (2014) verified that backstroke swimmers specialists used a feet-partial-out-of-the-water start, and tended to register greater mean 5 m start time than participants of Nguyen et al. (2014). This might indicate superiority of the variation performed with feet entirely out-of-the-water over the method with partially emerged. De Jesus et al. have not displayed performance differences during above- (2013) and underwater phases (2012), between the variation with feet entirely out and under the water; thereby disagreeing with the Nguyen et al.'s findings (2014). These contradictions might be explained by the larger sample size and greater swimmers' preference for feet positioned out of the water displayed by Nguyen et al. (2014). De Jesus et al. (2011a, 2013) and Nguyen et al. (2014) stressed that swimmers should generate greater horizontal and vertical take-off velocities when the feet were positioned out of the water to achieve the most appropriate aerial trajectory (de Jesus et al., 2013). The inclusion of the new device for backstroke starts potentially improves the parabolic flight trajectory due to minimized take-off friction force. However, since greater vertical flight trajectory

implies deeper water entry, future research should also examine underwater phase variables, which can indicate risk of injury, as previously pointed out during youth competitions (Cornett et al., 2011).

Summary and future directions

The main research findings can be summarized as follows: (1) the phase definitions used in analyzing backstroke starts are inconsistent and unclear. Hence, this makes it difficult to determine how many changes over time can be attributed to a real change, or mere differences between definitions; (2) studies conducted in laboratory settings have adopted kinematics, kinetics and EMG; however, many research challenges remain in both settings to improve the methods of quantifying valid, reliable and accurate data; (3) the temporal variables, particularly the starting time, were most studied; and backstroke start movements were predominantly described using linear kinematics; (4) most of the experimental and competition research findings are now out of date since the backstroke start rules have been recently changed, and the studies were completed under swimming rules which are now obsolete.

Future research would help coaches and swimmers by exploring issues not yet fully addressed in the literature. For example: (1) determination of a consistent observational model for categorization and study of the backstroke start technique; (2) development of appropriate biomechanical measurements and research methodologies as standard tools; for scientific purposes and training support, competition preparation and analysis; (3) reinforcement of more holistic and process-oriented biomechanical approaches in laboratory procedures: involving interactions of kinematics, kinetics and EMG variables; from aerial, aerial/in-water and underwater phases; definitions for more detailed parameters which better describe the overall backstroke start in competitions, beyond the starting time; (4) focusing on studies based on the actual FINA rules and the new starting block configurations.

Acknowledgments

This work was supported by the CAPES Foundation under doctoral grant (BEX 0761/12-5/2012-2015) and FCT Foundation under grant (EXPL/DTL-DES/2481/2013).

References

Arellano, R., Cossor, J., Wilson, B., Chatard, J-C., Riewald, S., & Mason, B. (2001). Modelling competitive swimming in different strokes and distances upon regression analysis: a study of the female participants of Sydney 2000 Olympic Games. In J.R. Blackwell, & R.H. Sanders (eds.), XIX International Symposium on Biomechanics in Sports: University of San Francisco, 53-56.

Arellano, R., Sanchez-Molina, J., Navarro, F., & De Aymerich, J. (2003). Analysis of 100 m backstroke, breaststroke, butterfly, freestyle swimmers at the 2001 European Youth Olympic days. In J-C Chatard (ed.), IX Biomechanics and Medicine in Swimming: University of Saint Etienne, 255-260.

Bartlett, R. (2007). Introduction to sports biomechanics: analyzing human movement patterns. New York: Routledge, 191-195.

Chatard, J-C., Girold, S., Caudal, N., Cossor, J., & Mason B. (2003). Analysis of the 200 m events in the Sydney Olympic Games. In J-C Chatard (ed.), IX Biomechanics and Medicine in Swimming: University of Saint Etienne, 261-264.

Clarys, J. P., & Cabri, J. (1993). Electromyography and the study of the sports movements: a review. *Journal of Sports Sciences, 11*(5)*,* 1155-1162.

Cornett, A.C., White, J.C., Wright, B.V., Willmont, A.P., & Stager, J.M. (2001). Racing start safety: head depth and head speed during competitive backstroke starts. *International Journal of Aquatic Research, 5*(4), 389-401.

Burnley, M., & Jones, A. (2007). Oxygen uptake kinetics as a determinant of sports performance. *European Journal of Sports Science, 7*(2), 63-79.

Cossor, J.M., & Mason, B.R. (2001). Swim start performances at the Sydney 2000 Olympic Games. In J.R. Blackwell & R.H. Sanders (eds.), XIX International Symposium on Biomechanics in Sports: University of San Francisco, 70-73.

de Jesus, K., de Jesus, K., Figueiredo, P., Gonçalves, P., Pereira, S., Vilas-Boas, J.P., & Fernandes, R.J. (2010). Biomechanical characterization of the backstroke start in immersed and emerged feet conditions. In P-L. Kjendlie, R.K. Stallman, & J. Cabri (eds.), XI Biomechanics and Medicine in Swimming: Norwegian School of Sport Science, 64-66.

de Jesus, K., de Jesus, K., Figueiredo, P., Gonçalves, P., Pereira, S., Vilas-Boas, J.P., & Fernandes, R. (2011a). Biomechanical analysis of backstroke swimming starts. *International Journal of Sports and Medicine, 32*(7)**,** 546-551.

de Jesus, K., de Jesus, K., Figueiredo, P., Gonçalves, P., Pereira, S. M., Vilas-Boas, J.P., Fernandes, R. (2011b). Electromyographic analysis of two different feet positions in backstroke start. In J.P. Vilas-Boas, L. Machado, W. Kim, A.P. Veloso, F. Alves, R.J. Fernandes, & F. Conceição (eds.), XXIX International Symposium on Biomechanics in Sports: University of Porto, 191-194.

de Jesus, K., de Jesus, K., Machado, L., Fernandes, R., Vilas-Boas, J. P. (2012). Linear kinematics of the underwater undulatory swimming phase performed after two backstroke starting techniques. In E.J. Bradshaw, A. Burnett, & P.A. Hume (eds.), XXX International Symposium on Biomechanics in Sports: Australian Catholic University, 371-373.

de Jesus, K., de Jesus, K., Figueiredo, P., Gonçalves, P., Pereira, S. M., Vilas-Boas, J.P., & Fernandes, R.J. (2013). Backstroke start kinematic and kinetic changes due to different feet positioning. *Journal of Sports Sciences, 31*(15), 1665-1675.

FINA. Federation International de Natation, 2013. Available at: http://www.fina.org/H2O/index.php?option=com_content&view=article&id=4161&Itemid1; accessed on 17.10.2013.

Girold ,S., Chatard, J-C., Cossor, J., & Mason, B. (2001). Specific strategy for the medalists versus finalists and semi-finalists in the men's 200 m backstroke at the Sydney Olympic Games. In J.R. Blackwell & R.H. Sanders (eds.), XIX International Symposium on Biomechanics in Sports: University of San Francisco, 27-30.

Green, R.C. (1987). A biomechanical analysis comparing the whip start with the conventional backstroke start. Unpublished doctoral dissertation, Brigham Young University, Idaho; 1987.

Green, R.C., Cryer, W., Bangerter, B., Lewis, K., & Walker, J. (1987). Comparative analyses of two methods of backstroke starting: conventional and whip. In L. Tsarouchas, J. Terauds, B.A. Gowitzke, & L.E. Holt (eds.), V International Symposium on Biomechanics in Sports. University of Greece, 281-289..

Guimarães, A.C.S., & Hay, J.G. (1985). A mechanical analysis of the grab starting technique in swimming. *International Journal of Sports Biomechanics, 1*, 25-35.

Hermes, H.J., & Freriks, B. (1999). European recommendations for surface electromyography: results of the SENIAM project. Enschede, Netherlands: Roessingh research and development.

Hohmann, A., Fehr, U., Kirsten, R., & Krueger, T. (2008). Biomechanical analysis of the backstroke start technique in swimming. *E-Journal Bewegung und Training, 2*, 28-33.

Ikuta, Y., Mason, B., & Cossor, J. (2001). A comparison of Japanese finalists to other finalists in the 100 m swimming races at the Sydney Olympic Games. In J.R. Blackwell & R.H. Sanders (eds.), XIX International Symposium on Biomechanics in Sports: University of San Francisco, 75-77.

Kudo, S., & Lee, M.K. (2010). Prediction of propulsive force exerted by the hand in swimming. In P-L. Kjendlie, R.K. Stallman, & J. Cabri (eds.), XI Biomechanics and Medicine in Swimming: Norwegian School of Sport Science, 112-114.

Maglischo, E.W. (2003). Swimming fastest: the essential reference on technique, training, and program design. Champaign, Illinois: Human Kinetics, 283-287.

Miller, J. A., Hay, J. G., & Wilson, B. D. (1984). Starting techniques of elite swimmers. *Journal of Sports Sciences, 2*, 403-410.

NCAA. National College Athletic Association. NCAA men's and women's swimming and diving rules. Available at: http://www.naia.org/fls/27900/1NAIA1/resources/sid/Rule%20Books/SW; accessed on 20.06.2013.

Nguyen, C., Bradshaw, E.J., Pease, D., & Wilson, C. (2014). Is the starting with the feet out of the water faster in backstroke swimming? *Sports Biomechanics, 13*(2), 154-165.

Rea, W. M, & Soth, S. (1967). Revolutionary backstroke start. *Swimming Technique, 3*, 94-95.

Schwameder, H. (2008). Aspects and challenges of applied sport biomechanics research. XXVI International Symposium on Biomechanics in Sports: Seoul National University, 25-28.

Stratten, G. (1970). A comparison of three backstroke starts. *Swimming Technique, 7*, 55-60.

Siljeg, K., Leko, G., & Mikulic, P. (2011). Situational success in 100-m backstroke event at the 2004 and 2008 European Swimming Championships. *Sports Sciences, 4*, 28-31.

Takeda, T., Takagi, H., & Tsubakimoto, S. (2012). Effect of inclination and position of new swimming starting block's back plate on track-start performance. *Sports Biomechanics, 11*(3), 370-381.

Takeda, T., Itoi, O., Takagi, H., & Tsubakimoto, S. (2014). Kinematic analysis of the backstroke start: differences between backstroke specialists and non-specialists. *Journal of Sports Sciences, 32*(7), 635-641.

Thanopoulos, V., Rozi, G., Okici, T., Dopsaj, M., Jorgic, B, Madic, D., Velickovid, S., Milanovic, Z., Spanou, F., & Batis, E. (2012). Differences in the efficiency between the grab and track starts for both genders in Greek young swimmers. *Journal of Human Kinetics, 32*, 43-51.

Theut, K. M., & Jensen, R. L. (2006). A comparison of two backstroke starts. In H. Schwameder, G. Strutzenberger, V. Fastenbauer, S. Lindinger, & E. Muller (eds.), XXIV International Symposium on Biomechanics in Sports: University of Salzburg, 1-5.

Thow, J. L., Naemi, R., & Sanders, R. H. (2012). Comparison of modes of feedback on glide performance in swimming. *Journal of Sports Sciences, 30*(1), 43-52.

Toubekis, A. G., Drosou, E., Gourgoulis, V., Thomaidis, S., Douda, H., & Tokmakidis, S.V. (2013). Competitive performance, training load and physiological responses during tapering in young swimmers. *Journal of Human Kinetics, 38*(8), 125-134.

Vantorre, J., Seifert, L., Fernandes, R. J., Vilas-Boas, J.P., & Chollet, D. (2010). Comparison of grab start between elite and trained swimmers. *International Journal of Sports Medicine, 31*(12), 887-893.

Vantorre, J., Chollet, D., & Seifert, L. (2014). Biomechanical analysis of the swim-start: a review. *Journal of Sports Science and Medicine, 13*(2), 223-231.

Vilas-Boas, J.P., & Fernandes, R.J. (2003). Swimming starts and turns: determinant factors of swimming performance. In P. Pelayo (ed.), Actes des 3èmes journées spécialisées de natation: Université Lille, 84-95.

Wilson, B. D., & Howard, A. (1983). The use of cluster analysis in movement description and classification of the backstroke swim start. In H. Matsui, & K. Kobayashi (eds), VIII-B Biomechanics: Human Kinetics, 1223-1230.

.

Chapter 3

The backstroke starting variants performed under the current swimming rules and block configuration.

Karla de Jesus[1], Kelly de Jesus[1], Alexandre I. A. Medeiros[1], Ricardo J. Fernandes[1,2], João Paulo Vilas-Boas[1,2].

[1] Centre of Research, Education, Innovation and Intervention in Sport, Faculty of Sport, University of Porto, Porto, Portugal
[2] Porto Biomechanics Laboratory (LABIOMEP), Porto, Portugal

Published on Journal of Swimming Research (2014), 22, 1-5.

Abstract

Backstroke start has evolved since last 10 years due to modifications on international rules and block configuration; however, researchers have not yet attempted to verify the combined effects of these changes on the backstroke start technique. Therefore, this study aimed to identify the backstroke starting variants performed at elite swimming events considering the effects of the current FINA rules and the starting block handgrip actualizations. Video images from individual backstroke events recorded during 2012 Olympic Games and 2013 Swimming World Championships were analyzed from official FINA's videos. Frequency analysis was calculated to verify the starting variants distribution by gender, event and classification. Considering 100 and 200 m backstroke heats, semi-finals and finals, male and female swimmers adopted four and six different starting variants, respectively. Analyzing only the semi-finals and finals, males performed two variants at 50 and 100 m and three variants at 200 m event, respectively, while females adopted three variants at 50 and 200 m and four variants at 100 m event, respectively. Independently of the gender, event and classification, swimmers frequently performed one variant with feet parallel and partially emerged and hands grasping the highest horizontal handgrip and the other one with feet parallel and partially emerged and hands grasping the vertical handgrip. In order to complement these findings, further studies are required to provide coaches and swimmers with biomechanical evidences of the different backstroke starting variants.

Key words: video analysis, swimming competition, backstroke event, dorsal start

Introduction

Researchers have been interested since long, in targeting swimming race analysis rather than only simple split times. According to Hay and Guimarães (1983) the swimming race time can be divided into the starting, stroking and turning sections. Starting performance, usually defined as the period between the starting signal and the first 15 m mark is crucial in short (Arellano, et al., 2003; Cossor & Mason, 2001; Ikuta, et al., 2001; Maglischo, 2003; Thanopoulos, et al., 2012) and middle distance swimming events (Girold, et al., 2001; Miller, et al., 1984). In fact, the difference between the best and worst starters at elite swimming level is likely to achieve 0.5 s, which may determine the final classifications (Mason, et al., 2012; Seifert, et al., 2010, Vilas-Boas & Fernandes, 2003; Wilson & Howard, 1983). For example, less than 0.5 s has separated the second place from the winner at men's 50, 100 and 200 m backstroke at Barcelona 2013 Long Course Swimming World Championships.

Swimming competitions hold starting techniques for ventral and dorsal events. Conversely, few studies have been drawing their attention towards the backstroke start technique (de Jesus, et al., 2013; Hohmann, et al., 2008, Theut & Jensen, 2006) opposing lots of others, which have analyzed the mechanics of different ventral starting techniques (e.g. Hanin, et al., 2004; Vantorre, et al., 2010a, 2010b). This lack might be explained by the higher number of swimming events beginning from a standing position on the starting block rather than in water (Theut & Jensen, 2006) and by the previous lower number of options and controversy about the backstroke starting variants performed under the Fédération Internationale de Natation (FINA) old rules (Vilas-Boas & Fernandes, 2003). From the available data regarding the backstroke start, almost all studies are outdated or limited as the international swimming rules have changed and most of the starting variants analyzed were deemed to be illegal (Vantorre, et al., 2010a). To date, only de Jesus et al. (2011a, 2011b, 2013), Nguyen et al., (2014) and Takeda et al., (2014) have conducted studies under FINA's current

backstroke starting rules (FINA, SW 6.1), considering the different feet positioning and the respective effects on biomechanical parameters.

No study has yet considered the current starting block update in backstroke starting analysis. However, the combination of different upper and lower limbs positioning might substantially affect the backstroke starting performance, highlighting the need for further investigation. An overview of the backstroke starting technique considering current FINA rules and block facilities is imperative for the purposes of highlighting the most popular starting variants performed and future research stimulation. In fact, Green et al. (1987) had already mentioned that as soon as this skill is successfully approved by swimmers, biomechanists will carry on a careful review. Therefore, it was necessary to identify the starting variants which have been performed by elite backstroke swimmers after the FINA's rule changes and the implementation of the current starting block configuration. It was hypothesized that most of the elite male and female swimmers would perform starting variants with the feet positioned entirely or partially above the water level and hands grasping on the highest horizontal or vertical handgrip to uplift the body as high as possible out of the water during the set positioning.

Methods

Participants

The sample has comprised swimmers of both genders who have competed at 100 and 200 m backstroke heats, semi-finals and finals at London 2012 Olympic Games and at 50, 100 and 200 m backstroke semi-finals and finals at Barcelona 2013 Swimming World Long Course Championships. Swimmers competing more than once at the classification series (i.e., heats, semi-finals and finals) got in the sample procedure only once, since the variant performed was unchanged. Only swimmers who have competed in lanes five to eight were observed due to camera view obstruction.

Mean (± SD), minimum and maximum values of body mass, height, age, and time obtained at each scrutinized event for male and female swimmers at the three individual backstroke competitive distances are presented in Table 1. The 100 and 200 m backstroke data for males and females was calculated including 2012 Olympic Games and 2013 Swimming World Championships participants, since the 50 m backstroke was not included as an Olympic event. Personal and anthropometric data were retrieved from web portals, particularly from London 2012 Olympic Games and FINA swimmers' biographies. Performance data at each event and distance for male and female swimmers was taken from the event organizer official website.

Table 1. Mean (±SD), minimum and maximum values of body mass, height, age and time for male and female swimmers at each individual backstroke competitive distance. The 100 and 200 m backstroke data for males and females were calculated including the Olympic Games and Swimming World Championships participants.

		Body mass (Kg)		Height (m)		Age (yr)		Time (s)	
		Male (n=8)	Female (n=8)	Male (n=8)	Female (n=8)	Male (n=10)	Female (n=10)	Male (n=11)	Female (n=10)
50m	Mean	90.3	62.5	1.94	1.74	26.1	22.2	24.84	28.07
	SD	3.4	4.4	0.07	0.02	3.4	3.6	0.03	0.04
	Minimum	73.0	59.0	1.84	1.70	21.0	18.0	24.39	27.29
	Maximum	113.0	69.0	2.03	1.76	31.0	29.0	25.28	28.61
		Male (n=33)	Female (n=34)	Male (n=32)	Female (n=34)	Male (n=36)	Female (n=37)	Male (n=36)	Female (n=37)
100m	Mean	78.9	66.6	1.87	1.77	23.8	22.4	54.42	61.00
	SD	7.2	6.9	0.07	0.07	3.2	3.4	1.04	2.14
	Minimum	62.0	57.0	1.77	1.60	17.0	16.0	52.97	58.23
	Maximum	95.0	85.0	2.00	1.87	29.0	29.0	57.94	68.19
		Male (n=31)	Female (n=31)	Male (n=31)	Female (n=31)	Male (n=34)	Female (n=34)	Male (n=33)	Female (n=34)
200m	Mean	77.2	64.8	1.86	1.75	22.7	21.4	118.14	130.49
	SD	8.0	4.9	0.06	0.05	3.8	3.3	1.90	3.17
	Minimum	62.0	57.0	1.73	1.64	17.0	14.0	113.94	124.06
	Maximum	91.0	76.0	2.05	1.85	36.0	29.0	122.12	138.60

Data collection

Backstroke starts performed at individual 50, 100 and 200 m events were analyzed from an aerial video camera (FINA official video images). Missing data were noted in the Olympic Games videos at 5th women's 100 m backstroke heat, 1st women's 200 m backstroke heat and lanes six, seven and eight of 4th men's 200 m backstroke heat.

Data analysis

Backstroke starting technique performed by each swimmer was classified according to different combinations of upper and lower limbs positioning at the command of “take-your marks”. These combinations were defined based on the current FINA’s backstroke starting rules (FINA, 2013), the starting block configuration (Omega, OSB11, Corgémont, Swiss Timing Ltd.) and on literature (Figure 1). None of the swimmers who had been analyzed at Barcelona 2013 Swimming World Championships used the recently authorized ledge device (FINA, 2013).

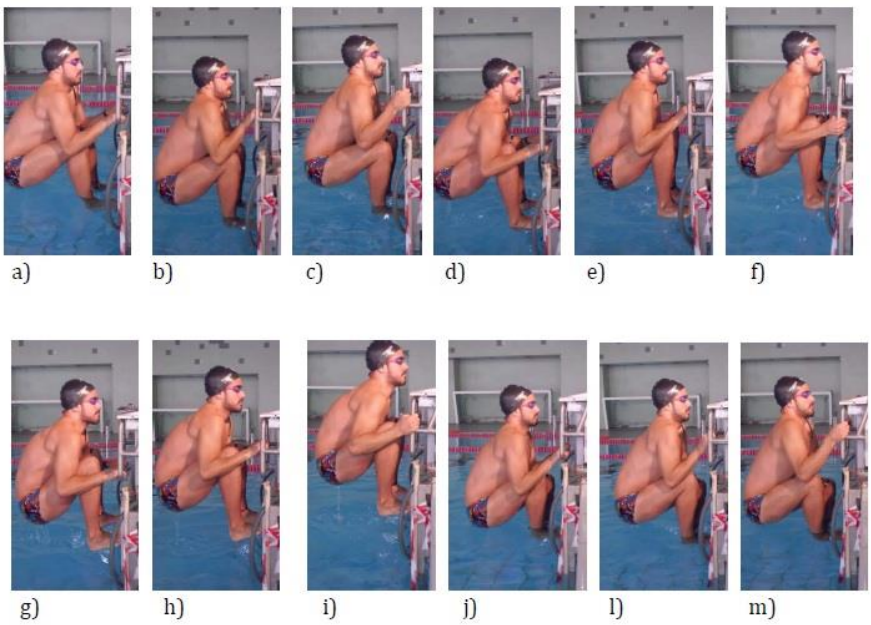

Figure 1. The backstroke starting variants, characterized by the combination of different upper and lower limbs positioning. Feet immersed and lowest and highest horizontal, and vertical, handgrip (Panels a, b and c, respectively). Feet partially emerged and lowest and highest horizontal, and vertical, handgrip (Panels d, e and f, respectively). Feet entirely emerged and lowest and highest horizontal and vertical, handgrip (Panels g, h and i, respectively). Feet staggered and lowest and highest horizontal, and vertical, handgrip (Panels j, l and m, respectively).

Statistical procedures

Frequency analyses were conducted aiming to verify the starting variants distribution by gender, swimming events (50, 100 and 200 m) and classifications (heats, semi-finals and finals). The 1st frequency analysis calculated for male and

females and for 100 and 200 m backstroke included swimmers who participated at heats, semi-finals and finals at London 2012 Olympic Games and at semi-finals and finals at 2013 Barcelona Swimming World Championships. To analyze the starting distributions among the most proficient backstroke Olympic and World Championships swimmers, the 2nd frequency analysis for both genders has included only swimmers from the semi-finals and finals of 50 m backstroke at Barcelona 2013 Swimming World Championships and 100 and 200 m backstroke at both competitive events.

To test the intra and inter observer reliability, a second video analysis was conducted after 15 days from the 1st observation, being observed both competition overall heats, semi-finals and finals. The value obtained (98.4%) corresponds to a high intra and inter observer reliability (Van Der Mars, 1989). The statistical procedures were conducted through IBM®SPSS® Statistics system 20.

Results

From the overall combinations of upper and lower limbs positioning (cf. Figure 1) seven starting variants were observed (Figure 1, Panels b, c, d, e, f, i, j). Considering 100 and 200 m backstroke heats, semi-finals and finals at 2012 Olympic Games and semi-final and finals at 2013 Swimming World Championships, male swimmers adopted four different backstroke starting variants (Table 2), with the most frequent one (with feet positioned parallel and partially emerged and hands grasping on the vertical handgrip, Figure 1, Panel f) found on the 100 m event. Conversely, in 200 m male backstroke, swimmers often used the variant with feet parallel and partially emerged and hands grasping on the highest horizontal handgrip (Figure 1, Panel e). In the same events, female swimmers used six different starting variants (cf. Table 2). The starting variant with feet parallel and partially emerged and hands positioned on the highest

horizontal handgrip (Figure 1, Panel e) was the most common used at 100 and 200 m backstroke.

Table 2. Absolute and relative frequency distribution of the backstroke starting variants performed by male and female swimmers at 100 and 200 m backstroke heats, semi-finals and finals of 2012 Olympic Games and at semi-finals and finals of 2013 Swimming World Championships.

	100m			200m		
	Variants	Count	% of variants	Variants	Count	% of variants
Male	1	1	2.8%	3	2	7.4%
	5	17	47.2%	5	15	55.6%
	6	18	50.0%	6	10	37.0%
Female	2	1	2.9%	2	1	3.2%
	4	4	11.4%	3	1	3.2%
	5	16	45.7%	5	18	58.1%
	6	13	37.1%	6	11	35.5%

The frequency analysis on the men's semi-finalists and finalists at 50 m backstroke at 2013 Swimming World Championship and at 100, 200 m backstroke in both competitions (Table 3), showed two variants for 50 and 100 m and three variants for 200 m event commonly used by backstroke swimmers. The starting variant performed with feet parallel and partially emerged and hands grasped on the highest horizontal handgrip (Figure 1, Panel e) was the most adopted on 50 and 200 m backstroke, while the variant performed with feet parallel and partially emerged and hands positioned on the vertical handgrip (Figure 1, Panel f) was the most used on 100 m backstroke event. In the same events, female swimmers displayed three variants for 50 and 200 m and four variants for 100 m event, respectively (Table 3). Female backstrokers performing the 50 m event rather adopted the starting variant with feet parallel and partially emerged and hands grasping on the vertical handgrip (Figure 1, Panel f). Regarding 100 and 200 m backstroke, swimmers commonly performed the variant with feet parallel and partially emerged and hands grasping on the highest horizontal handgrip (Figure 1, Panel e).

Table 3. Absolute and relative frequency distribution of the backstroke starting variants performed by male and female swimmers at 50, 100 and 200 m backstroke (semi-finals and finals) at London 2012 Olympic Games and Barcelona 2013 Swimming World Championships.

	50m			100m			200m		
	Variants	Count	% of variants	Variants	Count	% of variants	Variants	Count	% of variants
Male	5	6	54.5%	5	9	42.9%	3	1	6.3%
	6	5	45.5%	6	12	57.1%	5	8	50.0%
							6	7	43.8%
Female	4	2	20.0%	2	1	2.7%	2	1	5.0%
	5	3	30.0%	4	2	10.0%	5	11	55.0%
	6	5	50.0%	5	9	45.0%	6	8	40.0%
				6	8	40.0%			

Note: 1=Entirely emerged and vertical handgrip; 2=Entirely immersed and vertical handgrip; 3=Entirely immersed and highest horizontal handgrip; 4=Partially emerged and lowest horizontal handgrip; 5=Partially emerged and highest horizontal handgrip; 6=Partially emerged and vertical handgrip.

Discussion

The backstroke swimming start has been increasingly evolving after the last FINA's rule changes and starting block configuration, with swimmers being currently allowed to perform several starting variants (Figure 1). Hence, considering the obvious importance of the starting phase on the overall swimming race time (Mason, et al., 2012; Vilas-Boas & Fernandes, 2003) andthat most of the studies have dealt with obsolete backstroke starting rules (Arellano, et al., 2003; Cossor & Mason, 2001; Girold, et al., 2001; Ikuta, et al., 2001; Miller, et al., 1984; Stratten, 1970; Theut & Jensen, 2006; Wilson & Howard, 1983) or have not yet considered the starting block actualizations (de Jesus, et al., 2013; Hohmann, et al., 2008; Takeda, et al., 2014), this study is original and pertinent once it describes the backstroke starting technique and respective variants adopted at individual elite events. Nevertheless, a better understanding on the competition data may be crucial to establish specific training programs and to impart new researching areas. Our findings revealed that independently of gender, event and classification, backstroke swimmers performed mainly two starting variants: one, with feet parallel and partially emerged and hands grasping on the highest horizontal handgrip (Figure 1, Panel e), and other with feet parallel

and partially emerged and hands positioned on the vertical handgrip (Figure 1, Panel f). These results partially agree with our hypothesis.

Considering men's 100 and 200 m backstroke heats, semi-finals and finals, swimmers have adopted a small starting variants number rather than females, probably due to the previous mentioned gender effects (Takeda, et al., 2014). At 100 m backstroke, most of the swimmers have chosen the variant with feet positioned parallel and partially emerged and hands grasping on the vertical handgrips (Figure 1, Panel f). In opposition, 200 m swimmers have performed often the feet positioned parallel and partially emerged and hands grasping on the highest horizontal handgrip (Figure 1, Panel e). Since a previous backstroke starting research mentioned that the Biceps Brachii is mainly activated during the hands-off phase (de Jesus, et al., 2011b), the forearm positioned laterally potentiates this muscle action to pull the swimmer's body out of water in a crouched position at the "take-your marks" command. Swimmers in a high setting positioning and closer to the pool wall may generate great vertical force during the hands-off and take-off phases (de Jesus, et al., 2011a; Maglischo, 2003), and, consequently, a clearer flight and water immersion (de Jesus, et al., 2011a, 2013; Seifert, et al., 2010; Takeda, et al., 2014). New kinematic, kinetic and EMG studies would be useful to verify in detail the influence of different handgrips when the backstroke start is performed with feet parallel and partially emerged.

In the same events, female swimmers performed, in total, six different starting variants. The higher quantity of starting variants carried out by female swimmers might be explained mainly due to strength differences, compared to males. In fact, de Jesus et al. (2011a, 2011b) and Hohmann et al. (2008) have mentioned the essential role-played by the upper limb muscles to fix the body in a high starting position close to the wall. Despite these results, the starting variant with feet parallel and partially above the water surface with the hands grasping on the highest horizontal handgrip (Figure 1, Panel e) was the most used by female swimmers welcomed best the horizontal positioning on the highest handgrip to sufficiently raise the center of mass and achieve a better support, consequently

generating a meaningful magnitude of upper limbs propulsive force, as previously suggested by Maglischo (2003), but not confirmed by de Jesus et al. (2011a, 2013). Further studies are needed to identify if swimmers' hands positioned on the highest horizontal handgrip increase the upper limbs vertical reaction force contribution on the resultant impulse during the upward thrust from the swimming pool wall.

Analyzing the starting variants distribution including only the semi-finalists and finalists of 100 and 200 m backstroke in both competitive events, male and female swimmers seem to adopt a more reduced variants number. It might indicate that some starting variants present common biomechanical advantages, which should be analyzed in detail. The starting variants most frequently used by male semi-finalists and finalists at 50, 100 and 200 m backstroke were the feet partially emerged and hands grasping on the highest horizontal (Figure 1, Panel e) and vertical handgrips (Figure 1, Panel f). The 50 and 200 m backstroke swimmers rather performed the variant with feet partially emerged and hands grasping on the highest horizontal handgrip, while 100 m swimmers adopted similar feet positioning, but with the hands vertically positioned. These findings highlight the need of further investigation to understand the possible mechanical advantages that starting variants performed with feet partially above the water level might generate over the feet entirely immerged or emerged. In addition, since Miller et al. (1984) have recommended swimmers to use similar starting variants at short and middle distance events, it might be speculated that elite backstrokers are able to perform with excellence the backstroke start with feet parallel and partially above the water level independently of the highest horizontal or vertical handgrip.

Considering the same classifications, female swimmers participants of 50, 100 and 200 m backstroke events commonly used similar starting variants as males, particularly the feet parallel and partially emerged and hands grasping on the highest horizontal and vertical handgrips. These findings suggest that elite swimmers have prioritized less body water contact during the setting positioning, with less water resistance needed to be moved through the push off the wall (de

Jesus, et al., 2011a; Maglischo, 2003). As also observed for male swimmers, females used different handgrips positioning depending on the distance. At 50 m backstroke swimmers adopted the hands positioned vertically, while at 100 and 200 m events, females used the hands positioned at the highest horizontal handgrips. According to Miller et al. (1984) swimmers participants at shorter distances may use a starting variant, which allows them to remain in the air after take-off for longer than those in longer events. Despite researchers have provided important findings about the influence of different lower limbs positioning at ventral (e.g. Thanopoulos, et al., 2012; Theut & Jensen, 2006) and dorsal (de Jesus, et al., 2011a, 2011b, 2013; Stratten, 1970) starts, this study highlights the need for further analysis regarding the role played by upper limbs at backstroke start, since it may represent an advantage of hundredths of a second at final race time.

Conclusion

This study is a first step to convey the implications of the current FINA backstroke starting rules combined to the recent starting block configuration on the backstroke starting technique. Considering genders, competitions and classifications, seven out of twelve possible different starting variants were observed. The most common variants performed by male and female backstroke swimmers, independently of the swimming events and classifications were: with feet parallel and partially emerged and hands grasping on the highest horizontal handgrip, and with feet parallel and partially emerged and hands grasping on the vertical handgrip. These two variants collectively accounted for an average 91.3% of all the male and female participants in the study. Notwithstanding the originality and relevance of the current data, it is acknowledged that the camera view obstruction represents a significant limitation, since only images of four lanes in each swimming event were analysed.

Future studies should analyze biomechanically each backstroke starting variant advantages and disadvantages, clarifying how swimmers should perform each one to achieve better performance. It is recommended that coaches and swimmers should spend time in adapting to current FINA rules and new block facilities previously to decision about which backstroke starting variant to be adopted.

Acknowledgments

This research was supported by CAPES (BEX 0761/12-5/2012-2014), Santander Totta Bank (PP-IJUP2011-123) and FCT (EXPL/DTP-DES/2481/2013- FCOMP-01-0124-FEDER-041981).

References

Arellano, R., Sanchez-Molina, J., Navarro, F., & Aymerich, J. (2003). Analysis of 100 m backstroke, breastroke, butterfly and freestyle swimmers at the 2001 European Youth Olympic Days. In J-C Chatard (ed.), IX Biomechanics and Medicine in Swimming: University of Saint Etienne, 249-253.

Cossor, J.M., & Mason, B.R. (2001). Swim start performances at the Sydney 2000 Olympic Games. In J.R. Blackwell & R.H. Sanders (eds.), XIX International Symposium on Biomechanics in Sports: University of San Francisco, 70-73.

de Jesus, K., de Jesus, K., Figueiredo, P., Gonçalves, P., Pereira, S., Vilas-Boas, J.P., & Fernandes, R.J. (2011a). Biomechanical analysis of backstroke swimming starts. *Internation Journal of Sports Medicine, 32*(7), 546-551.

de Jesus, K., de Jesus, K., Figueiredo, P., Gonçalves, P., Pereira, S. M., Vilas-Boas, J.P., Fernandes, R.(2011b). Electromyographic analysis of two different feet positions in backstroke start. In J.P. Vilas-Boas, L. Machado, W. Kim, A.P. Veloso, F. Alves, R.J. Fernandes, & F. Coinceição (eds.), XXIX International Symposium on Biomechanics in Sports: University of Porto, 191-194.

de Jesus, K., de Jesus, K., Figueiredo, P., Gonçalves, P., Pereira, S., Vilas-Boas, J.P., & Fernandes, R.J. (2013). Backstroke start kinematic and kinetic changes due to different feet positioning. *Journal of Sports Sciences, 31*(15),1665-1675.

Federation Internationale de Natation (FINA; 2013). Swimming rules and regulations.

Girold, S., Chatard, J., Cossor, J., & Mason, B. (2001). Specific Strategy for the medalists versus finalists and semi-finalists in the men`s 200 m backstroke at the Sydney Olympic Games. In J.R. Blackwell & R.H. Sanders (eds.), XIX International Symposium on Biomechanics in Sports: University of San Francisco, 6-9.

Green, R.C., Cryer, W., Bangerter, B., Lewis, K., & Walker, J. (1987). Comparative analyses of two methods of backstroke starting: conventional and whip. In L. Tsarouchas, J. Terauds, B.A. Gowitzke, & L.E. Holt (eds.), V International Symposium on Biomechanics in Sports. University of Greece, 281-289.

Hanin, Y., Malvela, M., & Hanina, M. (2004). Rapid Correction of Start Technique in an Olympic-level Swimmer: A Case Study Using Old Way/New Way. *Journal of Swimming Research, 16*, 11-17.

Hay, J., & Guimarães, A. (1983). A quantitative look at swimming biomechanics. *Swimming Technique, 20*, 11-17.

Hohmann, A., Fehr, U., Kirsten, R., & Krueger, T. (2008). Biomechanical analysis of the backstroke start technique in swimming. *E-Journal Bewegung und Training, 2*, 28-33.

Ikuta, Y., Mason, B., & Cossor J. (2001). A comparison of Japanese finalists to other finalists in the 100 m swimming races at the Sydney Olympic Games. In J.R. Blackwell, & R.H. Sanders (eds.), XIX International Symposium on Biomechanics in Sports: University of San Francisco, 75-77.

Maglischo, E.W. (2003). Swimming fastest: the essential reference on technique, training, and program design. Champaign, Illinois: Human Kinetics.

Mason, B., Mackintosh, C., & Pease, D. (2012). The development of an analysis system to assist in the correction of inefficiencies in stars and turns for elite competitive swimming. In: Proceedings of the 30th Annual Conference of Biomechanics in Sports.

Miller, J.A., Hay, J.G., & Wilson, B.D. (1984). Starting techniques of elite swimmers. *Journal of Sports Sciences, 2*(3), 213-223.

Nguyen, C., Bradshaw, E.J., Pease, D., & Wilson, C. (2014). Is the starting with the feet out of the water faster in backstroke swimming? *Sports Biomechanics, 13*(2), 154-165..

Seifert, L., Vantorre, J., Lemaitre, F., Chollet, D., Toussaint, H., & Vilas-Boas, J.P. (2010). Different profiles of the aerial start phase in front crawl. *Journal of Strength and Conditioning Research, 24*(2), 507-516.

Stratten, G. (1970). A comparison of three backstroke starts. *Swimming Technique, 7*, 55-60.

Takeda, T., Itoi, O., Takagi, H., & Tsubakimoto, S. (2014). Kinematic analysis of the backstroke start: differences between backstroke specialists and non-specialists. *Journal of Sports Sciences, 32*(7), 635-641.

Thanopoulos, V., Rozi, G., Okicic, T, Dopsaj, M., Jorgic, B., Madic, D., Velickovic, S., Milanovic, Z., Spanou, F., & Batis, E. (2012). Differences in the efficiency between the grab and track starts for both genders in Greek young swimmers. *Journal of Human Kinetics, 32*, 43-51.

Theut, K., & Jensen, R. (2006). A comparison of two backstroke starts. In H. Schwameder, G. Strutzenberger, V. Fastenbauer, S. Lindinger, & E. Muller (eds.), XXIV International Symposium on Biomechanics in Sports: University of Salzburg, 1-5.

Van Der Mars, H. (1989). Observer Reliability: issues and procedures. In P.W. Darst, D.B. Zakrajsek, V.H. Mancini, (eds). Analysing physical education and sport instrucion: Champaign, Illinois: Human Kinetics, 53-79.

Vantorre, J., Seifert, L., Fernandes, R.J., Vilas-Boas, J.P., & Chollet, D. (2010a). Comparison of grab start between elite and trained swimmers*. International Journal of Sports Medicine, 31*(12), 887-893.

Vantorre, J., Seifert, L., Fernandes, R.J., Vilas-Boas, J.P., & Chollet, D. (2010b). Kinematical profiling of the front crawl start. *International Journal of Sports Medicine, 31*,16-21.

Vilas-Boas, J.P., & Fernandes, R.J. (2003). Swimming starts and turns: determinant factors of swimming performance In P. Pelayo (ed.), Actes des 3èmes journées spécialisées de natation, 84-95.

Wilson, B., & Howard, A. (1983). The use of cluster analysis in movement description and classification of the backstroke swim start. In H. Matsui, & K. Kobayashi (eds.), VIII-B Biomechanics: Human Kinetics, 1223-1230.

Chapter 4

Design and validation of a 3D-6DoF instrumented swimming starting block for backstroke start external kinetics assessment.

Karla de Jesus[1], Luis Mourão[1,2], Hélio Roesler[3], Kelly de Jesus[1], Ricardo Fernandes[1,4], Mário A. P. Vaz[4,5,], Nuno Viriato[5], João Paulo Vilas-Boas[1,4].

[1]Centre of Research, Education, Innovation and Intervention in Sport, Faculty of Sport, University of Porto, Porto, Portugal

[2] Superior School of Industrial and Management Studies, Polytechnic Institute of Porto, Vila Conde, Portugal, Vila do Conde, Portugal.

[3] Centre of Physical Education, Physiotherapy and Sports, Aquatic Biomechanics Research Laboratory, University of the State of Santa Catarina, Florianópolis, Santa Catarina, Brazil

[4] Porto Biomechanics Laboratory, University of Porto, Porto, Portugal

[5] Institute of Mechanical Engineering and Industrial Management, Faculty of Engineering, University of Porto

Unsubmitted for publication, under patent request (PPP 108229).

Abstract

The backstroke start technique has evolved due to swimming rules and starting block configuration changes. To know such effects on performance, instrumented starting block updating is needed. This study described the development and validation of an instrumented starting block for tridimensional (3D-6DoF) backstroke start external kinetic analysis. Four force plates, a starting block, an underwater structure and one pair of handgrips and other of wedges were designed according to the Fédération Internationale de Natation rules, numerically simulated, manufactured and validated. Two force plates were laterally positioned on the starting block, and the two other were fixed vertically on the underwater structure. The handgrips pair were positioned each over each lateral force plate top, and the wedge pair was fixed each on each underwater force plate top. The force plates were instrumented with 24 strain gauges each connected in full Wheatstone bridges. A custom-designed software was created to acquire, plot and save strain readings from each force plate. Static and dynamic calibration revealed linearity and non-meaningfully cross talk. Experimental laboratory and ecological tests indicated similarity between force-time curves. The instrumented starting block showed reliability and accuracy for backstroke kinetic measurements and could be applied for other analysis proposed, as swimming turns and resistive drag.

Key words: Sports engineering, biomechanics, swimming start technique, dorsal starts, start variants.

Introduction

Swimming competitive performance has been assessed by the sum of starting, stroking and turning times (Guimarães & Hay, 1985). The start component is the fastest part of the swimming race and is usually defined from the auditory signal until the swimmers' vertex passes a point 15 m into the pool (Slawson et al., 2013). Three primary interdependent phases contribute towards total start time, namely wall/block, flight and underwater (de Jesus et al., 2014a; Vantorre et al., 2014), being actions performed during the two latter dependents upon preceding block/wall actions (Thow et al., 2012). Nearly all the small temporal differences in the short distance events might be explained by the starting efficiency (Vantorre et al., 2014) and proficient starters can be 0.5 s faster than their poorer counterparts (Mason et al., 2012). In fact, other authors have noticed that differences between individual 15 m performances of international level swimmers might achieve 0.30 s (cf. Seifert et al., 2010).

In backstroke events, unlike other swimming techniques, swimmer's starting position is in water. In accordance with the Fédération Internationale de Natation (FINA) from ~1960s to 2005 backstroke swimmers should grasp the handgrips and place their feet on the wall entirely immersed. Using the pool gutter was not allowed. From ~1960s until 1990s, FINA rules were adapted by the National Collegiate Athletic Association (NCAA) to allow swimmers to position their feet over the wall gutter (de Jesus et al., 2014a, b). By the beginning of 1990s, the NCAA used backstroke start rules similar to FINA. From mid-2005 until now, FINA established that swimmers must position their hands on starting grips and their feet totally or partially immersed, or entirely emerged without the gutter use (SW 6.1). By the end of 2008, FINA authorised a starting block with different handgrips, allowing backstrokers to perform different variants by combining upper and lower limbs positioning. In mid-2013 a new feet support was approved to mask friction force and maximize vertical force component during backstroke start performance (FR 2.10).

There is a growing research concern about the backstroke start technique performed in current competitions (de Jesus et al., 2014a) and part of this rise in interest may be related to the on going modifications in FINA rules (de Jesus et al., 2014b; Vantorre et al., 2014). However, most of the backstroke start studies are either out-dated or limited as current rules and starting block configurations have not been considered (de Jesus et al., 2014 a, b). Moreover, measuring detailed external kinetics depends upon proper instrumentation; limiting most of backstroke start researches to kinematics assessment (e.g. Takeda et al., 2014). External forces explain how starting movements are generated; however they have been predominantly measured at ventral starts (e.g. Tor et al., 2015). In fact, researchers have instrumented swimming start blocks for ventral technique analysis since 70s (Elliot & Sinclair's) using strain gauges or piezoelectric sensors (Mourão et al., 2014).

In backstroke start, few research groups have instrumented starting blocks and pool wall for bi-dimensional (2D) or tri-dimensional (3D) upper (e.g. de Jesus et al., 2011) and/or lower limb (e.g. Nguyen et al., 2014) force assessments. Hohmann et al. (2008) and Nguyen et al. (2014) used a 3D commercial piezoelectric force plate to measure the added lower limbs force profile, while Tor et al. (2015) presented the same sensors in a starting block for upper limbs dynamometry. De Jesus et al. (2011, 2013) instrumented the starting block handgrip and the pool wall with uniaxial strain gauge load cells. To date, beyond disregarding about the current backstroke start FINA facility rules (FR 2.7 and 2.10), none research has concerned eventual asymmetries by implementing separated right and left body side analysis. This study aimed to describe the development and validation of a new-instrumented starting block composed by four force plates able to measure forces and moments at six degrees of freedom of backstroke start movement in three-dimensional space (3D-6DoF) based on current FINA rules.

Material and Methods

Tridimensional (3D) geometric computer aided design

The force plates, starting block, underwater structure and handgrips were 3D designed using a solid modelling computer aided design software (SolidWorks 2012, Dassault Systèmes, SOLIDWORKS Corp., USA). Each force plate and handgrip was designed to achieve proper sensibility with as high rigidity as possible. Starting block project prioritize low deformation to support force plates and handgrips, and an underwater structure was designed to support overall force plates, handgrips and starting block. In addition, force plates, starting block, underwater structure and handgrips dimension was conditioned to comply FINA rules (FR 2.7). The geometric design evolution of each component is depicted below.

Force Plates

Two geminate force plates were projected to be laterally fixed on a starting block, and two other, also geminated, were projected to be fixed vertically on an underwater structure. Based on previous experiments conducted with a cylindrical geometry some conclusions were taken allowing next force plate improvements (Mourão et al., 2015a). It was chosen Roesler's (1997) design for waterproof force plates, which should bear 8000 N in vertical load for independent use in other dynamometric analyses (Roesler et al., 1997). According to Mourão et al. (2015a), Roesler's (1997) topology allows most accurate centre of pressure determination and direct 3D forces and moments measurement. Each force plate core was designed to be manufactured in galvanized steel and is essentially composed by two vertical and two horizontal beams and two lateral boxes. The beams, as oppose to the ring or pylon, can acquire the applied load with better accuracy and precision and can better capture minute changes in the strain throughout the top plate, not just at the corners (Wright, 2011).

The force plate core dimensions were 280 mm x 230 mm and 540 mm x 280 mm, for upper and lower limb force measurements, respectively. Top and bottom

above and below water force plates were projected in duralumin to reduce weight and presented 300 mm x 250 mm and 600 mm x 300 mm, respectively. Minimizing weight and maintaining structural strength is important for a couple of reasons (Wright, 2011): (i) practicality of the user and that is to make physical transportation of the force plate easier; (ii) minimizing the weight to ensure accurate readings, especially when a very small force is being applied to the plate; (iii) to distinguish the very small load from the internal stresses to convey large enough strain change to be accurately measured. In Figure 1, it is presented the final version of the upper (Figure 1a) and lower (Figure 1b) limb force plate core and top.

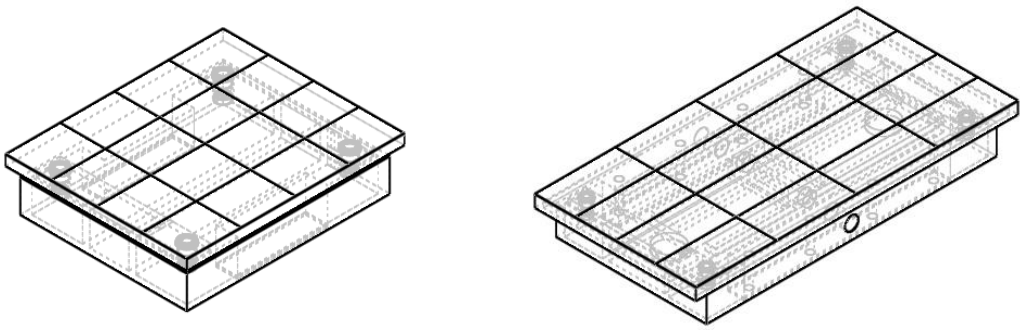

a) b)

Figure 1. Force plates core and top. a) Upper limb measurements. b) Lower limb measurements.

The mounting apparatus has a crucial role in providing measurements accuracy and reliability. The force plate top and core were separated using commercial bushings (cf. Roesler, 1997). Figure 2 depicts the upper (Figure 2a) and lower limbs (Figure 2b) force plates core and mounting apparatuswere performed in a 25 m indoor and heated (27ºC) swimming pool.

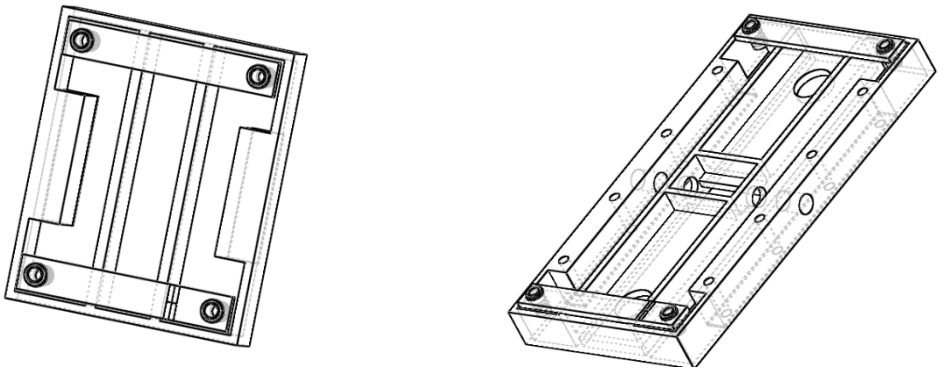

a) b)

Figure 2. Force plate core and mounting apparatus. a) Upper limb measurements. b) Lower limb measurements.

Starting block, underwater structure and handgrips design

Two starting block projects were made previous to the final prototype: (i) a bulky and solid structure (Figure 3a) and (ii) a lattice block with a declination support (Figure 3b). These projects were replaced by a lattice galvanized steel structure with zero inclination (Figure 3c) due to excessive weight and reduced stability, showed by the 1st and 2nd structures, respectively.

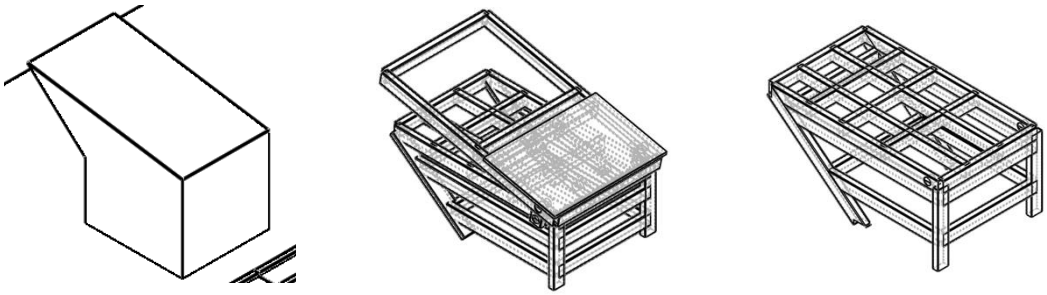

a) b) c)

Figure 3. Starting block design evolution. a) Bulky and solid starting block. b) Lattice starting block with a declination angle. c) Lattice structure with zero inclination.

The starting block was fixed over an underwater structure, which would be attached vertically to the swimming pool wall by front and rear edges. A previous underwater structure used by de Jesus et al. (2011, 2013) for backstroke start kinetics was adopted as design for the project and Figure 4 displays respective front (Figure 4a) and back view (Figure 4b).

a) b)

Figure 4. Underwater structure used by de Jesus et al. (2011; 2013) to fix one force plate, frontal (a) and posterior view (b).

First underwater structure projected was very similar to de Jesus et al. (2013) design. However, it was projected to support two independent force plates (Figure 5a). The underwater structure evolved from a heavier (Figure 5b) to a lattice (Figure 5c) form. The final underwater structure was slighter and embodied holes (100 mm distance between them) for both force plates positioning at different heights regarding the surface level. The underwater structure contemplated a flat rectangular surface for swimming turn analysis with a hollow area for underwater force plates embedding (Figure 5d), as previously used in turn analysis (Araujo et al., 2010).

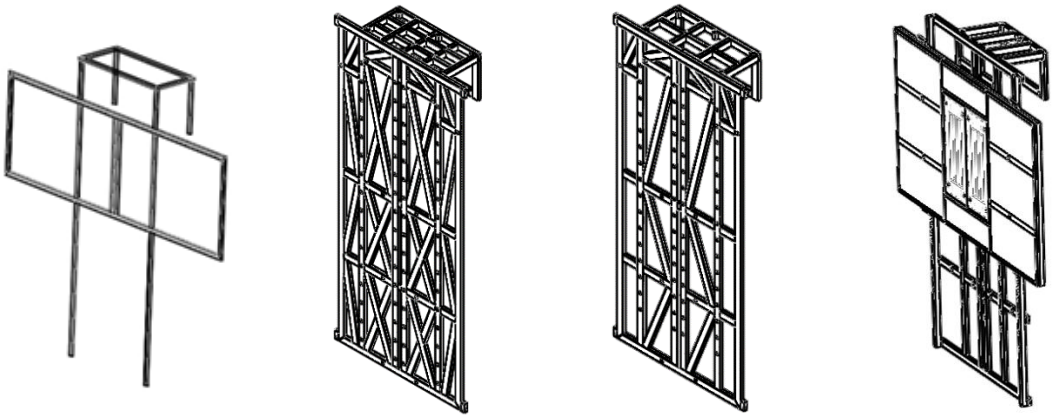

a) b) c) d)

Figure 5. Underwater structure design evolution. a) First project. b) Second project. c) Third project. d) Final project with false starting pool wall.

The handgrips were projected to be independent and framed in galvanized steel, being the 1st design very versatile to be easily used in dorsal and ventral start

technique analysis (Figure 6a). However this first design showed a handgrip positioning dependency on measured strain signals, which did not allow real training and competitive swimmers' movement. In fact, strain gauges would be bonded in the handgrip pipes, which would oblige swimmers to position their hands in a fixed place to allow comparisons. This limitation was solved in the next projects that proposed to fix the handgrips on each lateral force plate top. With this project, forces and moment of force could be measured and handgrips positioning could be found. The 1st handgrip project design considering this handgrip positioning limitation was based on a simple and out-dated handgrip version (Figure 6b), and updated for two horizontal (i.e. highest and lowest, 0.43 and 0.56 m above water surface, respectively) and vertical (Figure 6c), following OSB11 configurations. The final prototype received fine adjustments due to the existent pipe profile (Figure 6d).

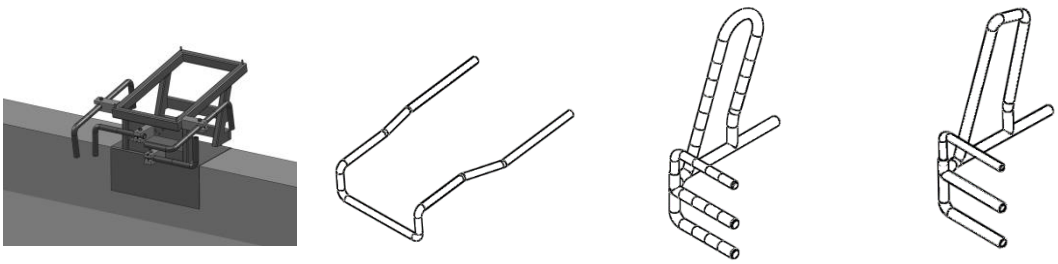

a) b) c) d)

Figure 6. Handgrips design evolution. a) First project. b) Second project. c) Third project. d) Last project.

Finite element analysis

Finite element method is a computer-based technique in which structure is broken down into many small simple blocks or elements and their respective behaviour is assessed by computer from solutions and stress and deflection of all structure parts can be calculated (Pierrisnard et al., 2002). Static structural simulations were conducted using modelling software for finite element analysis Ansys v.12.1 (ANSYS Inc., USA) enabling predictions about how force plates, starting block, underwater structure and handgrips would strain under different conditions. Dynamic simulations were applied to verify resonance frequency, equivalent stress, equivalent strain and deformations. Based on Roesler's (1997)

geometry and sensor location definition, 8000 N load was vertically and anterior-posteriorly applied to confirm the previous determined sensors location. This load was simulated due to the independent force plate use in other sports that depict increased ground reaction forces (e.g. jumping). Static and dynamic force plate simulations were performed with core, top and mounting apparatus (i.e. polyethylene bushing and screw). Simulations with the starting block and handgrips were conducted with 2500 N (centrally located) and 2000 N load (vertically and anterior-posteriorly in the three most common used handgrip positioning, cf. de Jesus et al., 2014b), respectively. The underwater structure with respective force plates vertically mounted was simulated with the standard sea level Earth gravity (i.e. 9.80 m/s2) and values of total deformation, equivalent stress and equivalent elastic strain were obtained. The most refined mesh for force plates, starting block, underwater structure and handgrips simulations was composed of pyramids and cobbled with 1 mm length and 39197 nodes and 12431 elements, 76344 nodes and 15724 elements, 273837 nodes and 107653 elements, 46372 nodes and 17459 elements, respectively.

Strain gauges bonding, electric and electronic circuit

Strain gauges were chosen as force sensors due to short budget and previous research group background, reported in Mourão et al. (2015a). Following structures design, numerical simulations and manufacturing, each force plate was instrumented with 24 waterproof strain gauges (Kyowa, Electronic Instruments, KFW-5-120-C1-5M2B, Japan), arranged in six independent full Wheatstone bridges to minimize temperature effects. All strain gauges were bonded internally to each force plate core and positioning are depicted in Figure 7 with different views (panels a to d).

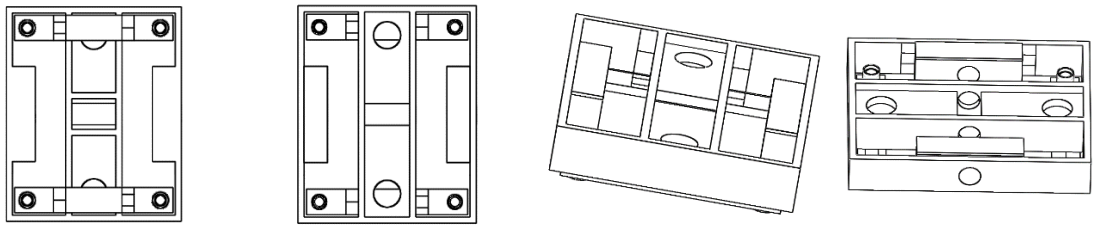

a) b) c) d)

Figure 7. Strain gauge positioning. a) Vertical load up view. b) Vertical load down view. c) Anterior-posterior load view. d) Lateral load view.

After bonded, each strain gauge received an additional protection of two-part polybutadiene resin encapsulated designed for re-enterable splice protection (Scotchcast TM re-enterable electrical insulation resin 2123, 3M TM, USA), which minimized chlorine wear. Each strain gauge wire was brazed in a full Wheatstone bridge configuration (six in total for each force plate, Figure 8a), which was protected with silicone. Each full Wheatstone bridge was connected to a shielded unfiled cable and provided data from each variable of interest (i.e. horizontal, vertical and lateral forces and moments) (Figure 8b). The six-shielded unfiled cables were connected to an analogue-to-digital converter module for full Wheatstone bridge signals (NI9237 50 kS/s/ch 24 bit-4Channels) and respective chassis (NI CompactDAQ USB-9178 with 8 slots) (Figure 8c) through RJ50 connectivity, which interface with the PC. National Instruments Corporation (NI™, USA) manufactured both devices.

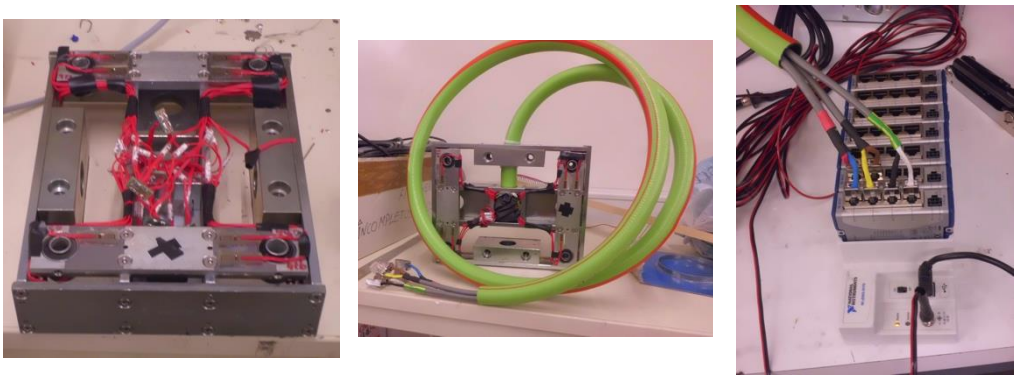

a) b) c)

Figure 8. Force plates electric and electronic circuit. a) Wheatstone bridges brazed. b) Shielded unfiled cables connected to each Wheatstone bridge. c) Each shielded unfiled cables connected to each analogue-to-digital converter module.

Each strain signal was recorded in 2000 Hz sampling rate and a custom-designed data processing software (executable file) was created in LabView 2013 (SP1, NI™, USA) to acquire, plot and save the strain readings from each force plate. The software was programmed to record data in a total of eight seconds, being four seconds before and after the trigger signal, respectively. It was possible to observe each force and moment of force curve profile in real data time-acquisition (Figure 9).

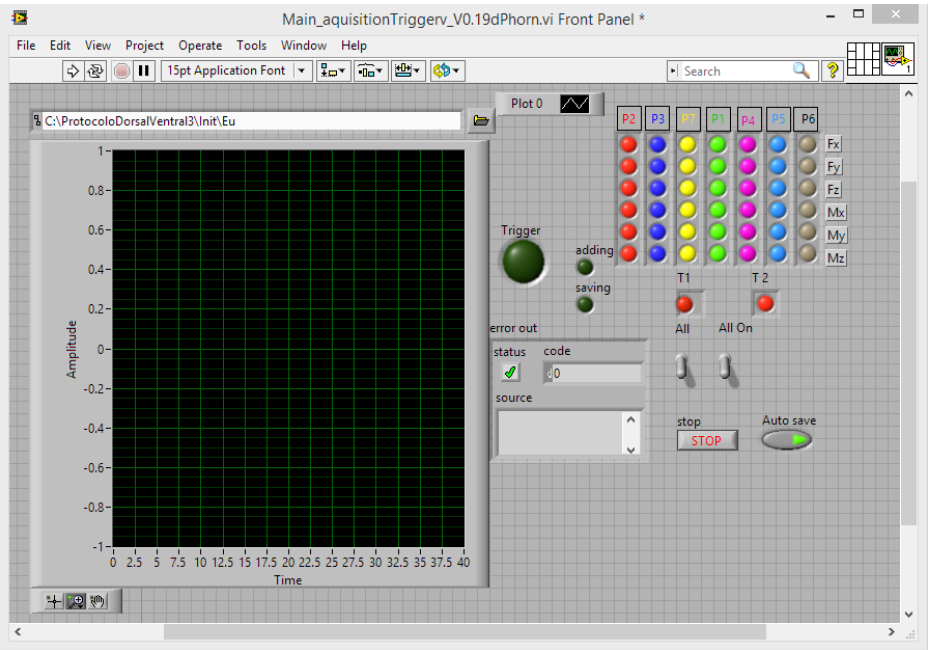

Figure 9. LabView force data acquisition view.

Static calibration

Calibration procedures allow verifying if known applied load is compatible to registered force plate load. The static calibration was performed on dry land before the force plate's proper use in backstroke swimming start condition. Static calibrations of each force plate were conducted in load and unload sequence with 10 kg individual masses (up to 50 kg), which allow correspondences between strain and applied load (Cedraro et al., 2009). Vertical force component was calibrated with the use of a compressor machine that laid the knowing load on each force plate top centre (Figure 10a). For anterior-posterior (Figure 10b) and lateral axis (Figure 10c) force calibration, force plates were vertically fixed on the

wall and load (laid on a plate) was applied on each centre of interest through a stainless steel cable connection. The stainless steel cables were fixed through holes made on the lateral of each force plate top (three per edge). The forces were calibrated using the central holes and moments the lateral ones.

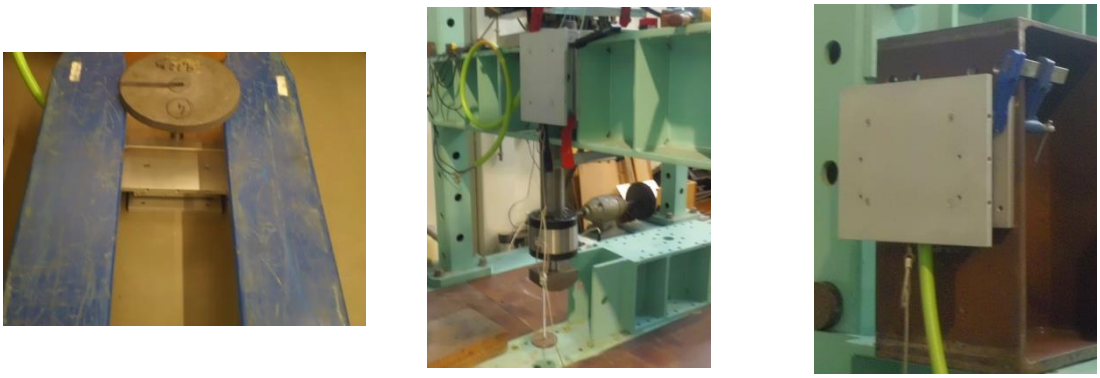

a) b) c)

Figure 10. Force plates static calibration. a) Vertical force. b) Anterior-posterior force. c) Lateral force.

Laboratory experimental validation

An experimental validation was completed comparing the results of the theoretical free fall rigid body force pattern (Mourão et al., 2015b) and the registered strain signal pattern generated by the experimental free fall. Inertia moment of the rigid body has to be assessed previously by knowledge of mass distribution and allocating its centre of mass, as well as, centre of mass to centre of pressure distance (Mourão et al., 2015b). This assessment implies the exclusive geometrical dependency of moment of inertia obviating the use of any force platform except for gravity acceleration knowledge.

Ecological experimental validation

Dynamometric central for backstroke start measurements (i.e. four force plates, starting block, underwater structure and handgrips) is depicted in front (Figure 11a) and lateral view (Figure 11b). The force plates were tested in swimming pool for real data acquisitions, which were then qualitatively analysed. Upper limbs horizontal force was validated with data previously presented by de Jesus et al. (2011, 2013) using a uniaxial strain gauge load cell (Globus Ergo Meter, Globus,

Italy) fixed on the handgrips. Lower limbs horizontal force was validated with data presented by Hohmann et al. (2008), Nguyen et al. (2014) and de Jesus et al. (2013) when using piezoelectric and strain gauge force plates, respectively.

a) b)

Figure 11. Manufactured and instrumented starting block mounted in the swimming pool for backstroke start dynamometric measurements. a) Front view. b) Lateral view.

Results and discussion

Simulations

Table 1 shows force plates strain in vertical, anterior-posterior and lateral axes (8000 N centred) and resonance frequency from the 1st to the final prototype, evidencing project designs that undergone most significant structural changes. According to Roesler (1997) strain values should be between 100 and 500 με, which were obtained in the current project for both force plates.

Table 1. Anterior-posterior and vertical strain and respective resonance frequency in each force plate from 1st project to final prototype.

Project evolution	Static and dynamic simulations	Upper limbs	Lower limbs
1st	Anterior-posterior (με)	323.0	470.0
	Vertical (με)	464.0	489.0
	Resonance frequency (Hz)	235.7	153.0
2nd	Anterior-posterior (με)	397.8	329.0
	Vertical (με)	528.1	578.0
	Resonance frequency (Hz)	229.7	192.0
3rd	Anterior-posterior (με)	388.0	357.0
	Vertical (με)	526.0	521.0
	Resonance frequency (Hz)	300.8	197.0
4th	Anterior-posterior (με)	357.6	383.0
	Vertical (με)	501.0	541.0
	Resonance frequency (Hz)	332.4	200.7
5th	Anterior-posterior (με)	290.0	375.0
	Vertical (με)	545.4	541.0
	Resonance frequency (Hz)	328.6	199.2

The last resonance frequency was obtained in the lateral axis for both force plates pair (Figure 12a and b). Specific force plate application determines proper resonance frequencies and maximal vertical load supported. The waterproof force plate used by Roesler (1997), with 500 mm x 500 mm framed in galvanized steel, obtained 35 Hz resonance frequency, which was considered at that time sufficient for underwater applications due to over damping effects. However, in the current project, the force plates versatility was prioritized and as they can be used independently from the starting block and out of the water, a considerable resonance frequency was required. However, in the current project, the force plates versatility was prioritized and as they can be used independently from the starting block and out of the water, a considerable resonance frequency was required.

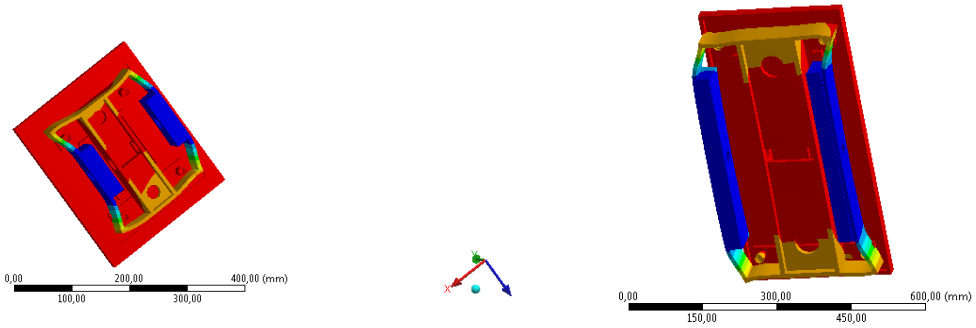

a) b)

Figure 12. Resonance frequency vibration mode. a) Upper limbs. b) Lower limbs.

Table 2 shows results from one example of static simulation from each force plate considering all 24 strain gauges responses, which indicates cross talk. Strain gauge 1 to 12, 13 to 16 and 17 to 24 were positioned for vertical, anterior-posterior and lateral responses, respectively. The upper limbs force plate was simulated with 2000 N load applied vertically on the handgrips and indicating what an expectable relevant anterior-posterior and vertical strain responses. When 8000 N was vertically centred applied at lower limbs force plate only strain gauges responsible for this respective measurement responded (i.e. 1 to 12). According to Roesler (1997) findings, ~ 3% was the maximal interference among loads, when applied 800 N.

Table 2. The 24 strain gauge responses when applied 2000 N and 8000 N vertical load at upper and lower limbs force plate.

Strain gauges	Upper limbs (με)	Lower limbs (με)
1	-4.542	78.129
2	84.66	301.17
3	-23.727	157.09
4	-149.79	108.67
5	200.78	316.68
6	83.29	93.083
7	-40.008	-215.51
8	133.75	-282.81
9	-74.945	-205.9
10	9.5103	-160.94
11	55.697	-188.2
12	-72.427	-238.46
13	-104.08	1.6002
14	93.305	0.51818
15	-177.25	0.61774
16	176.88	0.13888
17	249.58	14.55
18	256.12	-10.409
19	-26.399	-7.7072
20	-45.34	13.114
21	7.0879	13.1
22	33.936	-8.2178
23	-222.66	-10.196
24	-264.68	15.832

Starting block total deformation when applied 2500 N centre vertical load was 0.00030553 m (Figure 13a). The standard sea level Earth gravity (9.8066 m/s2) exposition over the underwater structure and two force plates vertically fixed on

it revealed maximal deformation of 0.00012322 m (Figure 13b). Moreover, using the same standard sea level Earth gravity, underwater structure with force plates showed maximum of 0.00000813 Pa and 0.0000409 m/m, considering equivalent von-Mises stress and equivalent von-Mises elastic strain, respectively, indicating short stress gradients in the underwater structure regions. Anterior–posterior 2000 N load applied on the lowest and highest horizontal and vertical handgrips (Figure 13c) revealed 200, 165 and 115 maximal με. Vertical 2000 N load applied on the lowest and highest horizontal and vertical handgrips revealed 591, 585 and 205 maximal με.

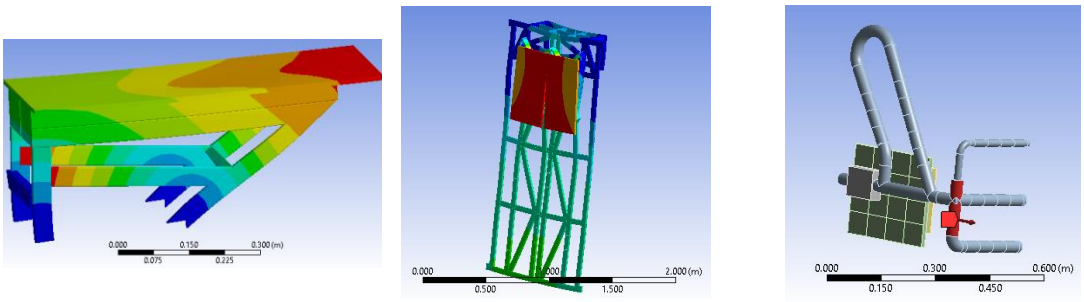

a) b) c)

Figure 13. Static structure simulations. a) Starting block. b) Underwater structure with two force plates. c) Handgrips.

Calibrations

Figure 14 (panel a to h) shows the calibration regression equation for horizontal and lateral axis of each upper and lower limb force plate. Results evidenced the previous noticed linearity (R2 ranging between 0.97 to 0.99) and non-meaningful cross talk when quantified any couple of force plate's output signals (Roesler, 1997). Calibration results for upper limb force plates are depicted considering the forces applied on handgrips positioning previously simulated using finite element analysis. Since only 3D backstroke start forces were measured in the current Thesis, calibration regression equations are presented for 3D forces, without moments.

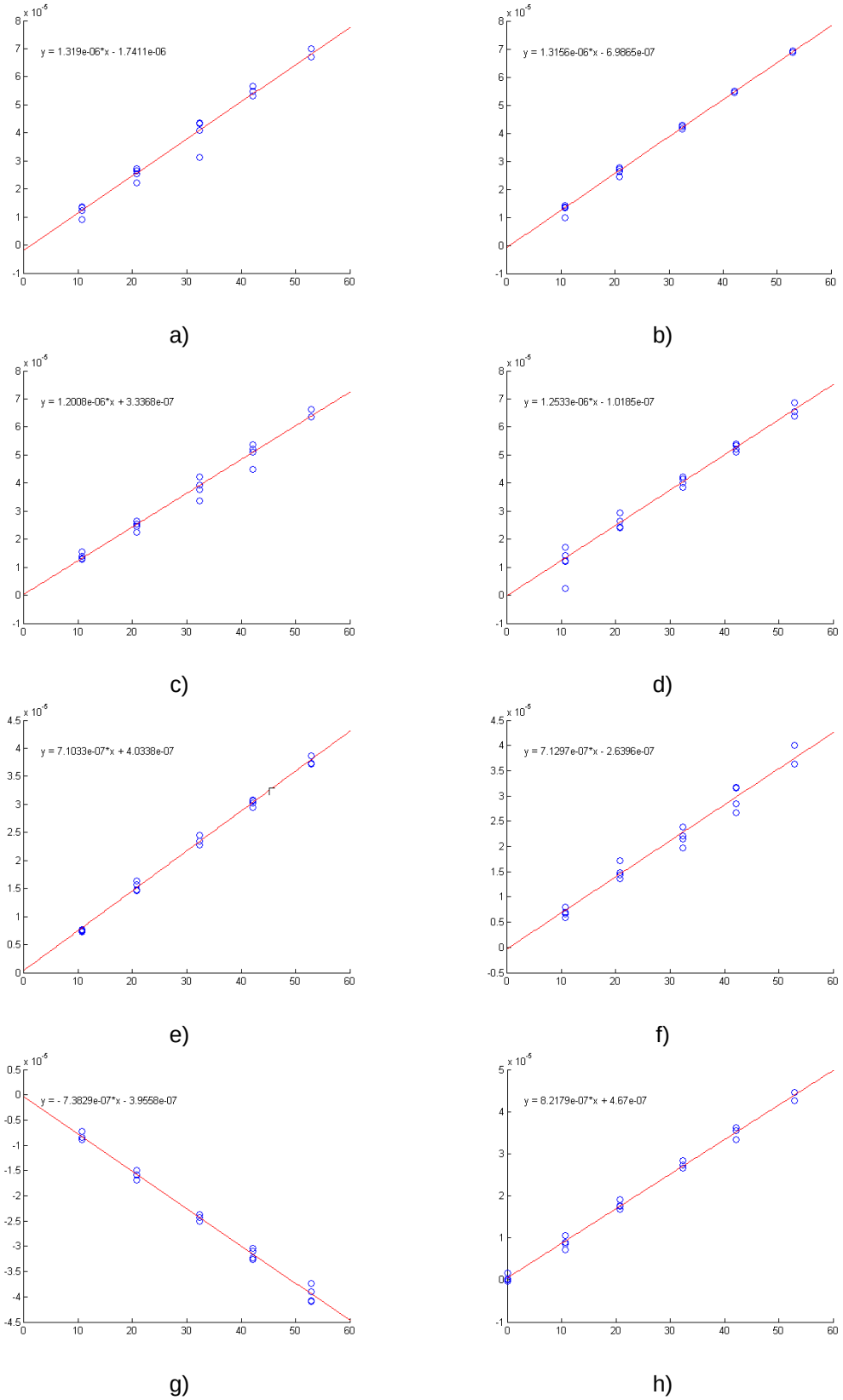

Figure 14. Force plates calibration results. Upper limb force plates horizontal (Panel a and c) and lateral axis (Panel b and d). Lower limb force plates horizontal (Panel e and g) and lateral axis (Panel f and h).

Figure 15 presents the calibration graph for each of the lower limb force plates (Panel a and b).

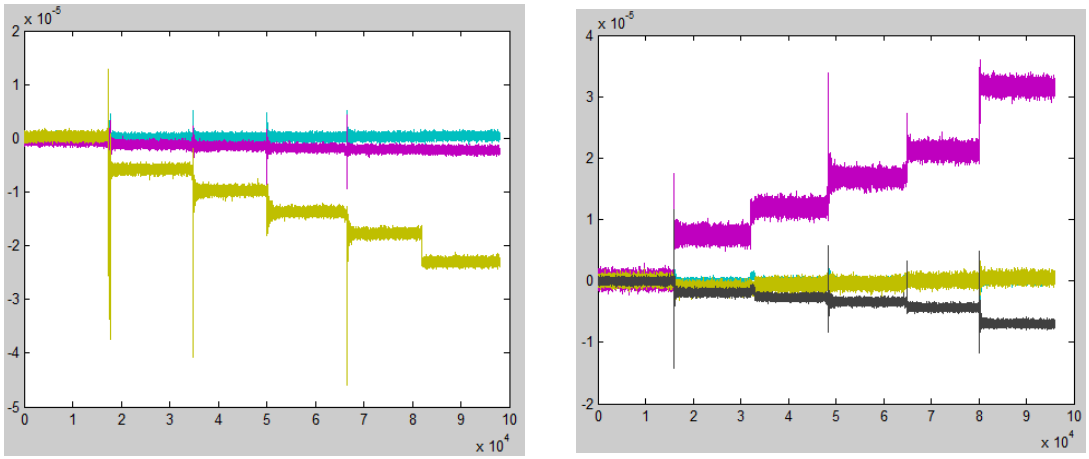

a) b)

Figure 15. Underwater force plate vertical load. Right (a) and left (b).

Due to in-situ installation procedures, usage and aging, force plates accuracy may decrease, which can be propagate to calculated kinetic quantities (Cedraro et al., 2009). Based on these limitations, some research groups developed systems to assess force plate accuracy using ad hoc designed devices (e.g. framework attached pendulum, Fairburn et al., 2000). In the current study, static calibrations were followed by dynamical calibrations performed with a rigid body falling procedure (Mourão et al., 2015b) and revealed homogeneity of static calibration results.

Experimental validation

Simultaneous correlation coefficient between posterior strain filtered signal (moving average 32 samples) and the theoretical generated by previous application in MatLab R2014a (The MathWorks Inc., USA) (Mourão et al., 2015b) showed values of 0.95. Figure 16 illustrates the anterior-posterior and vertical force-time curve profile of the rigid body free falling in one of the underwater force plates.

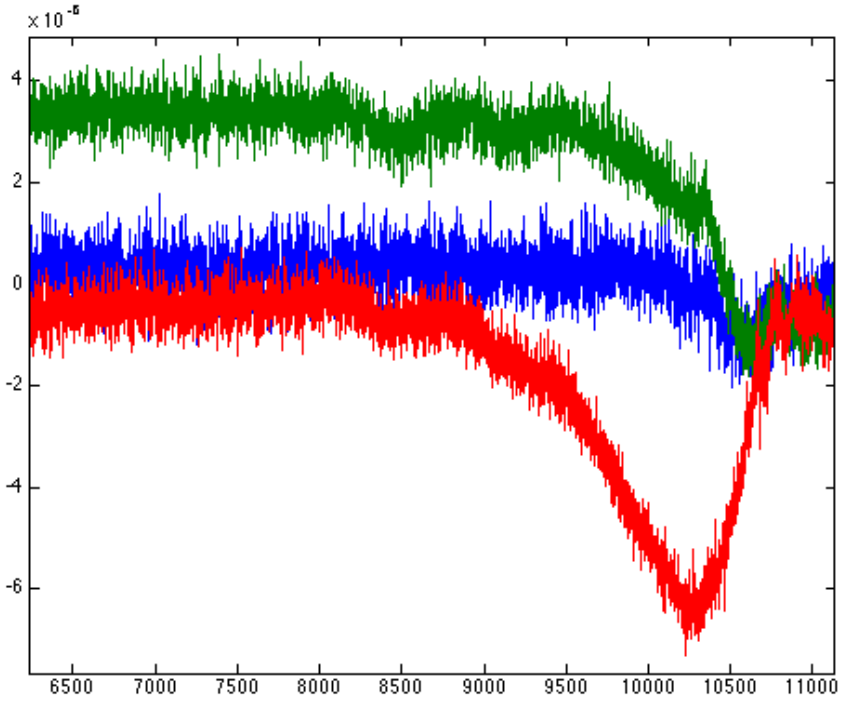

Figure 16. Anterior posterior and vertical force-time curve profile of the rigid body free falling.

Ecological validation

Horizontal upper limbs force time curve obtained during a backstroke start data acquisition (Figure 17a) is qualitatively similar to the horizontal forces obtained by de Jesus et al. (2013; Figure 17b).

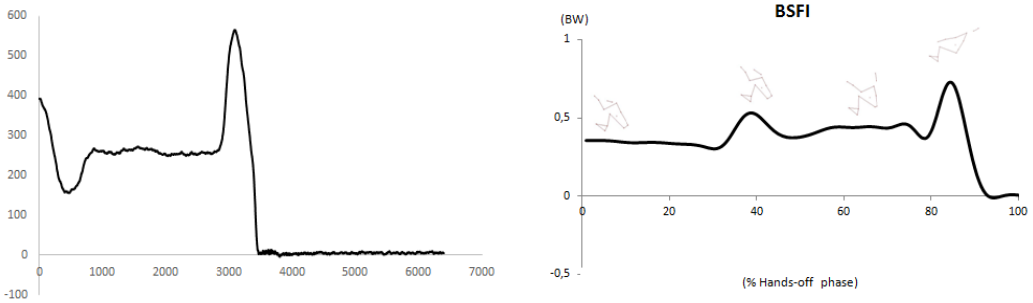

a) b)

Figure 17. Horizontal upper limbs force-time curve. a) de Jesus et al. (2015). b) de Jesus et al. (2013).

Horizontal lower limb force-time curve obtained in the current study (Figure 18a) is qualitatively similar to the horizontal forces obtained by Hohmann et al. (2008) (Figure 18b), de Jesus et al. (2013; Figure 18c) and Nguyen et al. (2014; Figure 18d).

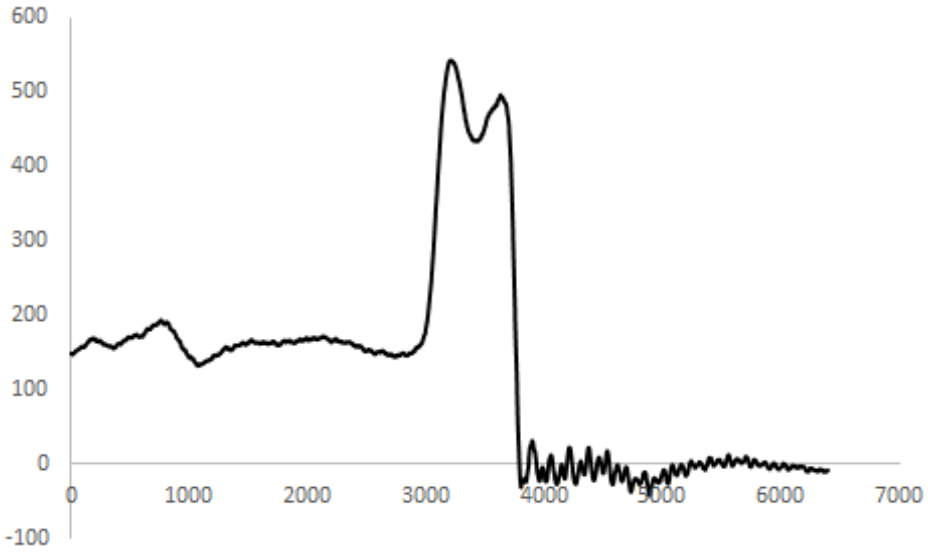

a)

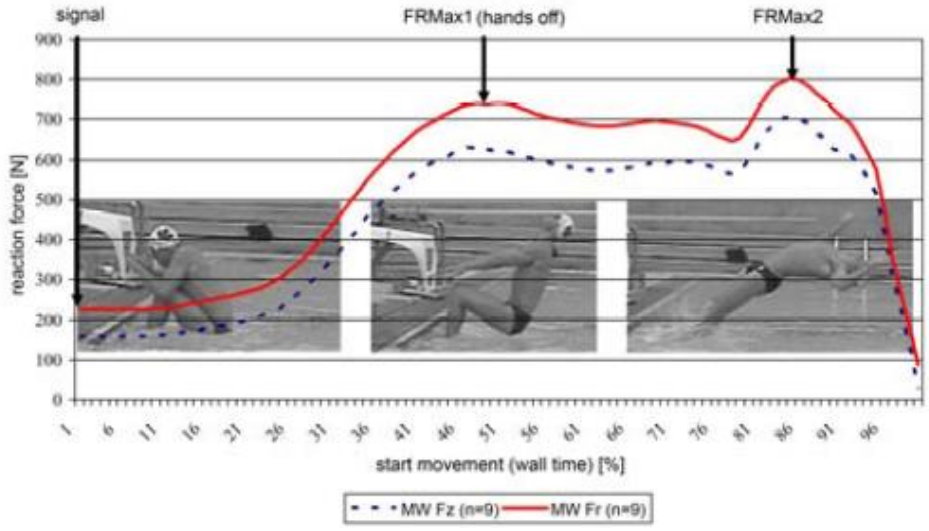

b)

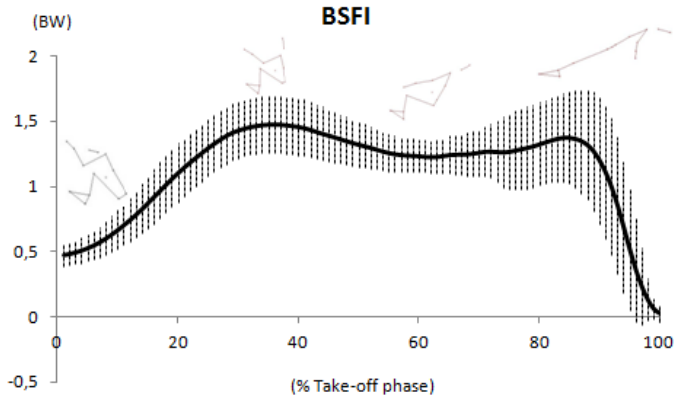

c)

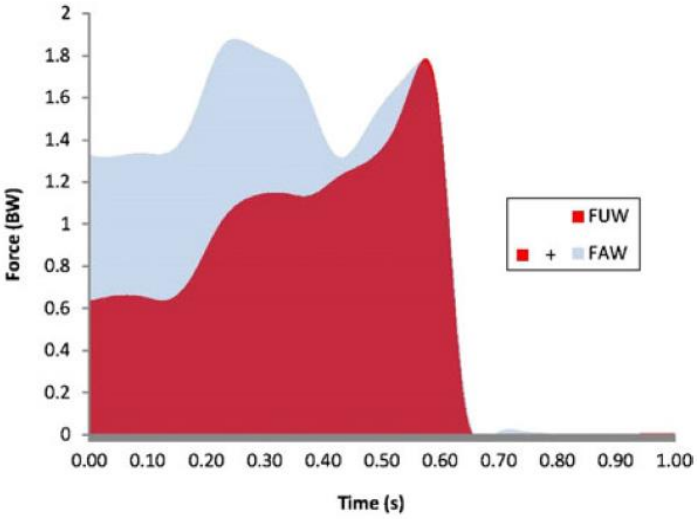

d)

Figure 18. Horizontal lower limbs force-time curve. a) de Jesus et al. (2015). b) Hohmann et al. (2008). c) de Jesus et al. (2013). d) Nguyen et al. (2014). Frmax – maximum resultant force. FAW – feet above water surface. FUW – feet underwater.

The dynamometric central affixation on the starting pool wall was evolving since the first data collection. Affixation procedure evolved from manually efforts (Figure 19a) to pulley system (Figure 19b).

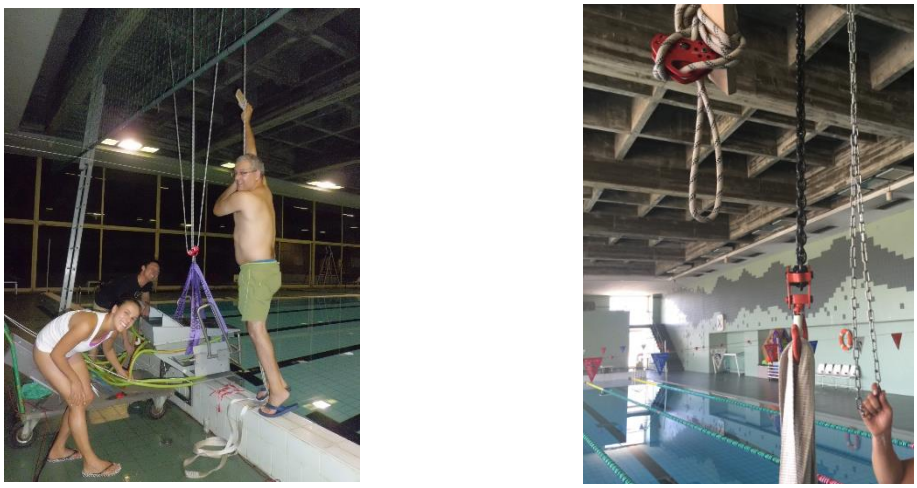

a) b)

Figure 19. Affixation dynamometric central system procedures. a) Manual. b) Pulley.

The dynamometric central showed to be reliable and accurate for backstroke start kinetic analysis considering the current FINA swimming (SW 6.1) and facility (FR 2.7 and 2.10) rules. Furthermore, the device can be adapted to evaluate swimming turns and resistive and wave drag. However, as a prototype, two major limitations should be considered: i) Finite element analysis revealed important data for project manufacturing; however, irregularities in starting pool wall cannot be controlled and could affect measurements and (ii) despite static and dynamic calibration procedures revealed force plates linear responses, an in-situ calibration procedure should be developed to minimize time-consuming process by avoiding withdraw each force plate from the dynamometric central for calibration.

Acknowledgements

This work was supported by the CAPES Foundation under doctoral grant (BEX 0761/12-5/2012-2015) and FCT Foundation under grant (EXPL/DTP-DES/2481/2013- FCOMP-01-0124-FEDER-041981).

References

Araujo, L., Pereira, S., Gatti, R., Freitas, E., Jacomel, G., Roesler, H., & Vilas-Boas, J.P. (2010). Analysis of the lateral push-off in the freestyle flip turn. Journal of Sports Sciences, 28(11), 1175-1181.

Cedraro, A., Capello, A., & Chari, L. (2009). A portable system for in-situ re-calibration of force platforms: experimental validation. Gait & Posture, 29(3) 449-453.

de Jesus, K. , de Jesus, K., Figueiredo, P., Gonçalves, P., Pereira, S. M., Vilas-Boas, J.P., & Fernandes, R.J. (2011). Biomechanical analysis of backstroke swimming starts. International Journal of Sports Medicine, 32(7), 546-551.

de Jesus, K., de Jesus, K., Figueiredo, P., Gonçalves, P., Pereira, S., Vilas-Boas, J.P., & Fernandes, R.J. (2013). Backstroke start kinematic and kinetic changes due to different feet positioning. Journal of Sports Sciences, 31(15), 1665-1675.

de Jesus, K., de Jesus, K., Fernandes, R.J., Vilas-Boas, J.P., & Sanders, R. (2014a). The backstroke swimming start: state of the art. Journal of Human Kinetics, 42, 27-40.

de Jesus, K., de Jesus, K., Medeiros, A., Fernandes, R.J., & Vilas Boas, J.P. (2014b). The bacstroke starting variants performed under the current swimming rules and block configuration. Journal of Swimming Research, 22(1), 1-11

Guimarães, A.C.S., & Hay, J.G. (1985). A mechanical analysis of the grab starting technique in swimming. International Journal of Sport Biomechanics, 1, 25-35.

Fairburn, P.S., Palmer, R., Whybrow, J., Fielden, S., & Jones, S. (2000). A prototype system for testing force platform dynamic performances. Gait & Posture, 12(1), 25-33.

Hohmann, A., Fehr, U., Kirsten, R., & Krueger, T. (2008). Biomechanical analysis of the backstroke start technique in swimming. E-Journal Bewegung und Training, 2, 28-33.

Mourão, L., de Jesus, K, de Jesus, K., Fernandes, R.J., Vaz, M.A.P., Vilas-Boas, J.P. (2014). External kinetics measurements in individual and relay swimming starts: a review. In B. Mason (Ed.), XII International Symposium for Biomechanics and Medicine in Swimming: Australian Institute of Sport. Canberra, Australia, 112-117.

Mourão, L., de Jesus, K., Viriato, N., Fernandes, R.J., Vilas-Boas, J.P., Vaz, M.A. P. (2015a). Preliminary tests for developing an instrumented swimming starting block for starting technique improvements. Unpublished.

Mourão, L., de Jesus, K., Roesler, H., Machado, L.J., Fernandes, R.J., Vilas-Boas, J.P., Vaz, M.A.P. (2015b). Effective swimmer's action during the grab start techniques. Plos One, 10(5), e0123001.

Nguyen, C., Bradshaw, E., Pease, D., & Wilson, C. (2014). Is starting with the feet out of the water faster in backstroke swimming? Sports Biomechanics, 13(1), 1-12.

Pierrisnard, L., Barquins, M., & Daniel C. (2002). Two dental implants designed for immediate loading: a finite element analysis. International Journal of Oral Maxillofac, 17(3), 353-362.

Roesler, H. (1997). Desenvolvimento de plataforma subaquática para medições de forças e momentos nos três eixos coordenados para utilização em biomecânica. PhD Thesis, Post Graduation in Mechanical Engineering, Universidade Federal do Rio Grande do Sul, Porto Alegre.

Seifert, L., Vantorre, J., Lemaitre, F., Chollet, D., Toussaint, H.M., & Vilas-Boas, J.P. (2010). Different profiles of the aerial start phase in front crawl. Journal of Strength and Conditioning Research, 24(2), 507-516.

Slawson, S.E., Conway, P.P., Cossor, J., Chakravorti, N., & West, A.A. (2013). The categorisation of swimming start performance with reference to force generation on the main block and footrest components of the Omega OSB start blocks. Journal of Sports Sciences, 31(5), 468-478.

Takeda, T., Itoi, O., Takagi, H., & Tsubakimoto, S. (2014). Kinematic analysis of the backstroke start: differences between backstroke specialists and non-specialists. Journal of Sports Sciences, 32(7), 635-641.

Thow, J.L., Naemi, R., & Sanders, R.H. (2012). Comparison of modes of feedback on glide performance in swimming. Journal of Sports Sciences, 30(1), 43-52.

Tor, E., Pease, D.L., Ball, & K.A. (2015). The reliability of an instrumented start block analysis system. Journal of Applied Biomechanics, 31(1), 62-67.

Vantorre, J., Chollet, D., & Seifert, L. (2014). Biomechanical analysis of the swim-start: a review. Journal of Sports Science and Medicine, 13(2), 223-231.
Wright, D.A. (2011). Development of a waterproof force plate for pool applications. Ohio State University. Master Thesis.

Chapter 5

Effects of diverse feet and hands positioning on backstroke start performance.

Karla de Jesus[1], Kelly de Jesus[1], J. Arturo Abraldes[2], Luis Mourão[1,3], Márcio B. Santos[1,4], Alexandre I. A. Medeiros[1,5], Pedro Gonçalves[1], Phornpot Chainok[1,6], Ricardo J. Fernandes[1,4], Mário A. P. Vaz [4,7], João Paulo Vilas-Boas[1,4].

[1] Centre of Research, Education, Innovation and Intervention in Sport, Faculty of Sport, University of Porto, Porto, Portugal.

[2] Department of Physical Activity and Sport, Faculty of Sports Sciences. University of Murcia. Murcia, Spain.

[3] Superior School of Industrial Studies and Management, Porto Polytechnic Institute, Vila do Conde, Portugal.

[4] Porto Biomechanics Laboratory, Porto, Portugal.

[5] Department of Physical Education, University of Fortaleza, Fortaleza, Brazil.

[6] Faculty of Sport, Burapha University, Chonburi, Thailand.

[7] Institute of Mechanical Engineering and Industrial Management, Faculty of Engineering, University of Porto, Porto, Portugal.

Submitted for publication on Sports Biomechanics (2015)

Abstract

This study analysed feet and handgrips positioning effects on backstroke start performance. Ten swimmers completed randomly 27 backstroke starts grouped in trials (n=3) of each start variant, changing feet (utterly immersed, partially and utterly emerged) and handgrips positioning (lowest and highest horizontal and vertical). Fifteen cameras recorded kinematics from auditory signal until 15 m. Four force plates collected horizontal and vertical upper and lower limb forces. Standardized mean difference and 95% confidence interval were used. Feet utterly immersed, regardless handgrips positioning, implied 0.16 m shorter vertical centre of mass (CM) set positioning and 0.28, 0.41 and 0.16 (N/BW.s) vertical upper limbs, horizontal and vertical lower limbs impulse (respectively) than feet emerged and hands on highest horizontal and vertical handgrip. Variants with feet partially emerged registered greater and shorter vertical upper limbs impulse than feet utterly immersed and emerged (e.g. vertical handgrip, 0.13 and 0.15 N/BW.s, respectively). Variant with feet utterly emerged and hands on lowest horizontal handgrip depicted shorter horizontal (0.23 and 0.26 m) and vertical CM positioning (0.16 and 0.15 m) at flight than highest horizontal and vertical handgrip, respectively. Despite variant adopted initial biomechanical advantages should be preserved throughout entry and underwater phases for shorter 15 m time.

Keywords: Biomechanics, kinematics, kinetic, swimming, dorsal start performance.

Introduction

In competitive swimming the start phase effectiveness (commonly assessed from the auditory signal until swimmers' vertex passes the 15 m mark) is essential, particularly in shorter events (Elipot et al., 2009; Tor et al., 2015a, 2015b), leading biomechanists to invest in new methods and technologies for detailed kinematic and kinetic analyses (e.g. Mourão et al., 2015). Greater scientific relevance has been given to the ventral start techniques (de Jesus et al., 2014a), which has been noticed in the deterministic models developed through standardized key starting performance indicators (e.g. centre of mass coordinates – CM - at set positioning; e.g. Guimaraes & Hay, 1985).

From 1960s to early 2005, the Fédération Internationale de Natation (FINA) determined that backstrokers should perform the start with hands on the block grips with feet utterly immersed. Performing this start variant is strongly influenced by the peak force before take-off, horizontal lower limbs impulse and also by CM resultant glide velocity (de Jesus et al., 2011; Hohmann et al., 2008). Following the FINA authorization to position feet above water level in mid-2005, many backstrokers are using the start variant with feet utterly emerged (Nguyen et al., 2014). Successful performance of this start variant depends upon shorter CM horizontal set positioning, greater take-off angle and horizontal velocity and CM resultant glide velocity (de Jesus et al., 2011), looking complex if not performed in a proper handgrips height above water level (de Jesus et al., 2013).

From Beijing 2008 Olympic Games, the start block configuration has changed, with swimmers being authorized to use three backstroke start handgrip types (two horizontal and one vertical) combined with different feet positioning (de Jesus et al., 2014b). Therefore, variants with feet partially emerged and hands on highest horizontal and vertical handgrips have been often chosen by elite swimmers regardless the backstroke event (de Jesus et al., 2014b). It seems expectable that swimmers prioritize a set position allowing to lift their body out of water, minimizing water resistance during flight, entry and underwater phases (Nguyen

et al., 2014). Contrarily to ventral starts, where swimmers take off 0.7 m above water level, backstrokers have to perform the start motion close to the water surface, evidencing the importance of choosing proper start variant for less resistance flight and entry phases (Takeda et al., 2014). Higher back arc angle and lesser deceleration during flight and entry phases have been considered more relevant than the generation of a greater lower limbs impulse (de Jesus et al., 2013; Takeda et al., 2014).

The lack of studies analysing biomechanical advantages/disadvantages when using different feet and handgrip positioning combinations for backstroke start has not favoured a start variant for training and competition (Seifert et al., 2010). Despite the set positioning adopted, one could expect that backstrokers would reveal different motor profile organization to achieve similar 15 m start time (Rodacki & Fowler, 2001; Seifert et al., 2010). The current study compared nine backstroke start variants (combining different feet and hands positioning), being assumed that those performed with feet partially or utterly emerged and hands on highest horizontal and vertical handgrips would imply higher CM set positioning, upper and lower limbs impulse, greater take-off and entry angle, longer and higher flight and reduced 15 m backstroke start time.

Methods

Participants

Ten male competitive backstroke swimmers (mean ± SD: age 20.6 ± 6.0 yrs., stature 1.75 ± 0.05 m, body mass 71.63 ± 12.14 kg, training background 12.7 ± 8.02 yrs. and 60.56 ± 2.29 s 100 m backstroke mean performance in 25 m pool representing 80.91 ± 3.09 % of the 100 m backstroke short course World Record) volunteered to participate. The institutional ethics committee approved training intervention and data collection and all experimental procedures corresponded to Declaration of Helsinki requirements. Swimmers and parents

and/or guardians (when subjects were under 18 yrs.) provided written informed consent before the start.

Backstroke start variants

Nine backstroke start variants were determined based on FINA start (SW 6.1) and facility rules (FR 2.7) (Figure 1), combining three different feet (always parallel to each other) and hands positioning: (i) feet utterly immersed and hands on lowest and highest (0.43 and 0.56 m above the water level, respectively) horizontal and vertical handgrips (Figure 1 a, b and c); (ii) feet partially emerged and hands on the positioning described in (i) (Figure 1 d, e and f); and (iii) feet utterly emerged and hands on the above described positioning (Figure 1 g, h and i).

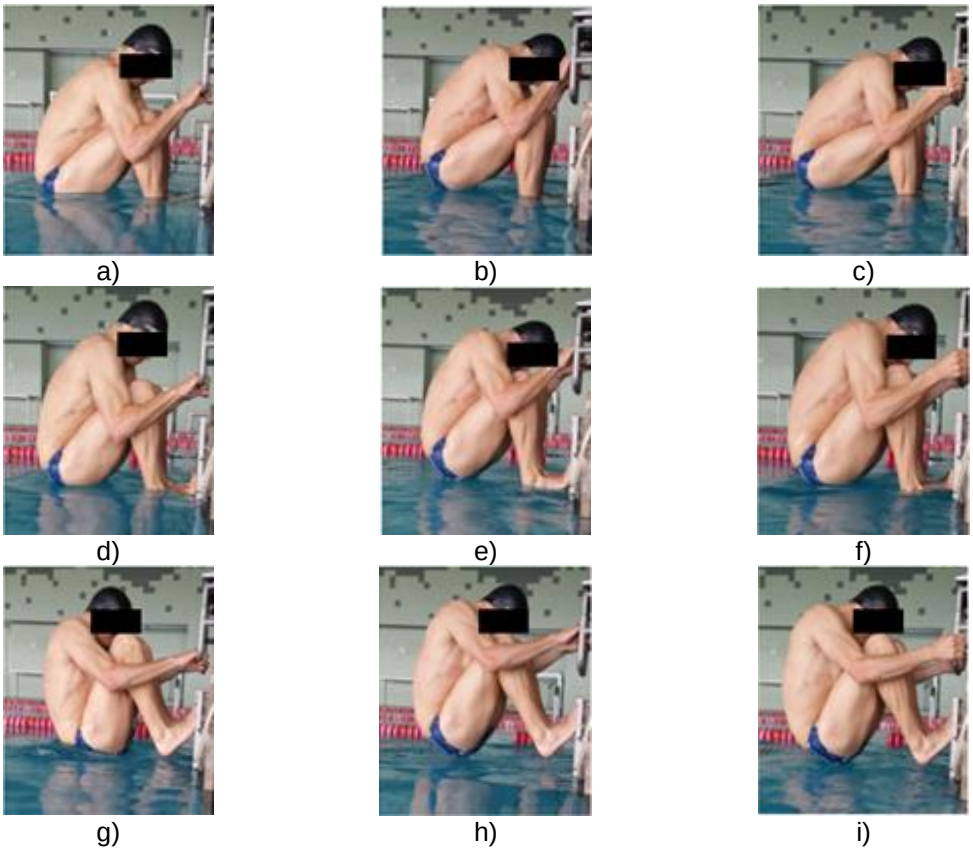

Figure 1. Backstroke start variants: (i) feet utterly immersed and hands on lowest and highest horizontal and vertical handgrips (Figure 1 a, b and c, respectively); (ii) feet partially emerged and hands on the positioning described in (i) (Figure 1 d, e and f, respectively); and (iii) feet utterly emerged and hands on the above described positioning (Figure 1 g, h and I, respectively).

Training protocol

One month backstroke start training was conducted for familiarization with the studied variants, as previously done (Blanksby et al., 2002; Breed & Young, 2003). In each session, swimmers performed randomly three maximal 15 m trials of each variant (2 min resting between trials) on an instrumented starting block, which met OSB11 block specifications (Swiss Timing Ltd., Switzerland) (cf. Tor et al., 2015a, 2015b). To standardize the starting procedure, an auditory buzzer signal similar to the one adopted in official events was used following FINA rules (SW 4.2). After diving, participants crossed maximally the 15 m mark and return to the starting block for the next following repetition. Swimmers were supervised two sessions a week to receive qualitative (i.e. video images) and quantitative (i.e. 15 m time) feedback. Familiarization and subsequent experimental backstroke starting protocol were performed in a 25 m indoor and heated (27ºC) swimming pool.

Testing protocol

Swimmers answered a questionnaire about their training and competitive 100 m backstroke performance background and height and body mass were measured. A warm-up consisting of 600 m front crawl and backstroke and one repetition of each start variant before each of the two testing sessions (2 h rest between each session) took place. Each swimmer performed 13 and 14 maximal 15 m starts (1st and 2nd session, respectively), namely three of each start variant (3 min rest in-between) on the same starting block previously outlined, being the mean values calculated. Starting signals were produced through a device (StartTime IV, Swiss Timing Ltd., Switzerland) complying with FINA rules (SW 4.2), which was instrumented to simultaneously export a light to digital cameras, and a trigger to motion capture (MoCap) system and to force plates, being all synchronized with a trigger box.

Data collection

A three-dimensional (3D) kinematic setup consisting of eight (four surface and four underwater) stationary digital video cameras (HDR CX160E, Sony

Electronics Inc., Japan), operating at 50 Hz sampling frequency and 1/250 s exposure time was used to record starts from the auditory signal to water immersion. Each camera was fixed to a tripod (Hama Star 63, Hama Ltd., UK) at 0.8 m height (surface) and 1.4 m deep (underwater), with underwater cameras being inside a waterproof housing (Sony SPK-HCH, Sony Electronics Inc., Japan) and the angles between adjacent surface and underwater camera axes varying from 70 to 110º (de Jesus et al., 2015; Figueiredo et al., 2012). A ninth stationary and synchronized surface camera fixed on a tripod at 3 m height was positioned perpendicularly to swimmer's start lane. A prism to calibrate starting space (4 m length [horizontal axis, x], 2.5 m height [vertical axis, y] and 2 m width [lateral axis, z]) was used (de Jesus et al., 2015; Psycharakis & McCabe, 2011), and was placed 0.80 m above water level with the horizontal axis aligned towards starting direction. A pair of lights emitting diodes (LED), visible in each camera view, was fixed to this frame.

Simultaneously, another 3D kinematic MoCap setup consisting of six cameras recording at 100 Hz (Oqus, Qualisys AB, Sweden) was implemented to automatically track swimmers' body right side from full immersion until 15 m mark. Cameras were alternatively placed at 0.10 m below water level and at swimming pool bottom (2 m depth) with respective lens targeting to swimmers' trajectory. Each camera was configured to: (i) mask, and cover unwanted area and sunlight reflections, (ii) to adjust exposure delay/flash time and marker threshold (values ranged between 0.0002 to 0.0012 s and 5 and 20, respectively), and (iii) filter and remove background light. Calibration was firstly performed with a static L- frame (positioned 5 m further from the starting wall) to create virtual origin in 3D environment followed by a wand dynamic calibration with two markers fixed with 0.75 m inter-point distance (covering expected performance volume). All camera calibration mean values were achieved with ~ 0.008 m wand length standard deviations, agreeing with previous studies using smaller calibrated volume (e.g. Silvatti et al., 2012). A short data acquisition was performed to determine the water level and orientation relative to the calibration frame origin.

To enable swimmers' tracking in both digital video and MoCap system a complete swimsuit was used (Fastskin, Speedo International Limited, UK) with fixed anatomical landmarks. Twenty-four anatomical markers (16 body segments, cf. Barbosa et al., 2008) were defined for digital cameras (cf. de Leva, 1996): the vertex of the head (using a swim cap), mid-gonion, the right and left of the acromion, lateral epicondyle of humerus, ulnar styloid process of the wrist, 3rd hand distal phalanx, xyphoid, iliac crest, great trochanter of the femur, lateral epicondyle of the femur, lateral malleolus, calcaneus and tip of 1st foot distal phalanx. An additional reflective spherical marker (19 mm diameter) was fixed on swimmers' hip (cf. Nguyen et al., 2014).

The starting block (under patent request: INPI nº 108229) integrates four 3D waterproof force plates (one surface – upper limbs and one underwater pair – lower limbs force measurements (cf. Roesler et al., 2006). Surface force plates (300 Hz resonance frequency) were laterally fixed on each side of a starting block with an independent handgrip fixed on each force plate top. Underwater force plates (200 Hz resonance frequency) were vertically fixed on a starting pool wall support (0.3 m above and below water level). Dynamical calibration followed previous study steps with a rigid body falling (Mourão et al., 2015), revealing homogeneity of static calibrations. The two force plate pairs have a sensitivity of 0.5 N and error < 5%, considered acceptable for accurate and reliable measurements (Roesler et al., 2006). All strain outputs were converted to digital data through an analogue to digital converter via strain gauge input modules NI 9237 connected to a chassis CompactDAQ USB-9172 and Ethernet-9188 National Instruments Corporation, USA (both from National Instruments, NI Corporation, USA). Figure 2 illustrates the instrumented starting block, digital video and MoCap system positioning.

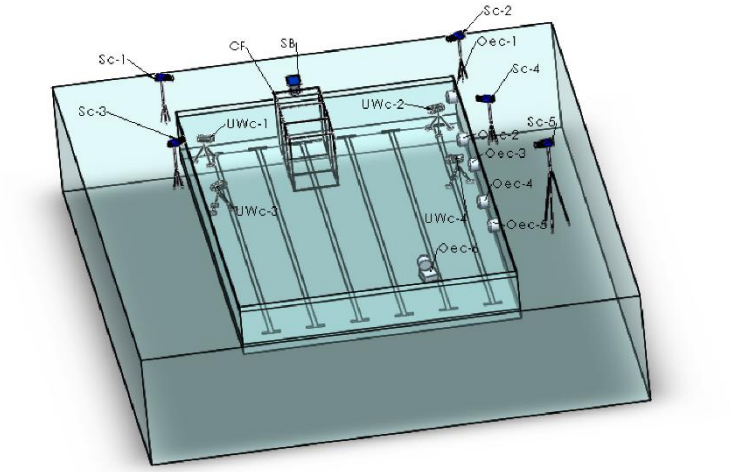

Figure 2. Digital video cameras, MoCap system and start block and respective positioning in the swimming pool. Sc-1 to Sc-5 and UWc-1 to UWc-4, digital surface and underwater cameras, respectively. Oec 1 to Oec-6, opto-electronic cameras. SB, starting block. CF, calibration frame.

Data processing

Surface and underwater video images were digitised independently and manually frame-by-frame by the same operator using Ariel Performance Analysis System (Ariel Dynamics Inc., USA) (Barbosa et al., 2015; de Jesus et al., 2012; Gourgoulis et al., 2008). Digitising accuracy calculation is described in detail by Barbosa et al. (2015) and has revealed unclear differences in-between digitized-re-digitized trials for each variable of interest (with trivial magnitude of thresholds; cf. Hopkins, 2010). Independent digitisation was 3D reconstructed (Direct Linear Transformation algorithm, (Abdel-Aziz & Karara, 1971) with 12 calibration points (four surface, four underwater and four common to both camera view; (de Jesus et al., 2012; Gourgoulis et al., 2008; Puel et al., 2012). Reconstruction accuracy was tested with root mean square error using 12 validation points (de Jesus et al., 2012), which did not serve as control points and were as follows (for the x, y and z axis, respectively): (i) 2.96, 2.84, 2.10 mm representing 0.074, 0.11 and 0.10% of the calibrated dimension for surface view; and (ii) 3.46, 4.80 and 3.01 mm, representing 0.08, 0.19 and 0.15% of the calibrated dimension for underwater view. It was selected a 5 Hz cut-off value for data filtering done according to residual analysis (Barbosa et al., 2015).

Qualisys Track Manager (QTM, Qualisys AB, Sweden) processed hip velocity-time curves and a referential transformation was applied to the original calibration referential to align it with the water level at the starting block, setting this point as the new referential origin to the system. Each individual velocity time-curve was filtered with a fit to 2nd degree curve and subsequently normalized in time from swimmers' hallux water immersion until beginning of upper limbs propulsion. Data processing software was created in LabView2013 (SP1, National Instruments, NI Corporation, USA) to acquire, plot and save the four force plates data in real-time (2000 Hz sampling rate). Two processing routines created in MatLab R2014a (The MathWorks Incorporated, USA) were used to convert strain readings into force values and to filter upper and lower limb force curves (4th order zero-phase digital Butterworth filter with a cut-off 10 Hz frequency). Upper and lower limb right and left force data were summed and normalized to each swimmer's body weight.

Data analysis

Backstroke start variants were divided into five phases (cf. de Jesus et al., 2011; Hohmann et al., 2008): (i) hands-off – between auditory signal and swimmers' hands left handgrips (1st positive horizontal swimmers' hand 3rd distal phalanx coordinate); (ii) take-off – from hands-off until swimmers' feet left wall (1st positive horizontal swimmers' foot 1st distal phalanx coordinate); (iii) flight – from take-off until swimmers' CM immersion (1st negative swimmers' CM vertical coordinate); (iv) entry – from flight ending until swimmers' feet immersion (1st negative swimmers' foot 1st distal phalanx vertical coordinate); and (v) underwater – from full swimmers' immersion until beginning of upper limbs propulsion. Linear and angular kinematic and kinetic parameters are described in Table 1.

Table 1. Linear and angular kinematical and kinetic parameters and their respective definition.

Parameters	Definition
Centre of mass horizontal positioning at auditory signal	Centre of mass horizontal coordinate at 1st frame
Centre of mass vertical positioning at auditory signal	Centre of mass vertical coordinate at 1st frame
Horizontal upper limbs impulse	Upper limbs time integral normalized of horizontal force component from auditory signal until swimmers' hands left handgrips
Vertical upper limbs impulse	Upper limbs time integral normalized of vertical force component from auditory signal until the swimmers' hands left handgrips
Horizontal lower limbs impulse	Lower limbs time integral normalized of horizontal force component from auditory signal until swimmers' feet left the platform
Vertical lower limbs impulse	Lower limbs time integral normalized of vertical force component from auditory signal until swimmers' feet left the platform
Take-off angle	Angle formed by right great trochanter of femur, lateral malleolus and horizontal axis
Centre of mass horizontal positioning at flight	Centre of mass horizontal coordinate at 3rd distal phalanx water contact
Centre of mass vertical positioning at flight	Centre of mass vertical coordinate at 3rd distal phalanx water contact
Entry angle	Angle formed by right acromion, styloid process of wrist and horizontal axis
Intracyclic velocity variation during the underwater phase	Horizontal hip intracyclic velocity variation from full immersion until beginning of upper limbs propulsion (SD / mean)
15 m starting time	Time between auditory signal and swimmers' vertex reached 15 m mark

Statistical analysis

Data are presented as mean and respective standard deviation. Magnitude-based inference and precision of estimation approach was calculated (Hopkins, 2010) to assess practical differences in kinematic and kinetic parameters (dependent variables) between backstroke start variants (independent variable). Differences were assessed via standardized mean differences computed with pooled variance and respective 95% confidence intervals (Cohen, 1988). Magnitude thresholds for difference in a mean were described using the following scale: 0-0.2 trivial, > 0.2-0.6 small, > 0.6-1.2 moderate, > 1.2-2.0 large, and > 2.0 very large (Hopkins, 2010). Effects with 95% confidence intervals overlapping zero and/or the smallest worthwhile change (i.e. 0.2 standardized units) were defined as unclear.

Results

Descriptive analysis

Table 2 depicts the mean and respective standard deviation of the linear and angular kinematic and kinetic parameters calculated for each backstroke start variant.

Table 2. Mean and respective standard deviations of each kinematical and kinetic parameter for each backstroke start variant.

Variables	Starting variants								
	1	2	3	4	5	6	7	8	9
CMssx (m)	0.51±0.03	0.50±0.03	0.49±0.03	0.51±0.03	0.49±0.04	0.49±0.04	0.51±0.04	0.49±0.05	0.49±0.04
CMssy (m)	0.16±0.08	0.21±0.07	0.19±0.08	0.20±0.09	0.26±0.10	0.23±0.10	0.28±0.08	0.35±0.12	0.34±0.15
ULimpx ((N/BW).s)	-0.77±0.18	-0.88±0.22	-0.80±0.11	-0.68±0.14	-0.92±0.22	-0.82±0.17	-0.61±0.12	-0.79±0.23	-0.72±0.16
ULimpy ((N/BW).s)	0.52±0.13	0.52±0.10	0.52±0.11	0.74±0.12	0.64±0.12	0.65±0.12	0.90±0.16	0.81±0.13	0.80±0.17
LLimpx ((N/BW).s)	1.02±0.27	0.94±0.25	0.95±0.26	1.27±0.23	1.17±0.25	1.19±0.24	1.56±0.19	1.38±0.27	1.39±0.29
LLimpy ((N/BW).s)	0.46±0.08	0.44±0.07	0.44±0.07	0.52±0.10	0.52±0.06	0.51±0.05	0.56±0.12	0.61±0.08	0.61±0.13
TOA (º)	28.95±8.18	31.60±5.05	29.47±8.44	23.52±6.41	25.54±4.63	26.68±5.42	20.10±6.80	25.08±7.37	31.46±4.85
CMflx (m)	1.70±0.20	1.69±0.13	1.64±0.12	1.69±0.17	1.69±0.17	1.72±0.17	1.55±0.16	1.78±0.16	1.81±0.21
CMfly (m)	0.24±0.07	0.25±0.08	0.24±0.07	0.23±0.09	0.28±0.06	0.25±0.07	0.16±0.13	0.32±0.08	0.31±0.05
EA (º)	8.69±4.00	7.06±3.31	8.27±4.14	9.19±4.51	8.60±5.21	8.82±4.59	13.97±7.56	12.12±7.20	11.77±7.08
IVVx	0.26±0.03	0.25±0.02	0.26±0.03	0.26±0.03	0.25±0.03	0.26±0.03	0.24±0.03	0.25±0.03	0.25±0.04
15 m ST (s)	7.23±0.45	7.19±0.45	7.23±0.49	7.23±0.45	7.14±0.50	7.12±0.51	7.25±0.36	7.17±0.53	7.21±0.53

Note: 1, 2 and 3 - Feet utterly immersed and hands on lowest, highest horizontal and vertical handgrips. 4, 5 and 6 - Feet partially emerged and hands on lowest, highest horizontal and vertical handgrips. 7, 8 and 9 - Feet utterly emerged and hands on lowest, highest horizontal and vertical handgrips. CMssx and CMssy, centre of mass horizontal and vertical coordinate at 1st frame, respectively; ULimpx and ULimpy, upper limbs horizontal and vertical impulse, respectively; LLimpx and LLimpy, lower limbs horizontal and vertical impulse, respectively; TOA, take-off angle; CMflx and CMfly, centre of mass horizontal and vertical coordinate at 3rd distal phalanx water contact, respectively; EA, entry angle; IVVx, horizontal hip intracyclic velocity variations; 15 m ST, 15 m start time.

Table 3 to 7 display standardized mean difference and respective 95% confidence intervals of comparisons between variants. Start variant with feet utterly immersed and hands on lowest horizontal handgrip depicted shorter CM vertical coordinate at 1st frame, as well as upper limbs vertical and lower limbs horizontal and vertical impulse rather than variants with feet utterly emerged, notwithstanding handgrips positioning (Table 3).

Table 3. Standardized mean difference and respective 95% confidence interval of comparisons between start variant with feet utterly immersed and hands on lowest horizontal handgrip and the other eight variants for kinematic and kinetic parameters.

Variables	Comparisons between start variants							
	1x2	1x2	1x2	1x2	1x2	1x2	1x2	1x2
CMssx	-0.31	-0.49	0.04	-0.49	-0.61	-0.07	-0.60	-0.49
(m)	(-1.19, 0.56)	(-1.36, 0.38)	(-0.90, 0.97)	(-1.51, 0.53)	(-1.57, 0.35)	(-1.16, 1.02)	(-1.90, 0.70)	(-1.55, 0.58)
CMssy	0.46	0.31	0.43	0.97	0.75	0.99	1.97	1.92
(m)	(-0.35, 1.28)	(-0.57, 1.19)	(-0.47, 1.34)	(0.00, 1.94)	(-0.22, 1.72)	(0.01, 1.98)	(0.85, 3.08)	(0.58, 3.26)
ULimpx	-0.55	-0.14	0.46	-0.70	-0.23	0.82	-0.10	0.27
((N/BW).s)	(-1.53, 0.44)	(-0.87, 0.59)	(-0.32, 1.23)	(-1.69, 0.28)	(-1.08, 0.62)	(0.08, 1.56)	(-1.09, 0.89)	(-0.55, 1.10)
ULimpy	-0.02	0.02	1.46	0.83	0.83	2.52	1.89	1.83
((N/BW).s)	(-0.78, 0.75)	(-0.79, 0.83)	(0.64, 2.27)	(0.00, 1.66)	(0.02, 1.65)	(1.55, 3.50)	(1.03, 2.76)	(0.83, 2.83)
LLimpx	-0.23	-0.21	0.83	0.51	0.55	1.74	1.18	1.20
((N/BW).s)	(-1.07, 0.61)	(-1.08, 0.64)	(0.03, 1.63)	(-0.32, 1.34)	(-0.27, 1.36)	(0.98, 2.49)	(0.32, 2.05)	(0.30, 2.10)
LLimpy	-0.16	-0.12	0.70	0.64	0.62	1.13	1.60	1.69
((N/BW).s)	(-0.96, 0.63)	(-0.92, 0.68)	(-0.26, 1.67)	(-0.12, 1.41)	(-0.12, 1.36)	(0.01, 2.26)	(0.74, 2.47)	(0.50, 2.87)
TOA	0.30	0.06	-0.47	-0.35	-0.25	-0.99	-0.43	0.28
(º)	(-0.43, 1,03)	(-0.82, 0.94)	(-1.25, 0.31)	(-1.09, 0.38)	(-0.99, 0.49)	(-1.86, -0.12)	(-1.25, 0.39)	(-0.44, 1.00)
CMflx	-0.03	-0.26	-0.05	0.16	0.09	-0.65	0.33	0.49
(m)	(-0.76, 0.71)	(-0.99, 0.47)	(-0.86, 0.75)	(-0.66, 0.98)	(-0.71, 0.90)	(-1.43, 0.12)	(-0.47, 1.11)	(-0.39, 1.36)
CMfly	0.04	0.00	-0.19	0.45	0.03	-1.00	0.86	0.83
(m)	(-0.84, 0.92)	(-0.85, 0.85)	(-1.16, 0.79)	(-0.33,1.23)	(-0.79, 0.85)	(-2.27, 0.26)	(-0.04, 1.76)	(-0.07, 1.59)
EA	-0.35	-0.09	0.11	-0.02	0.03	1.14	0.74	0.67
(º)	(-1.14, 0.44)	(-1.00, 0.82)	(-0.81, 1.03)	(-1.03, 0.99)	(-0.90, 0.96)	(-0.19, 2.48)	(-0.53, 2.02)	(-0.59, 1.93)
	-0.26	-0.08	0.05	-0.21	-0.10	-0.44	-0.20	-0.18
IVVx	(-1.01, 0.50)	(-0.93, 0.77)	(-0.78, 0.88)	(-0.98, 0.57)	(-0.93, 0.73)	(-1.25, 0.38)	(-1.03, 0.63)	(-1.07, 0.71)
15 m ST	-0.09	-0.01	0.00	-0.17	-0.21	0.04	-0.11	-0.05
(s)	(-0.99, 0.82)	(-0.95, 0.93)	(-0.90, 0.91)	(-1.12, 0.79)	(-1.17, 0.75)	(-0.78, 0.85)	(-1.09, 0.87)	(-1.03, 0.94)

Note: 1, 2 and 3- Feet utterly immersed and hands on lowest, highest horizontal and vertical handgrips. 4, 5 and 6 - Feet partially emerged and hands on lowest, highest horizontal and vertical handgrips. 7, 8 and 9 - Feet utterly emerged and hands on lowest, highest horizontal and vertical handgrips. CMssx and CMssy, centre of mass horizontal and vertical coordinate at 1st frame, respectively; ULimpx and ULimpy, upper limbs horizontal and vertical impulse, respectively; LLimpx and LLimpy, lower limbs horizontal and vertical impulse, respectively; TOA, take-off angle; CMflx and CMfly, centre of mass horizontal and vertical coordinate at 3rd distal phalanx water contact, respectively; EA, entry angle; IVVx, horizontal hip intracyclic velocity variations; 15 m ST, 15 m start time.

Comparisons between start variants with feet utterly immersed and hands on highest horizontal handgrips and that performed with feet partially and utterly emerged (regardless handgrips positioning) have shown greater vertical upper and lower limbs impulse for the latest. In addition, those former start variants have shown shorter horizontal lower limbs impulse rather than variants with feet utterly emerged (Table 4).

Table 4. Standardized mean difference and respective 95% confidence interval of comparisons between start variant with feet utterly immersed and hands on highest horizontal handgrip and the other seven variants for kinematic and kinetic parameters.

Variables	Comparisons between starting variants						
	2x3	2x4	2x5	2x6	2x7	2x8	2x9
CMssx	-0.17	0.34	-0.17	-0.29	0.24	-0.28	-0.17
(m)	(-1.03, 0.69)	(-0.58, 1.27)	(-1.18, 0.83)	(-1.24, 0.66)	(-0.83, 1.31)	(-1.55, 0.99)	(-1.21, 0.88)
CMssy	-0.18	-0.03	0.58	0.32	0.60	1.71	1.65
(m)	(-1.12, 0.76)	(-1.01, 0.94)	(-0.48, 1.64)	(-0.73, 1.38)	(-0.49, 1.69)	(0.48, 2.93)	(0.16, 3.15)
ULimpx	0.32	0.79	-0.12	0.25	1.08	0.35	0.65
((N/BW).s)	(-0.38, 1.02)	(0.07, 1.52)	(-0.99, 0.74)	(-0.52, 1.02)	(0.37, 1.78)	(-0.52, 1.22)	(-0.11, 1.40)
ULimpy	0.05	1.96	1.13	1.13	3.38	2.54	2.46
((N/BW).s)	(-0.89, 0.98)	(1.02, 2.91)	(0.16, 2.09)	(0.19, 2.07)	(2.18, 4.58)	(1.52, 3.57)	(1.22, 3.69)
LLimpx	0.02	1.12	0.78	0.82	2.08	1.50	1.52
((N/BW).s)	(-0.85, 0.89)	(0.30, 1.94)	(-0.07, 1.63)	(-0.02, 1.66)	(1.32, 2.85)	(0.61, 2.39)	(0.59, 2.45)
LLimpy	0.05	1.04	0.97	0.94	1.57	2.13	2.23
((N/BW).s)	(-0.81, 0.92)	(0.06, 2.14)	(0.15, 1.79)	(1.16, 1.73)	(0.25, 2.88)	(1.17, 3.09)	(0.85, 3.61)
TOA	-0.39	-1.24	-1.05	-0.89	-2.09	-1.18	-0.03
(º)	(-1.61, 083)	(-2.25, -0.24)	(-1.93, -0.17)	(-1.79, 0.00)	(-3.31, -0.86)	(-2.27, -0.09)	(-0.87, 0.82)
CMflx	-0.36	-0.04	0.29	0.19	-0.96	0.55	0.80
(m)	(-1.21, 0.49)	(-1.06, 0.98)	(-0.76, 1.33)	(-0.83, 1.20)	(-1.92, -0.01)	(-0.43, 1.53)	(-0.36, 1.95)
CMfly	-0.04	-0.22	0.03	-0.01	-1.01	0.78	0.75
(m)	(-0.88, 0.79)	(-1.17, 0.73)	(-0.03, 0.10)	(-0.82, 0.79)	(-2.23, 0.22)	(-0.10, 1.66)	(0.00, 1.50)
EA	0.32	0.56	0.40	0.46	1.81	1.33	1.23
(º)	(-0.71, 1.34)	(-0.48, 1.59)	(-0.75, 1.55)	(-0.59, 1.51)	(0.00, 3.38)	(-0.18, 2.83)	(-0.25, 2.72)
IVVx	0.25	0.42	0.07	0.21	-0.25	0.08	0.11
	(-0.78, 1.27)	(-0.56, 1.41)	(-0.82, 0.96)	(-0.77, 1.20)	(-1.21, 0.71)	(-0.91, 1.07)	(-0.98, 1.19)
15 m ST	0.08	0.09	-0.08	-0.12	0.12	-0.03	0.04
(s)	(-0.87, 1.02)	(-0.82, 1.00)	(-1.04, 0.88)	(-1.09, 0.84)	(-0.69, 0.94)	(-1.01, 0.96)	(-0.95, 1.03)

Note: 1, 2 and 3- Feet utterly immersed and hands on lowest, highest horizontal and vertical handgrips. 4, 5 and 6 - Feet partially emerged and hands on lowest, highest horizontal and vertical handgrips. 7, 8 and 9 - Feet utterly emerged and hands on lowest, highest horizontal and vertical handgrips. CMssx and CMssy, centre of mass horizontal and vertical coordinate at 1st frame, respectively; ULimpx and ULimpy, upper limbs horizontal and vertical impulse, respectively; LLimpx and LLimpy, lower limbs horizontal and vertical impulse, respectively; TOA, take-off angle; CMflx and CMfly, centre of mass horizontal and vertical coordinate at 3rd distal phalanx water contact, respectively; EA, entry angle; IVVx, horizontal hip intracyclic velocity variations; 15 m ST, 15 m start time.

Comparisons between start variants with feet utterly immersed and hands on vertical handgrips and the one with feet partially and utterly emerged revealed greater upper limbs vertical impulse for the last two. Start variants with feet utterly emerged have also depicted greater horizontal and vertical lower limbs impulse rather than that former start variant (Table 5).

Table 5. Standardized mean difference and respective 95% confidence interval of comparisons between start variant with feet utterly immersed and hands on vertical handgrip and the other six variants for kinematic and kinetic parameters.

Variables	Comparisons between starting variants					
	3x4	3x5	3x6	3x7	3x8	3x9
CMssx	0.54	0.00	-0.13	0.43	-0.12	0.00
(m)	(-0.43, 1.52)	(-1.06, 1.05)	(-1.13, 0.87)	(-0.70, 1.56)	(-1.47, 1.23)	(-1.11, 1.11)
CMssy	0.13	0.67	0.45	0.69	1.68	1.64
(m)	(-0.81, 1.06)	(-0.33, 1.68)	(-0.55, 1.45)	(-0.33, 1.72)	(0.55, 2.82)	(0.27, 3.01)
ULimpx	0.95	-0.90	-0.14	1.53	0.06	0.66
((N/BW).s)	(-0.02, 1.92)	(-2.30, 0.51)	(-1.28, 0.99)	(0.63, 2.42)	(-1.36, 1.48)	(-0.43, 1.75)
ULimpy	1.66	0.94	0.94	2.89	2.16	2.09
((N/BW).s)	(0.79, 2.53)	(0.05, 1.83)	(0.07, 1.81)	(1.81, 3.96)	(1.23, 3.10)	(0.98, 3.19)
LLimpx	1.08	0.75	0.79	2.02	1.45	1.47
((N/BW).s)	(0.27, 1.89)	(-0.09, 1.59)	(-0.05, 1.62)	(1.26, 2.78)	(0.57, 2.33)	(0.55, 2.39)
LLimpy	0.98	0.91	0.88	1.50	2.06	2.16
((N/BW).s)	(-0.11, 2.07)	(0.09, 1.73)	(0.10, 1.66)	(0.20, 2.80)	(1.10, 3.01)	(0.79, 3.53)
TOA	-0.53	-0.41	-0.32	-1.06	-0.50	0.22
(º)	(-1.34, 0.28)	(-1.18, 0.35)	(-1.09, 0.46)	(-1.96, 0.15)	(-1.34, 0.35)	(-0.53, 0.98)
CMflx	0.35	0.70	0.60	-0.66	0.99	1.26
(m)	(-0.75, 1.45)	(-0.42, 1.83)	(-0.50, 1.69)	(-1.68, 0.37)	(0.06, 2.04)	(0.01, 2.51)
CMfly	-0.20	0.49	0.03	-1.09	0.93	0.90
(m)	(-1.25, 0.85)	(-0.34, 1.31)	(-0.84, 0.91)	(-2.46, 0.28)	(-0.03, 1.89)	(-0.09, 1.70)
EA	0.19	0.07	0.11	1.17	0.79	0.72
(º)	(-0.73, 1.10)	(-0.92, 1.06)	(-0.81, 1.04)	(-0.11, 2.46)	(-0.45, 2.03)	(-0.51, 1.95)
IVVx	0.13	-0.13	-0.03	-0.37	-0.13	-0.11
	(-0.71, 0.97)	(-0.91, 0.65)	(-0.87, 0.81)	(-1.19, 0.45)	(-0.97, 0.71)	(-1.00, 0.79)
15 m ST	0.01	-0.14	-0.18	0.05	-0.09	-0.03
(s)	(-0.87, 0.89)	(-1.07, 0.78)	(-1.11, 0.74)	(-0.76, 0.85)	(-1.04, 0.85)	(-0.98, 0.91)

Note: 1, 2 and 3- Feet utterly immersed and hands on lowest, highest horizontal and vertical handgrips. 4, 5 and 6 - Feet partially emerged and hands on lowest, highest horizontal and vertical handgrips. 7, 8 and 9 - Feet utterly emerged and hands on lowest, highest horizontal and vertical handgrips. CMssx and CMssy, centre of mass horizontal and vertical coordinate at 1st frame, respectively; ULimpx and ULimpy, upper limbs horizontal and vertical impulse, respectively; LLimpx and LLimpy, lower limbs horizontal and vertical impulse, respectively; TOA, take-off angle; CMflx and CMfly, centre of mass horizontal and vertical coordinate at 3rd distal phalanx water contact, respectively; EA, entry angle; IVVx, horizontal hip intracyclic velocity variations; 15 m ST, 15 m start time.

When comparing start variant with feet partially emerged and hands on lowest handgrips with feet utterly emerged and hands on highest horizontal and vertical handgrips, these last two displayed greater CM vertical coordinate at set positioning and at first fingertip water contact. Start variant with feet partially emerged and hands on highest horizontal handgrips revealed shorter upper limbs vertical impulse than variants with feet utterly emerged (Table 6).

Table 6. Standardized mean difference and respective 95% confidence interval of comparisons between start variant with feet parallel and partially emerged and hands on lowest and highest horizontal handgrip and the other start variants for kinematic and kinetic parameters.

Variables	Comparisons between starting variants								
	4x5	4x6	4x7	4x8	4x9	5x6	5x7	5x8	5x9
CMssx	-0.45	-0.56	-0.09	-0.55	-0.45	-0.09	0.32	-0.08	0.00
(m)	(-1.38, 0.47)	(-1.44, 0.33)	(-1.07, 0.89)	(-1.70, 0.60)	(-1.41, 0.51)	(-0.92, 0.74)	(-0.59, 1.22)	(-1.13, 0.96)	(-0.89, 0.90)
CMssy	0.49	0.29	0.51	1.41	1.36	-0.18	0.22	0.80	0.76
(m)	(-0.43, 1.42)	(-0.63, 1.21)	(-0.43, 1.45)	(0.36, 2.45)	(0.12, 2.61)	(-1.04, 0.68)	(-0.58, 1.02)	(-0.16, 1.76)	(-0.36, 1.89)
ULimpx	-1.50	-0.89	0.46	-0.72	-0.24	0.37	1.20	0.47	0.77
((N/BW).s)	(-2.68, -0.31)	(-1.86, 0.09)	(-0.34, 1.27)	(-1.92, 0.47)	(-1.18, 0.70)	(-0.40, 1.15)	(0.50, 1.91)	(-0.39, 1.34)	(0.02, 1.53)
ULimpy	-0.71	-0.70	1.20	0.49	0.42	0.00	1.83	1.15	1.08
((N/BW).s)	(-1.59, 0.17)	(-1.56, 0.16)	(0.14, 2.26)	(-0.43, 1.42)	(-0.67, 1.51)	(-0.84, 0.85)	(0.80, 2.86)	(0.25, 2.06)	(0.03, 2.14)
LLimpx	-0.37	-0.33	1.07	0.42	0.44	0.04	1.34	0.74	0.76
((N/BW).s)	(-1.27, 0.52)	(-1.22, 0.55)	(0.28, 1.87)	(-0.52, 1.36)	(-0.55, 1.43)	(-0.81, 0.89)	(0.57, 2.12)	(-0.17, 1.64)	(-0.19, 1.70)
LLimpy	-0.05	-0.07	0.35	0.74	0.81	-0.03	0.66	1.28	1.40
((N/BW).s)	(-0.78, 0.68)	(-0.78, 0.64)	(-0.62, 1.33)	(-0.05, 1.53)	(-0.22, 1.83)	(-0.85, 0.78)	(-0.76, 2.07)	(0.26, 2.31)	(-0.11, 2.90)
TOA	0.15	0.27	-0.65	0.05	0.94	0.15	-0.99	-0.13	0.97
(º)	(-0.64, 0.93)	(-0.52, 1.06)	(-1.65, 0.35)	(-0.87, 0.96)	(0.17, 1.70)	(-0.72, 1.02)	(-2.17, -0.19)	(-1.18, 0.92)	(0.15, 1.80)
CMflx	0.24	0.17	-0.69	0.44	0.63	-0.07	-0.90	0.19	0.37
(m)	(-0.64, 1.12)	(-0.69, 1.03)	(-1.52, 1.13)	(-0.40, 1.28)	(-0.32, 1.58)	(-0.92, 0.77)	(-1.71, -0.09)	(-0.63, 1.01)	(-0.56, 1.30)
CMfly	0.51	0.17	-0.65	0.84	0.81	-0.54	-1.87	0.53	0.48
(m)	(-0.22, 1.23)	(-0.58, 0.93)	(-1.72, 0.41)	(0.03, 1.64)	(0.09, 1.53)	(-1.47, 0.39)	(-3.44, -0.30)	(-0.52, 1.58)	(-0.35, 1.32)
EA	-0.11	-0.07	0.92	0.56	0.50	0.04	0.89	0.59	0.53
(º)	(-1.05, 0.82)	(-0.94, 0.80)	(-0.29, 2.13)	(-0.60, 1.73)	(-0.65, 1.64)	(-0.78, 0.85)	(-1.19, 1.98)	(-0.46, 1.63)	(-0.51, 1.56)
IVVx	-0.28	-0.17	-0.53	-0.27	-0.25	0.13	-0.30	0.01	0.03
	(-1.07, 0.52)	(-1.03, 0.69)	(-1.37, 0.31)	(-1.13, 0.59)	(-1.17, 0.67)	(-0.82, 1.08)	(-1.23, 0.63)	(-0.94, 0.96)	(-1.00, 1.07)
15 m ST	-0.17	-0.21	0.03	-0.11	-0.05	-0.04	0.18	0.05	0.11
(s)	(-1.13, 0.79)	(-1.17, 0.75)	(-0.78, 0.85)	(-1.10, 0.87)	(-1.03, 0.93)	(-0.95, 0.87)	(-0.61, 0.97)	(-0.88, 0.98)	(-0.82, 1.03)

Note: 1, 2 and 3- Feet utterly immersed and hands on lowest, highest horizontal and vertical handgrips. 4, 5 and 6 - Feet partially emerged and hands on lowest, highest horizontal and vertical handgrips. 7, 8 and 9 - Feet utterly emerged and hands on lowest, highest horizontal and vertical handgrips. CMssx and CMssy, centre of mass horizontal and vertical coordinate at 1st frame, respectively; ULimpx and ULimpy, upper limbs horizontal and vertical impulse, respectively; LLimpx and LLimpy, lower limbs horizontal and vertical impulse, respectively; TOA, take-off angle; CMflx and CMfly, centre of mass horizontal and vertical coordinate at 3rd distal phalanx water contact, respectively; EA, entry angle; IVVx, horizontal hip intracyclic velocity variations; 15 m ST, 15 m start time.

Start variant with feet partially emerged and hands on vertical handgrips depicted shorter upper limbs vertical impulse than start variants with feet utterly emerged. Start variants performed with feet utterly emerged and hands on highest horizontal and vertical handgrips have shown longer and higher CM vertical coordinate at first fingertip water contact than that with feet utterly emerged but hands on the lowest horizontal handgrips (Table 7).

Table 7. Standardized mean difference and respective 95% confidence interval of comparisons between start variants with feet partially emerged and hands on vertical handgrip, feet utterly emerged and hands on lowest and highest horizontal handgrip and the other variants for kinematic and kinetic parameters.

Variables	Comparisons between starting variants					
	6x7	6x8	6x9	7x8	7x9	8x9
CMssx	0.44	0.01	0.10	-0.36	-0.28	0.06
(m)	(-0.51, 1.39)	(-1.10, 1.12)	(-0.83, 1.04)	(-1.34, 0.62)	(-1.14, 0.57)	(-0.71, 0.84)
CMssy	0.41	0.99	0.95	0.72	0.68	-0.03
(m)	(-0.39, 1.21)	(0.03, 1.95)	(-0.18, 2.08)	(-0.41, 1.86)	(-0.68, 2.04)	(-1.01, 0.95)
ULimpx	1.08	0.13	0.52	-1.37	-0.81	0.29
((N/BW).s)	(0.33, 1.83)	(-0.88, 1.14)	(-0.32, 1.35)	(-2.71, -0.03)	(-1.85, 0.22)	(-0.46, 1.05)
ULimpy	1.91	1.20	1.13	-0.50	-0.56	-0.07
((N/BW).s)	(0.85, 2.97)	(0.27, 2.13)	(0.03, 2.22)	(-1.29, 0.28)	(-1.44, 0.32)	(-1.06, 0.93)
LLimpx	1.33	0.71	0.73	-0.78	-0.75	0.02
((N/BW).s)	(0.55, 2.11)	(-0.20, 1.63)	(-0.22, 1.69)	(-1.84, 0.28)	(-1.88, 0.37)	(-0.88, 0.92)
LLimpy	0.78	1.48	1.61	0.31	0.36	0.08
((N/BW).s)	(-0.80, 2.36)	(0.36, 2.60)	(-0.08, 3.30)	(-0.43, 1.04)	(-0.53, 1.25)	(-1.10, 1.26)
TOA	-1.11	-0.27	0.81	0.64	1.45	0.79
(º)	(-2.26, 0.04)	(-1.30, 0.76)	(-0.01, 1.62)	(-0.32, 1.59)	(0.60, 2.30)	(0.05, 1.53)
CMflx	-0.87	0.27	0.46	1.25	1.46	0.20
(m)	(-1.69, -0.04)	(-0.57, 1.11)	(-0.49, 1.41)	(0.37, 2.13)	(0.45, 2.47)	(-0.78, 1.18)
CMfly	-1.15	0.92	0.88	1.05	1.03	-0.03
(m)	(-2.53, 0.23)	(-0.03, 1.87)	(0.10, 1.67)	(0.32, 1.77)	(0.34, 1.72)	(-0.77, 0.71)
EA	0.97	0.62	0.56	-0.21	-0.25	-0.04
(º)	(-0.22, 2.17)	(-0.52, 1.77)	(-0.58, 1.69)	(-1.05, 0.63)	(-1.09, 0.58)	(-0.90, 0.81)
IVVx	-0.36	-0.11	-0.08	0.27	0.29	0.02
	(-1.21, 0.48)	(-0.97, 0.76)	(-1.01, 0.84)	(-0.61, 1.15)	(-0.66, 1.24)	(-0.95, 1.00)
15 m ST	0.22	0.09	0.14	-0.19	-0.11	0.06
(s)	(-0.57, 1.01)	(-0.84, 1.01)	(-0.78, 1.07)	(-1.34, 0.97)	(-1.26, 1.05)	(-0.85, 0.96)

Note: 1, 2 and 3 - Feet utterly immersed and hands on lowest, highest horizontal and vertical handgrips. 4, 5 and 6 - Feet partially emerged and hands on lowest, highest horizontal and vertical handgrips. 7, 8 and 9 - Feet utterly emerged and hands on lowest, highest horizontal and vertical handgrips. CMssx and CMssy, centre of mass horizontal and vertical coordinate at 1st frame, respectively; ULimpx and ULimpy, upper limbs horizontal and vertical impulse, respectively; LLimpx and LLimpy, lower limbs horizontal and vertical impulse, respectively; TOA, take-off angle; CMflx and CMfly, centre of mass horizontal and vertical coordinate at 3rd distal phalanx water contact, respectively; EA, entry angle; IVVx, horizontal hip intracyclic velocity variations; 15 m ST, 15 m start time.

Discussion

This study has compared nine backstroke start variants (three feet vs. hands positioning) to verify the biomechanical advantages/disadvantages provided by the combination of current FINA start (SW 6.1) and facility (FR 2.7) rules on start performance. The main results were: (i) variants performed with feet utterly immersed depicted shorter vertical upper and lower limbs impulse than those with feet utterly emerged (regardless handgrips positioning); (ii) variants with feet partially emerged displayed greater vertical upper limbs impulse than those with feet positioned utterly immersed; and (iii) variants with feet utterly emerged with hands on highest horizontal and vertical handgrip presented greater CM horizontal and vertical coordinate at 1st fingertip water contact than that with feet utterly emerged but hands on lowest horizontal handgrip. Findings partially corroborate the established assumptions, since entry angle, horizontal hip intracyclic velocity variation during underwater phase and 15 m start time were similar in spite of the start variant used.

When swimmers perform backstroke start variants with feet utterly immersed (independently of the handgrips positioning), hydrostatic pressure increases in comparison with those performed with feet utterly emerged (Aspenes & Karlsen, 2012), reducing vertical upper and lower limbs impulse. Moreover CM was positioned lower than when using their feet utterly emerged and hands on highest horizontal and vertical handgrips, which is considered a biomechanical disadvantage, hampering low resistance flight and entry phases (Nguyen et al., 2014). Despite these authors have not mentioned the adopted handgrips, they have verified that feet utterly emerged set the hip higher regarding water level (~0.18 m) than feet utterly immersed (~0.07 m). To position CM higher out of the water and to generate greater vertical impulse during the hands-off phase is crucial because it was already noticed that the angle formed by the CM, centre of pressure and horizontal axis progressively reduce until the take-off, restricting the conditions to generate vertical displacement (Mourão et al., 2015).

Notwithstanding the handgrips used, positioning feet partially emerged has implied greater upper limbs vertical impulse than feet utterly immersed, which can also be explained by the hydrostatic pressure influencing the force profile. Most of the vertical upper limbs impulse has been accounted for sustaining swimmers out of the water and for changing trunk's moment of inertia (de Jesus et al., 2011, 2013). Upper limbs role has already been described as to guide swimmers' lower limbs impulse (Breed & Young, 2003; Guimarães & Hay, 1985; Mourão et al., 2015), and strong positive correlations have been found between upper and lower limbs impulse (Guimarães & Hay, 1985). Moreover, only focusing on greater upper limbs vertical impulse during the hands-off phase, coaches should attempt to transfer this biomechanical advantage throughout take-off, flight, entry and underwater phase (Elipot et al., 2009; Thow et al., 2012; Vantorre et al., 2014).

Start variants with feet utterly emerged can provide swimmers with more biomechanical advantages, but using hands positioned at lowest horizontal handgrip seem to be detrimental for the flight path. Indeed, swimmers adopting the above-referred variant have depicted shorter CM horizontal position at the fingertip water contact than variant with feet utterly immersed with hands on highest horizontal handgrip and feet partially and utterly emerged with hands on highest horizontal and vertical handgrip. Despite backstrokers constrains in performing similar ventral starts take-off angle (Breed & Young, 2003; Mourão et al., 2015) due to the proximity with the water level (Takeda et al., 2014), swimmers should prioritize a start variant that allows longer flight path due to less air resistance (Blanksby et al., 2002; Takeda et al., 2009). The current findings suggest that swimmers can succeed when adopting the variant with feet utterly emerged, as already mentioned (Nguyen et al., 2014), but they should preferentially position their hands on highest horizontal or vertical handgrip.

In summary, any biomechanical advantage obtained when standing with feet positioned partially or utterly emerged during wall contact phases was not transferred along entry and underwater phase, being similar to the 15 m start times. It seems that despite the variant used proficient backstrokers had depicted

similar motor profile to perform the entry and undulatory movements and, consequently achieving similar performance (Seifert et al., 2010). Based on these findings, it might be recommended to use higher setting positioning (i.e. with feet partially or entirely above water level with hand on highest or vertical handgrip), although focusing on entry and underwater biomechanics improvement, as previously mentioned (de Jesus et al., 2013; Takeda et al., 2014).

Notwithstanding the relevance of the current data, some limitations should be addressed. In the current study ten swimmers were evaluated, which can be considered a reasonable sample size when swimmers' availability is required for familiarization and testing using complex data collection methodology (e.g. Puel et al., 2012). It is recognized that enhanced statistical power depends upon a large number of observations; thus, future studies should verify how reproducible these findings could be in a larger sample. Start variants familiarization period has followed previous studies (e.g. Blanksby et al., 2002), however future studies should consider taking a longer familiarization period, as already mentioned (cf. Blanksby et al., 2002). Lastly, as the new wedge availability for feet support is restricted for many swimmers, yet, we have not included it in this study. Further studies should consider analysing its effects when used in different heights and handgrips positioning.

Conclusion

The current study has compared nine backstroke start variants (combining three feet and three hands positioning), being noticed clear biomechanical advantages during wall contact phase in variants performed with feet partially and utterly emerged over feet utterly immersed, regardless handgrip adopted. In spite of these findings, none clear difference was noticed among start variants considering entry and underwater phases, as well as 15 m start time. Therefore, coaches should focus on maintaining these advantages onwards during entry and underwater phases, and consequently improving overall 15 m start time.

Acknowledgments

This work was supported by the Coordination for the Improvement of Higher Education under doctoral grant (BEX 0761/12-5/2012-2015), Foundation for Science and Technology under grant (EXPL/DTP-DES/2481/2013- FCOMP-01-0124-FEDER-041981) and Séneca Foundation under grant (19615/EE/14). The authors acknowledge M.Sc. Mariana Marques and M.Sc. Sara Tribuzi Morais for their involvement in the data collection and treatment.

Disclosure Statement

The authors declare that they have no conflict of interest.

References

Abdel-Aziz, Y., & Karara, H. (1971). Direct linear transformation: from comparator coordinates into object coordinates in close range photogrammetry. Symposium on Close-Range Photogrammetry Falls Church, VA: American Society of Photogrammetry, United States, 1-18.

Aspenes, S.T., & Karlsen, T. (2012). Exercise-training intervention studies in competitive swimming. *Sports Medicine, 42*(6), 527-543.

Barbosa, T., Fernandes, R.J., Morouco, P., & Vilas-Boas, J.P. (2008). Predicting the intra-cyclic variation of the velocity of the centre of mass from segmental velocities in butterfly stroke: A pilot study*. Journal of Sports Science and Medicine, 7*(2), 201-209.

Barbosa, T., de Jesus, K., Abraldes, A., Ribeiro, J., Figueiredo, P., Vilas-Boas, J.P., & Fernandes, R.J. (2015). Effects of protocol step length on biomechanical measures in swimming. *International Journal of Sports Physiology and Performance, 10*(2), 211-218.

Blanksby, B., Nicholson, L., & Elliott, B. (2002). Biomechanical analysis of the grab, track and handle swimming starts: An intervention study. *Sports Biomechanics, 1*(1), 11-24.

Breed, R., & Young, W. (2003). The effect of a resistance training programme on the grab, track and swing starts in swimming. *Journal of Sports Sciences, 21*(3), 213-220.

Cohen, J. (1988). Statistical power analysis for the behavioral sciences (2nd ed.): Hillsdale, NJ: Lawrence Erlbaum Associates.

de Jesus, K., de Jesus, K., Figueiredo, P., Gonçalves, P., Pereira, S., Vilas-Boas, J.P., & Fernandes, R.J. (2011). Biomechanical analysis of backstroke swimming starts. *International Journal of Sports Medicine, 32*(7), 546-551.

de Jesus, K., Figueiredo, P., de Jesus, K., Pereira, F., Vilas-Boas, J.P., Machado, L., & Fernandes, R.J. (2012). Kinematic analysis of three water polo front crawl styles. *Journal of Sports Sciences, 30*(7), 715-723.

de Jesus, K., de Jesus, K., Figueiredo, P., Gonçalves, P., Pereira, S., Vilas-Boas, J.P., & Fernandes, R.J. (2013). Backstroke start kinematic and kinetic changes due to different feet positioning. *Journal of Sports Sciences, 31*(15), 1665-1675.

de Jesus, K., de Jesus, K., Fernandes, R.J., Vilas-Boas, J.P., & Sanders, R. (2014a). The backstroke swimming start: state of the art. *Journal of Human Kinetics, 42*, 27-40.

de Jesus, K., de Jesus, K., Medeiros, A., Fernandes, R.J., & Vilas-Boas, J.P. (2014b). The bacstroke starting variants performed under the current swimming rules and block configuration. *Journal of Swimming Research, 22*(1), 1-11.

de Jesus, K., de Jesus, K., Figueiredo.P., Vilas-Boas, J.P., Fernandes, R.J., & Machado, L. (2015). Reconstruction accuracy assessment of surface and underwater 3D motion analysis: a new approach. *Computational and Mathematical Methods in Medicine*; 2015:269264.

de Leva, P. (1996). *Adjustments to Zatsiorsky-Seluyanov's segment inertia parameters. Journal of Biomechanics, 29*(9), 1223-1230.

Elipot, M., Hellard, P., Taiar, R., Boissière, E., Rey, J., Lecat, S., & Houel, N. (2009). Analysis of swimmers' velocity during the underwater gliding motion following grab start. *Journal of Biomechanics, 42*(9), 1367-1370.

Figueiredo, P., Seifert, L., Vilas-Boas, J.P., & Fernandes, R.J. (2012). Individual profiles of spatio-temporal coordination in high intensity swimming. *Human Movement Science, 31*(5), 1200-1212.

Gourgoulis, V., Aggeloussis, N., Vezos, V., Kasimatis, P., Antoniou, P., & Mavromatis, G. (2008). Estimation of hand forces and propelling efficiency during front crawl swimming with hand paddles. *Journal of Biomechanics, 41*(1), 208-215.

Guimarães, A., & Hay, J. (1985). A mechanical analysis of the grab starting technique in swimming. *International Journal of Sport Biomechanics, 1*, 25-35.

Hohmann, A., Fehr, U., Kirsten, R., & Krueger, T. (2008). Biomechanical analysis of the backstroke start technique in swimming. *E-Journal Bewegung und Training, 2*, 28-33.

Hopkins, W. (2010). Linear models and effect magnitudes for research, clinical and practical applications. *Sport science, 14*, 49-58.

Mourão, L., de Jesus, K., Roesler, H., Machado, L., Fernandes, R.J., Vilas-Boas, J.P., & Vaz, M. (2015). Effective swimmer's action during the grab start technique. *PLoS ONE, 15*, e0123001.

Nguyen, C., Bradshaw, E., Pease, D., & Wilson, C. (2014). Is starting with the feet out of the water faster in backstroke swimming? *Sports Biomechanics, 13*(2), 154-165.

Psycharakis, S., & McCabe, C. (2011). Shoulder and hip roll differences between breathing and non-breathing conditions in front crawl swimming. *Journal of Biomechanics, 44*(9), 1752-1756.

Puel, F., Morlier, J., Avalos, M., Mesnard, M., Cid, M., & Hellard, P. (2012). 3D kinematic and dynamic analysis of the front crawl tumble turn in elite male swimmers. *Journal of Biomechanics, 45*(3), 510-515.

Rodacki, A.L., & Fowler, N. (2001). Intermuscular coordination during pendulum rebound exercises. *Journal of Sports Sciences, 19*(6), 411-425.

Roesler, H., Haupenthal, A., Schutz, G., & Souza, P. (2006). Dynamometric analysis of the maximum force applied in aquatic human gait at 1.3 m of immersion. *Gait & Posture, 24*(4), 412-417.

Seifert, L., Vantorre, J., Lemaitre, F., Chollet, D., Toussaint, H.M., & Vilas-Boas, J.P. (2010). Different profiles of the aerial start phase in front crawl. *Journal of Strength and Conditioning Research, 24*(2), 507-516.

Silvatti, A., Cerveri, P., Telles, T., Dias, F., Baroni, G., & Barros, R. (2012). Quantitative underwater 3D motion analysis using submerged video cameras: accuracy analysis and trajectory reconstruction. *Computer Methods in Biomechanics and Biomedical Engineering, 16*(11), 1240-1248.

Takeda, T., Ichikawa, H., Takagi, H., & Tsubakimoto, S. (2009). Do differences in initial speed persist to the stroke phase in front-crawl swimming? *Journal of Sports Sciences, 27*(13), 1449-1454.

Takeda, T., Itoi, O., Takagi, H., & Tsubakimoto, S. (2014). Kinematic analysis of the backstroke start: differences between backstroke specialists and non-specialists. *Journal of Sports Sciences, 32*(7), 635-641.

Thow, J., Naemi, R., & Sanders, R. (2012). Comparison of modes of feedback on glide performance in swimming. *Journal of Sports Sciences, 30*(1), 43-52.

Tor, E., Pease, D., & Ball, K. (2015a). How does drag affect the underwater phase of a swimming start? *Journal of Applied Biomechanics, 31*(1), 8-12.
Tor, E., Pease, D., & Ball, K. (2015b). The reliability of an instrumented start block analysis system. *Journal of Applied Biomechanics, 31*(1), 62-67.
Vantorre, J., Chollet, D., & Seifert, L. (2014). Biomechanical analysis of the swim-start: a review. *Journal of Sports Science and Medicine, 13*(2), 223-231.

Chapter 6

Neuromuscular activity of upper and lower limbs during two backstroke swimming start variants.

Karla de Jesus[1], Kelly de Jesus[1], Alexandre I. A. Medeiros[1,2], Pedro Gonçalves[1], Pedro Figueiredo[1,3], Ricardo Fernandes[1,4], João Paulo Vilas-Boas[1,4].

[1] Centre of Research, Education, Innovation and Intervention in Sport, Faculty of Sport, University of Porto, Porto, Portugal

[2] Department of Physical Education, University of Fortaleza, Fortaleza, Brazil.

[3] School of Physical Education, Federal University of Rio Grande do Sul, Porto Alegre, Brazil

[4] Porto Biomechanics Laboratory (LABIOMEP), Porto, Portugal

Submitted for publication on Journal of Sports Science and Medicine.

Abstract

A proficient start is decisive in sprint competitive swimming events and requires the swimmer's to exert maximal forces in a short period to complete the task successfully. The aim of this study was to compare the electromyographic (EMG) activity in-between the backstroke start with feet positioned parallel and partially emerged performed with the hands on the highest horizontal and on the vertical handgrip at hands-off, take-off, flight and entry start phases. EMG comparisons between starting variants were supported by upper and lower limb joint angles at starting position and 15 m start time data. Following a four-week start training to familiarize participants with each start variant, 10 male competitive backstroke swimmers performed randomly six 15 m maximal trials, being three of each start variant. Surface EMG of Biceps Brachii, Triceps Brachii, Rectus Femoris, Biceps Femoris, Gastrocnemius Medialis and Tibialis Anterior was recorded and processed using the time integral EMG (iEMG). Eight video cameras (four surface and four underwater) were used to determine backstroke start phases and joint angles at starting position. EMG, joint angles and temporal parameters have not evidenced changes due to the different handgrips. Nevertheless, clear differences were observed in both variants for upper and lower limb muscles activity among starting phases (e.g. Biceps Brachii at take-off vs. flight phase, 15.17% ± 2.76% and 22.38% ± 4.25%; 14.24% ± 7.11% and 25.90% ± 8.65%, for variant with hands horizontal and vertically positioned, respectively). It was concluded that different handgrips did not affect EMG, kinematics and temporal profile in backstroke start. Despite coaches might plan similar strength training for both start variants, further attention should be given on the selection of proper exercises to maximize the contribution of relevant muscles at different starting phases.

Key words: Biomechanics, surface electromyography, starting technique, backstroke events

Introduction

A successful start is essential in swimming competition, being composed of several phases (block, flight, entry and underwater), which are interdependent (Vantorre et al., 2014). Backstroke is the only competitive swimming technique in which the swimmers start in the water. The start technique performed in backstroke events regulated by the Fédération Internationale de Natation Amateur (FINA) authorizes swimmers to position their feet above the water level (SW 6.1, FINA). This rule determination has led researchers to investigate the kinematic and/or kinetic effects on different start variants performance (i.e. feet entirely immersed or emerged) (de Jesus et al., 2013; Nguyen et al., 2014; Takeda et al., 2014). According to Nguyen et al. (2014), swimmers often adopt the feet positioned above the water surface.

In 2008, FINA approved the Omega OSB11 starting block (Swiss Timing Ltd., Switzerland) with two horizontal and one vertical backstroke start handgrip. With this in mind, de Jesus, et al. (2014) has shown that the backstroke start variants with feet parallel and partially emerged but with hands positioned on the highest horizontal or vertical handgrips were often used by ~40% of swimmers regardless of the backstroke event (i.e. 50, 100 and 200 m) at London 2012 Olympic Games and Barcelona 2013 Swimming World Championships. As other high-velocity movements (e.g. squat jump, Van Soest et al., 1994), the backstroke start performance is related to the exertion of maximal force in the shortest time (de Jesus et al., 2011; Nguyen et al., 2014), which can be influenced by the set positioning used on the starting block/wall. In fact, handgrip start positioning might imply different upper and lower limb joint angles, influencing the muscular activity level from the starting signal throughout the flight and underwater phases. Therefore, it became indispensable for training support the study of current backstroke start variants from a neuromuscular standpoint, as also done in swimming turns (Pereira et al., 2015).

The handgrip effects on upper limbs electromyography (EMG) have been extensively studied in lat pull-down exercises, however contradiction remains about the upper limb muscles intervention across grip biacromial diameter and forearm orientation (e.g. Andersen et al., 2014). A wider grip, such as the vertical backstroke start handgrip might reduce the flexion and extension of the elbow and increase shoulder abduction compared with a narrow grip, such as the highest horizontal backstroke start handgrip, altering working conditions (Andersen et al., 2014). These changes at initial backstroke start instants might affect the upper body joints movement during the take-off and flight (i.e. shoulder adducted or abducted) (de Jesus et al., 2011), changing intrinsic muscle properties (e.g. force-length) and EMG amplitude (McGowan et al., 2013). Different handgrips might also alter lower limb joint angles at start positioning, a critical factor influencing jump EMG output (Bobbert et al., 2013; Mackala et al., 2013a, 2013b; Zajac, 2002), and consequently affect the lower limb muscular activity level throughout the start phases. Despite the above-mentioned findings, Rodacki and Fowler (2001), Camomilla et al. (2009) and Van Soest et al. (1994) reported an overall consistency between EMG activity in extremely fast movements performed with different set positioning. According to Van Soest et al (1994), the variability of important movement patterns decreases as the instant of time on which achievement depends (e.g. take-off in jumping is approached).

Scarce EMG literature in backstroke start has analyzed the upper and lower limb muscles activation sequence (Hohmann et al., 2008) and amplitude (de Jesus et al., 2011) during the wall, flight and underwater phases of outdated start variants. Hohmann et al. (2008) have shown that the backstroke start movement initiated with upper limb muscles, and the lower limb muscles contributed maximally during the take-off and underwater phase. de Jesus et al. (2011) have evidenced that greater Rectus Femoris activity during underwater phase has increased starting time, probably due to increased drag. Several authors have quantified and compared the EMG in-between movement phases in other sports (e.g. Escamilla & Andrews, 2009), which seems relevant due to the remaining confusion of some upper (Youm et al., 2009) and lower limb biarticular muscles

(Cleather et al., 2015) contribution. In the light of these considerations, this study has a twofold aim: (i) to compare the EMG of upper and lower limb muscles between variants with hands positioned horizontally or vertically on the starting handgrips from the starting signal to the water immersion, supported by angular kinematic and temporal data and (ii) to compare the EMG of each muscle between start phases for each variant. We hypothesized that EMG response of upper limb muscles from the starting signal until the hands-off would be sensitive to different handgrips. Furthermore, once kinematical differences between start variants are expectedly detailed (with the exception for the first one) it is expected that the biarticular upper and lower limb muscles contribute similarly from the starting signal to the water immersion in both.

Methods

Participants

Ten swimmers (mean and standard deviations (± s): age 20.6 ± 6.0 yrs., stature 1.75 ± 0.05 m, body mass 71.63 ± 12.14 kg, body fat percentage 10.8 ± 1.6%, training background 12.8 ± 8.43 yrs. and a personal best of 80.91 ± 3.09 % of the 100 m backstroke short course World Record) volunteered to participate in the study. Participants were healthy (no serious injury or illness in the last 6 months), able-bodied and were at the time of this study participating in national competitions with backstroke as their main specialty. Six swimmers preferred to use the variant with feet parallel and partially emerged and the highest horizontal handgrip, two preferred the feet parallel and partially emerged and the vertical handgrip, and two swimmers often used the variant with staggering feet positioned and hands on the lowest horizontal handgrip. After being informed of the benefits and potential risks of the investigation, each participant (or parent/guardian when subjects were under 18 yrs.) provided written informed consent by signing a document approved by the local Ethics Committee. The procedures were conformed to the recommendations of the Declaration of Helsinki.

Procedures

Starting trials

Two backstroke start variants with feet parallel and partially emerged were studied (cf. de Jesus et al., 2014): (i) hands on the highest horizontal (Figure 1a) and (ii) vertical handgrip (Figure 1b). Previous to data collection, a 1-month starting training intervention (3 sessions per week) was conducted to minimize performance bias and to provide similar standards in each of the two variants studied. In each session, swimmers performed 10 x 15 m maximal trials of each starting variant and were supervised two sessions a week to receive qualitative (i.e. video images) and quantitative (i.e. 15 m time) performance feedback.

A B

Figure 1. The backstroke start variants with feet partially emerged. A) The hands grasping the highest horizontal handgrip. B) The hands grasping the vertical handgrip.

In a 25 m indoor swimming pool, participants performed randomly six maximal 15 m trials, being three of each variant (2 min rest in-between trials), from which a mean value for each swimmer in each variant was calculated for statistical analysis. A starter device (Omega StartTime IV, Swiss Timing Ltd., Switzerland) produced the starting signals conform to swimming rules (SW 4.2, FINA) and simultaneously exported a light and trigger to the cameras and the analogue-to-digital (A/D) converter (MP150, BIOPAC Systems Inc., USA), respectively.

Video recording, starting phases and kinematical parameters

The swimmers' movements from the starting signal to the full water immersion were recorded by eight stationary and synchronized digital cameras (HDR CX160E, Sony Electronics Inc., Japan), four surface and four underwater, operating at a sampling frequency of 50 Hz with exposure time of 1/250 s. The angles between the axes of adjacent surface and underwater cameras varied from 75º to 110º (cf. de Jesus et al., 2012). To calibrate the starting space, a rectangular frame (4 m length [horizontal axis], 2.5 m height [vertical axis] and 2 m width [lateral axis]) was used. This frame was 0.80 m above the water surface and 0.50 m far from the starting pool wall with the horizontal axis aligned with the starting direction. A ninth stationary and synchronized surface camera was positioned perpendicularly to the swimming start lane to register 15 m start time. A pair of LEDs was fixed to the calibration volume visible in each camera view. Figure 2 illustrates the nine digital cameras and calibration volume positioning regarding to the starting block.

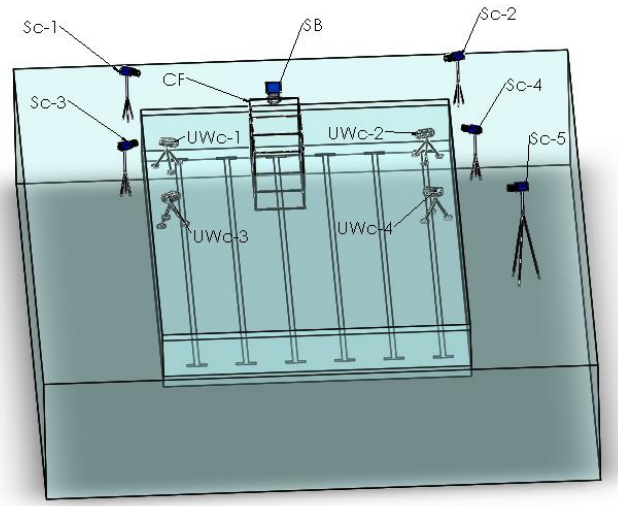

Figure 2. Experimental 3D kinematic set up. SB, starting block. CF, calibration frame. Sc, surface camera - 0.8 m height: 1, 2, 3 and 4 (5.5 and 7 m away from swimmers' plane of movement, aligned or 5 m away from SB). Sc-5, 3 m height, 8 m away from swimmer´s plane of movement and 15 m away from SB. UWc, underwater camera - 1.4 m deep: 1, 2, 3 and 4 (4.5 and 6.5 m away from the swimmers' plane of movement, 0.5, 1.0 and 5 m away from SB).

To enable swimmer's tracking the following 24 anatomical markers (being 22 fixed on the complete swim suit, Fastskin ©Speedo International Limited, UK) were defined: the vertex of the head (using a swim cap), mid-gonion, the right and left of the acromion, lateral epicondyle of humerus, styloid process of the wrist, 3rd hand distal phalanx, xyphoid, iliac crest, great trochanter of the femur, lateral epicondyle of the femur, lateral malleolus, calcaneus and tip of 1st foot distal phalanx. The anthropometric model assumed (de Leva, 1996) was similar to previous studies (Barbosa et al., 2008). Using the Ariel Performance Analysis System (Ariel Dynamics, Inc., USA) the video images were digitized manually and frame-by-frame. The independent digitization from the eight cameras was reconstructed with the help of calibration volume. Twelve calibration points were used and the image coordinates were transformed into three-dimensional object-space coordinates using the linear transformation algorithm (Abdel-Aziz & Karara, 1971), as done before (Barbosa et al., 2008). A 5 Hz cut-off value for data filtering (with a low pass digital filter) was selected according to residual analysis (residual error vs. cut-off frequency).

The variants were divided into four phases (de Jesus et al., 2013): (i) hands-off - the time between the starting signal and the instant the swimmer's hands left the handgrips; (ii) take-off – from the hands-off until the swimmer's feet left the wall; (iii) flight – from the take-off until the swimmer's fingertip water contacts; and (iv) entry – from the final instant of the flight until the swimmer's toe immersion. The critical instants used to define the starting phases (i.e., hands-off, take-off, 1st water contact and full water immersion) roughly corresponded to the respective 3D resultant right joint angles: maximal elbow extension, 1st maximal knee extension, maximal shoulder flexion and 2nd maximal knee extension. The 15 m starting time was defined between the auditory signal and the swimmers' vertex reached the 15 m mark. The resultant joint angles of the right shoulder (upper arm and upper trunk), elbow (upper and forearm), hip (lower trunk and thigh), knee (thigh and shank) and ankle (shank and feet) were determined at the 1st starting position frame.

The accuracy of the digitising procedure for the joint angles assessed was determined based on data from two repeated digitisations of a randomly selected trial (de Jesus et al., 2012), and subsequently tested with the statistical analysis described below.

EMG recordings and parameters

Biceps Brachii, Triceps Brachii, Rectus Femoris, Biceps Femoris, Gastrocnemius Medialis and Tibialis Anterior were right body side selected based on their main function in backstroke start and anatomic localization (de Jesus et al., 2011; Hohmann et al., 2008). Swimmer's skin was shaved and cleaned with alcohol-soaked cotton to reduce skin impedance. Active silver/silver chloride surface electrodes (Dormo, Telic, S.A., Spain) with preamplifiers (AD621BNZ, Analog Devices Inc., USA) recorded bipolar EMG (2 cm apart) with an eight-channel device (de Jesus et al., 2011). EMG system presents Zin ≥ 10 Ω//2*10-12F, common rejection mode of 110 dB and a total gain of 1100 (Basmajian & De Luca, 1985). Modern pre-amplifier design reduces the importance of measuring EMG with low level of electrode skin-impedance (Day, 2002). Electrodes were placed in the mid-point of the contracted muscle belly, in line with the fibber orientation (Hermes et al., 2000) and a reference electrode was attached to the patella.

Preceding the electrodes insulation and cables immobilization (for more information see de Jesus et al., 2011; Figueiredo et al., 2013; Stirn et al., 2011), each swimmer performed three dry land maximal voluntary isometric contractions (MVIC) for each muscle studied. Each MVIC was held for 5 s (followed by 5 min rest) and verbal encouragement was given to the subjects. The maximum value of the three measurements was defined for normalization. Raw EMG signals were sampled at 1000 Hz per channel with a 16-bit A/D conversion and recording system (BIOPAC System, Inc., USA) and stored on a computer for later analysis. EMG data analysis was performed with MATLAB R2014a (The MathWorks Inc., USA) (Conceição et al., 2014; de Jesus et al., 2011; Figueiredo et al., 2013).

Baseline and MVIC values were recorded sequentially and in the same file. After the trigger, baseline was assessed between 1500 to 2500 ms, followed by the MVIC test. Each raw EMG signal was filtered with a 4^{th} order band-pass Butterworth filter with cut-off frequencies of 35 and 500 Hz, full-wave rectified and smoothed with a 4^{th} order low pass Butterworth filter of 10 Hz to get the linear envelope. All filtering actions were implemented to assure that zero-phase distortion exists, by processing the input data in both the forward and reverse directions. The mean values plus two standard deviations (Hodges & Bui, 1996) were calculated from the baseline, and the MVIC maximum values were extracted from above referred files. Dynamic EMG signals were considered active or inactive when located above or below the baseline values, respectively, and then normalized to each respective MVIC value. Integration of the resulting linear envelope signal (iEMG) of active signals, in each phase, was calculated for active EMG normalized time, instead of each respective normalized total phase time. The time normalization results, in any case, in a time vector from 0 to 100%. The relative activation time was a percentage of each start phase time.

Statistical Analysis

The reconstruction accuracy was tested with the root mean square error of 12 validation points, which did not serve as control points, being noticed resultant errors < 6.5 mm for both the surface and underwater cameras. EMG, temporal and kinematical data are presented as mean and respective standard deviation. It was used the magnitude-based inferences and precision of estimation approaches (Hopkins, 2010), for the digitization error, kinematical and EMG parameters. Magnitude based inference assessed the practical difference in joint angle values between digitization and re-digitization procedures, in phase time, iEMG and relative activation time in-between starting variants and upper and lower limb joint angles at 1^{st} backstroke starting position and starting time between start variants. Differences were assessed via standardized mean differences (SMD), computed with pooled variance, and respective 95% confidence interval (95% CI) (Cohen, 1988). Magnitude thresholds for difference in a mean were described using the following scale: 0-0.2 trivial, > 0.2-0.6 small,

> 0.6-1.2 moderate, > 1.2-2.0 large, and > 2.0 very large (Hopkins, 2010). Effects with 95% CI overlapping zero and/or the smallest worthwhile change (i.e., 0.2 standardized units) were unclear. Statistical computations were performed using the software ESCI (Exploratory Software for Confidence Intervals) (Cumming, 2013).

The iEMG and relative activation time repeatability among starting trials was tested for each upper and lower limb muscle in each start phase and in both start variants by calculating the intraclass correlation coefficient (ICC). It was considered a good reproducibility if ICC ≥ 0.75, moderate if 0.4 ≤ ICC < 0.75 and poor if ICC < 0.4 (Asseldonk et al., 2014).

Results

Unclear differences were noticed for shoulder, elbow, hip, knee and ankle joint angles between digitizing and re-digitizing procedures with trivial magnitude of effect. ICC correlation coefficients calculated among trials for iEMG and relative activation time in each start phase ranged from moderate to good reproducibility values for both variants: (i) hands positioned on the highest horizontal handgrip (ICC = 0.46 to 0.93) and (ii) hands positioned on the vertical handgrip (ICC = 0.49 to 0.82).

Table 1 depicts mean and respective standard deviation of each phase and 15 m start time in both variants.

Table 1. Mean (± standard deviations) of each phase and 15 m time for both backstroke start variants.

Phase	Upper limbs horizontally positioned	Upper limbs vertically positioned
Hands-off (s)	0.55±0.06	0.55±0.06
Take-off (s)	0.21±0.02	0.21±0.03
Flight (s)	0.17±0.08	0.17±0.07
Entry (s)	0.39±0.12	0.39±0.11
15 m (s)	7.14±0.54	7.12±0.57

Figure 3 displays standardized mean difference and respective 95% CI of comparisons between variants for the phase and 15 m start time. All differences were rated as unclear.

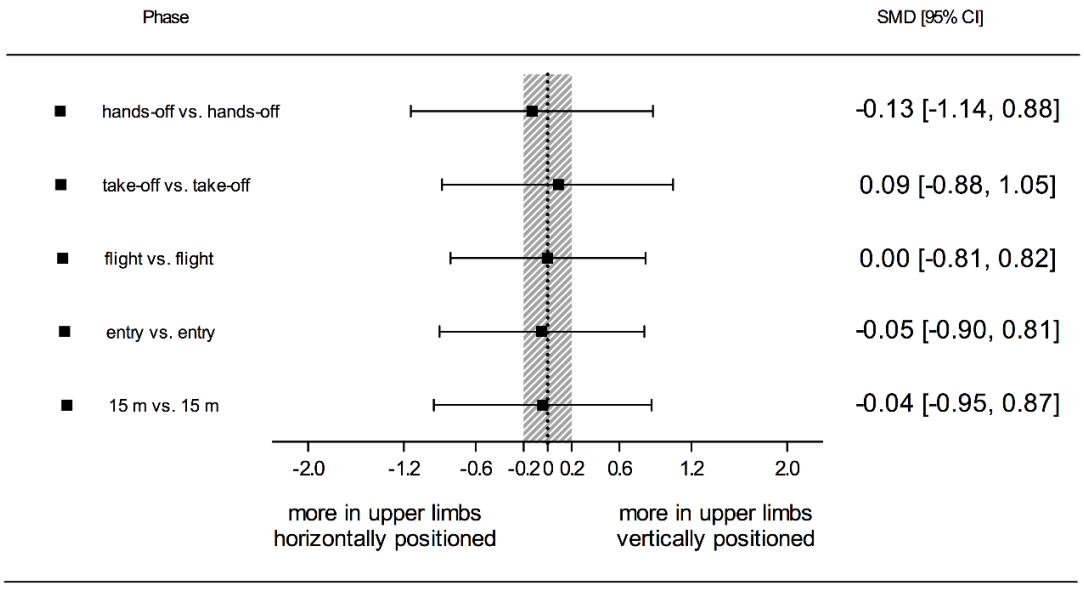

Figure 3. Standardized mean difference (SMD) and 95% confidence intervals (CI) for start phase and 15 m time from comparisons between start variants. The shaded area represents the smallest (trivial differences) worthwhile change.

Table 2 exhibits mean and respective standard deviation of shoulder, elbow, hip, knee and ankle angles at the backstroke start position instant for both variants. All differences between start variants were rated as unclear (i.e. effects with 95% CI overlapping zero and/or the smallest worthwhile change).

Table 2. Mean (± standard deviations) of shoulder, elbow, hip, knee and ankle joint angles for both backstroke start variants.

Joint angle	Upper limbs horizontally positioned	Upper limbs vertically positioned
Shoulder (º)	77.86±14.86	73.70±16.10
Elbow (º)	89.08±26.93	90.07±20.82
Hip (º)	57.77±7.06	58.64±15.45
Knee (º)	52.44±5.34	53.35±7.99
Ankle (º)	38.01±8.97	44.29±10.76

Table 3 depicts iEMG mean and respective standard deviation for each muscle, starting phase and variant.

Table 3. Mean (± standard deviations) of iEMG of each muscle in each phase for both starting variants.

Variant	Variable	Phase	Biceps Brachii	Triceps Brachii	Tibialis Anterior	Gastrocnemius Medialis	Rectus Femoris	Biceps Femoris
Upper limbs horizontally positioned	Active IEMG (%MVIC)	Hands-off	15.12±6.76	12.37±6.80	17.19±5.92	12.38±6.18	9.13±3.78	17.43±4.16
		Take-off	15.17±2.76	2.76±0.26	8.94±5.79	14.47±5.40	24.92±8.88	19.89±9.73
		Flight	22.38±4.25	3.51±2.31	8.48±4.00	11.35±4.65	15.40±6.62	18.06±10.65
		Entry	22.14±6.74	7.59±5.36	10.29±4.56	11.84±6.39	19.22±9.95	10.40±5.87
Upper limbs vertically positioned		Hands-off	18.15±9.54	12.02±8.45	15.54±7.70	15.20±7.07	9.66±4.77	19.45±6.70
		Take-off	14.24±7.11	8.06±4.30	12.94±4.73	27.66±9.84	16.94±8.44	17.20±10.65
		Flight	25.90±8.65	3.40±1.93	6.65±3.94	11.88±5.24	14.20±5.14	16.47±8.41
		Entry	24.59±10.22	7.14±3.41	11.68±4.72	15.19±8.94	18.81±8.27	10.02±6.22

Figure 4 shows standardized mean difference and respective 95% CI for each muscle when comparing the iEMG of each starting phase between start variants. All differences were rated as unclear.

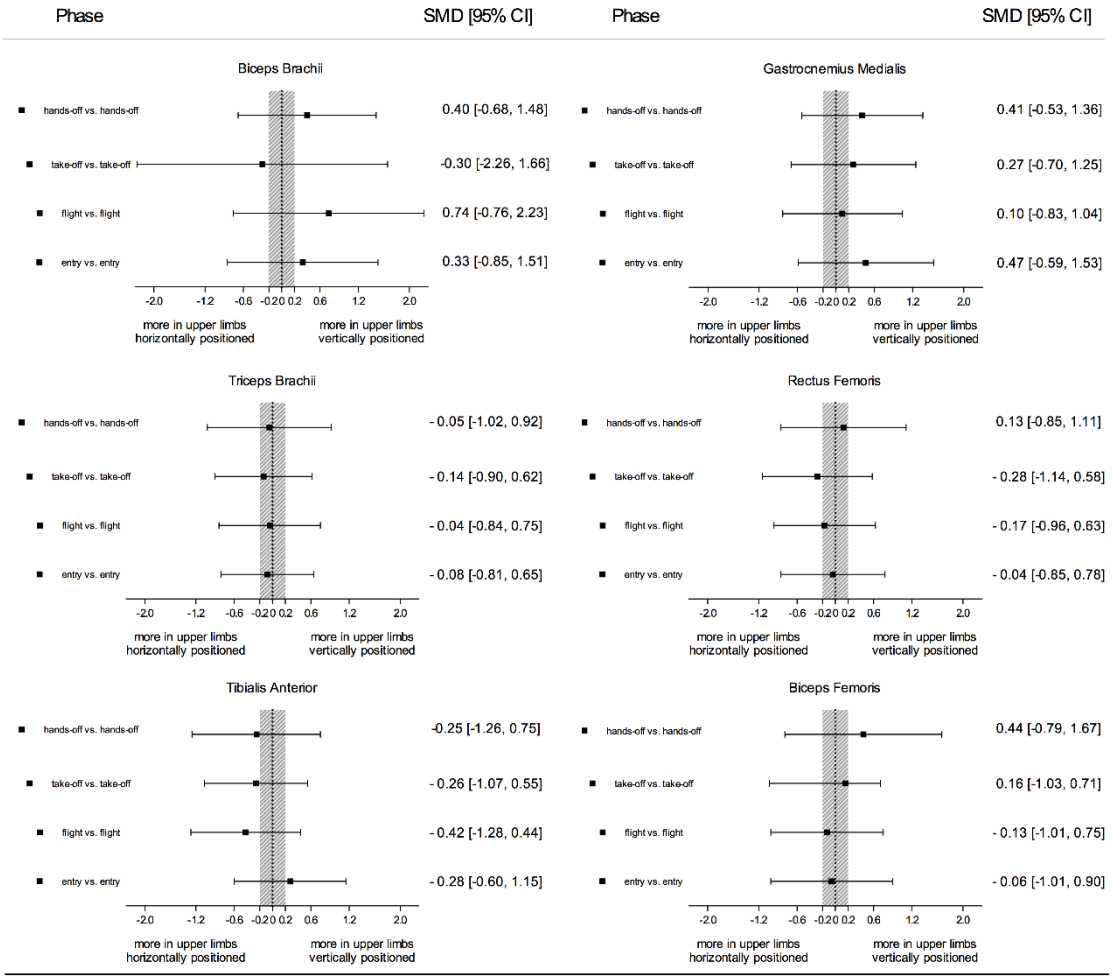

Figure 4. Standardized mean difference (SMD) and 95% confidence intervals (CI) for active iEMG from comparisons between start variants for each muscle and starting phase. The shaded area represents the smallest (trivial differences) worthwhile change.

Table 4 shows standardized mean difference and respective 95% CI for each muscle iEMG when comparing the starting phases for both variants. For upper limbs, the clear differences of the Biceps Brachii comparing flight and entry with the take-off phase presented large to very large magnitude of effect. Triceps Brachii depicted substantial differences between hands-off, take-off and entry and the flight phase (moderate to large magnitude of effect). For lower limbs,

Tibialis Anterior displayed clear differences (moderate to large practical effects) between hands-off and take-off with flight phase. Gastrocnemius Medialis has revealed meaningful differences comparing take-off with hands-off, flight and entry phases (moderate to large magnitude of effect). Rectus Femoris and Biceps Femoris have demonstrated clear differences with large meaningful inferences comparing entry and hands-off phase.

Table 4. Standardized mean difference and 95% CI for iEMG from comparisons between starting phases of each muscle and for both backstroke start variants.

	Phase	Biceps Brachii	Triceps Brachii	Tibialis Anterior	Gastrocnemius Medialis	Rectus Femoris	Biceps Femoris
Upper limbs horizontally positioned	Hands-off vs Take-off	0.01 [-0.76, 0.77]	-0.46 [-1.26, 0.34]	-0.42 [-1.25, 0.41]	1.83 [0.64, 3.03]	2.61 [0.85, 4.37]	0.37 [-1.53, 2.27]
	Hands-off vs Flight	0.96 [0.14, 1.77]	-1.65 [-2.30, -0.99]	-1.35 [-2.09, -0.60]	-0.15 [-0.96, 0.66]	1.52 [0.27, 2.77]	0.14 [-2.05, 2.32]
	Hands-off vs Entry	0.92 [0.03, 1.82]	-1.57 [-2.23, -0.91]	-1.07 [-1.84, -0.29]	-0.08 [-1.00, 0.84]	2.44 [0.54, 4.34]	-1.53 [-2.71, -0.35]
	Take-off vs Flight	2.32 [1.07, 3.58]	-0.86 [-1.54, -0.17]	-1.02 [-1.78, -0.25]	-1.36 [-2.14, -0.58]	-0.42 [-1.17, 0.32]	-0.09 [-1.05, 0.88]
	Take-off vs Entry	2.25 [0.60, 3.89]	-0.21 [-1.04, 0.62]	-0.71 [-1.51, 0.09]	-1.31 [-2.14, -0.48]	-0.06 [-0.96, 0.84]	-0.72 [-1.47, 0.04]
	Flight vs Entry	-0.05 [-1.21, 1.11]	1.61 [0.03, 3.20]	0.41 [-0.51, 1.34]	0.10 [-1.00, 1.19]	0.53 [-0.64, 1.70]	-0.63 [-1.46, 0.21]
Upper limbs vertically positioned	Hands-off vs Take-off	-0.38 [-1.18, 0.43]	-0.43 [-1.13, 0.27]	-0.31 [-1.04, 0.42]	1.61 [0.51, 2.71]	1.39 [-0.03, 2.82]	0.00 [-0.90, 0.90]
	Hands-off vs Flight	0.74 [-0.11, 1.59]	-0.93 [-1.60, -0.26]	-1.06 [-1.76, -0.35]	-0.43 [-1.19, 0.33]	0.87 [-0.06, 1.80]	-0.40 [-1.43, 0.63]
	Hands-off vs Entry	0.62 [-0.31, 1.54]	-0.53 [-1.21, 0.16]	-0.46 [-1.19, 0.27]	0.00 [-0.99, 0.98]	1.75 [0.51, 2.99]	-1.27 [-2.15, -0.40]
	Take-off vs Flight	1.46 [0.43, 2.48]	-0.99 [-1.68, -0.30]	-1.22 [-2.01, -0.42]	-1.45 [-2.19, -0.71]	-0.29 [-1.09, 0.51]	-0.40 [-1.43, 0.63]
	Take-off vs Entry	1.29 [0.16, 2.43]	-0.19 [-0.97, 0.58]	-0.24 [-1.11, 0.62]	-1.15 [-1.99, -0.30]	0.20 [-0.69, 1.09]	-1.27 [-2.15, -0.40]
	Flight vs Entry	-0.14 [-1.13, 0.86]	1.77 [0.51, 3.03]	1.17 [0.22, 2.12]	0.58 [-0.65, 1.80]	0.81 [-0.36, 1.98]	-0.69 [-1.50, 0.11]

Table 5 presents mean and respective standard deviation of relative activation time for each muscle in each starting phase and for both backstroke start variants.

Table 5. Table 5 presents mean and respective standard deviation of relative activation time for each muscle in each starting phase and for both backstroke start variants.

Variant	Variable	Phase	Biceps Brachii	Triceps Brachii	Tibialis Anterior	Gastrocnemius Medialis	Rectus Femoris	Biceps Femoris
Upper limbs horizontally positioned	Activation time (%)	Hands-off	90.63±12.43	73.47±23.91	74.91±15.48	53.50±14.35	53.71±17.23	86.86±11.76
		Take-off	95.14±10.28	72.76±17.59	83.77±15.98	89.46±13.41	86.34±13.08	90.68±12.00
		Flight	95.59±12.18	55.39±20.90	68.46±14.55	79.76±21.01	72.42±19.48	87.77±14.52
		Entry	90.84±19.54	64.56±13.22	65.45±15.49	69.22±21.59	71.93±19.88	88.75±11.13
Upper limbs vertically positioned		Hands-off	94.84±9.87	64.83±27.95	71.29±19.45	54.05±16.60	50.96±21.63	92.86±7.33
		Take-off	97.51±3.86	73.15±23.71	84.45±22.83	93.31±6.24	85.16±14.87	94.24±10.11
		Flight	91.81±11.35	52.23±24.83	59.70±26.92	82.37±21.59	73.72±16.70	91.12±11.43
		Entry	91.06±13.44	55.82±27.44	65.03±17.99	75.14±15.88	80.13±15.32	89.42±9.17

Standardized mean difference and respective 95% CI for each muscle when compared relative activation time between variants are presented in Figure 5. All differences were rated as unclear.

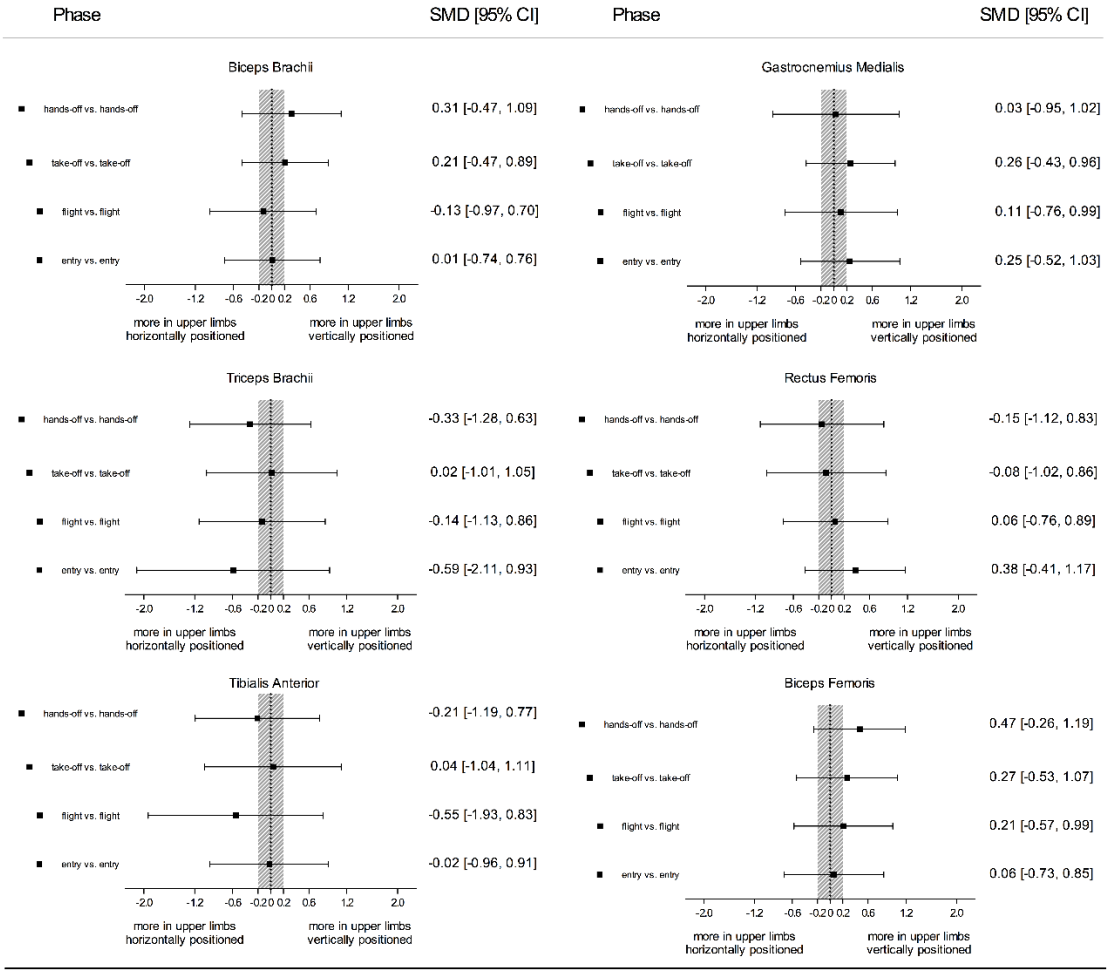

Figure 5. Standardized mean difference (SMD) and 95% confidence intervals (CI) for relative activation time from comparisons between start variants for each muscle and starting phase. The shaded area represents the smallest (trivial differences) worthwhile change.

Table 6 shows standardized mean difference and respective 95% CI for each muscle comparing relative activation time between starting phases for both variants. Considering upper limbs, Biceps Brachii and Triceps Brachii depicted unclear differences at most comparisons. For lower limbs, Tibialis Anterior has shown clear differences between take-off and flight phase (moderate magnitude of effect). Gastrocnemius Medialis and Rectus Femoris displayed substantial differences between take-off and flight, and hands-off phase (moderate to large

meaningful inference). For all starting phase comparisons Biceps Femoris depicted unclear differences.

Table 6. Standardized mean difference and 95% CI for relative activation time from comparisons between starting phases of each muscle and for both backstroke start variants.

	Phase	Biceps Brachii	Triceps Brachii	Tibialis Anterior	Gastrocnemius Medialis	Rectus Femoris	Biceps Femoris
Upper limbs horizontally positioned	Hands-off vs Take-off	0.33 [-0.46, 1.12]	-0.03 [-0.81, 0.76]	0.52 [-0.38, 1.43]	2.26 [1.41, 3.12]	1.73 [0.95, 2.52]	0.30 [-0.57, 1.17]
	Hands-off vs Flight	0.22 [-0.64, 1.07]	-0.68 [-1.54, 0.17]	-0.38 [-1.22, 0.46]	1.65 [0.56, 2.75]	0.99 [0.07, 1.91]	0.07 [-0.90, 1.04]
	Hands-off vs Entry	0.02 [-1.13, 1.16]	-0.34 [-1.10, 0.42]	-0.56 [-1.42, 0.30]	0.99 [-0.13, 2.11]	0.97 [0.04, 1.90]	0.15 [-0.69, 0.99]
	Take-off vs Flight	-6.47 [-7.17, -5.78]	-0.90 [-1.89, 0.08]	-0.87 [-1.71, -0.02]	-0.66 [-1.81, 0.48]	-0.96 [-2.07, 0.15]	-0.22 [-1.18, 0.74]
	Take-off vs Entry	-0.38 [-1.72, 0.96]	-0.43 [-1.23, 0.38]	-1.04 [-1.90, -0.17]	-1.38 [-2.55, -0.21]	-0.99 [-2.12, 0.13]	-0.15 [-0.98, 0.68]
	Flight vs Entry	-0.21 [-1.37, 4.96]	0.40 [-0.39, 1.18]	-0.19 [-1.08, 0.70]	-0.46 [-1.33, 0.42]	-0.02 [-0.89, 0.85]	0.06 [-0.71, 0.83]
Upper limbs vertically positioned	Hands-off vs Take-off	0.25 [-0.44, 0.93]	0.27 [-0.53, 1.07]	0.62 [-0.32, 1.56]	2.14 [1.42, 2.85]	1.45 [0.70, 2.19]	0.17 [-0.87, 1.22]
	Hands-off vs Flight	-0.28 [-1.21, 0.65]	-0.41 [-1.25, 0.43]	-0.54 [-1.64, 0.55]	1.54 [0.53, 2.55]	0.96 [0.17, 1.75]	-0.22 [-1.36, 0.92]
	Hands-off vs Entry	-0.35 [-1.39, 0.69]	-1.89 [-2.55, -1.23]	-0.29 [-1.13, 0.54]	1.15 [0.26, 2.04]	1.23 [0.47, 2.00]	-0.43 [-1.40, 0.55]
	Take-off vs Flight	-1.35 [-3.32, 0.63]	-0.81 [-1.72, 0.11]	-0.99 [-1.97, -0.01]	-1.60 [-3.92, 0.72]	-0.70 [-1.65, 0.25]	-0.28 [-1.20, 0.64]
	Take-off vs Entry	-1.52 [-3.86, 0.81]	-0.67 [-1.64, 0.30]	-0.78 [-1.55, 0.00]	-2.66 [-4.50, -0.82]	-0.31 [-1.21, 0.60]	-0.44 [-1.26, 0.39]
	Flight vs Entry	-0.06 [-1.01, 0.89]	0.13 [-0.83, 1.09]	0.18 [-0.59, 0.95]	-0.31 [-1.08, 0.47]	0.35 [-0.52, 1.22]	-0.14 [-0.92, 0.65]

Discussion

This study compared the muscular activity level and relative activation time in-between two actual backstroke start variants (Figure 1a and 1b). Comparisons were made from the starting signal to the water immersion, underpinned by temporal and angular kinematic data. Our main findings have shown that, independently of the starting phase, all differences between the two variants were considered unclear with magnitude of effect ranging from trivial to moderate in iEMG (Figure 4) and relative activation time (Figure 5), which did not agree with the previous hypothesis established in this study. It was assumed that clear differences between start variants would be observed in upper limbs EMG parameters from the starting signal to the hands-off instant. Secondly, upper and lower limb biarticular muscles were not recruited similarly by the two start variants in hands-off, take-off, flight and entry start phases, in opposite with our initial supposition.

To assess iEMG calculation per phase and relative activation time, the absolute starting phase time was assessed in both variants. Like starting phase times, the two start variants did not differ for the starting performance indicator (i.e. 15 m starting time) (Figure 3). These similarities in performance may justify previous observations (de Jesus, et al., 2014), that elite backstroke swimmers tend to use both starting variants, independently of the gender and competitive event Van Soest et al. (1994) stated that performance will be successful as long as starting postures are close to the preferred position and the jumping execution did not seem to be hampered when the movement has to be started from widely different starting positions. Despite those resemblances, different motor profiles might lead to similar performances (Vantorre et al., 2014). In terms of muscular activity, different body geometries assumed at set positioning have affected the EMG signal amplitude in lat-pull down exercise (Andersen et al., 2014), in throwing (Escamilla & Andrews, 2009) and in jumping (Bobbert et al., 2013; Mackala et al., 2013a, 2013b). These findings are often attributed to the effects of muscle length

changes on their ability to generate force during high velocity contractions (McGowan et al., 2013; Zajac, 2002).

Following the temporal findings, the different handgrip positioning showed an overall similitude between start variants for shoulder, elbow, hip, knee and ankle joint angles at set positioning frame and upper and lower limb EMG parameters thorough the different starting phases. The unclear muscular activation changes during the initial backstroke start phase is probably due to similar intrinsic muscle properties (i.e. muscle length) (McGowan et al., 2013) and seem to reflect similar solicitation of the nervous system as maximal effort is intended (Giroux et al., 2015). As we are dealing with proficient backstroke swimmers, their ability to keep constant the already planned and learned motor task is somewhat prevalent with respect to the necessity to suddenly modify the specific motor task substantially (Camomilla et al., 2009). According to Van Soest et al. (1994) for specific task groups (e.g. explosive leg extensions) a muscle stimulation pattern stored at present in some unspecified form within the central nervous system, which drives to a muscle stimulation pattern that yields successful performance for a wide range of, for instants, starting positions. Complementarily, Rodacki and Fowler (2001) mentioned that the past experiences of individuals could have a meaningful influence on movement output, as they tend to select a stereotyped strategy similar to that previously learnt.

In both variants clear differences in upper and lower limb muscles activation between starting phases were observed. Monoarticular muscles have been pointed out to generate more propulsive energy (Zajac, 2002); however, biarticular muscles were already identified as the most important to increase jumping performance (Pandy & Zajac, 1991). This fact reinforce the still remaining contradictions in biarticular muscles role (Cleather et al., 2015; Youm et al., 2009) highlighting the need to study the respective activation in different backstroke start phases, as previously conducted in upper limbs sports (e.g. Escamilla & Andrews, 2009). In this study, despite Biceps Brachii and Triceps Brachii have displayed several unclear differences between start phases for the relative

muscle activation time, indicating that they were involved in sustaining, propelling and stabilization movements (Hohmann et al., 2008), muscle activity level revealed that these biarticular muscles were more required in specific phases. Regardless of the start variant, Biceps Brachii was more recruited during the flight and entry compared to take-off phase, which might be due to the important glenohumeral stabilizer role. Youm et al. (2009) mentioned that with elbow and forearm movements controlled, Biceps Brachii long head plays an essential active compensatory role in the unstable shoulder. For both start variants, Biceps Brachii also revealed similar iEMG during hands-off and take-off phase, corroborating previous findings in lat pull-down exercises that observed similar Biceps Brachii activation throughout the entire movement (Andersen et al., 2014). Antagonist Triceps Brachii was highly recruited during hands-off and entry compared to the flight phase, suggesting a predominant elbow extension during hands-off followed by the synergistically contraction for shoulder adduction and anterior-posterior stabilization (Hohmann et al., 2008). Biarticular muscles involved in simultaneous joint actions produce less energy themselves, since they are activated to distribute net joint moments to control the direction of force applied externally by the limb (Zajac, 2002).

Considering the mono and biarticular lower limb muscles in both variants, only Biceps Femoris relative activation time was consistent throughout the starting phases, corroborating (Takeda et al., 2014) statement that coaches should focus on hip motion during backstroke start. In fact, swimmers are required to extend their hip joint since the hands-off until the entry phase. Possible great activation of Tibialis Anterior during take-off compared to flight phase can be explained by the antagonist co-activation to prevent ankle hyper-extension (Giroux et al., 2015). To date, none research conducted previously to the current study had concerned about the Tibialis Anterior EMG during backstroke start. Gastrocnemius Medialis was confirmed as the most important contributor to the plantar flexor (Giroux et al., 2015; Zajac, 2002) due to the greater activation displayed during take-off rather than in hands-off and flight phase. Pandy and Zajac (1991) noted that the Gastrocnemius Medialis contributed similarly to the

monoarticular ankle plantarflexors during to improve vertical jump performance. The slight Rectus Femoris relative activation time at hands-off compared to take-off, flight and entry might be explained by lower limb joint rotations sequence timing, which is initiated by the hip extensors during hands-off phase (Takeda et al., 2014). Following take-off, Rectus Femoris is activated to decelerate hip joint extension during flight phase (Giroux et al., 2015) and to extend the knee during the entry phase to maintain the hole-entry (Takeda et al., 2014).

Notwithstanding the originality and relevance of the current data, limitations should be mentioned. Firstly, considering the complexity of our methodology and consistency with previous findings, these results should be considered as preliminary, however important, and used with caution until data on a larger sample can be obtained. Authors recognize that enhanced statistical inference power of results depend upon substantial number of observations, though, ten swimmers is a common mean number used in complex EMG swimming scenarios (Figueiredo et al., 2013; Hohmann et al., 2008; Stirn et al., 2011), being reported noticeable signal variability even in larger sample study designs using normalization procedures (Martens et al., 2015; Pereira et al., 2015). Secondly, five from the six studied muscles have biarticular characteristics (i.e., generating torque, transferring energy and protecting joint passive structures), which are considered to develop less propulsive energy than mono-articular muscles (Zajac, 2002). As contribution of mono and bi-articular muscles were not compared in this study, as previously done for jumping (e.g. Pandy & Zajac, 1991), further researches should analyze if bi-articular muscles display nuanced activity than mono-articular independently of the starting phase. Thirdly, measuring EMG in water is challenging (Martens et al., 2015; Stirn et al., 2011) and findings obtained are considered essential for neuromuscular responses understanding. Nevertheless, it is recommended that further research should integrate EMG, kinematic and kinetic data for better understanding about eventual influence of the new feet wedge on biomechanics of the backstroke start variants. Based on the results reported in this article, it is suggested that similar strength training can be planned for both backstroke start variants; however,

coaches should attempt to select proper exercises for muscles activated at different starting phases to enhance neuromuscular function.

Conclusions

This study has shown unclear differences between two backstroke start variants in EMG parameters (i.e., iEMG and relative activation time) throughout hands-off, take-off, flight and entry starting phases, highlighting swimmers' ability to keep constant the already planned and learned motor task. These results were supported by temporal (15 m time) and angular kinematics (upper and lower limb joint angles at starting position) data, which also displayed similarities between start variants. In addition, comparison of upper and lower limb muscles activation between starting phases evidenced that the bi-articular muscles had contribute differently along starting phases, suggesting a crucial role in backstroke start propulsive actions, as mono-articular muscles. These findings provide coaches with some initial objective evidence to understand the biomechanical effects of different handgrips in backstroke start performance. Coaches should plan similar strength training to improve backstroke start performance of both variants. However further attention should be given on the selection of exercises that activates properly the involved muscles at different starting phases.

Acknowledgments

This work was supported by the CAPES Foundation under doctoral grant (BEX 0761/12-5/2012-2015) and FCT Foundation under grant (EXPL/DTP-DES/2481/2013- FCOMP-01-0124-FEDER-041981).

References

Abdel-Aziz, Y.I., & Karara, H.M. (1971). Direct linear transformation: from comparator coordinates into object coordinates in close range photogrammetry. Symposium on Close-Range Photogrammetry: Urbana, Illinois, 1-18.

Andersen, V., Fimland, M., Wiik, E., Skoglund, A., & Saeterbakken, A. (2014). Effects of grip width on muscle strength and activation in the lat pull-down. *Journal of Strength & Conditioning Research, 28*(4), 1135-1142.

Asseldonk, E., Campfens, S., Verwer, S., Putten, M., & Stegeman, D. (2014). Reliability and agreement of intramuscular coherence in tibialis anterior muscle. *PLoS ONE, 9*(2), 1-10.

Barbosa, T., Fernandes, R., Morouco, P., & Vilas Boas, J. P. (2008). Predicting the intra-cyclic variation of the velocity of the centre of mass from segmental velocities in butterfly stroke: A pilot study. *Journal of Sport Science and Medicine, 7*(2), 201-209.

Basmajian, V., & De Luca, J. (1985). Muscles alive: Their functions revealed by electromyography (5th ed.). Baltimore.

Bobbert, M., Casius, L., & Kistemaker, D. (2013). Humans make near-optimal adjustments of control to initial body configuration in vertical squat jumping. *Neuroscience, 1*(237), 232-242.

Camomilla, V., Sbriccoli, P., Di Mario, A., Arpante, A., & Francesco, F. (2009). Comparison of two variants of a Kata technique (Unsu): The neuromechanical point of view. *Journal of Sports Science and Medicine, 8*(3), 29-35.

Cleather, D., Southgate, D., & Bull, A. (2015). The role of the biarticular hamstrings and gastrocnemius muscles in closed chain lower limb extension. *Journal of Theoretical Biology, 365*(21), 217-225.

Cohen, J. (1988). Statistical power analysis for the behavioral sciences (2nd ed.). Hillsdale, NJ: Lawrence Erlbaum Associates.

Conceição, A., Silva, A., Barbosa, T., Karsai, I., & Louro, H. (2014). Neuromuscular Fatigue during 200 M Breaststroke. *Journal of Sports Science and Medicine, 13*(1), 200-210.

Cumming, G. (2013). The new statistics: Estimation for better research. Retrieved from http://www.thenewstatistics.com.

Day, S. (2002). Important factors in surface EMG measurement, Bortec Biomedical Ltd., Calgary.

de Jesus, K., de Jesus, K., Figueiredo, P., Gonçalves, P., Pereira, S., Vilas-Boas, J.P., & Fernandes, R. (2011). Biomechanical analysis of backstroke swimming starts. *International Journal of Sport Medicine, 32*(7), 546-551.

de Jesus, K., Figueiredo, P., de Jesus, K., Pereira, F., Vilas-Boas, J., Machado, L. , & Fernandes, R.J. (2012). Kinematic analysis of three water polo front crawl styles. *Journal of Sport Science, 30*(7), 715-723.

de Jesus, K., de Jesus, K., Figueiredo, P., Gonçalves, P., Pereira, S., Vilas-Boas, J.P., & Fernandes, R.J. (2013). Backstroke start kinematic and kinetic changes due to different feet positioning. *Journal of Sports Sciences, 31* (15), 1665-1675.

de Jesus, K., de Jesus, K., Medeiros, A, Fernandes, R. J., & Vilas Boas, J. P. (2014). The bacstroke starting variants performed under the current swimming rules and block configuration. *Journal of Swimming Research, 22*(1), 1-11.

Escamilla, R., & Andrews, J. (2009). Shoulder muscle recruitment patterns and related biomechanics during upper extremity sports. *Sports Medicine, 39*(7), 569-590.

Figueiredo, P., Rouard, A., Vilas Boas, J. P., & Fernandes, R.J. (2013). Upper-and lower-limb muscular fatigue during the 200-m front crawl. *Applied Physiology, Nutrition, and Metabolism, 38*, 716-724.

Giroux, C., Guilhem, G., Couturier, A., Chollet, D., & Rabita, G. (2015). Is muscle coordination affected by loading condition in ballistic movements? *Journal of Electromyography and Kinesiology, 25*(1), 69-76.

Hermes, J., Freriks, B., Disselhorst-Klug, C., & Rau, G. (2000). Development of recomendation for SEMG sensors and sensor placement procedures. *Journal of Electromyography and Kinesiology, 10*(5), 361-374.

Hodges, P., & Bui, B. (1996). A comparison of computer-based methods for determination of on set of muscle contraction using electromyography. *Electroencephalography and Clinical Neurophysiology, 101*(6), 511-519.

Hohmann, A., Fehr, U., Kirsten, R., & Krueger, T. (2008). Biomechanical analysis of the backstroke start technique in swimming. *E-Journal Bewegung und Training, 2*, 28-33.
Hopkins, W. (2010). Linear models and effect magnitudes for research, clinical and practical applications. *Sport science, 14*, 49-57.
Mackala, K., Stodółka, J. , Siemienski, A., & Coh, M. (2013a). Biomechanical analysis of standing long jump from varying starting positions. *Journal of Strength and Conditioning Research, 27*(10), 2674-2684.
Mackala, K., Stodółka, J., Siemienski, A., & Coh, M. (2013b). Biomechanical analysis of squat jump and countermovement jump from varying starting positions. *Journal of Strength and Conditioning Research, 27*(10), 2650-2661.
Martens, J., Figueiredo, P., & Daly, D. (2015). Electromyography in the four competitive swimming strokes: A systematic review. *Journal of Electromyography and Kinesiology, 25*(2), 273-291.
McGowan, C., Neptune, R., & Herzog, W. (2013). A phenomenological muscle model to assess history dependent effects in human movement. *Journal of Biomechanics, 46*(1), 151-157.
Nguyen, C., Bradshaw, E., Pease, D., & Wilson, C. (2014). Is starting with the feet out of the water faster in backstroke swimming? *Sports Biomechanics, 13*(2), 154-165.
Pandy, M., & Zajac, F. (1991). Optimal muscular coordination strategies for jumping. *Journal of Biomechanics, 24*(1), 1-10.
Pereira, S.M., Ruschel, C., Hubert, M., Machado, L., Roesler, H., Fernandes, R.J., & Vilas-Boas, J.P. (2015). Kinematic, kinetic and EMG analysis of four front crawl flip turn techniques. *Journal of Sports Sciences, 27*, 1-10.
Rodacki, A., & Fowler, N. (2001). Intermuscular coordination during pendulum rebound exercises. *Journal of Sport Science, 19*(6), 411-425.
Stirn, I., Jarm, T., Kapus, V., & Strojnik, V. (2011). Evaluation of muscle fatigue during 100-m front crawl. *European Journal of Applied Physiology, 111*(1), 101-113.
Takeda, T., Itoi, O. , Takagi, H., & Tsubakimoto, S. (2014). Kinematic analysis of the backstroke start: differences between backstroke specialists and non-specialists. *Journal of Sports Sciences, 32*(7), 635-641.
Van Soest, A.J., Bobbert, M.F., & Van Ingen Schenau, G.J. (1994). A control strategy for the execution of explosive movements from varying starting positions. *Journal of Neurophysiology, 71*(4), 1390-1402.
Vantorre, J., Chollet, D., & Seifert, L. (2014). Biomechanical analysis of the swim-start: a review. *Journal of Sports Science and Medicine, 13*(2), 223-231.
Youm, T., ElAttrache, N.S., Tibone, J.E., McGarry, M.H., & Lee, T.Q. (2009). The effect of the long head of t he biceps on glenohumeral kinematics. *Journal of Shoulder and Elbow Surgeons, 18*(1), 122-129.
Zajac, F. (2002). Understanding muscle coordination of the human leg with dynamical simulations. *Journal of Biomechanics, 35*(8), 1011-1018.

Chapter 7

Are the new starting block facilities beneficial for backstroke start performance?

Karla de Jesus[1], Kelly de Jesus[1], J. Arturo Abraldes[2], Alexandre I.A. Medeiros[1,3], Ricardo J. Fernandes[1,4], João Paulo Vilas-Boas[1,4].

[1] Centre of Research, Education, Innovation and Intervention in Sport, Faculty of Sport, University of Porto, Porto, Portugal.
[2] Department of Physical Activity and Sport, Faculty of Sports Sciences. University of Murcia. Murcia, Spain.
[3] Department of Physical Education, University of Fortaleza, Fortaleza, Brazil.
[4] Porto Biomechanics Laboratory (LABIOMEP), Porto, Portugal

Submitted for publication on Journal of Sports Sciences.

Abstract

We aimed to analyse the handgrip positioning and the wedge effects on the backstroke start performance and technique. Ten swimmers completed randomly eight 15 m backstroke starts (four with hands on highest horizontal and four on vertical handgrip) performed with and without wedge. One surface and one underwater camera recorded kinematic data. Standardized mean difference (SMD) and 95% confidence intervals (CI) were used. Handgrip positioning did not affect kinematics with and without wedge use. Handgrips horizontally positioned and feet over wedge displayed greater knee angular velocity than without it (SMD = -0.82; 95% CI: -1.56, -0.08). Hands vertically positioned and feet over wedge presented greater take-off angle (SMD = -0.81; 95% CI: -1.55, -0.07), centre of mass (CM) vertical positioning at first water contact (SMD = -0.97; 95% CI: -1.87, -0.07) and CM vertical velocity at CM immersion (SMD = 1.03; 95% CI: 0.08, 1.98) when comparing without wedge use. Swimmers extended the hip previous to the knee and ankle joints, except for the variant with hands vertically positioned without wedge (SMD = 0.75; 95% CI: -0.03, 1.53). Swimmers should preserve biomechanical advantages achieved during flight with variant with hands vertically positioned and wedge throughout entry and underwater phase.

Key words: Biomechanics, kinematics, competitive swimming, swimming facility rules, dorsal start

Introduction

An effective swimming start, from the auditory signal to the 15 m mark, can represent up to ~ 30% of the final time in short-distance events (Slawson, et al., 2013; Vantorre et al., 2014), leading the biomechanists to examine it in detail. Three primary and interdependent phases have contributed to the scanning of the overall start time, the block/wall (11%), flight (5%) and underwater (84%) (Houel et al., 2013; Slawson et al., 2013). In 2009 and 2013, the Federation Internationale de Natation (FINA) had authorized facility rule changes that could allow swimmers to take the most out of each backstroke start phase. This fact combined with the complexity to perform successful backstroke start technique comparing with those for ventral events (de Jesus et al., 2013; Nguyen et al., 2014) had led the scientific community to a growing concern about the backstroke start technique (de Jesus et al., 2014a).

Recently, studies have been conducted to show the effects of positioning feet entirely immersed and emerged (FINA rules, SW 6.1) on backstroke start performance indicators, regardless handgrips configuration (de Jesus et al., 2013; Nguyen et al., 2014). In those, authors have assessed start phase times, time to reach 5 - 15 m mark, hip or centre of mass (CM) horizontal and vertical position at auditory signal and at swimmers' hands or head water contact, hip or CM horizontal and vertical velocity at swimmers' hands-off, take-off and hip or CM immersion, take-off and entry angles. Despite researchers having mentioned that many competitive backstrokers have altered their starting technique to place their feet entirely emerged (Nguyen et al., 2014), findings have revealed contradictory results regarding which starting variant should be the most recommended for improving performance (de Jesus et al., 2013; Nguyen et al., 2014).

In 2014, researchers revealed that ~ 40% of the 2012 London Olympic Games and 2013 Barcelona Swimming World Championships swimmers used the backstroke start variants with feet parallel and partially immersed and hands on

the highest horizontal and vertical handgrips (de Jesus et al., 2014b). The great acceptance of these variants independent of backstroke event could indicate few biomechanical differences between them. The use of the wedge in those start variants could increase the vertical CM displacement, take-off angle and flight distance, considered decisive for successful backstroke start performance (de Jesus et al., 2011; Nguyen et al., 2014; Takeda et al., 2014). In fact, the wedge obviates part of friction mechanism, allowing better feet wall contact and masking pure static friction effects, which lead to the need of vertical force component hybridization including the vertical wall reaction force.

To understand how the handgrips and wedge might affect backstroke start technique, using deterministic model variables (Guimaraes & Hay, 1985) would provide coaches with initial objective evidence about backstroke start variant selection. However, to explain how swimmers organize the most propulsive segment actions when facing those new facilities could reveal technique adaptations for coaches' feedback at backstroke start training sessions. Researchers have highlighted that successful backstroke start performance depends upon greater hip and knee maximal angular velocity and former joint earlier extension (Takeda et al., 2014). Despite authors having shown similar joint couplings regardless of varying rebound jump starting position (Rodacki & Fowler, 2001), it would be expectable that the new wedge could allow swimmers to benefit from a proximal-to-distal lower limb extension sequence (Van Ingen Schenau, 1989). The current study aimed to analyse the handgrip positioning and the wedge use effects on the backstroke start performance and technique.

Methods

Participants

Ten male national-level swimmers (mean and respective standard deviations: age 21.1 ± 5.36 years, stature 1.78 ± 0.04 m, body mass 72.82 ± 10.05 kg, training background 12.6 ± 6.13 years, mean performance for the 100 m

backstroke in 25 m pool of 59.67 ± 2.89 s, representing 78.7 ± 3.6 % of the 100 m backstroke short course World Record) volunteered to participate in the study. All participants were healthy (no serious injury or illness occurred in the last 6 months), able-bodied and had participated in national level competitions. Data collection was approved according to the local research ethics committee, and all experimental procedures conformed to requirements stipulated in the Declaration of Helsinki. Swimmers and parents and/or guardians (when participants were under 18 years) provided informed written consent before data collection.

Backstroke start variants

Two backstroke start variants were studied, both with the feet parallel and partially emerged and the hands on the highest horizontal or vertical handgrip, but performed with (Figure 1a and b, respectively) and without wedge (Figure 1c and d, respectively). The horizontal handgrip was positioned 0.56 m above water level and the vertical was welded to join the lowest (0.43 m above water level) and highest horizontal handgrip. The selection of those two starting variants was based on the high swimmers' percentage that perform backstroke start with feet partially emerged and hands grasping horizontally or vertically the grips (de Jesus et al., 2014b). The starting block, handgrips and wedge pair were custom-built complying with FINA facility rules (FR 2.7 and 2.10), and each wedge pair was positioned 0.04 m above the water level and fixed on an instrumented pool wall.

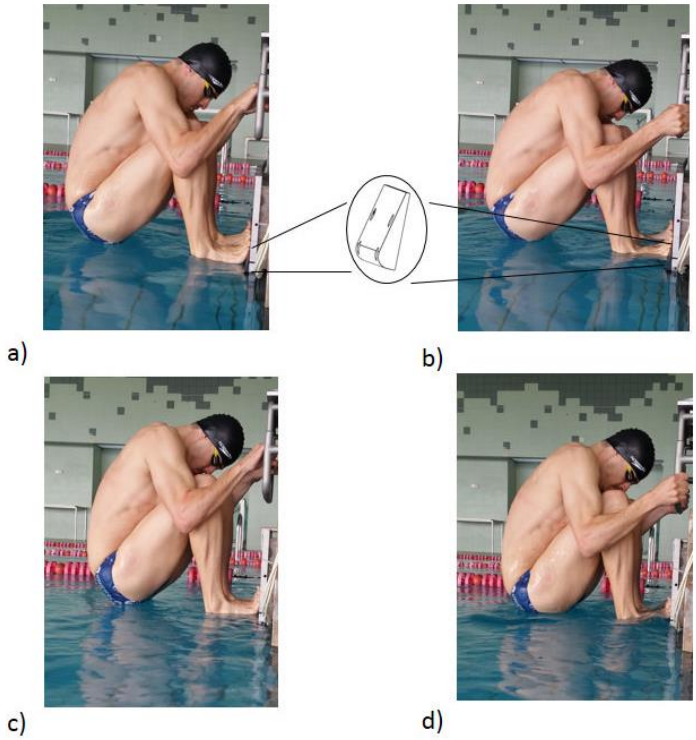

Figure 1. Backstroke start variants positioning at auditory signal. Hands on highest horizontal handgrip and feet positioned over wedge (a). Hands on vertical handgrip and feet positioned over wedge (b). Hands on highest horizontal handgrip and feet positioned without wedge (c). Hands on vertical handgrip and feet positioned without wedge (d).

Starting trials

Swimmers' height and body mass were measured and they answered a questionnaire for background information assessment about their 100 m backstroke start performance. Each swimmer performed a standardized warm up consisting of 600 m front crawl and backstroke swimming, followed by a familiarisation period of each backstroke start variant studied. For that purpose, both variants were verbally described by the research team (complying with FINA rules, SW 6.1), as well as visually depicted by video recordings. Moreover, verbal instruction and feedback were given during familiarisation to ensure that the start variants were performed correctly (Nguyen et al., 2014). Participants were marked at joint centres with black waterproof tape (0.018 m) for tracking during digitizing process.

Swimmers participated on two testing sessions of 1 h each in a 25 m indoor and heated (27ºC) swimming pool. Between sessions the wedge pair was fixed (or removed) from the instrumented pool wall. Each swimmer randomly performed four maximal 15 m repetitions of each backstroke start variant (with and without wedge), a total of 16 repetitions, with 2 min and 1h rest in-between each trial and sessions (respectively), with the mean values being calculated and used in subsequent statistical analysis. Starting signals were produced through a starter device (StartTime IV acoustic start, Swiss Timing Ltd., Switzerland) conformed to FINA swimming rules (SW 4.2) and instrumented to simultaneously generate the auditory starting signal and export a light to the video system.

Data collection

Swimmers were videotaped in the sagittal plane for 2D kinematic analysis using a dual media set-up with two stationary and synchronized cameras (HDR CX160E, Sony Electronics Inc., Japan), operating at 50 Hz sampling frequency with 1/250 digital shutter speed. Each camera was placed in a waterproof housing (SPK-CXB, Sony Electronics Inc., Japan) and fixed on a specially designed support for video image-recording. This support was placed at the lateral pool wall, 2.6 m from the starting wall and 6.78 m away from the backstroke start trajectory and perpendicularly to the line of swimmers' motion. Surface and underwater cameras were aligned and placed 0.15 m above and 0.20 m below water level, respectively. A rectangular frame (4 m length [horizontal axis], 2.5 m height [vertical axis] and 2 m width [lateral axis]) was used for starting space calibration and was leaned on the starting pool wall and 0.80 m above the water level with the horizontal axis aligned with the starting direction (cf. de Jesus et al., 2015). A pair of light emitting diodes, visible in each 4.5 m long camera view, was fixed at one of the vertical calibration frame rods.

To enable swimmers' tracking, the following 13 anatomical landmarks were identified on the right side of the body: the vertex of the head (using a swim cap), mid-gonion, acromion, lateral epicondyle of humerus, ulnar styloid process of the wrist, 3rd hand distal phalanx, xyphoid, iliac crest, great trochanter of the femur,

lateral epicondyle of the femur, lateral malleolus, calcaneus and 1st foot distal phalanx. These markers have defined a 10-segment anthropometric model (de Leva, 1996), as used before (de Jesus et al., 2013).

Data processing

The surface and underwater video images were independently digitised frame-by-frame by the same operator using the Ariel Performance Analysis System (Ariel Dynamics Inc., USA) (Gourgoulis et al., 2015). Image coordinates were transformed into 2D object-space coordinates using the Direct Linear Transformation algorithm (Abdel-Aziz & Karara, 1971) with six calibration points, as done before (Barbosa et al., 2015; de Jesus et al., 2013). Following these studies, a 5 Hz cut-off value for data filtering was selected (with a low pass digital filter) done according to residual analysis (residual error vs. cut-off frequency). To determine the accuracy of calibration procedure, the root mean square error of six validation points on the calibration frame, which did not serve as control points, was calculated (respectively for horizontal and vertical axes): (i) 2.32 and 2.22 mm, representing 0.05% and 0.08% of the calibrated space for surface and (ii) 4.72 and 4.59 mm, representing 0.10% and 0.16% of the calibrated space for underwater camera. The accuracy of the digitising procedure of each variable of interest was determined based on data from two repeated digitisations of a randomly selected trial (de Jesus et al., 2013; Figueiredo et al., 2009), and subsequently tested with the statistical analysis described below.

Data analysis

Backstroke start variants were divided into four phases (adapted from de Jesus et al., 2013; Hohmann et al., 2008): (i) hands-off – between the auditory signal and the instant the swimmers' hand left the handgrips (1st positive horizontal swimmers' hand 3rd distal phalanx coordinate); (ii) take-off – from the hands-off until the swimmers' foot left the wall (1st positive horizontal swimmers' foot 1st distal phalanx coordinate); (iii) flight – from the take-off until the swimmers' CM immersion (1st negative swimmers' CM vertical coordinate); and (iv) entry – from the final instant of the flight phase until the swimmers' foot immersion (1st negative

swimmers' foot 1st distal phalanx vertical coordinate). Linear and angular kinematical variables were: (i) absolute hands-off, take-off, flight and entry phase time; (ii) starting time when the middle of the swimmers' head reaches the 5 m distance; (iii) CM horizontal and vertical position at the auditory signal, in relation to the starting pool wall and water surface, respectively; (iv) CM horizontal and vertical position at the swimmers' hand 3rd distal phalanx immersion, in relation to the starting pool wall and water surface, respectively; (v) CM horizontal and vertical velocity at hands-off, take-off, CM and swimmers' full immersion; (vi) take-off angle, formed by the lateral epicondyle of the femur, the lateral malleolus and the horizontal axis; (vii) upper limbs entry angle at the swimmers' hand 3rd distal phalanx immersion (formed by the lateral epicondyle of humerus, the ulnar styloid process of the wrist and the horizontal axis); (viii) upper trunk entry angle at the swimmers' hand 3rd distal phalanx immersion (formed by the acromion, the xyphoid and the horizontal axis); and (ix) maximum hip, knee and ankle angular velocity and respective time. Each individual hip, knee and ankle joint angular velocity curve was normalized from the auditory signal to the CM immersion to assess the respective maximum values and time using a customised module (MatLab R2014a, The MathWorks Inc., USA).

Statistical procedures

Data are presented as mean and respective standard deviations. Magnitude-based inference and precision of estimation approach (Hopkins, 2010) was calculated to assess digitizing reliability and practical differences in linear and angular kinematical parameters in-between backstroke start variants. Differences were assessed via standardized mean differences (SMD) computed with pooled variance, and respective 95% confidence intervals (CI) (Cohen, 1988). Magnitude thresholds for difference in a mean were described using the following scale: 0-0.2 trivial, > 0.2-0.6 small, > 0.6-1.2 moderate, > 1.2-2.0 large and > 2.0 very large (Hopkins, 2010). Effects with 95% CI overlapping zero and/or the smallest worthwhile change (i.e. 0.2 standardized units) were defined as unclear. All statistical computations were performed using a specifically designed Excel

spreadsheet (Cumming, 2013). Differences between digitized and re-digitized trials for linear and angular kinematic variables were unclear.

Results

Table 1 depicts mean and respective standard deviations of linear and angular kinematic parameters for backstroke start variant with hands horizontal and vertically positioned (performed in both conditions with and without wedge.

Table 1. Mean and respective standard deviations of linear and angular kinematic parameters for each backstroke start variant performed in both conditions, with and without wedge.

Variables	Horizontal		Vertical	
	With wedge	Without wedge	With wedge	Without wedge
Hands off phase time (s)	0.56±0.06	0.57±0.05	0.57±0.07	0.57±0.07
Take off phase time (s)	0.22±0.04	0.21±0.04	0.22±0.04	0.21±0.04
Flight phase time (s)	0.35±0.08	0.33±0.07	0.35±0.08	0.31±0.07
Entry phase time (s)	0.26±0.10	0.26±0.12	0.28±0.07	0.23±0.13
5 m time (s)	1.97±0.14	2.03±0.14	1.97±0.16	2.05±0.14
CM horizontal position at starting signal (m)	0.39±0.05	0.40±0.03	0.38±0.05	0.40±0.03
CM vertical position at starting signal (m)	0.28±0.09	0.25±0.08	0.26±0.09	0.24±0.08
CM horizontal position at water contact (m)	1.77±0.20	1.71±0.17	1.77±0.19	1.67±0.16
CM vertical position at water contact (m)	0.33±0.07	0.29±0.05	0.33±0.06	0.27±0.06
CM horizontal velocity at hands-off ($m.s^{-1}$)	1.73±0.34	1.86±0.48	1.80±0.28	1.85±0.40
CM vertical velocity at hands-off ($m.s^{-1}$)	0.70±0.28	0.60±0.29	0.71±0.23	0.56±0.31
CM horizontal velocity at take-off ($m.s^{-1}$)	3.85±0.31	3.68±0.27	3.85±0.37	3.76±0.28
CM vertical velocity at take-off ($m.s^{-1}$)	-0.22±0.46	-0.28±0.42	-0.27±0.43	-0.38±0.38
CM horizontal velocity at CM immersion ($m.s^{-1}$)	3.14±0.39	2.84±0.35	3.16±0.49	2.87±0.15
CM vertical velocity at CM immersion ($m.s^{-1}$)	-2.34±0.26	-2.11±0.29	-2.32±0.26	-2.03±0.29
CM horizontal velocity at body immersion ($m.s^{-1}$)	2.40±0.40	2.28±0.31	2.44±0.36	2.34±0.32
CM vertical velocity at body immersion ($m.s^{-1}$)	-1.61±0.31	-1.62±0.37	-1.57±0.20	-1.61±0.35
Take off angle (º)	27.24±6.84	23.04±4.88	26.85±6.26	21.31±3.98
Upper limbs entry angle (º)	51.29±9.07	55.12±6.91	52.61±8.88	59.14±10.63
Upper trunk entry angle (º)	31.73±8.67	25.46±6.61	35.79±13.85	24.94±7.60
Maximum hip angular velocity (rad/s)	7.67±0.72	7.00±1.24	7.76±1.03	6.66±1.29
Maximum hip angular velocity time (%)	54.90±3.22	54.63±6.52	53.41±7.08	56.61±8.21
Maximum knee angular velocity (rad/s)	15.79±1.72	14.40±0.88	15.53±2.05	14.50±1.45
Maximum knee angular velocity time (%)	62.45±5.01	61.89±5.18	62.30±6.10	63.86±5.39
Maximum ankle angular velocity (rad/s)	13.76±1.00	13.50±1.93	13.84±0.83	14.25±2.95
Maximum ankle angular velocity time (%)	62.70±5.33	63.11±5.07	61.63±6.07	64.75±5.97

Table 2 shows SMD and respective 95% CI of comparisons between start variant with hands horizontally and vertically positioned when both performed with and without wedge. Despite only comparisons with small magnitude of effect being displayed, magnitude of effects ranged from trivial to small and all differences were unclear.

Table 2. Standardized mean difference and respective 95% confidence interval of comparisons between start variant with hands horizontally and vertically positioned performed in both conditions, with and without wedge for linear and angular kinematic parameters that displayed small or greater magnitude of effect (threshold).

Variables	With wedge		Without wedge	
	Horizontal vs. vertical	Magnitude of thresholds	Horizontal vs. vertical	Magnitude of thresholds
Entry phase time	-	-	-0.30 (-1.30, 0.70)	Small
CM horizontal position at water contact	-	-	-0.23 (-1.12, 0.65)	Small
CM vertical position at water contact	-	-	-0.43 (-1.41, 0.54)	Small
CM horizontal velocity at take-off	-	-	0.00 (-0.94, 0.94)	Small
CM vertical velocity at take-off	-	-	-0.21 (-1.07, 0.66)	Small
CM vertical velocity at CM immersion	-	-	0.24 (-0.66, 1.15)	Small
Take off angle	-	-	-0.32 (-1.15, 0.51)	Small
Upper limbs entry angle	0.53 (-0.67, 1.72)	Small	0.43 (-0.73, 1.59)	Small
Upper trunk entry angle	0.43 (-0.73, 1.59)	Small	-	-
Maximum hip angular velocity	-	-	-0.25 (-1.17, 0.68)	Small
Maximum hip angular velocity time	-0.40 (-1.92, 1.12)	Small	0.26 (-0.77, 1.29)	Small
Maximum knee angular velocity	-0.21 (-1.17, 0.75)	Small	-	-
Maximum knee angular velocity time	-	-	0.32 (-0.60, 1.25)	Small
Maximum ankle angular velocity	-	-	0.25 (-0.86, 1.36)	Small
Maximum ankle angular velocity time	-	-	0.28 (-0.72, 1.27)	Small

Table 3 shows SMD and respective 95% CI of comparisons between starting conditions (with and without wedge) for start variants with hands horizontally and vertically positioned. Only comparisons with small to greater magnitude of effect were shown, and few variables registered clear differences, being all with

moderate magnitude of effect. Start variant with hands horizontally positioned and with wedge depicted greater knee angular velocity. Start variant with hands vertically positioned performed with the wedge displayed greater CM vertical position at first water contact, take-off angle and CM vertical velocity at CM immersion.

Table 3. Standardized mean difference and respective 95% confidence interval of comparisons between wedge conditions (with and without) in both start variants, horizontal and vertical handgrips positioning for linear and angular kinematic parameters that displayed small or greater magnitude of effect (threshold).

Variables	Horizontal		Vertical	
	With vs. Without wedge	Magnitude of thresholds	With vs. Without wedge	Magnitude of thresholds
Take off phase time	-0.24 (-1.08, 0.58)	Small	-0.35 (-1.20, 0.49)	Small
Flight phase time	-0.24 (-1.08, 0.58)	Small	-0.35 (-1.20, 0.49)	Small
Entry phase time	-	-	-0.69 (-2.04, 0.66)	Moderate
5 m time	0.42 (-0.47, 1.31)	Small	0.47 (-0.37, 1.30)	Small
CM horizontal position at starting signal	0.30 (-0.40, 1.00)	Small	0.45 (-0.33, 1.23)	Small
CM vertical position at starting signal	-0.29 (-1.11, 0.54)	Small	0.25 (-1.10, 0.59)	Small
CM horizontal position at water contact	-0.29 (-1.10, 0.53)	Small	-0.47 (-1.28, 0.35)	Small
CM vertical position at water contact	-0.51 (-1.28, 0.27)	Small	-0.97 (-1.87, -0.07)	Moderate
CM horizontal velocity at hands-off	0.35 (-0.76, 1.46)	Small	-	-
CM vertical velocity at hands-off	-0.33 (-1.24, 0.57)	Small	-0.59 (-1.68, 0.50)	Small
CM horizontal velocity at take-off	-0.49 (-1.31, 0.34)	Small	-0.22 (-1.01, 0.56)	Small
CM vertical velocity at take-off	-	-	-0.23 (-1.07, 0.61)	Small
CM horizontal velocity at CM immersion	-0.72 (-1.57, 0.12)	Moderate	-0.55 (-1.22, 0.13)	Moderate
CM vertical velocity at CM immersion	0.81 (-0.14, 1.76)	Moderate	1.03 (0.08, 1.98)	Moderate
CM horizontal velocity at body immersion	-0.27 (-1.07, 0.52)	Small	-0.25 (-1.10, 0.59)	Small
Take off angle	-0.56 (-1.33, 0.20)	Small	-0.81 (-1.55,- 0.07)	Moderate
Upper limbs entry angle	0.39 (-0.40, 1.17)	Small	0.67 (-0.32, 1.66)	Moderate
Upper trunk entry angle	-0.66 (-1.45, 0.13)	Moderate	-0.72 (-1.43, 0.00)	Moderate

Maximum hip angular velocity	-0.85 (-2.16, 0.46)	Moderate	-0.97 (-1.98, 0.05)	Moderate
Maximum hip angular velocity time	-	-	0.39 (-0.58, 1.37)	Small
Maximum knee angular velocity	-0.82 (-1.56, -0.08)	Moderate	-0.48 (-1.24, 0.28)	Small
Maximum knee angular velocity time	-	-	0.22 (-0.62, 1.06)	Small
Maximum ankle angular velocity	-	-	0.32 (-1.87, 2.51)	Small
Maximum ankle angular velocity time	-	-	0.45 (-0.44, 1.33)	Small

Figure 2 shows SMD and respective 95% CI of comparisons between times of maximum hip, knee and ankle joint angular velocity in the start variants performed with hands horizontally and vertically positioned (with and without wedge). Comparisons that revealed trivial magnitude of effect were excluded from Figure 2. It was observed that the hip was the first joint to be extended (magnitude of effects ranging from moderate to very large), followed by the simultaneous knee and ankle extension, excepting the variant with upper limbs vertically positioned performed without wedge.

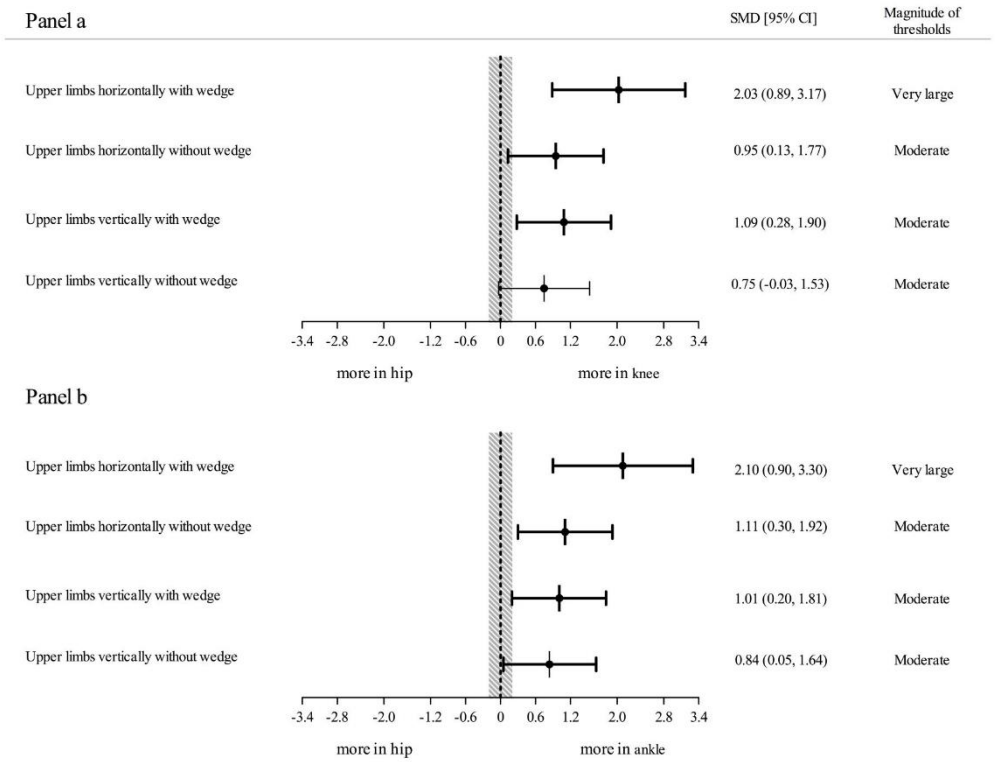

Figure 2. SMD (standardized mean difference) and respective 95% CI (confidence interval) of comparisons between time at maximum joint velocity in backstroke start variant with hands horizontally and vertically positioned performed in both conditions, with and without wedge, whose magnitude of effect (threshold) was small or greater. Comparison between time at maximum hip and knee angular velocity (a). Comparison between time at maximum hip and ankle angular velocity (b).

Discussion

The current study is the first that analyzed the handgrip positioning and the wedge use effects on the backstroke start performance and technique. Main findings have revealed that: (i) different handgrips positioning had not affected the linear and angular kinematic parameters; (ii) the variant with hands horizontally positioned displayed greater knee extension angular velocity with the wedge; (iii) the start variant with hands vertically positioned increased the take-off angle, CM vertical position at first water contact and CM vertical velocity at CM water immersion with the wedge; and (iv) the wedge use had not implied a proximal-to-

distal lower limb joint extension sequence when swimmers starting with hands horizontally or vertically positioned, being the hip the first joint to be extended, excepting the variant with hands vertically positioned performed without the wedge. The above-mentioned findings partially confirm the assumptions already established in this study, since it was presumed that the handgrips would not affect backstroke start kinematics and the wedge use would increase vertical CM displacement, take-off angle, flight distance, and consequently, reducing start time through a proximal-to-distal lower limb joint extension sequence.

After the implementation of the current starting block configuration (Omega OSB11, Swiss Timing, Ltd., Switzerland), which has been depicted in ventral start studies (Slawson et al., 2013; Takeda et al., 2012), researchers have observed that, regardless the competitive event, elite swimmers have often adopted the start variant with feet positioned partially emerged and hands on the highest horizontal and vertical handgrips (de Jesus et al., 2014b). As expected, the handgrips positioning had not changed backstroke start performance and swimmers had used similar lower limb joint extension couplings to propel themselves out of the starting wall. In fact, starting performance seems to be successful as long as initial set positioning is sufficiently close to the preferred backstroke start variant, as previously noticed in rebound jumping (Rodacki & Fowler, 2001). Previous ventral start studies revealed that several similar start styles could lead to similar start performance (Seifert et al., 2010; Vantorre et al., 2014). It is important to note that previous researches considering the start variant with feet parallel and positioned entirely emerged (without wedge) have shown swimmers' CM or hip starting position ~ 0.20 m above the water level (de Jesus et al., 2013; Nguyen et al., 2014). In the current study, the two start variants performed with and without wedge registered mean values of CM vertical coordinate at starting position ranging from 0.24 to 0.28 m. Therefore, it is suggested that both handgrip configurations performed with and without wedge contribute to a better-suited CM setup position, which is considered a backstroke start performance determinant (Nguyen et al., 2014; Takeda et al., 2014).

The wedge implementation is based upon previous biomechanical advantages reported in studies analyzing the outdated start variants performed with the gutter supporting (for a more detailed description see de Jesus et al., 2014a). Backstrokers who hold themselves on the wedge might benefit from greater vertical force that can provide a less resistant CM aerial pathway reducing swimmers' deceleration (de Jesus et al., 2013; Takeda et al., 2014). In this study, the wedge use increased the knee extension angular velocity when swimmers performed start variants with hands horizontally positioned, which did not imply a greater CM vertical positioning, as previously reported (Takeda et al., 2014). Contrarily, the wedge use in the starting variant with hands vertically positioned depicted greater take-off angle, CM vertical position at first water contact and CM vertical velocity at CM immersion, considered decisive to reduce start time (de Jesus et al., 2011; Guimaraes & Hay, 1985). Based on these evidence, it seems that the use of the wedge combined with the vertical handgrips might allow swimmers obtaining biomechanical advantages that, if sustained throughout the underwater phases, could result in reduced start time, as previously recommended (de Jesus et al., 2013). Despite the confidence intervals having indicated unclear 5 m start time differences between wedge conditions in both start variants, it could be evidenced clear feet support benefits in backstroke start performance if a larger sample had been studied. In addition, it would take longer for proficient competitive swimmers to familiarize themselves enough to improve their start performance using the new facilities (Nguyen et al., 2014).

The underwater phase impact on overall start time is well reported (de Jesus et al., 2014a; Vantorre et al., 2014); however, the wall/block phase determines what happens in the flight and subsequently, in the underwater phase (Slawson et al., 2013; Takeda et al., 2009; Vantorre et al., 2014). In the light of this start phases interdependency, the authors have attempted to clarify coaches how swimmers coordinate their lower limb joint actions to generate proper take-off angle with less resistant flight and entry phases, and consequently improving overall backstroke start performance (Takeda et al., 2014). For those authors, proficient backstrokers perform the start extending the hip prior to the knee joint with high

angular velocity. Despite most of the current findings corroborating previous backstroke start (Takeda et al., 2014) and rebound jump studies (Rodacki & Fowler, 2001) regarding the anticipated hip join extension, the improved feet indentation provided by the wedge had not resulted in a clear proximal-to-distal joint extension sequence. Much research has suggested that throwing, striking, jumping and kicking skills all exhibit aspects of proximal-to-distal sequencing to produce the largest possible velocity at the end of a linked chain of segments (Marshall & Elliott, 2000; Van Ingen Schenau, 1989). The simultaneous knee and ankle joint extension observed in the current study seems to be explained by a swimmer's strategy to deal with short take-off angle to generate a maximum horizontal force before swimmers' feet contact to the wall (de Jesus et al., 2013; Hohmann et al., 2008). Indeed, the authors have mentioned that different explosive movements might impose constraints of an external and/or anatomical nature, which could imply the requirements of either a sequential or simultaneous strategy (Ravn et al., 1999). In addition, those authors have indicated that the level of trunk inclination explains the choice of a sequential or simultaneous strategy (Ravn et al., 1999).

Notwithstanding the originality and relevance of the current data, some study's limitations should be addressed. Firstly, the sample size, which undermines the confidence intervals and, therefore, the precision of the presented effect size estimations. Ten participants were selected in the current study, which is a reasonable number in experiments that require swimmers' availability for familiarization and testing protocols using complex data methodology (Houel et al., 2013; Nguyen et al., 2014; Takeda et al., 2009). Secondly, the familiarization period followed previous study protocols and strategies were implemented to reduce the start variant bias (e.g. Nguyen et al., 2014). However, future studies should consider taking a longer training period to allow swimmers to improve their performance using the new starting block facilities, as previously suggested (Nguyen et al., 2014; Takeda et al., 2012). Lastly, the recent approved wedge can be adjusted in five heights related to the water level, as the ventral start back plate (Takeda et al., 2012), and in the current study only the highest positioning

was chosen (i.e. 0.04 m above water level) due to the high percentage of swimmers that prefer to perform backstroke start with feet above water level (de Jesus et al., 2014b). Future studies should investigate in detail how swimmers overcome the task constraints imposed by the combination of different handgrip and wedge positioning from the auditory signal to the 15 m mark.

Conclusions

The current study analyzed the handgrips configuration and wedge effects on backstroke start performance and technique. The results have shown that positioning the hands on the highest horizontal or vertical handgrip had not affected backstroke start performance and the intralimb coordinative strategy before take-off propulsion. However, the wedge use revealed biomechanical advantages during the flight phase when combined to the vertical handgrip, as greater take-off angle, CM vertical positioning and CM vertical velocity at partial immersion, even when swimmers were using similar lower limb coordination. From a practical perspective, the present results would suggest that swimmers could take backstroke start performance advantages if they used the variant with vertical handgrip and the wedge. However, swimmers should maintain the biomechanical advantages resulting from a more vertical flight pathway throughout the entry and underwater phase for successful start performance. In spite of the apparent restricted lower limb coordination strategy disregarding the start variant and wedge condition (with or without), coaches should consider training with other wedge positioning to decide upon which start variant is the most appropriated for each swimmer.

Disclosure statement

No potential conflict of interest was reported by the authors.

Funding

This work was supported by the Brazil Coordination for the Improvement of Higher Education Personnel Foundation, Ministry of Education of Brazil (0761-12-5/2012-2015); the Foundation for Science and Technology of Portugal (EXPL/DTP-DES/2481/2013-FCOMP-01-0124-FEDER-041981) and the Séneca Foundation (19615/EE/14).

References

Abdel-Aziz, Y., & Karara, H. (1971). Direct linear transformation: from comparator coordinates into object coordinates in close range photogrammetry. In: ASP *Symposium on Close-Range Photogrammetry*, United States. 1-18.

Barbosa, T.M., de Jesus, K., Abraldes, A., Ribeiro, J., Figueiredo, P., Vilas-Boas, J.P., & Fernandes, R.J. (2015). Effects of protocol step length on biomechanical measures in swimming. *International Journal of Sports Physiology and Performance, 10*(2), 211-218.

Cohen, J. (1988). Statistical power analysis for the behavioral sciences (2nd ed.): Hillsdale, NJ: Lawrence Erlbaum Associates.

Cumming, G. (2013). The new statistics: Estimation for better research. Retrieved from http://www.thenewstatistics.com.

de Jesus, K., de Jesus, K., Figueiredo, P., Gonçalves, P., Pereira, S., Vilas-Boas, J.P., & Fernandes, R.J. (2011). Biomechanical analysis of backstroke swimming starts. *International Journal of Sports Medicine, 32*(7), 546-551.

de Jesus, K., de Jesus, K., Figueiredo, P., Gonçalves, P., Pereira, S., Vilas-Boas, J.P., & Fernandes, R.J. (2013). Backstroke start kinematic and kinetic changes due to different feet positioning. *Journal of Sports Sciences, 31*(15), 1665-1675.

de Jesus, K., de Jesus, K., Fernandes, R.J., Vilas-Boas, J.P., & Sanders, R. (2014a). The backstroke swimming start: state of the art. *Journal of Human Kinetics, 42*, 27-40.

de Jesus, K., de Jesus, K., Medeiros, A., Fernandes, R.J., & Vilas-Boas, J.P. (2014b). The backstroke starting variants performed under the current swimming rules and block configuration. *Journal of Swimming Research, 22*(1), 1-11.

de Jesus, K., de Jesus, K., Figueiredo, P., Vilas-Boas, J.P., Fernandes, R.J., & Machado, L. (2015). Reconstruction accuracy assessment of surfasse and underwater 3D motion analyis: a new approach. *Computational and Mathematical Methods in Medicine*, ID 269264, doi: 10.1155/2015/269264.

de Leva, P. (1996). Adjustments to Zatsiorsky-Seluyanov's segment inertia parameters. *Journal of Biomechanics, 29*(9), 1223-1230.

Figueiredo, P., Vilas-Boas, J.P., Maia, J., Gonçalves, P., & Fernandes, R.J. (2009). Does the hip reflect the centre of mass swimming kinematics? *International Journal of Sports Medicine, 30*(11), 779-781.

Gourgoulis, V., Boli, A., Aggeloussis, N., Antoniou, P., Toubekis, A., & Mavromatis, G. (2015). The influence of the hand's acceleration and the relative contribution of drag and lift forces in front crawl swimming. *Journal of Sports Sciences, 33*(7), 696-712.

Guimaraes, A., & Hay, J. (1985). A mechanical analysis of the grab starting technique in swimming. *International Journal of Sport Biomechanics, 1*, 25-35.

Hohmann, A., Fehr, U., Kirsten, R., & Krueger, T. (2008). Biomechanical analysis of the backstroke start technique in swimming. *E-Journal Bewegung und Training, 2*, 28-33.

Hopkins, W. (2010). Linear models and effect magnitudes for research, clinical and practical applications. *Sport science, 14*, 49-58.

Houel, N., Elipot, M., André, F., & Hellard, P. (2013). Influence of angles of attack, frequency and kick amplitude on swimmer's horizontal velocity during underwater phase of a grab start. *Journal of Applied Biomechanics, 29*(1), 49-54.

Marshall, R., & Elliott, B. (2000). Long-axis rotation: The missing link in proximal-to-distal segmental sequencing. *Journal of Sports Sciences, 18*(4), 247-254.

Nguyen, C., Bradshaw, E., Pease, D., & Wilson, C. (2014). Is starting with the feet out of the water faster in backstroke swimming? *Sports Biomechanics, 13*(1), 1-12.

Ravn, S., Voight, M., Simonsen, E. B., Alkjaer, T., BØjsen-Moller, F., & Klausen, K. (1999). Choice of jumping strategy in two standard jumps, squat and countermovement jump-effect of training background or inherited preference? *Scandinavian Journal of Medicine and Science in Sports, 9*(4), 201-208.

Rodacki, A.L., & Fowler, N. (2001). Intermuscular coordination during pendulum rebound exercises. *Journal of Sports Sciences, 19*(6), 411-425.

Seifert, L., Vantorre, J., Lemaitre, F., Chollet, D., Toussaint, H.M., & Vilas-Boas, J.P. (2010). Different profiles of the aerial start phase in front crawl. *Journal of Strength and Conditioning Research, 24*(2), 507-516.

Slawson, S.E., Conway, P.P., Cossor, J., Chakravorti, N., & West, A.A. (2013). The categorisation of swimming start performance with reference to force generation on the main block and footrest components of the Omega OSB11 start blocks. *Journal of Sports Sciences, 31*(5), 468-478.

Takeda, T., Ichikawa, H., Takagi, H., & Tsubakimoto, S. (2009). Do differences in initial speed persist to the stroke phase in front-crawl swimming? *Journal of Sports Sciences, 27*(13), 1449-1454.

Takeda, T., Takagi, H., & Tsubakimoto, S. (2012). Effect of inclination and position of new swimming starting block's back plate on track-start performance. *Sports Biomechanics, 1*(3), 370-381.

Takeda, T., Itoi, O., Takagi, H., & Tsubakimoto, S. (2014). Kinematic analysis of the backstroke start: differences between backstroke specialists and non-specialists. *Journal of Sports Science, 32*(7), 635-641.

Van Ingen Schenau, G.J. (1989). From rotation to translation: constraints on multi-joint movements and the unique action of bi-articular muscles. *Human Movement Science, 8*(4), 301-337.

Vantorre, J., Chollet, D., & Seifert, L. (2014). Biomechanical analysis of the swim-start: a review. *Journal of Sports Science and Medicine, 13*(2), 223-231.

Chapter 8

Lateral kinetic proficiency and asymmetry in backstroke swimming start.

Karla de Jesus[1], Kelly de Jesus[1], Diogo Duarte[1], Daniel Pires[1], Marcelo C. Torres[1], Pedro Gonçalves[1], Luis Mourão[1,2], Hélio Roesler[3], Maria O. Vasconcelos[1], Ricardo J. Fernandes[1,4], Mário A. P. Vaz[5], João Paulo Vilas-Boas[1,4].

[1] Centre of Research, Education, Innovation and Intervention in Sport, Faculty of Sport, University of Porto, Porto, Portugal

[2] Superior School of Industrial Studies and Management, Porto Polytechnic Institute, Vila do Conde, Portugal.

[3] Aquatic Biomechanics Research Laboratory, Health and Sports Science Centre University of the State of Santa Catarina, Florianópolis, Santa Catarina, Brazil

[4] Porto Biomechanics Laboratory (LABIOMEP), Porto, Portugal

[5] Institute of Mechanical Engineering and Industrial Management, Faculty of Engineering, University of Porto, Porto, Portugal

Submitted for publication on Journal of Applied Biomechanics.

Abstract

This study aimed to compare preferred and non-preferred upper and lower limb kinetics and respective asymmetry between two backstroke start variants. It has also correlated upper and lower limb kinetics asymmetry with 5 m start time. Ten competitive swimmers completed randomly eight 15 m backstroke starts, four with horizontal and four with vertical hands positioning. Handedness and footedness were assessed via questionnaires. An instrumented starting block registered right and left upper and lower limb kinetics and an underwater video camera recorded 5 m time. The following results could be found when using hands horizontally and vertically positioned, respectively: (i) preferred upper limb depicted shorter horizontal force peak (N/BW) before hands-off (-0.40 [-0.46 and -0.31] vs. -0.31 [-0.38 and -0.28]), and (ii) preferred lower limb displayed greater horizontal force at 2nd peak before take-off (0.83 [0.78 and 0.86] vs. 0.83 [0.75 and 0.91]). Variant with hands vertically positioned depicted greater lower limb asymmetry for horizontal impulse [(N/BW).s, 0.14 (0.05 and 0.17)]. Lower limb horizontal force asymmetry at 1st peak contributed 82% in 5 m start time variation with hands horizontally positioned. It is recommended that coaches evaluate and control lateral kinetic differences to attenuate force discrepancies and improve backstroke start performance.

Key words: Biomechanics, Ground reaction forces, Limb proficiency, Swimming start, Performance.

Introduction

An effective swimming start (from auditory signal to the 15 m mark) is crucial to the final race result especially at short distance events (Hardt et al, 2009). It is elucidative that during the 2013 Long-Course Swimming World Championship, men's 2nd place finisher in 100 m backstroke was 0.20 s slower at the 15 m mark than the winner, with the final race time differing only 0.19 s. Since 2005 to 2013, the Fédération Internationale de Natation (FINA) introduced new backstroke start rules (SW 6.1), authorising swimmers to emerge their feet, as well as innovative handgrips and a feet support changing the block configuration (FR 2.7 and 2.10, respectively). Those innovations triggered an increasing enthusiasm towards research in swimming starts, being recently described that elite swimmers perform the backstroke start using the highest horizontal or vertical handgrip regardless the competitive level and event length (de Jesus et al., 2014b).

Researches in backstroke start have focused mainly on kinematics assessment to explain 5, 7.5, 10 and 15 m performance, without taking into account the recent FINA rule changes (e.g. Takeda et al., 2014). Kinetic studies are still scarce and have prioritized lower limbs horizontal and resultant force pattern as an important precursor to understand how backstroke start movement was performed with feet entirely immersed and emerged (de Jesus et al., 2011, 2013; Nguyen et al., 2014). Authors have revealed a double peak force profile corresponding to instants just before hands-off and take-off and also have found strong relationships between the 2nd resultant peak force and 7.5 m start performance (Nguyen et al., 2014), as well as between the horizontal lower limbs impulse and 5 m start performance (de Jesus et al., 2013). Upper limbs horizontal reaction force was assessed twice, being noticed a single peak force generated before the hands-off, which was related to traction force exerted to compensate the lower limbs extension movement (de Jesus et al., 2011, 2013).

Despite the existence of previous meaningful backstroke start kinetic contributions, no study has considered limb lateral dominance according to

preference, proficiency and asymmetry, as done for ventral starts (Hardt et al., 2009). As in bilateral countermovement jump (Stephens et al., 2007), it is expectable that upper and lower limbs would contribute equally to generate backstroke start propulsion. In fact, it seems mechanically disadvantageous to generate unbalanced forces in swimming starts, since it could impair symmetric steering goal (Mourão et al., 2015) and, consequently, overall start performance due to interdependency of swimming start phases (Vantorre, et al., 2014). However, it is natural to develop one body side as the accuracy-dominant and the other as the strength-dominant, which may promote unequal use and development of skill across age span (Carpes et al., 2010; Gabbard & Hart, 1996). Thus, a certain degree of asymmetry has been accepted as no detrimental to swimming (Mouroço et al., 2015), countermovement and squat jump performance (Yoshioka et al., 2010, 2011); but it should be evaluated and controlled during training season (Luk et al., 2014; Sanders et al., 2015).

It has been noticed that high-level athletes of bilateral sports present reduced lateralization in regularly practiced tasks than their less skilled counterparts, suggesting that reduced one-hand/foot bias is a performance advantage (dos Santos et al., 2013; Stockel & Valter, 2014; Teixeira et al., 2011). In addition, this reduced one limb preference bias was not considered a specific adaptation of preferred limb to the bilateral sports demands (Stockel & Valter, 2014). The current study compared preferred and non-preferred upper and lower limb kinetics in two backstroke start variants (with horizontal vs. vertical handgrip) and has analysed respective handgrip effects on kinetics asymmetry. In addition, relationships between upper and lower limbs kinetic asymmetry and start performance were analysed for both start variants. It was hypothesized that backstroke swimmers would report kinetic differences between preferred and non-preferred upper and lower limbs in both start variants, rather than similarities between variants of kinetic asymmetry. Furthermore, it was expected that greater upper and lower limbs kinetic asymmetry would increase backstroke start time regardless the used hands positioning.

Methods

Participants

Ten male competitive backstroke swimmers, all right-hand and footed (mean ± s: age 21.1 ± 5.36 yrs., stature 1.78 ± 0.04 m, body mass 72.82 ± 10.05 kg, training background 12.6 ± 6.13 yrs. and mean performance for the 100 m backstroke in 25 m pool of 59.67 ± 2.89 s representing 78.7 ± 3.6 % of the 100 m backstroke short course World Record) volunteered to participate. All participants were healthy (no serious injury or illness occurred in the last six months), able-bodied and had participated in national level competitions. Data collection was approved according to the local research ethics committee and all experimental procedures corresponded to requirements stipulated in the Declaration of Helsinki. Swimmers and parents and/or guardians (when subjects were under 18 yrs.) were provided informed written consent before data collection.

Procedures

Swimmers answered a questionnaire to assess background information about their 100 m backstroke performance, handedness (Van Strien, 2002) and footedness (Coren, 1993), in accordance with the literature (Freitas et al., 2014). After measuring height and body mass, swimmers performed a standardized warm up consisting of 600 m freestyle and backstroke swimming (cf. Hardt et al., 2009) in a 25 m indoor and heated (27ºC) swimming pool, followed by a familiarisation period of each studied starting variant (Figure 1). Both start variants were performed with feet over a wedge, but with hands on highest horizontal (0.56 m above water level) or vertical handgrip (Figure 1, a and b panels, respectively). Selection of those variants was based on the high percentage of swimmers that choose perform them as previously described (de Jesus et al., 2014b). Backstroke start variants were verbally described and visually depicted by video recordings to each participant, and verbal instruction and feedback were given during familiarisation to ensure that start variants were performed correctly (Nguyen et al., 2014). Each swimmer performed randomly eight maximal 15 m repetitions, being four of each backstroke start variant, with

2 min rest in-between. Median value of the four trials for each swimmer in each start variant was calculated and used in subsequent statistical analysis (cf. de Jesus et al., 2013).

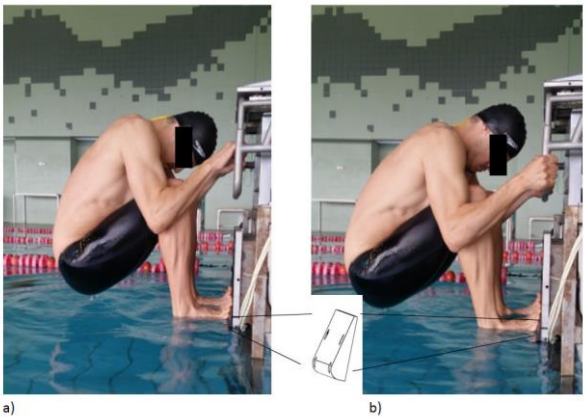

Figure 1. The two backstroke start variants, both with the feet parallel in two wedge conditions (with or without), but with hands on the highest horizontal (Figure 1a) or vertical (Figure 1b) handgrip.

Data collection

All start trials were performed on an instrumented starting block complying with FINA facility rules (FR. 2.7 and 2.10) (under patent request – INPI 108229) with four tri-axial waterproof force plates (designed according to Roesler et al., 2006), two for upper and two for lower limbs independent force measurements. Upper limbs force plates were laterally fixed on a custom-built starting block, with one pair of independent handgrips fixed each one over each force plate top. Lower limb force plates were vertically positioned on a custom-built underwater structure fixed on starting pool wall. Two independent wedges were fixed each one over each underwater force plate top at 0.04 m above water level (FR 2.10). The two force plate pairs (for upper and lower limbs kinetic analysis) have a sensitivity of 0.5 N, error < 5% and resonance frequency of 300 and 200 Hz, respectively. Dynamic calibration followed similar steps used in unanimated rigid body falling (Mourão et al., 2015), revealing homogeneity of results for static calibration. Each force plate was instrumented with waterproof strain gauges (Kyowa, Electronic Instruments, Japan), arranged in independent Wheatstone bridges. Each cable from each Wheatstone bridge was connected to an analogue-to-digital converter

module for strain signals reading (NI9237, National Instruments Corp., USA) fixed on respective chassis (CompactDAQ USB-9172 and Ethernet-9188 National Instruments Corporation, USA). A custom-designed data processing software (executable file) was created in LabView 2013 (SP1, National Instruments Corp., USA) to acquire (2000 Hz sampling rate), plot and save the strain readings from each force plate.

Swimmers were videotaped with one underwater stationary and synchronized (using lighting emitting diode) video camera (HDR CX160E, Sony Electronics Inc., Japan) placed in a waterproof housing (SPK-CXB, Sony Electronics Inc., Japan) and fixed on a special built support. It operated at 50 Hz sampling frequency with 1/250 s exposure time and was positioned in the lateral (2.6 m away from the starting block wall), perpendicular to the line of swimmers' motion (6.78 m away from the backstroke start trajectory) and 0.20 m below the water surface. Starting signals were produced through a starter device (Omega StartTime IV acoustic start, Swiss Timing Ltd., Switzerland) conform to FINA swimming rules (SW 4.2), allowing kinetic and kinematic data synchronization through simultaneously starting command generation, analogue-to-digital converter module triggering and light emitting diode lightning for video camera view.

Data analysis

For handedness assessment, participants indicated the hand they would use (left/right/any preference) for a particular activity (e.g. throw a ball, stir with a spoon or hold an eraser when rubbing out something) involving a certain object (e.g. ball, spoon or eraser). Each questionnaire item from a total of ten items was coded from -1 to 1, with "left" receiving a score of -1, "right" receiving a score of 1 and "both" receiving a score of 0, with the total score ranging from -10 to 10. For the purpose of the current study, swimmers were considered to be left-handed or right-handed if their total questionnaire score ranged from -10 and -4 and from 4 and 10, respectively (Van Strien, 2002).

For footedness determination, each questionnaire item from a total of five items (e.g. foot selected to catch a little stone with toes or to climb a step) was coded as 1 for “left” and “right”, and “both” receiving a score of 1 for the simultaneous “right” and “left” preference. The laterality coefficient (Porac & Coren, 1981) was calculated as described in Equation 1. If laterality coefficient was ≤ 0, swimmers were classified as left-footed and if it was > 0 right-footed (Coren, 1993).

$$Laterality\ coefficient = \left(\frac{right\ foot\ total\ tasks - left\ foot\ total\ tasks}{total\ task\ number}\right) * 100 \qquad (1)$$

All swimmers were right-handed and footed. Two processing custom-designed routines created in MatLab R2014a (The MathWorks Inc., USA) were used to: (i) convert strain readings (με) to force values (N) and (ii) filter the horizontal and vertical upper and lower limbs force curves (4th order zero-phase digital Butterworth filter with a cut-off frequency of 10 Hz; cf. de Jesus et al., 2011). Kinetic data from right and left upper and lower limbs were normalized to each swimmer’s body weight and to time (i.e. from auditory signal to hands-off and to take-off, for upper and lower limb force, respectively). Horizontal and vertical normalized impulse was assessed from right and left upper and lower limb force-time curves as time integral of horizontal and vertical force component from auditory signal to hands-off and to take-off, respectively. The following critical instants from each individual’s right and left upper and lower limb horizontal force-time curve were selected: (i) upper limb force at auditory signal; (ii) upper limb peak force and time before hands-off; (iii) lower limb force at auditory signal; (iv) 1st lower limb peak force and time before hands-off; (v) intermediate lower limb force and time at hands-off; and (vi) 2nd lower limb peak force and time before take-off (cf. Figure 2). Functional motor asymmetry index was calculated from each kinetic parameter by subtracting the preferred and non-preferred limb values (absolute value; cf. dos Santos et al., 2013).

The time from auditory signal until the swimmers’ head reaches the 5 m distance was determined.

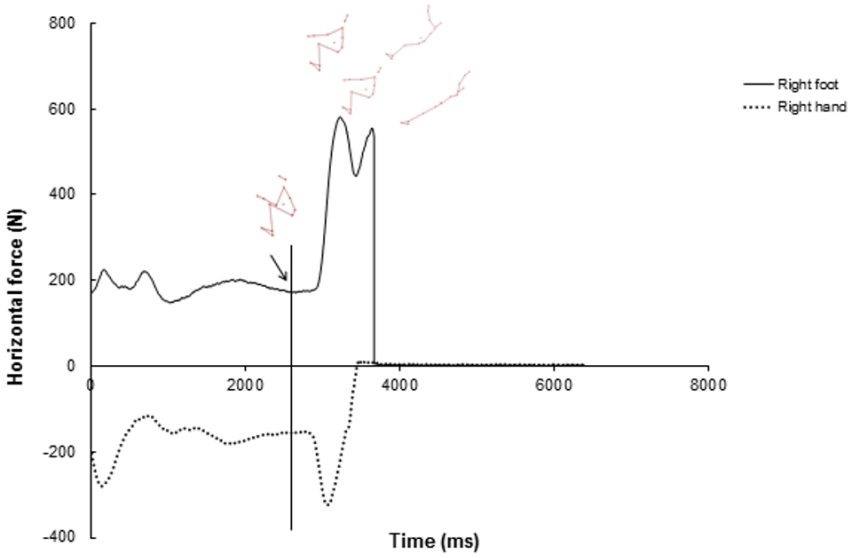

Figure 2. The critical force instants determined in each individual horizontal upper and lower limb force-time curve: (i) upper limb force at auditory signal; (ii) upper limb peak force and time before hands-off instant; (iii) lower limb force at auditory signal; (iv) 1st lower limb peak force and time before hands-off instant; (v) intermediate lower limb force and time at hands-off instant; and (vi) 2nd lower limb peak force and time before take-off instant.

Statistical Analysis

Tests were performed using Statistical Package for Social Sciences 21 software (SPSS, IBM, USA) and significance level was set at $p \leq 0.05$. Since kinetic variables did not satisfy assumptions of normality and homogeneity of variance, median and interquartile range (Q1-Q3) were used, which are considered suitable values of central tendency and dispersion for non-parametric data. Wilcoxon signed-rank test was used to determine if: (i) kinetic (dependent variables) differed between preferred and non-preferred upper and lower limbs (independent variables) for both backstroke starting variants and (ii) upper and lower limbs functional motor kinetic asymmetries (dependent variables) differed between backstroke starting variants (independent variables). Effect size was calculated using the following Equation (2).

$$r = \frac{Z}{\sqrt{N}} \quad (2)$$

Where N is the total number of observations on which Z is based. Criterion for interpreting absolute effect size considered a trivial effect size if $0 \leq r \leq 0.09$, small if $0.1 \leq r < 0.3$, medium if $0.3 \leq r < 0.5$, large if $0.5 \leq r \leq 0.69$, and very large if ≥ 0.7 (Cohen's, 1988).

Spearman's correlation coefficient was calculated between upper and lower limbs kinetic asymmetry and 5 m start time for both starting variants. Correlations magnitude was based on the following scale (Munro, 2001): very weak if $0 \leq r \leq 0.25$, weak if $0.26 \leq r \leq 0.49$, moderate if $0.50 \leq r \leq 0.69$, strong if $0.70 \leq r \leq 0.89$, and very strong $0.90 \leq r \leq 1.0$.

Results

Median and respective interquartile range values for upper limb kinetic parameters for starting variants with hands horizontally and vertically positioned, as well as Z, exact p and effect size (r) values of comparisons between preferred and non-preferred upper limbs were presented (Table 1). For the backstroke start with hands horizontally positioned it was noticed greater horizontal force at auditory signal and peak force for non-preferred upper limb (with very large effect size). Upper limb horizontal and vertical impulses were greater for non-preferred (very large effect size) and preferred limb (large effect size), respectively. For the backstroke start variant with hands vertically positioned, it was observed greater horizontal force at auditory signal and peak force and time for non-preferred upper limb (all with very large effect size). Upper limb horizontal and vertical impulse was greater for non-preferred and preferred upper limb (very large effect size), respectively.

Table 1. Median and interquartile range (Q1 and Q3) of kinetic parameters for both starting variants (hands horizontally and vertically positioned) with Z, exact p and effect size (r) reported for comparisons between preferred and non-preferred upper limb.

	Variables	Preferred Upper Limb	Non-Preferred Upper Limb	Wilcoxon Test		Effect Size
		Median (IQ)	Median (IQ)	Z	exact P-value	r
Horizontal handgrip	P1UL	-0.22 (-0.24 - -0.18)	-0.26 (-0.31 - -0.23)	-2.803	0.002*	-0.886
	P2UL	-0.40 (-0.46 - -0.31)	-0.52 (-0.56 - -0.41)	-2.805	0.002*	-0.887
	T2UL	65.00 (55.25 - 83.25)	64.50 (54.25 - 79.25)	-1.809	0.117	-0.572
	IMPFXUL	-0.25 (-0.26 - -0.18)	-0.28 (-0.34 - -0.26)	-2.803	0.002*	-0.886
	IMPFYUL	0.34 (0.30 - 0.37)	0.30 (0.25 - 0.33)	-2.090	0.037*	-0.661
Vertical handgrip	P1UL	-0.17 (-0.19 - -0.15)	-0.25 (-0.28 - -0.21)	-2.805	0.002*	-0.887
	P2UL	-0.31 (-0.38 - -0.28)	-0.49 (-0.54 - -0.38)	-2.805	0.002*	-0.887
	T2UL	62.50 (58.25 - 79.00)	63.00 (56.50 - 78.00)	-2.310	0.031*	-0.730
	IMPFXUL	-0.19 (-0.21 - -0.17)	-0.28 (-0.31 - -0.24)	-2.803	0.002*	-0.886
	IMPFYUL	0.36 (0.31 - 0.39)	0.32 (0.28 - 0.34)	-2.293	0.020*	-0.725

Note: P1UL (upper limb horizontal force at auditory signal, N/BW), P2UL and T2UL (upper limb peak horizontal force and time before hands-off, N/BW and %, respectively), IMPFXUL (upper limb horizontal impulse from auditory signal to hands-off ((N/BW).s))) and IMPFYUL (upper limb vertical impulse from auditory signal to hands-off, ((N/BW).s))). * Significant at exact $p \leq 0.05$.

Median and respective interquartile range values for lower limb kinetic parameters for both starting variants, as well as Z, exact p and effect size (r) values of comparisons between preferred and non-preferred lower limb were presented (Table 2). Backstroke start variant with hands horizontally positioned has shown preferred lower limb superiority for all force values at selected critical instants (medium to very large effect size). Lower limb horizontal and vertical impulse was both greater for preferred lower limb (very large and medium effect size, respectively). Backstroke start variant with hands vertically positioned revealed preferred lower limb superiority for horizontal force at auditory signal and 2nd peak force before take-off (both with very large effect size). Time of intermediate force at hands-off instant was greater for non-preferred lower limb (medium effect size).

Table 2. Median and interquartile range (Q1 and Q3) of kinetic parameters for both starting variants (hands horizontally and vertically positioned) with Z, exact p and effect size (r) reported for the comparisons between preferred and non-preferred lower limb.

	Variables	Preferred Lower Limb	Non-Preferred Lower Limb	Wilcoxon Test		Effect Size
		Median (IQ)	Median (IQ)	Z	exact P-value	r
Horizontal handgrip	P1LL	0.32 (0.26 – 0.36)	0.23 (0.18 – 0.30)	-2.601	0.006*	-0.823
	P2LL	0.85 (0.81 – 0.94)	0.63 (0.54 – 0.74)	-1.988	0.049*	-0.629
	P3LL	0.60 (0.55 – 0.64)	0.47 (0.43 – 0.56)	-2.192	0.027*	-0.693
	P4LL	0.83 (0.78 – 0.86)	0.61 (0.53 – 0.71)	-2.497	0.010*	-0.790
	T2LL	54.00 (50.50 – 57.25)	53.00 (48.00 – 59.50)	-.359	0.801	-0.114
	T3LL	71.00 (65.75 – 73.25)	71.50 (68.00 – 74.00)	-1.378	0.250	-0.436
	T4LL	86.50 (82.25 – 88.25)	86.00 (83.00 – 88.25)	-1.382	0.219	-0.437
	IMPFXLL	0.50 (0.49 – 0.52)	0.37 (0.32 – 0.43)	-2.499	0.010*	-0.790
	IMPFYLL	0.28 (0.25 – 0.30	0.26 (0.21 – 0.27)	-1.988	0.049*	-0.629
Vertical handgrip	P1LL	0.34 (0.28 – 0.40)	0.69 (0.52 – 0.88)	-2.66	0.004*	-0.841
	P2LL	0.86 (0.71 – 0.96)	0.25 (0.18 – 0.35)	-1.784	0.084	-0.564
	P3LL	0.58 (0.54 – 0.66)	0.50 (0.42 – 0.60)	-1.784	0.084	-0.564
	P4LL	0.83 (0.75 – 0.91)	0.64 (0.55 – 0.77)	-2.293	0.020*	-0.725
	T2LL	53.00 (48.75 – 56.75)	54.00 (47.00 – 57.75)	-0.476	0.664	-0.151
	T3LL	69.50 (65.00 – 72.25)	70.00 (67.00 – 73.75)	-2.043	0.047*	-0.646
	T4LL	84.50 (80.50 – 89.50)	85.00 (82.50 – 87.75)	-0.172	0.938	-0.054
	IMPFXLL	0.51 (0.47 – 0.53)	0.42 (0.35 – 0.50)	-1.786	0.076	-0.565
	IMPFYLL	0.30 (0.26 – 0.32)	0.27 (0.23 – 0.28)	-1.682	0.105	-0.532

Note: P1LL (lower limb horizontal force at auditory signal, N/BW), P2LL and T2LL (1st lower limb horizontal peak force and time before hands-off, N/BW and %, respectively), P3LL and T3LL (intermediate lower limb horizontal force and time at hands-off, N/BW and %, respectively), P4LL and T4LL (2nd peak lower limb horizontal force and time before take-off, N/BW and %, respectively), IMPFXLL (lower limb horizontal impulse from auditory signal to take-off, ((N/BW).s))) and IMPFYLL (lower limb vertical impulse from auditory signal to take-off, ((N/BW).s))). * Significant at exact $p \leq 0.05$..

Median and respective interquartile range values for each upper and lower limb kinetic asymmetry, as well as Z, exact p and effect size (r) comparison values between starting variants were presented (Table 3). Backstroke start variant with vertical handgrip has shown greater horizontal lower limb impulse asymmetry than variant with hands horizontally positioned (medium effect size).

Table 3. Median and interquartile range (Q1 and Q3) of each upper and lower limb dynamometric parameter when considering the functional motor asymmetry with Z, exact p and effect size (r) reported for the comparisons between starting variants.

	Variables	Horizontal Handgrip	Vertical Handgrip	Wilcoxon Test		Effect Size
		Median (IQ)	Median (IQ)	Z	exact P-value	r
Upper Limb	P1UL	0.06 (0.01 – 0.07)	0.07 (0.04 – 0.12)	-1.887	0.064	-0.597
	P2UL	0.11 (0.05 – 0.16)	0.15 (0.11 – 0.18)	-1.682	0.105	-0.532
	T2UL	1 (0.00-1.25)	1.00 (0.00-1.25)	-0.412	0.813	-0.130
	IMPFXUL	0.07 (0.04 – 0.09)	0.09 (0.07 – 0.12)	-1.886	0.064	-0.596
	IMPFYUL	0.04 (0.01 – 0.07)	0.04 (0.02 – 0.06)	-0.764	0.492	-0.242
Lower Limb	P1LL	0.08 (0.03 – 0.12)	0.08 (0.05 – 0.11)	-0.051	1.000	-0.016
	P2LL	0.21 (0.17 – 0.28)	0.23 (0.15 – 0.37)	-0.051	1.000	-0.016
	P3LL	0.12 (0.05 – 0.20)	0.15 (0.04 – 0.21)	-0.764	0.492	-0.242
	P4LL	0.23 (0.13 – 0.31)	0.25 (0.15 – 0.29)	-0.561	0.625	-0.177
	T2LL	2.00 (1.00 –2.25)	2.50 (0.75 – 3.25)	-1.134	0.500	-0.359
	T3LL	2.00 (0.00 –3.25)	2.00 (.00 – 4.00)	-1.633	0.250	-0.516
	T4LL	1.00 (0.00 –1.25)	1.00 (0.75 – 2.00)	-1.000	0.531	-0.316
	IMPFXLL	0.13 (0.07 – 0.22)	0.14 (0.05 – 0.17)	-2.090	0.037*	-0.661
	IMPFYLL	0.04 (0.02 – 0.06)	0.04 (0.01 – 0.06)	-0.561	0.625	-0.177

Note: P1UL (upper limb horizontal force at auditory signal, N/BW), P2UL and T2UL (upper limb horizontal peak force and time before hands-off, N/BW and %, respectively), IMPFXUL (upper limb horizontal impulse from auditory signal to hands-off ((N/BW).s))), IMPFYUL (upper limb vertical impulse from auditory signal to hands-off, ((N/BW).s))), P1LL (lower limb horizontal force at auditory signal, N/BW), P2LL and T2LL (1st lower limb horizontal peak force and time before hands-off, N/BW and %, respectively), P3LL and T3LL (intermediate lower limb force and time at hands-off, N/BW and %, respectively), P4LL and T4LL (2nd lower limb horizontal peak force and time before take-off, N/BW and %, respectively), IMPFXLL (lower limb horizontal impulse from auditory signal to take-off, ((N/BW).s))) and IMPFYLL (lower limb vertical impulse from auditory signal to take-off, ((N/BW).s))). * Significant at exact $p \leq 0.05$.

Spearman's correlation coefficients between upper and lower limbs force, impulse asymmetry and 5 m start time for both start variants were depicted (Table 4). Backstroke start variant with hands horizontally positioned evidenced strong correlation between kinetic asymmetry in 1st lower limb horizontal peak force

before hands-off and start time, thus explaining 82% of 5 m start performance variance.

Table 4. Correlation coefficients and p-values between the upper and lower limb force and impulse values and the 5 m starting time for starting variant with hands horizontally and vertically positioned.

Kinetic variables	5 m starting time	
	Hands horizontally positioned	Hands vertically positioned
Upper limb horizontal force at auditory signal (N/BW)	-0.15 (0.673)	-0.23 (0.549)
Upper limb horizontal 1st peak force before hands-off (N/BW)	-0.23 (0.511)	-0.16 (0.676)
Upper limb horizontal impulse ((N/BW).s)	-0.09 (0.802)	-0.25 (0.513)
Upper limb vertical impulse ((N/BW).s)	-0.17 (0.623)	0.01 (0.961)
Lower limb horizontal force at auditory signal (N/BW)	0.46 (0.176)	0.30 (0.432)
Lower limb horizontal 1st peak force before hands-off (N/BW)	0.82 (0.001)	0.10 (0.803)
Intermediate lower limb horizontal force at hands-off (N/BW)	0.46 (0.173)	-0.09 (0.814)
Lower limb horizontal 2nd peak force before take-off (N/BW)	0.36 (0.314)	0.33 (0.387)
Lower limb horizontal impulse ((N/BW).s)	0.51 (0.135)	0.35 (0.359)
Lower limb vertical impulse ((N/BW).s)	0.23 (0.514)	-0.03 (0.937)

Note: * Significant at exact $p \leq 0.05$.

Discussion

The current study is the first attempt to compare preferred and non-preferred upper and lower limbs kinetic in two backstroke start variants with different handgrip positioning. We were also pioneers in analysing respective handgrip effects on kinetic asymmetry and relationships between this latter index and 5 m backstroke start time. Our findings revealed: (i) shorter preferred upper limb horizontal force at auditory signal and peak force before hands-off, and greater preferred horizontal lower limb force at auditory signal and 2nd peak force before take-off (in both starting variants); (ii) greater lower limbs asymmetry at horizontal impulse when swimmers performed start variant with hands vertically positioned; and (iii) strong correlation between asymmetry in 1st lower limbs horizontal peak force and 5 m start time at start variant with hands horizontally positioned. These partially agree the hypothesis that backstroke swimmers would display kinetic

differences between preferred and non-preferred upper and lower limbs and similar asymmetries between start variants. Moreover, it was partially confirmed the hypotheses that greater upper and lower limb kinetic asymmetry would increase backstroke start time for both variants.

In different sports, extensive practice with both preferred and non-preferred upper/lower limbs seems to potentiate task-specific modulations, being athletes able to show similar preferred and non-preferred proficiency (Stockel & Valter, 2014). However, due to human body innate characteristics, a certain level of difference in right and left upper and lower limbs proficiency is considered acceptable in bilateral sports (Carey et al., 2009; dos Santos et al., 2013; Mouroço et al., 2015). The greater non-preferred upper limb horizontal force at auditory signal and peak force before hands-off (noticed in both start variants) reveals a distinct upper limb preference for sustaining and steering backstroke start goals. In fact, upper limb motion can be adjusted to compensate body imbalances (probably due to performance differences between preferred and non-preferred lower limb), attempting to minimize centre of pressure displacements (Teixeira et al., 2011). Despite athletes can be trained to increase skill and use non-preferred limbs, preference for one of the limbs can persist (Carey et al., 2009; Carpes et al., 2010; Gabbard & Hart, 1996) and coaches should verify into what extent different preferred and non-preferred upper limb proficiency could affect backstroke start performance.

Both start variants revealed preferred lower limb superiority in horizontal force at auditory signal and 2nd peak before take-off, which might be explained by the above-mentioned differences observed between preferred and non-preferred upper limb force. In fact, these results seem to indicate force compensation generated by preferred lower limb to maintain swimmers' steering strategy and, consequently, longer and less resistive flight (Mourão et al., 2015). Meaningful lower limb joints extension peak torque imbalance between preferred and non-preferred collegiate softball players' lower limb was reported to harm vertical jump performance (Newton et al., 2006) and differences between preferred and non-

preferred lower limbs for vertical force during countermovement jump were also noticed in competitive volleyball players, although not affecting jumping height (Stephens et al., 2007). Greater preferred lower limb proficiency can be seen as a consequence of poor coaching and insufficient non-preferred lower limb practice in soccer (Carey et al., 2009). In backstroke start, horizontal peak force before take-off is considered determinant for propulsion (de Jesus et al., 2013) and, as it is a high velocity-movement might be influenced by the lateralised motor control system that biases the mechanism towards preferred limb, which provides more precise neuromuscular coordination (Carey et al., 2009; Sinclair et al., 2014).

The non-differences in upper limbs motor functional asymmetry between start variants considering force and time at horizontal force-curve critical instants might suggest that changing upper limbs positioning does not imply meaningful changes in backstroke start performance. In fact, ~ 40% of the swimmer participants in 2012 London Olympic Games and 2013 Barcelona Swimming World Championships used backstroke start variants with hands horizontally (highest handgrip) and vertically positioned (de Jesus, et al., 2014b). In opposition, when swimmers performed the backstroke start variant with hands vertically positioned, they had revealed greater horizontal lower limbs impulse asymmetry. As in front crawl tumble turn (Puel et al., 2012), the horizontal impulse was already pointed out as a determinant factor for backstroke start performance (de Jesus et al., 2011). The current finding could be expected, since swimmers seem not able to generate meaningful vertical propulsion after hands-off due to shorter angle formed by the centre of mass, hallux and horizontal axis (de Jesus et al., 2013; Mourão et al., 2015; Nguyen et al., 2014), obliging swimmers to apply greater propulsive horizontal effort. This greater asymmetry observed for start variant with hands vertically positioned might be explained by adjustments in upper limbs trajectory before take-off, since a vertical handgrip might imply a more lateral flight displacement and, consequently, take-off instability (de Jesus et al., 2014a). In countermovement jump, it was noticed that centre of mass moved towards the strong side during upper limbs counterbalance phase,

increasing stronger lower limb vertical ground reaction force (Yoshida et al., 2010).

Bearing in mind kinetic asymmetry displayed in backstroke start, it seems important to determine if these asymmetries could be disadvantageous for performance, as previously demonstrated in front crawl (Mouroço et al., 2015) and breaststroke swimming (Sanders et al., 2015). In the current study, it was noticed that greater motor functional asymmetry in the 1st horizontal lower limb force peak before hands-off impaired 5 m backstroke start time at variant performed with hands positioned on the horizontal handgrip. This finding is relevant for training, since swimmers might present greater horizontal propulsion during 1st peak, which often occurs before hands-off instant (de Jesus et al., 2013). Indeed, force disparity reduction between limbs was already pointed out as being relevant in bilateral sports that required maximum force generation in a shorter period of time, as field jumping (Luk et al., 2014; Sanders et al., 2015). In countermovement and squat jump, it was suggested that total muscle strength of preferred and non-preferred lower limb was the main determinant of jumping height instead of the muscle strength bilateral asymmetry (Yoshida et al., 2010, 2011). In ventral swimming start, the overall performance was not dependent only on lower limbs strength, but also on efficient interaction with upper limbs and trunk to maximize propulsion (Hard et al., 2009).

Current findings evidenced that, regardless the backstroke start variant used, swimmers displayed greater non-preferred upper limb and preferred lower limb proficiency in force-time curve critical instants. Nevertheless, most of those kinetic differences were not meaningful between start variants. Swimming coaches should use these findings to develop more precise resistance-training programs, minimizing force output discrepancies during backstroke start. Moreover, attention should also be given to lower limb peak force asymmetry before hands-off when swimmers use hands horizontally positioned, which might account to 82% of 5 m start time variance. Despite kinematical and kinetic assessments in swimming being naturally difficult due to challenges working in

and around water environment, it would be necessary to investigate in detail (kinematics, kinetic and electromyography) if handedness and footedness or the combination of both laterality indexes influences starting variants performance when they are conducted with different combinations of handgrip and wedge positioning.

Notwithstanding the originality and relevance of the current data, some study limitations should be addressed. Firstly, ten swimmers is a common sample size mean number used in experiments that require swimmers' availability for familiarization and testing protocols using complex data methodology (Puel et al., 2012). However, its has been recognized that generally much larger samples might be desired to increase the research inferential robustness; thus, future studies should consider verifying if greater sample size could lead to accuracy improvements. Secondly, the familiarization period followed previous study protocols (Nguyen et al., 2014), but could be carried out over a number of weeks if competitive swimmers were available. To minimize eventual start preference bias participants from the current study were provided with detailed demonstrations and feedback during familiarization with the two backstroke start variants, as previously recommended (Nguyen et al., 2014). Thirdly, the lateral kinetic responsiveness is not considered essentially as a propulsive component and should be minimized during swimming starts performance (Vantorre et al., 2014). In the current study, this force component was not assessed due to force sensor busts, but future studies could consider to assess the medio-lateral force axis to improve understanding about proper forces direction achievement (Mourão et al., 2015). Finally, the effectiveness of backstroke start has been assessed by the time to a set distance, ranging from 5 to 15 m from the starting wall, being the 5 m mark commonly used in recent studies (Takeda et al., 2014). The 5 m start time feedback can be more interesting for coaches since it is not influenced by underwater undulatory skill, although the 15 m time should be taken into account as a performance indicator in further studies.

References

Carey, D.P., Smith, D.T., Martin, D., Smith, G., Skriver, J., Rutland, A., & Shepherd, J.W. (2009). The bi-pedal ape: plasticity and asymmetry in footedness. *Cortex, 45*(5), 650-661.

Carpes, F.P., Mota, C.B., & Faria, I.E. (2010). On the bilateral asymmetry during running and cycling – a review considering leg preference. *Physical Therapy in Sports, 11*(4), 136-142.

Cohen, J. (1988). Statistical power analysis for the behavioural sciences (2nd ed.) Hillsdale, NJ: Erlbaum.

Coren, S. (1993). The lateral preference inventory for measurement of handedness, footedness, eyedness, and eardness. Norms for young adults. *Bulletin of the Psychonomic Society, 31*, 1-3.

de Jesus, K., de Jesus, K., Figueiredo, P., Gonçalves, P., Pereira, S.M., Vilas-Boas, J.P., & Fernandes, R.J. (2011). Biomechanical analysis of backstroke swimming starts. *International Journal of Sports Medicine, 32*(7), 546-551.

de Jesus, K., de Jesus, K., Figueiredo, P., Gonçalves, P., Pereira, S.M., Vilas-Boas, J.P., & Fernandes, R.J. (2013). Backstroke start kinematic and kinetic changes due to different feet positioning. *Journal of Sports Sciences, 31*(15), 1665-1675.

de Jesus, K., de Jesus, K., Fernandes, R.J., Vilas-Boas, J.P., & Sanders, R. (2014a). The backstroke swimming start: state of the art. *Journal of Human Kinetics, 10*, 42-47.

de Jesus, K., de Jesus, K., Medeiros, A., Fernandes, R.J., & Vilas-Boas, J.P. (2014b). The backstroke starting variants performed under the current swimming rules and block configuration. *Journal of Swimming Research, 22*, 1-5.

dos Santos, K.B., Pereira, G., Papoti, M., Bento, P.C., & Rodacki, A. (2013). Propulsive force asymmetry during tethered-swimming. *International Journal of Sports Medicine, 34*(7), 606-611.

Freitas, C., Vasconcelos, M.O., & Botelho, M. (2014). Handedness and developmental coordination disorder in Portuguese children: study with the M-ABS test. *Laterality, 19*(6), 655-676.

Gabbart, C. & Hart, S. (1996). A question of foot dominance. *Journal of General Psychology, 123*(4), 289-296.

Hardt, J. Benjanuvatra, N., & Blansky, B. (2009). Do footedness and strength asymmetry relate to dominant stance swimming track start? *Journal of Sports Sciences, 27*(11), 1221-1227.

Luk, H., Winter, C., O'Neil, E., & Thompson, B.A. (2014). Comparison of muscle strength imbalance in power lifters and jumpers. *Journal of Strength and Conditioning Research, 28(*1), 23-27.

Mourão, L., de Jesus, K., Roesler, H., Machado, L. J., Fernandes, R.J., Vilas-Boas, J.P., & Vaz, M.A.P. (2015). Effective swimmer's action during the grab start technique. *PLoS One, 10*(5): e0123001.

Mouroço, P.G., Marinho, D.A., Fernandes, R.J., & Marques, M.C. (2015). Quantification of upper limb kinetic asymmetries in front crawl swimming. *Human Movement Science, 40*(2), 185-192.

Munro, B. H. (2001). Correlation. In: Munro BH. Statistical methods for health care research. 4th ed. Philadelphia: Lippincott.

Newton, R.U., Gerber, A., Nimphius, S., Shim, J.K., Doan, B.K., Robertson, M., Pearson, D.R., Craig, B.W., Hakkinen, K., & Kraemer, W.J. (2006). Determination of functional strength imbalance of the lower extremities. *Journal of Strength and Conditioning Research, 20*(4), 971-977.

Nguyen, C., Bradshaw, E.J., Pease, D., & Wilson, C. (2014). Is starting with the feet out of the water faster in backstroke swimming? *Sports Biomechanics, 13*(2), 154-165.

Porac, C., & Coren, S. (1981). Lateral preferences and human behaviour. Springer-Verlag, New York.

Puel, F., Morlier, J., Avalos, M., Mesnard, M., Cid, M., & Hellard, P. (2012). 3D kinematic and dynamic analysis of the front crawl tumble turn in elite male swimmers. *Journal of Biomechanics, 45*(3), 510-515.

Roesler, H., Haupenthak, A., Schütz, G.R., & de Souza, P.V. (2006). Dynamometric analysis of the maximum force applied in aquatic human. *Gait & Posture, 24*(4) 412-417.

Sanders, R.H., Malcolm, M.F., Alcock, A., McCabe, C.B. (2015). An approach to identifying the effect of technique asymmetries on body alignment in swimming exemplified by a case study a breaststroke swimmer. *Journal of Sports Science and Medicine, 14*(2), 304-314.

Sinclair, J., Fewtrell, D., Taylor, P.J., Atkins, S., Bottoms, L., & Hobbs, S.J. (2014). Three-dimensional kinematic differences between the preferred and non-preferred limbs during maximal instep soccer kicking. *Journal of Sports Sciences, 32*(20), 1914-1923.

Stephens, T.M., Lawson, B.R., DeVoe, D.E., & Reiser, R.F. (2007). Gender and bilateral differences in single-leg countermovement jump performance with comparison to a double-leg jump. *Journal of Applied Biomechanics, 23*(3), 190-202.

Stockel, T. & Valter, C. (2014). Hand preference patterns in expert basketball players: interrelations between basketball-specific and everyday life behaviour. *Human Movement Science, 38*, 143-151.

Takeda, T., Itoi, O., Takagi, H., & Tsubakimoto, S. (2014). Kinematic analysis of the backstroke start: differences between backstroke specialists and non-specialists. *Journal of Sports Sciences, 32*(7), 635-641.

Teixeira, L.A., de Oliveira, D.L., Romano, R.G., & Correa, S.C. (2011). Leg preference and interlateral asymmetry of balance stability in soccer players. *Research Quarterly for Exercise and Sport, 82*(1), 21-27.

Vantorre, J., Chollet, D., & Seifert, L. (2014). Biomechanical analysis of the swim-start: a review. *Journal of Sports Science and Medicine, 13*(2), 223-231.

Van Strien, J.W. (2002). The Dutch handedness questionnaire. PhD Thesis. FSW, Department of Psychology, Erasmus University of Rotterdam.

Yoshioka, S., Nagano, A., Hay, D.C., & Fukashiro, S. (2010). The effect of bilateral asymmetry of muscle strength on jumping height of the countermovement jump: a computer simulation study. *Journal of Sports Sciences, 28*(2), 209-218.

Yoshioka, S., Nagano, A., Hay, D.C., & Fukashiro, S. (2011). The effect of bilateral asymmetry of muscle strength on the height of a squat jump: a computer simulation study. *Journal of Sports Sciences, 29*(8), 867-877.

Chapter 9

Modelling and predicting backstroke start performance using non-linear and linear approach.

Karla de Jesus[1], Helon V.H. Ayala[2], Kelly de Jesus[1], Leandro, S. Coelho[2,3], Luis Mourão[1,4], J. Arturo Abraldes[5], Ricardo J. Fernandes[1,6], Mário A.P. Vaz [7,6], João Paulo Vilas-Boas[1,6].

[1] Centre of Research, Education, Innovation and Intervention in Sport, Faculty of Sport, University of Porto, Porto, Portugal

[2] Industrial and Systems Engineering Graduate Program, Pontifical Catholic University of Paraná

[3] Electrical Engineering Graduate Program, Federal University of Paraná

[4] Superior School of Industrial Studies and Management, Porto Polytechnic Institute, Vila do Conde, Portugal.

[5] Department of Physical Activity and Sport, Faculty of Sports Sciences. University of Murcia. Murcia, Spain.

[6] Porto Biomechanics Laboratory (LABIOMEP), Porto, Portugal

[7] Institute of Mechanical Engineering and Industrial Management, Faculty of Engineering, University of Porto, Porto, Portugal

Submitted for publication on International Journal of Sports Medicine.

Abstract

Aiming to compare non-linear and linear tools for backstroke start performance modelling and prediction, ten swimmers randomly completed eight 15 m backstroke start trials with feet over the ledge (four of each variant, highest horizontal and vertical handgrip). Swimmers were videotaped in the sagittal plane for 2D kinematics using a dual media set-up with the starts being performed over an instrumented block with four force plates (upper and lower limbs measurement). Artificial neural networks and linear approach modelled and predicted 5 m start time using 26 parameters, with accuracy being determined by the mean absolute percentage error. Neural networks captured with greater accuracy 5 m time information using all input data than linear approach in horizontal and vertical handgrips (0.43 ± 0.19 vs. 0.98 ± 0.19%; 0.45 ± 0.19 vs. 1.38 ± 0.30%, respectively). The best neural network validation revealed for horizontal and vertical handgrips a smaller mean absolute error than linear model (0.007 vs. 0.04 s and 0.01 vs. 0.03 s, respectively). Neural networks revealed greater precision to be used in backstroke start performance estimation using kinematical and kinetic determinants, being a helpful tool to model technique adaptations and predict start time.

Keywords: neural networks, linear model, kinematics, kinetics, competitive swimming, backstroke start technique.

Introduction

In competitive swimming, start effectiveness has been usually measured by the time from the acoustic trigger until the swimmers' vertex passes the 15 m (Slawson et al., 2013) and it can be divided into interdependent phases as the wall/block, flight, entry and underwater (Hay & Guimarães, 1983; Tor et al., 2015; Vantorre et al., 2014). Researchers have suggested 5 to 7.5 m as proper set distances to assess start performance, since underwater propulsive actions mask the wall/block, flight and entry movements quality (Hohmann et al., 2008). As a result of starting practice, swimmers might reduce the start time by a minimum of 0.10 s (Blanksby et al., 2002), sufficient to differentiate the 1st and 2nd place in shorter distance events (Breed & Young, 2003; Hay & Guimarães, 1983; Vantorre et al., 2014). For example, during the 2015 Universiade Championships in Gwangju, the 2nd place finisher of men's 100 m backstroke was 0.07 s slower at the take-off than the winner, with the final race time differing in 0.15 s.

Most of official swimming events begin with an over water start and only backstroke and medley relay races start in-water. The backstroke start is more complex than the ventral techniques, since swimmers have to propel themselves out of the wall at the same level of the water (Takeda et al., 2014). However, research attention has been mainly dedicated to ventral starts (de Jesus et al., 2014), comparing different techniques and variants (Blanksby et al., 2002) and establishing biomechanical performance predictors (Elipot et al., 2009; Guimarães & Hay, 1985; Tor et al., 2015). In 2008 and 2013, the Fédération Internationale de Natation (FINA) authorized block configuration changes for backstroke start, including three handgrips and an ledge for feet support (FR 2.7. and 2.10, respectively). It has been noticed that the start variant with vertical handgrip and the ledge evidenced greater take-off angle and vertical centre of mass (CM) positioning during flight than without feet support (de Jesus et al., 2015), but key points that should be focused to drive backstrokers to greater levels of each start variant are unknown.

Biomechanical parameters that account for great variability in backstroke start time were identified before, under old FINA rules, with the 2nd resultant lower limbs force peak before the take-off explaining 82% of the 7.5 m start time variance (Hohmann et al., 2008) and the CM horizontal set positioning, lower limbs horizontal impulse, take-off horizontal velocity, take-off angle and CM resultant underwater velocity being also 5 m start time determinants (de Jesus et al., 2011; Nguyen et al., 2014). However, most relationships in sport science are not linear, as each unit change in an independent variable will not always bring about similar change in the dependent variable (Edelmann-Nusser et al., 2002; Pfeiffer & Hohmann, 2012; Zehr, 2005). Thus, the application of computational intelligent algorithms should be tested for backstroke start performance modelling and prediction, since they have become more widespread within the domain of complex sports training due to their capability of adapting to changing environment (Fister Jr. et al., 2015).

Artificial neural networks are encompassed by these computational intelligence algorithms and have received attention from researchers since 1980s (Ayala et al., 2014; Silva et al., 2007). It has been pointed out as superior than linear regression to explain more complex forms of human movement (Hahn, 2007; Maszczyk et al., 2012; Pfeiffer & Hohmann, 2012), but it was not determined yet such superiority to predict swimming start performance. In the current study, it was aimed to compare the accuracy of two methods (i.e. artificial neural networks vs. linear) for modelling and prediction of two actual backstroke start variants performance using kinematical and kinetic parameters. It was hypothesized that neural networks would outperform the linear model, being able to produce more accurate start performance modelling and prediction results. The current study might highlight with high accuracy the mechanism for achieving minimum 5 m backstroke start time under actual FINA rules.

Methods

Participants

The local Ethics Committee approved the study and all procedures followed requirements specified in the Declaration of Helsinki. The authors confirm that the study meets the ethical standards of the International Journal of Sports Medicine (Harris & Atkinson, 2013). Swimmers and parents and/or guardians (when participants were under 18 yrs.) freely provided their written consent before data collection. Ten male trained backstroke swimming competitors (mean ± s: age 21.1 ± 5.36 yrs., stature 1.78 ± 0.04 m, body mass 72.82 ± 10.05 kg, training background 12.6 ± 6.13 yrs. and mean performance for the 100 m backstroke in 25 m pool of 59.67 ± 2.89 s representing 78.67 ± 3.63% of the 100 m backstroke short course World Record) volunteered to participate.

Backstroke start variants

Two backstroke start variants were conducted, both with feet over a ledge (0.04 m above water level, FINA rule FR 2.10) and hands on the highest horizontal and vertical handgrip. The horizontal handgrip was positioned 0.56 m above water level and the vertical was welded joining the lowest (0.43 m above water level) and the highest horizontal handgrip. The selection of those variants was based on the high percentage of swimmers that performs them (de Jesus et al., 2015).

Backstroke start trials

Swimmers answered a questionnaire about their training and competitive 100 m backstroke background and were measured for height and body mass. A warm up consisting of 600 m front crawl and backstroke swimming, plus ten randomized backstroke start repetitions (five of each variant) took place in a 25 m indoor and heated pool (27ºC). Swimmers were enlightened with each variant, which were verbally described and visually depicted by video recordings. Verbal instruction and feedback during familiarisation were also given ensuring that variants were performed correctly (Nguyen et al., 2014). Swimmers performed randomly eight maximal 15 m backstroke start trials (four of each variant, with 2 min rest in-

between). Starting signals were produced conform to FINA rules (SW 6.1) through a device (StartTime IV acoustic start, Swiss Timing Ltd., Switzerland) instrumented to simultaneously generate the acoustic signal and export a light to the digital cameras and an electric pulse to the force plates (all synchronized with a trigger box).

Data collection

Swimmers were videotaped in the sagittal plane for bi-dimensional (2D) kinematical analysis using a dual media set-up with two stationary cameras (HDR CX160E, Sony Electronics Inc., Japan), operating at 50 Hz sampling rate with 1/250 s exposure time (de Jesus et al., 2015). Cameras were enclosed in a waterproof housing (SPK-CXB, Sony Electronics Inc., Japan) and fixed on a custom-built support, which was arranged at the lateral pool wall, 2.6 m from the starting wall and 6.78 m away from the start trajectory and perpendicularly to the movement line. Surface and underwater cameras were aligned and located 0.15 m above and 0.20 m below water level, respectively. A prism (4 m length - horizontal, 2.5 m height - vertical and 2 m width - lateral axis) was used for calibration, being leaned against the pool wall (0.80 m above water level) with horizontal axis aligned with starting direction (de Jesus et al., 2015; Seifert et al., 2014). A pair of light emitting diodes visible in each camera was fixed at one of the vertical calibration structure rods. To enable swimmers' tracking, 13 anatomical landmarks were identified (de Jesus et al., 2011), defining a 10 segment anthropometric model (de Leva, 1996), as follows: the vertex of the head (using a swim cap), mid-gonion, the right acromion, lateral epicondyle of the humerus, ulnar styloid process of the wrist, 3rd hand distal phalanx, xyphoid, iliac crest, great trochanter of the femur, lateral epicondyle of the femur, lateral malleolus, calcaneus and 1st foot distal phalanx.

Start trials were performed on an instrumented block (FINA rules FR. 2.7 and 2.10) and replicating OSB11 dimensions (Barlow et al., 2014; Omega Start Time IV, Swiss Timing Ltd., Switzerland) with four tri-axial force plates (Roesler et al.,

2006), two for upper and two for lower limbs independent force measurements (patent request – INPI nº 108229). Upper limb force plates were laterally fixed on a custom starting block with one pair of independent handgrips fixed each one over each force plate top. Lower limb force plates were vertically positioned on a custom underwater structure fixed on the pool wall with two independent ledges attached each one over each force plate top. These force plate pairs have a sensitivity of 0.5 N, error < 5% and resonance frequency of 300 and 200 Hz, respectively, and dynamic calibration revealed homogeneity of static calibration results (Roesler et al., 2006). Each force plate was connected to an analogue-to-digital converter module for strain reading (NI9237, National Instruments Corp., USA) fixed on two synchronized chassis (CompactDAQ USB-9172 and Ethernet-9188, National Instruments Corp., USA). Custom routine was created in LabView 2013 (SP1, National Instruments Corp., USA) to acquire with 2000 Hz sampling rate, plot and save the strain readings from each force plate.

Data processing

The surface and underwater video images were independently digitised frame-by-frame by the same operator using the Ariel Performance Analysis System (Ariel Dynamics Inc., USA) (de Jesus et al., 2015; Seifert et al., 2014). Image coordinates were transformed into 2D object-space coordinates with Direct Linear Transformation algorithm (Abdel-Aziz & Karara, 1971) using six calibration points (de Jesus et al., 2013; de Jesus et al., 2015). Following these studies, it was selected a 5 Hz cut-off value for data filtering (low pass digital filter) done according to residual analysis (residual error vs. cut-off frequency). Digitizing procedure accuracy was calculated using two repeated digitisations of a random selected trial and values from both digitisations were compared for each variable of interest and revealed unclear differences through magnitude based inference analysis (Hopkins et al., 2010). Root mean square reconstruction errors of six validation points on the calibration frame (which did not serve as control points) were shorter than 0.005 m for both axes and camera view, representing at most 0.16% of the calibrated space.

Two processing custom routines created in MatLab R2014a (The MathWorks Inc., USA) were used to convert strain readings into force values, to filter upper and lower limb force curves (4th order zero-phase digital Butterworth filter with a 10 Hz cut-off frequency; de Jesus et al., 2011, 2013), to sum right and left upper and lower limb and to normalize force values to each swimmer's body weight.

Data analysis

Backstroke start variants were divided into four phases (Hohmann et al., 2008): (i) hands-off - from acoustic signal and swimmers' hand left handgrips (1st positive horizontal swimmers' hand 3rd distal phalanx coordinate); (ii) take-off - from hands-off until swimmers' foot left the wall (1st positive horizontal swimmers' foot 1st distal phalanx coordinate); (iii) flight - from take-off until swimmers' CM immersion (1st negative swimmers' CM vertical coordinate); and (iv) entry - from final instant of flight phase until swimmers' foot immersion (1st negative swimmers' foot 1st distal phalanx vertical coordinate). Kinematic and kinetic selected variables are presented in Table 1.

Table 1. Linear and angular kinematic and linear kinetic variables selected in each start variant, respective units and definition.

Parameters	Definition
Hands-off phase relative time (%)	Time from auditory signal until swimmers' hands left the handgrips normalized to 5 m start time
Take-off phase relative time (%)	Time from hands-off until swimmers' feet left the starting wall normalized to 5 m start time
Flight phase relative time (%)	Time from the take-off until the CM water immersion normalized to 5 m start time
Entry phase relative time (%)	Time from CM water immersion until full swimmers' immersion normalized to 5 m start time
Resultant take-off velocity ($m.s^{-1}$)	Resultant (horizontal and vertical) CM velocity at take-off
Resultant flight velocity ($m.s^{-1}$)	Resultant (horizontal and vertical) CM velocity at center of mass water immersion
Resultant entry velocity ($m.s^{-1}$)	Resultant (horizontal and vertical) CM velocity at swimmers' full immersion
5 m start time (s)	Time between acoustic signal until swimmers' vertex achieve 5 m mark
Wrist entry angle (º)	Angle formed between forearm and horizontal axis at first fingertip water contact
Shoulder entry angle (º)	Angle formed between upper trunk and horizontal axis at acromion water immersion
Hip entry angle (º)	Angle formed between thigh and horizontal axis at greater trochanter water immersion
Back arc angle (º)	Angle formed between medium and lower trunk and horizontal axis at first fingertip water contact
Upper limb force at starting positioning (N/BW)	Horizontal upper limbs force at acoustic signal

Maximal upper limbs force and time (N/BW; %)	Horizontal upper limbs force before hands-off and respective normalized time
Upper limbs horizontal and vertical impulse ((N/BW).s)	Upper limbs time integral normalized of horizontal and vertical force component from acoustic signal until hands-off
Lower limbs force at starting positioning (N/BW)	Horizontal lower limbs force at acoustic signal
1st maximal lower limb force and time (N/BW)	1st maximal lower limbs horizontal force before the hands-off instant and respective normalized time
Intermediate lower limb force and time (N/BW; %)	1st minimum lower limbs horizontal force between the 1st and 2nd maximal value before hands-off and take-off and respective normalized time
2nd maximal lower limb force and time (N/BW; %)	2nd maximal horizontal lower limb horizontal force before the take-off and respective normalized time
Lower limb horizontal, vertical and medio-lateral impulse ((N/BW).s)	Lower limbs time integral normalized of horizontal, vertical and medio-lateral force from acoustic signal until take-off

Statistical procedures

An artificial neural network model was designed and implemented using Matlab's Neural Network Toolbox (v. 4.0.3, The MathWorks, Incorp., USA). The 11 kinematic and 15 kinetic parameters were used as input variables for the development of an artificial neural network (feed forward) with four neurons in a single hidden layer for modelling and predicting 5 m start time. The model complexity was arbitrarily chosen until we achieved a reasonable performance, as will be discussed in the next section. We have used the Levenberg-Marquardt algorithm (Levenberg, 1944; Marquardt, 1963) to optimize training procedure and measure performance with respect to the precision of the training and validation phase's outputs (Allen et al., 2014; Hahn, 2007), which had 90 and 10% of the data, respectively. Results have been analysed based on each model output accuracy by mean absolute percentage error calculation (Ayala et al., 2014).

To compare artificial neural network results we also built a linear model, which is a linear combination of the same inputs used in the artificial neural network model. The least squares problem in order to estimate the parameters of the linear model was solved by means of QR factorization.

Results

The average and standard deviation of mean absolute percentage error evidenced that neural networks obtained smaller mean absolute percentage error

values, being more robust with respect to changing the training and validation datasets (Table 2). The neural networks also obtained the best model in terms of accuracy in the validation phase. Fifty models were built by sorting randomly samples for training or validation.

Table 2. Average ± standard deviation of the mean absolute percentage error in training and validation phases, overall data and best validation for both start variants obtained by the artificial neural network (ANN) and the linear model (LM).

Start variant	Model type	Training (%)	Validation (%)	All data (%)	Best Validation (%)
Horizontal	ANN	8.78E-07 ± 1.99E-06	3.73 ± 1.62	0.43 ± 0.19	0.77
	LM	0.58 ± 0.13	4.06 ± 1.81	0.98 ± 0.19	4.68
Vertical	ANN	8.28E-07±1.50E-06	3.95 ± 1.67	0.45 ± 0.19	1.74
	LM	0.79 ± 0.18	5.92 ± 3.27	1.38 ± 0.30	3.72

True 5 m time obtained values of both start variants were confronted with mean and standard deviation of both models for each sample, considering all 50 runs. Through the mean of predictions Figure 1 evidenced that neural networks captured more precisely the 5 m time information in both variants, horizontal (Figure 1A) and vertical handgrips (Figure 1B), when compared to the linear model based on kinematic and kinetic data. In fact, on the basis of the mean of the predictions, neural networks outperformed the linear model in 77 and 83% for the horizontal and vertical handgrips, respectively. The variances of the predictions were similar for both models.

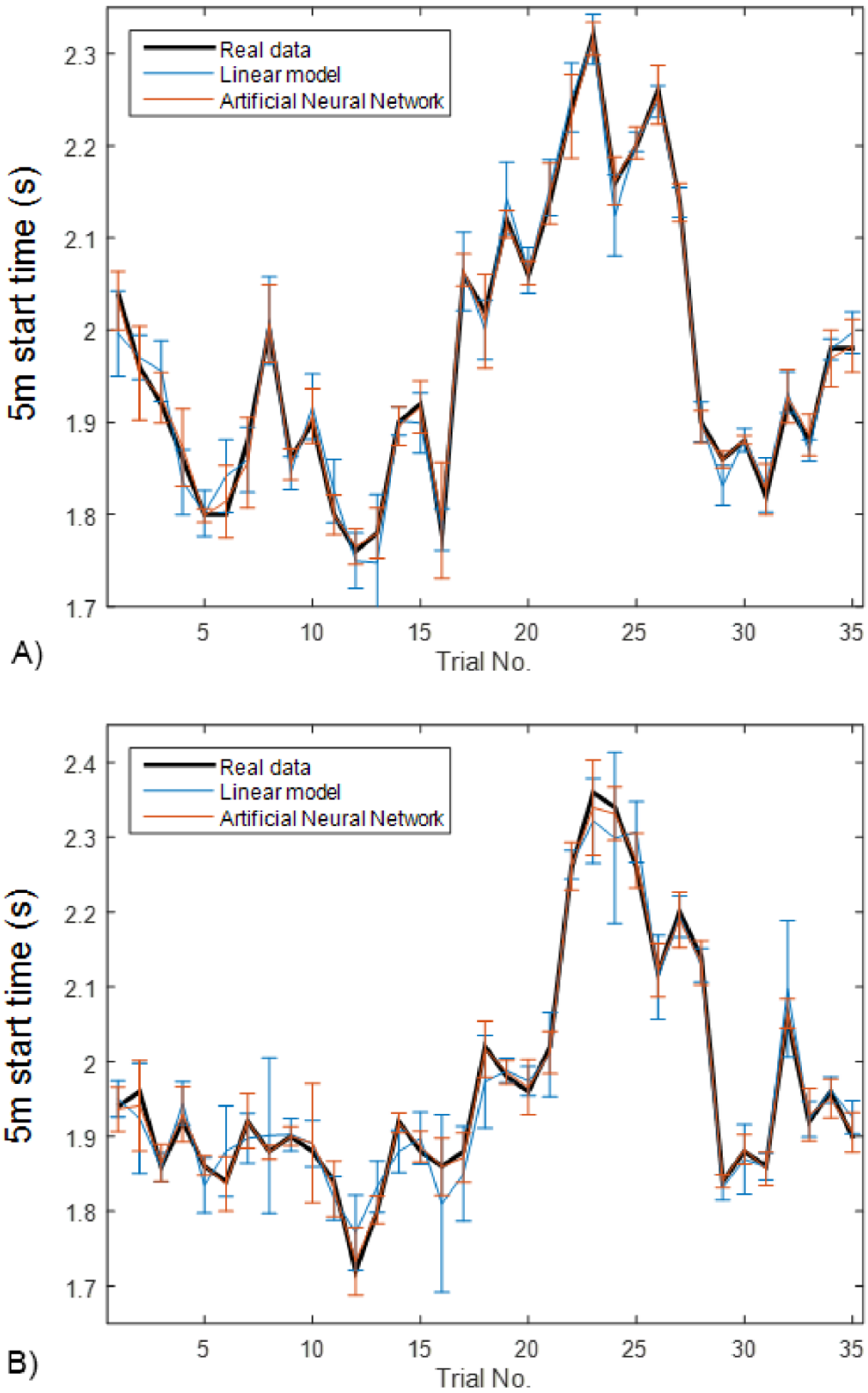

Figure 1. Real measured 5 m backstroke start times (black line) and model's predicted output, linear (blue line) and artificial neural network (red line), for backstroke start variants with horizontal (A) and vertical (B) handgrips. The variances observed from real and each model predictions are also presented.

Discussion

Movement patterns exhibit nonlinear self-organizing features (Dutt-Mazumder et al., 2011), thus neural networks evidence more robust and accurate results to model and predict sports performance than standard linear tools (Edelmann-Nusser et al., 2002; Hahn, 2007). Despite these evidences, correlations (e.g., Hay & Guimarães, 1983), principal components (e.g., Elipot et al., 2009) and multiple regression methods (e.g., Tor et al., 2015) have been used to explain swimming start performance variance. This is the first study that compared modeling and predictive accuracy of two backstroke start variants performance between artificial neural network and linear model methods using kinematical and kinetic parameters. The established hypothesis that neural networks would generate more precise modelling and prediction of the backstroke start variants performance was confirmed, being results analysed by mean absolute percentage error calculation and graphically

Nowadays, backstroke start is performed with different handgrips and a feet support, which might allow swimmers to lift their CM as high out of the water as possible and, consequently, reduce water-resistance during flight and entry phases (de Jesus et al., 2014; de Jesus et al., 2015). In fact, it was mentioned that coaches should focus on strategies that would improve flight and entry phase biomechanics, guaranteeing shorter backstroke start time (Takeda et al., 2014). In the current study, modeling and prediction was conducted using kinematic and kinetic parameters from the acoustic signal until full immersion as they have been reported as backstroke start performance determinants (de Jesus et al., 2011; Nguyen et al., 2014; Takeda et al., 2014). Based on the start phase's interdependency (Vantorre et al., 2014), coaches should attempt to take the most out of aerial phases and preserve these biomechanical advantages during entry and underwater actions. The smaller neural networks modeling and prediction error using already measured kinematic and kinetic parameters (Nguyen et al., 2014) might be useful for current backstroke start variants performance improvement.

Neural networks have been implemented as a valuable method to model and predict swimming performance since 1980s (Mujika et al., 1986) and have encompassed computational intelligence algorithms that can be used in different training phases (Fister Jr., et al., 2015). In accordance with the literature that evidenced a high correspondence between network response and swimmers' movement performance (Rejman & Ochmann, 2009), the current study confirmed the high quality of the used network model and indicated the poor estimation of linear model. Entering data into a regression equation is simple, but the accuracy results from this study's regression would be unacceptable in application (Hahn, 2007). In both variants, neural networks depicted mean absolute errors of 0.004 s between real and estimated 5 m start time (considering all data sets) compared to ~0.01 s of the linear model. Predictions errors were previously reported for short, middle and long distance swimming events using neural networks, being and 0.05 and 0.41 s for 200 m backstroke (Edelmann-Nusser et al., 2002; Pfeiffer & Hohmann, 2012), 0.58 and 1.04 s for 200 and 400 m individual medley (Silva et al., 2007) and 0.5 and 5 s for 50 and 800 m front crawl (Maszczyk et al., 2012).

Notwithstanding the pertinence and relevance of the current findings, some limitations should be addressed. In fact, ten swimmers is a reasonable sample size as this type of experiment requires swimmers' availability and highly methodological testing protocols; but, much larger samples are desired for neural networks (Hahn, 2007). This flaw was compensated by the inclusion of four trials for each participant, thereby increasing the available dataset for modelling. Start variants performed with feet above water level and hands on highest horizontal and vertical handgrip have been extensively applied in backstroke events (de Jesus et al., 2014; de Jesus et al., 2015), but, nowadays, swimmers might adopt different handgrips positioning and ledge height regarding water level. Thus, further studies should implement neural networks to verify if similar input variable sets might also be capable to accurately model and predict backstroke start effectiveness. The current study used the 5 m start time as output and biomechanical variables from the acoustic signal to full immersion as models

input, because these parameters reflect primarily the quality of starting activities (Hohmann et al., 2008; Tor et al., 2015). Future studies should also implement neural networks to model and predict underwater and swimming phase performance.

Acknowledgments

This work was supported by the Coordination for the Improvement of Higher Level or Education Personnel Foundation (0761/12-5/2012-2015) and Support Program for Graduate Private Education Institutions and by the Foundation for Science and Technology (EXPL/DTP-DES/2481/2013- FCOMP-01-0124-FEDER-041981).

References

Abdel-Aziz Y.I., & Karara H.M. (1971). Direct linear transformation: from comparator coordinates into object coordinates in close range photogrammetry. Symposium on Close-Range Photogrammetry. Urbana, Illinois, 1-18.

Allen, S.V., Vandenbogaerde, T.J., Pyne, D.B., & Hopkins, W.G. (2014). Predicting a nation's Olympic-qualifying swimmers. *International Journal of Sports Physiology and Performance, 10*(4), 431-435.

Ayala, H.V.H., da Cruz, L.F., Coelho, L.S., & Freire, R.Z (2014). Swim velocity profile identification through a dynamic self-adaptative multiobjective harmonic search and RBF neural networks. In M. Verleysen (ed.), XXIIthEuropean Symposium on Artificial Neural Networks, Computational Intelligence and Machine Learning: Bruges, 637-642.

Barlow, H., Malaki, M., Stuelcken, M., Green, A., & Sinclair, P.J. (2014). The effect of different kick start positions on OMEGA OSB11 blocks on free swimming time to 15 m in developmental level swimmers. *Human Movement Science, 34*, 178-186.

Blanksby, B., Nicholson, L., & Elliot, B. (2002). Biomechanical analysis of the grab, track and handle swimming starts: an intervention study. *Sports Biomechanics, 1*(1), 11-24.

Breed, R.V.P., & Young, W.B. (2003). The effect of a resistance-training program on the grab, track and swing starts in swimming. *Journal of Sports Sciences, 21*(3), 213-220.

de Jesus, K., de Jesus, K., Figueiredo, P., Gonçalves, P., Pereira, S., Vilas-Boas, J.P., & Fernandes, R.J. (2011). Biomechanical analysis of backstroke swimming starts. *International Journal of Sports Medicine, 32*(7), 546-551.

de Jesus, K., de Jesus, K., Figueiredo, P., Gonçalves, P., Pereira, S., Vilas-Boas, J.P., & Fernandes, R.J. (2013). Backstroke start kinematic and kinetic changes due to different feet positioning. *Journal of Sports Sciences, 31*(15), 1665-1675.

de Jesus, K., de Jesus, K., Fernandes, R.J., Vilas-Boas, J.P., & Sanders, R. (2014). The backstroke swimming start: state of the art. *Journal of Human Kinetics, 10*(42), 27-40.

de Jesus, K., de Jesus, K., Arturo-Abraldes, J., Medeiros, A.I.A., Fernandes, R.J., & Vilas-Boas, J.P. (2015). Are the new starting block facilities beneficial for backstroke start performance? *Journal of Sports Sciences*, doi.org/10.1080/02640414.2015.1076166.

de Leva, P. (1996). Adjustments to Zatsiorsky-Seluyanov's segment inertia parameters. *Journal of Biomechanics, 29*(9), 1223-1230.
Dutt-Mazumder, A., Button, C., Robins, A., & Bartlett, R. (2011). Neural network modelling and dynamical system theory: are they relevant to study the governing dynamics of association football players? *Sports Medicine, 41*(12), 1003-1017.
Edelmann-Nusser, J., Hohmann, A., & Henneberg, B. (2002). Modeling and prediction of competitive performance in swimming upon neural networks. *European Journal of Sport Science, 2*(2), 1-10.
Elipot, M., Hellard, P., Taiar, R., Boissière, E., Rey, J.L., Lecat, S., Houel, N. (2009). Analysis of swimmers' velocity during the underwater gliding motion following grab start. *Journal of Biomechanics, 42*(9), 1367-1370.
Fister, Jr I., Ljubic, K., Nagaratnam, P., Suganthan, P.N., Perc, M., & Fister, I. (2015). Computational intelligence in sports: challenges and opportunities within a new research domain. *Applied Mathematics and Computation, 262*(1), 176-186.
Galbraith, H., Scurr, J., Hencken, C., Wood, L., & Graham-Smith, P. (2008). Biomechanical comparison of the track start and the modified one-handed track start in competitive swimming: an intervention study. *Journal of Applied Biomechanics, 24*(4), 307-315.
Guimarães, A.C.S., & Hay, J.G. (1985). A mechanical analysis of the grab start starting technique in swimming. *International Journal of Sport Biomechanics, 1,* 25-35.
Hahn, M.E. (2007). Feasibility of estimating isokinetic knee torque using a neural network model. *Journal of Biomechanics, 40*(5), 1107-114.
Harriss, D.J., & Atkinson, G. (2013). Update – Ethical standards in sport and exercise science research: 2014 Update. *International Journal of Sports Medicine, 34*(12), 1025-1028.
Hay, J.G., & Guimarães, A.C.S. (1983). A quantitative look at swimming biomechanics. *Swimming Technique, 20*, 11-17.
Hohmann, A., Fehr, U., Kirsten, R., & Krueger, T. (2008). Biomechanical analysis of the backstroke start technique in swimming. *E-Journal Bewung und Training, 2*, 28-32.
Hopkins, W. (2010). Linear models and effect magnitudes for research, clinical and practical applications. *Sportscience, 14*, 49-58.
Levenberg, K.A. (1944). A method for the solution of certain non-linear problems in least squares. *Quarterly Journal of Applied Mathematics, 2*(2), 164-168.
Marquardt, D.W. (1963). An algorithm for least squares estimation of nonlinear parameters. *Journal of the Society for Industrial and Applied Mathematics, 11*, 431-441.
Maszczyk, A., Roczniok, R., Waskiewicz, Z., Czuba, M., Mikolajec, K., Zajac, A., & Stanula, A. (2012). Application of regression and neural models to predict competitive swimming performance. *Perceptual and Motor Skills, 114*(2), 610-626.
Mourão, L., de Jesus, K., Roesler, H., Machado, L., Fernandes, R.J, Vilas-Boas, J.P., & Vaz, M.A.P. (2015). Effective swimmer's action during the grab start technique. *PLoS ONE, 10*:e0123001
Mujika, I., Busso, T., Lacoste, L., Barale, F., Geyssant, A., & Chatard, J.C. (1986). Modelled responses to training and taper in competitive swimmers. *Medicine and Science in Sports and Exercise, 28(*2), 251-258.
Nguyen, C., Bradshaw, E., Pease, D., & Wilson, C. (2014). Is starting with the feet out of the water faster in backstroke swimming? *Sports Biomechanics, 13*(2), 1-12.
Pfeiffer, M., & Hohmann, A. (2012). Applications of neural networks in training science. *Human Movement Science, 31*, 344-359.
Rejman, M., & Ochmann, B. (2009). Modelling of monofin swimming technique: optimization of feet displacement and fin strain. *Journal of Applied Biomechanics, 25*(4), 340-350.
Roesler, H., Haupenthak, A., Schütz, G.R., & de Souza, P.V. (2006). Dynamometric analysis of the maximum force applied in aquatic human. *Gait & Posture, 24*(4), 412-417.
Seifert, L., Komar, J., Crettenand, F., & Millet, G. (2014). Coordination pattern adaptability: energy cost of degenerate behaviors. *PLoS ONE, 25*: e107839.
Silva, A.J., Costa, A.M., Oliveira, P.M., Reis, V.M., Saavedra, J., Perl, J., Rouboa, A., & Marinho, D.A. (2007). The use of neural netwrok technology to model swimming performance. *Journal of Sports Science and Medicine, 6*(1), 117-125.
Slawson, S.E., Conway, P.P., Cossor, J., Chakravorti, N., & West, A.A. (2013). The categorisation of swimming start performance with reference to force generation on the main block and

footrest components of the Omega OSB11 start blocks. *Journal of Sports Sciences, 31*(5), 468-478.

Takeda, T., Itoi, O., Takagi, H., & Tsubakimoto, S. (2014). Kinematic analysis of the backstroke start: differences between backstroke specialists and non-specialists. *Journal of Sports Sciences, 32*(7), 635-641.

Tor, E., Pease, D.L., & Ball, K.A. (2015). Key parameters of the swimming start and their relationship to start performance. *Journal of Sports Sciences, 33*(13), 1313-1321.

Vantorre, J., Chollet,, D., & Seifert, L. (2014). Biomechanical analysis of the swim-start: a review. *Journal of Sports Science and Medicine, 13*(2), 223-231.

Zehr, E.P. (2005). Neural control of rhythmic human movement: the common core hypothesis. *Exercise and Sport Sciences Reviews, 33*(1), 54-60.

Chapter 10

Effective swimmer's action during backstroke start technique.

Karla de Jesus[1], Kelly de Jesus[1], Luis Mourão[1,2], Hélio Roesler[3], Ricardo J. Fernandes[1,4], Mário A.P. Vaz[4,5], João Paulo Vilas-Boas[1,5], Leandro J. Machado[1,5].

[1] Centre of Research, Education, Innovation and Intervention in Sport, Faculty of Sport, University of Porto, Porto, Portugal

[2] Superior School of Industrial Studies and Management, Porto Polytechnic Institute, Vila do Conde, Portugal.

[3] Aquatic Biomechanics Research Laboratory, Health and Sports Science Centre University of the State of Santa Catarina, Florianópolis, Santa Catarina, Brazil

[4] Institute of Mechanical Engineering and Industrial Management, Faculty of Engineering, University of Porto, Porto, Portugal

[5] Porto Biomechanics Laboratory (LABIOMEP), Porto, Portugal

Submitted for publication on PLoS ONE.

.

Abstract

External force analysis in swimming starts has revealed how swimmers change their movements to achieve an outstanding performance. However, data should be properly interpreted for plenty understanding about force mechanisms generation. This study aimed to implement a previously developed tool for grab start technique to assess horizontal and vertical force based on structural (passive force due to dead weight) and swimmers' propulsive actions during the backstroke start. Three methodological steps were followed: the swimmer's matrix of inertia determination, the experimental starting protocol and the application of the algorithm on raw horizontal and vertical forces to split passive ($\vec{R}_{Passive}(t)$) from active ($\vec{R}_{Active}(t)$) components. Firstly, it was clarified the influence of $\vec{R}_{Passive}(t)$ component on backstroke start forces through the definition of two transient swimmer's start inter-segmental realistic body positions, most contracted and extended, just after the hands-off and before the take-off instant, respectively. Secondly, ten competitive backstroke swimmers performed four 15 m maximal backstroke start trials and horizontal and vertical force data were recorded using four force plates. Thirdly, $\vec{R}_{Passive}(t)$ was subtracted from experimental raw force (horizontal and vertical components) measured between the hands-off and take-off resulting in swimmers' $\vec{R}_{Active}(t)$ forces. Algorithm application evidenced that swimmers' horizontal and vertical $\vec{R}_{Passive}(t)$ components contributed with ~0.3% of swimmers' body weight during backstroke start propulsion, being these forces noticed between ~0.2 to 0.12 s before the take-off. Coaches can use provided data to improve direct transfer of resistance-training programs, consequently improving backstroke start output.

Keywords: biomechanics, ground reaction forces, algorithms, swimming, dorsal start

Introduction

In competitive swimming, time from auditory signal to swimmers' vertex passing the 15 m mark can have a meaningful impact on short and middle distance events overall performance (Slawson et al., 2013). The start is composed by the block/wall, flight, entry and underwater phases, considered interdependent, and the initial swimmers' actions are considered determinant to improve start effectiveness from then on (Guimarães & Hay, 1985; Vantorre et al., 2010). In ventral starts, swimmers have been advised to coordinate segmental actions on the starting block to generate proper partition between horizontal and vertical forces (Mourão et al., 2015), guarantying effective take-off angles and augmenting flight distances (Bartlett, 2007; Breed & Young, 2003; Mourão et al., 2015). However, in backstroke events the start is performed almost at the same level of the water surface, probably constraining force generation for optimum take-off angle (Takeda et al., 2014).

External forces analysis is an indicator of postural transformations (Chang et al., 2014) and in backstroke start has depicted a two-peak curve profile for horizontal and vertical components considering swimmers' lower limbs (de Jesus et al., 2011; Hohmann et al., 2008; Nguyen et al., 2014), being the 2nd maximum value pointed out as determinant for shorter start time (Hohmann et al., 2008; Nguyen et al., 2014). The horizontal impulse was also already included in regression equations to explain backstroke start time variation when this technique was performed under old Fédération Internationale de Natation rules (FINA, SW 6.1). Nowadays only one study has shown the force-time curve profile considering the recent backstroke start rules (FINA, SW 6.1, FR 2.7 and FR 2.10) (Sinistaj et al., 2015). Notwithstanding, no research has attempted to identify if, backstroke start forces generation are dependent upon effective and also postural forces, as previously evidenced during grab start the technique (Mourão et al., 2015).

In summary, starting with Newton's 3rd law, the total ground reaction force ($\overrightarrow{GRF}(t)$), is separated into its most relevant propulsive components (i.e.

horizontal and vertical) $\left(\overrightarrow{GRF}(t)=\left(GRF_h(t),GRF_v(t)\right)\right)$ (Vantorre et al., 2010), and this force is the opposite of the action force applied on the starting wall. In backstroke start the horizontal and vertical (just static friction ($\vec{F}_s$) without wedge use) force components might involve swimmers' muscular and respective body weight dynamical effects since their generation allows swimmers to maintain contact to the wall while moving in each successive body position. The new wedge availability can obviate part of the friction mechanism, allowing feet indentation and better wall contact (Figure 1), being the vertical component the sum of pure $\vec{F}_s$ and vertical reaction of the wedge.

Figure 1. Swimmer's feet supported over the wedge pair for backstroke start at auditory signal.

According to the previous proposed stepwise procedures (Mourão et al., 2015), in the absence of a swimmers' effective starting effort, impulse generation remains, which can be evidenced by considering a similar inactive rigid body falling. In the backstroke start technique the unanimated body falling would begin at ~40º with the horizontal axis, instead of ~90º which was observed in ventral start condition (Mourão et al., 2015), which would imply a later loss of contact instant in a smaller take-off angle. Therefore, in this particular case, the $\overrightarrow{GRF}(t)$ simply a passive force, that is:

$$\overrightarrow{GRF}(t) = \vec{R}_{Passive}(t) \quad (1)$$

The $\vec{R}_{Passive}(t)$ is the $\overrightarrow{GRF}(t)$ applied to the inertial structure of the swimmers' body and should be considered in this formalism as the one generated by a falling inert rigid body (inertia matrix and differential equation solutions calculations for force-time curves normalization may be formed; Mourão et al., 2015). Taking these ideas into account, it is recommended to decompose $\overrightarrow{GRF}(t)$ in the general (and real) case into passive and active backstroke start force components, as:

$$\overrightarrow{GRF}(t) = \vec{R}_{Passive}(t) + \vec{R}_{Active}(t) \quad (2)$$

where $\vec{R}_{Passive}(t)$ is the same as in equation (1) and is in the opposite direction to that of the propulsive force vector applied to the starting wall by the swimmers' muscular mechanical action.

This study aimed to apply the $\overrightarrow{GRF}(t)$ splitting formalism during backstroke start technique, which can be considered suitable after hands-off instant since swimmers' body is in contact with a wedge and the wall (FINA rules, SW 6.1) by means of the halluces-platform alignment whose centre should be the centre of pressure (COP). In fact, this particular geometry may be described as the CM rotation around the halluces lateral-medial axis, combined with the CM displacement along the anterior-posterior CM-COP direction (Mourão et al., 2015). It is hypothesised that it is possible to decompose $\overrightarrow{GRF}(t)$ into its $\vec{R}_{Passive}(t)$ and $\vec{R}_{Active}(t)$ using the same algorithm previously proposed for the grab start technique (Bartlett, 2007). The decomposition will allow coaches to understand the real mechanical load applied by the swimmers' musculoskeletal system during backstroke start.

Methods

Swimmers' matrix of inertia determination

Starting with a swimmer model (sagittal symmetry assumed), the minimum and maximum values of the moment of inertia around halluces (I_{zz}), defined by the last component of the inertia tensor matrix, were calculated (3D CAD, DS Solidworks, Dassault Systèmes S.A., USA) based on NASA's [13] human body anthropometrical inertial model and are presented in Table 1. These values were assessed using a model of a rigid articulated body with mass 85.71 kg, volume 89.4 dm3 and surface area of 3.26 m^2 compatible with two transient swimmer's inter-segmental realistic body positions assumed during the backstroke start variant performed with feet over the wedge at 0.04 m above water level and hands grasping vertically the grips, the most contracted - just before hands-off (Figure 2A) - and most extended - just before the take-off (Figure 2B) - with CM-COP of 0.668 m and 1.159 m, respectively. The start variant was selected based on its high acceptance by competitive swimmers (de Jesus et al., 2015) and the expression "articulated" refers to the reality-based effective transition from the 1st to the 2nd backstroke start positions. The minimum and maximum inertia matrix components are used to provide correction to the model considered in the rigid body fall simulation (cf. Mourão et al., 2015).

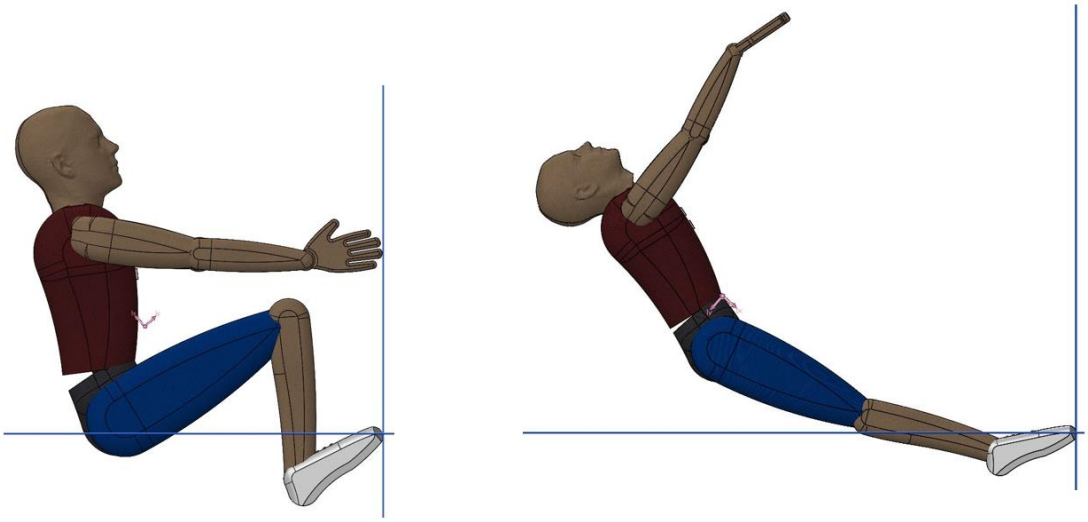

(a) (b)

Figure 2. Two rigid articulated body positions mimicking two limit transient backstroke start body positions: the most contracted (A) and the most extended (B).

Experimental start protocol

Ethics statement

The University of Porto Research Ethics Committee approved the study design (ethic review: CEFADE 222014) and all procedures corresponded to requirements stipulated in the Declaration of Helsinki. Swimmers and parents and/or guardians (when subjects were under 18 yrs.) freely provided their written informed consent before data collection.

Experimental measurements and analyses

Ten male competitive backstroke swimmers (mean ± SD: age 21.1 ± 5.36 y, stature 1.78 ± 0.04 m, body mass 72.82 ± 10.05 kg, training background 12.6 ± 6.13 y, mean performance for the 100 m backstroke in 25 m pool of 59.67 ± 2.89 s, representing 78.68 ± 3.63 % of the 100 m backstroke short course World Record) volunteered to participate in the study. All participants were healthy (no serious injury or illness occurred in the last six months), able-bodied and had participated in national level competitions.

Swimmers answered a questionnaire to assess their 100 m backstroke competitive background and height and body mass were measured. A standardized warm up consisting of 600 m front crawl and backstroke swimming (cf. Nguyen et al., 2014) and six repetitions of the backstroke start variant studied were performed in a 25 m indoor and heated (27ºC) swimming pool. During the familiarization period the start variant was verbally described and visually depicted by video recordings to each participant, being also verbal instruction and feedback given to ensure proficient performance (de Jesus et al., 2015; Nguyen et al., 2014). Each swimmer performed four 15 m maximal repetitions of the studied backstroke start variant following FINA starting rule requirements (SW 4.2 and 6.1) on an instrumented starting block that meets OSB11 block specifications (cf. Barlow et al., 2014; Tor et al., 2015); Swiss Timing Ltd., Switzerland) with 2 min rest in-between trials.

Data collection and analysis

All start trials were performed on the same instrumented starting block previously outlined (under patent request, INPI nº 108229), which is composed by four tri-axial strain gauge waterproof force plates (Roesler et al., 2006), two for upper and two for lower limb independent $\overrightarrow{GRF}(t)$ measurements. Upper limb force plates were laterally fixed on a custom-built starting block with one pair of independent handgrips fixed each one over each force plate top. Lower limb force plates were vertically positioned on a custom-built underwater structure fixed on the starting pool wall. Two independent wedges were attached each one over each lower limb force plate top at 0.04 m above the water level according to FINA facility rule determination (FR 2.10). The starting block was fixed over the underwater structure allowing the overall dynamometric unit to comply with FINA rules (FR 2.7).

The two force plate pairs (for upper and lower limb kinetic analysis) have a sensitivity of 0.5 N, error < 5% and resonance frequency of 300 Hz and 200 Hz, respectively. Dynamical calibration followed the same steps used by Mourão et al. (2015) in the rigid body fall and revealed homogeneity of results for static calibration. Custom-designed data processing software (executable file) was created in LabView 2013 (SP1, National Instruments Corporation, USA) to acquire, plot and save the strain readings from each force plate (2000 Hz sampling rate). Starting signals were produced conform to FINA rules (SW 4.2 and 6.1) using a starter device (Omega StartTime IV Acoustic Start, Swiss Timing Ltd., Switzerland), which was programmed and instrumented to simultaneously generate starting command and export a trigger signal to the force plates through a custom-built trigger box. $\overrightarrow{GRF}(t)$ curves were analogue-to-digital converted by a module for strain signals reading (NI9237, National Instruments Corporation, USA) and respective chassis (CompactDAQ USB-9172 and Ethernet-9188 National Instruments Corporation, USA).

Two processing custom-designed routines created in the MatLab R2014a (The MathWorks Incorporated, USA) were used to convert strain readings (με) into force values (N), to filter upper and lower limb force curves (4th order zero-phase digital Butterworth low-pass filter with a 10 Hz cut-off frequency (cf. de Jesus et al., 2011), to sum right and left upper and lower limb force data and to normalize force values to each swimmer's body weight. The splitting tool algorithm (detailed description in Mourão et al., 2015) was applied to each individual $\overrightarrow{GRF}(t)$ normalized to the take-off instant to subtract $\vec{R}_{h\_Passive}(t)$ and $\vec{R}_{v\_Passive}(t)$ from $\overrightarrow{GRFh}(t)$ and $\overrightarrow{GRFv}(t)$ (S1 files), defining $\vec{R}_{h\_Active}(t)$ and $\vec{R}_{v\_Active}(t)$ components, respectively.

The rigid body falling of the most contracted and extended backstroke start positioning at hands-off (Figure 2A and B, respectively) was simulated with different initial angular velocities, -10, 0, 10 and 60º/s to select the most proper angular velocity to be used with the splitting algorithm. The similarities noticed in the simulations for the CM-COP and horizontal axis angle (θ) and respective angular velocity (Figure 3A and B, respectively), as well as $\vec{R}_{h\_Passive}(t)$ and $\vec{R}_{v\_Passive}(t)$ profile (Figure 4A and B, respectively) were not sharp enough to clear the choice but the selection of the 0º/s initial condition at the hands-off instant, which suits for no descendent beginning direction rotation and for no maximum CM-COP segment angle to horizontal reflecting in greater wall contact time.

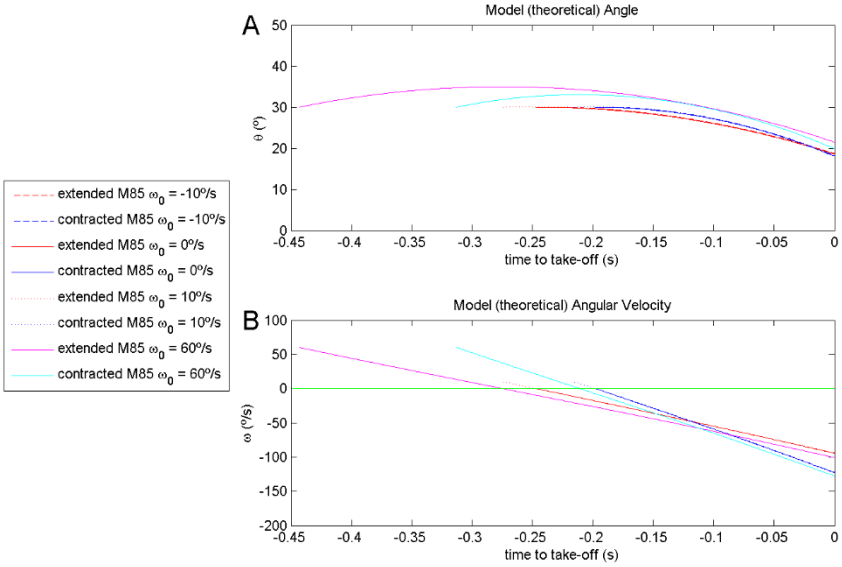

Figure 3. Two rigid Simulation results of the most extended and most contract rigid body falling, respectively at -10 (red and blue dashed line), 0 (red and blue continuous line), 10 (red and blue dotted line) and 60º/s angular velocity (rose and light blue continuous line): CM-COP segment and horizontal axis θ angle (A) and respective angular velocity (B). All data were normalized to the take-off-instant.

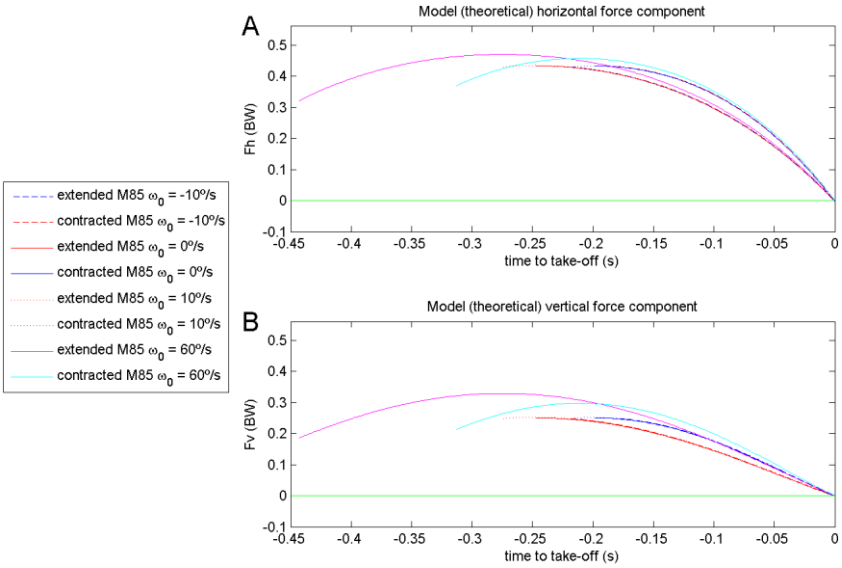

Figure 4. Simulation results of the most extended and most contract rigid body falling, respectively, at -10 (red and blue dashed line), 0 (red and blue continuous line), 10 (red and blue dotted line) and 60º/s angular velocity (rose and light blue continuous line). (Fh) and (Fv) data are presented as a fraction of the model's body weight (BW) and normalized to the take-off-instant.

Results

Complete matrix components were calculated and the minimum and maximum inertia matrix component I_{zz} obtained in the respective most contracted and extended rigid articulated body position was used to provide corrections to the model considered in the rigid body fall simulation (Table 1). The I_{zz} >> I_{yz}, I_{xz} justifies the non-meaningfulness of differences of I_{yz}, I_{xz} values between both rigid articulated body positions. Inertia I_{zz} value almost triplicates from the most contracted to the most extended rigid articulated body positions.

Table 1. Inertia tensors ($kg \cdot m^2$) calculated to hallux rotation point in the two rigid articulated body positions.

Rigid articulated body positions	Moment of Inertia matricial components
Most contracted	$\begin{bmatrix} I_{xx} & I_{xy} & I_{xz} \\ I_{yx} & I_{yy} & I_{yz} \\ I_{zx} & I_{zy} & I_{zz} \end{bmatrix} = \begin{bmatrix} +37.0068 & -16.0498 & -0.0006 \\ -16.0498 & +11.2819 & +0.0002 \\ -0.0006 & +0.0002 & +46.5009 \end{bmatrix}$
Most extended	$\begin{bmatrix} I_{xx} & I_{xy} & I_{xz} \\ I_{yx} & I_{yy} & I_{yz} \\ I_{zx} & I_{zy} & I_{zz} \end{bmatrix} = \begin{bmatrix} +37.0068 & -16.0498 & -0.0006 \\ -16.0498 & +11.2819 & +0.0002 \\ -0.0006 & +0.0002 & +46.5009 \end{bmatrix}$

The CM-COP segment and horizontal axis angle of the rigid body falling and all swimmers trials (Figure 5A) and respective angular velocity (Figure 5B) revealed that unanimated body and swimmers depict similar take-off angle ~20º, and angular velocity profile confirm that both described a descendent trajectory from the hands-off until the take-off.

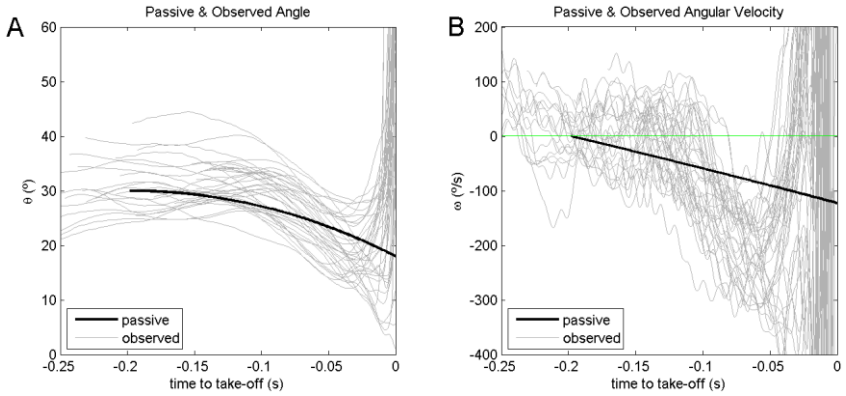

Figure 5. Passive (black continuous line) and observed (gray continuous line) CM-COP segment and horizontal axis θ angle (A) and respective angular velocity (B) at 0º/s angular velocity initial condition, normalized to the take-off.

$\overrightarrow{GRFh}(t)$ and $\overrightarrow{GRFv}(t)$ raw curves from all swimmers (Figure 6A and B, respectively) evidence a progressive profile from the hands-off until a peak just before the take-off, being $\overrightarrow{GRFh}(t)$ magnitude most outstanding and peak values occurring earlier than $\overrightarrow{GRFv}(t)$ (i.e. ~0.05 vs. 0.08 s before the take-off).

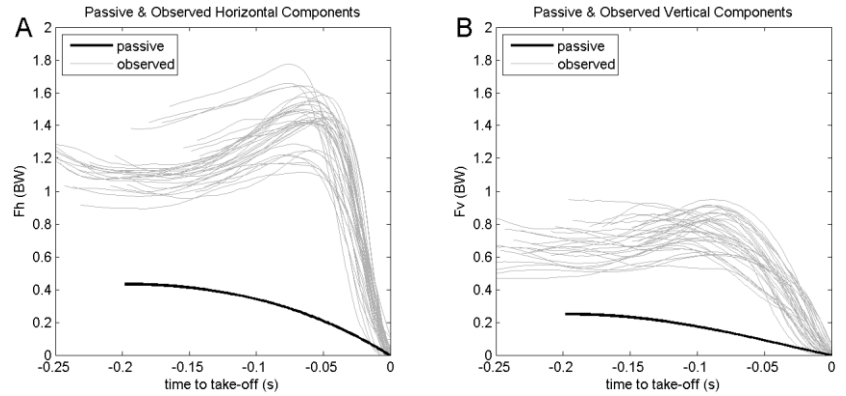

Figure 6. Passive (black continuous line) and observed (gray continuous line) $\overrightarrow{GRFh}(t)$ (Fh, A) and $\overrightarrow{GRFv}(t)$ (Fv, B) curves. Passive and observed forces are presented as a fraction of the swimmers' body weight (BW) and all data were normalized to the take-off instant and observed forces.

$\vec{R}_{h\_Passive}(t)$ and $\vec{R}_{v\_Passive}(t)$ displayed a stable curve with values of ~0.4 and 0.2 BW between -0.2 to 0.15 s before take-off, which was followed by a descendent

profile simultaneously to progressive $\vec{R}_{h\_Active}(t)$ and $\vec{R}_{v\_Active}(t)$ augment (Figure 7A and B, respectively).

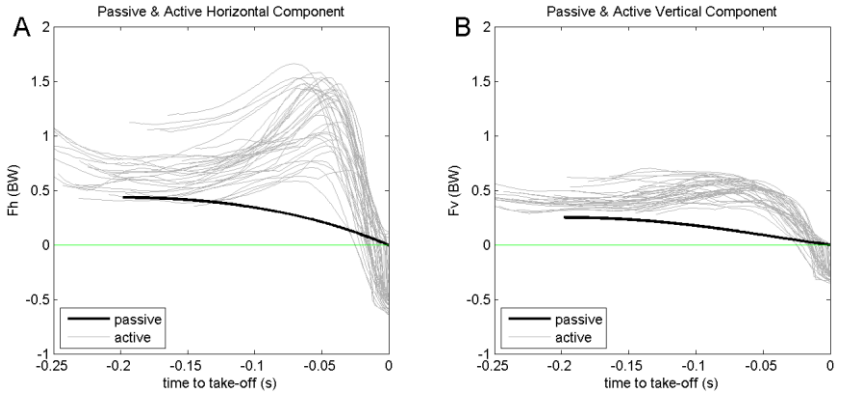

Figure 7. Passive (black continuous line) and active (gray continuous line) $\vec{R}_{h\_Passive}(t)$ and $\vec{R}_{h\_Active}(t)$ (Fh, A) and $\vec{R}_{v\_Passive}(t)$ and $\vec{R}_{v\_Active}(t)$ (Fv, B) curves. All data are presented as a fraction of the swimmers' body weight (BW) and are also normalized to the take-off instant.

Discussion

$\overrightarrow{GRFh}(t)$ and $\overrightarrow{GRFv}(t)$ measurement during swimming starts reveals all body segmental action strategies to achieve proper take-off angle, which would guarantee longer flight distance, as one of start performance indicators (Bartlett, 2007; Breed & Young, 2003; Mourão et al., 2015). Thus researchers have developed tools to accurately assess and analyse external forces during swimming starts, being useful for research proposes and training feedback in detail (Mourão et al., 2015; Slawson et al., 2013; Tor et al., 2015). This is the first study that implemented a previously developed algorithm for grab start technique (Mourão et al., 2015) to interpret the mechanisms responsible for backstroke start $\overrightarrow{GRFh}(t)$ and $\overrightarrow{GRFv}(t)$ generation based in fundamental mechanics. The algorithm application highlighted that $\overrightarrow{GRFh}(t)$ and $\overrightarrow{GRFv}(t)$ components are dependent on swimmers' muscular based biomechanical actions and on relevant body weight dynamical effects, as also evidenced in ventral start technique

(Bartlett, 2007). In fact, from the hands-off instant until ~0.12 s before the take-off $\vec{R}_{h\_Passive}(t)$ and $\vec{R}_{v\_Passive}(t)$ depicted a stable profile that was followed by gradual reduction and simultaneous $\vec{R}_{h\_Active}(t)$ and $\vec{R}_{v\_Active}(t)$ augment.

The changes in inertia moments due to different inter-segmental positions (i.e. most contract and extended, Figure 2A and B respectively) were used in simulations allowing the calculation of $\theta = \arctan(GRF_v / GRF_h)$ as a crucial parameter for the CM-COP direction and for the tool that separated $\vec{R}_{Passive}(t)$ from $\vec{R}_{Active}(t)$. Contrarily to ventral start technique (Vantorre et al., 2010), the I_{zz} value almost triplicates from the most contracted to the most extended swimmer's body position transition, justifying the complexity attributed to the backstroke start performance (de Jesus et al., 2013; Nguyen et al., 2014; Takeda et al., 2014). In the grab start, I_{zz} values almost doubles, which indicates that the CM-COP segment during the set positioning is greater than during the following backstroke start. The backstroke swimmers have to simultaneously coordinate their upper and lower limbs and trunk segment actions to ungroup their set positioning and to apportion $\overrightarrow{GRFh}(t)$ and $\overrightarrow{GRFv}(t)$ for an effective steering intention almost at the same level of water.

In the grab start technique, the symmetric $\overrightarrow{GRFh}(t)$ and $\overrightarrow{GRFv}(t)$ profile revealed the swimmers' intention to propel them out of the starting block using a steering strategy that targeted ~ 45º take-off angle (Vantorre et al., 2010). The similar apportion between $\overrightarrow{GRFh}(t)$ and $\overrightarrow{GRFv}(t)$ during the ventral track (Murrel and Dragunas, 2014; Slawson et al., 2013) and backstroke start (de Jesus et al., 2013; Hohmann et al., 2008) has not been observed, since swimmers using these techniques are constrained with a smaller take-off (Figure 5A), which implies a progressive negative angular velocity profile (Figure 5B) and greater $\overrightarrow{GRFh}(t)$ generation (Figure 6A). The take-off angle was already found as determinant for

backstroke start performance (de Jesus et al., 2011), which is comprehensible since propulsion with a ~20º angle become critical for less resistance flight phase. Thus, this backstroke start constrain has lead researchers to propose emphasizes in the lower limb joints coordination during extension for greater back arc angle (Takeda et al., 2014). The take-off angle calculated from kinematics when backstroke start was performed with the wedge revealed values of ~25º, being greater than without its use (de Jesus et al., 2015), which can be explained by the friction mechanism obviation.

The θ angle profile indicated that swimmers at ~ 0.1 s before the take-off revealed a sharply reduction of values (Figure 5A), which was a coincident instant of progressive $\overrightarrow{GRFh}(t)$ augment and $\overrightarrow{GRFv}(t)$ peak values achievement. Following the hands-off instant the reduced swimmers' degree of freedom due to small θ angles require swimmers to generate a maximum $\overrightarrow{GRFv}(t)$ earlier than $\overrightarrow{GRFh}(t)$ peak. The $\overrightarrow{GRFv}(t)$ peak value has already been presented clearly with the new wedge use (Nguyen et al., 2014) and it is not so pronounced as $\overrightarrow{GRFh}(t)$ due to essentially backward steering intention instants before the take-off. Notwithstanding the $\overrightarrow{GRFv}(t)$ maximum value had already been pointed out as determinant factor for successful swimming starts (Slawson et al., 2013), greater $\overrightarrow{GRFh}(t)$ peak just before the take-off seem to be more important in backstroke start (de Jesus et al., 2011; Hohmann et al., 2008). In fact, similar to the backstroke start, swimmers using the new kick-start have been advised to align their body into the most mechanically advantageous position to produce greater $\overrightarrow{GRFh}(t)$ (Murrel and Dragunas, 2014; Takeda et al., 2012).

The θ mapping methodology developed and implemented on $\overrightarrow{GRF}(t)$ grab start technique to decompose $\vec{R}_{Passive}(t)$ and $\vec{R}_{Active}(t)$ components (Mourão et al., 2015) was used in backstroke start and revealed an evident $\vec{R}_{h\_Passive}(t)$ and $\vec{R}_{v\_Passive}(t)$

contribution from ~0.2 to 0.12 s before take-off, which progressively decrease, being the opposite profile observed during grab start (Mourão et al., 2015). Indeed, the conditions in the grab start are different considering the θ angle, being swimmers undergone to $\vec{R}_{Passive}(t)$ effects during a longer period, and thus, revealing mainly greater $\vec{R}_{v\_Passive}(t)$ component effects. In the grab start technique swimmers evidence $\vec{R}_{h\_Active}(t)$ and $\vec{R}_{v\_Active}(t)$ just after the hands-off instant, which means that more than 60% of the block time is influence by inertial components. Considering the backstroke start, the $\vec{R}_{Passive}(t)$ influence revealed a more discreet profile for both components, $\vec{R}_{h\_Passive}(t)$ and $\vec{R}_{v\_Passive}(t)$, which was replaced by $\vec{R}_{h\_Active}(t)$ and $\vec{R}_{v\_Active}(t)$. The greater contribution of lower than upper limbs for propulsion during starts was evidenced since 80s (Hay & Guimarães, 1983; Guimarães & Hay, 1985;), leading researchers to propose diverse resistance-training programs to improve strength and power (Breed & Young, 2003; Rebutini et al., 2014). $\vec{R}_{Passive}(t)$ and $\vec{R}_{Active}(t)$ assessment might facilitate coaches to improve direct results transfer from backstroke start resistance training programs.

Notwithstanding the study's originality and pertinence, some limitations and future research directions should be considered. The force plates for lower limbs force measurements were vertically fixed on the starting pool wall, half part in-water and the other part above water as also previously done (de Jesus et al., 2013; Nguyen et al., 2014; Sinistaj et al., 2015). As the in-water part has been undergone to forces acting due to swimmers actions and wave vibrations during the last feet wall contact instants shorter positive and negative force values were measured, hampering proper θ angle calculations and consequently, splitting algorithm. The algorithm implementation developed firstly to separate $\vec{R}_{Passive}(t)$ from $\vec{R}_{Active}(t)$ components during grab start technique was suitable to be applied from the hands-off instant onward, but future studies should consider improving

algorithm capabilities to assess $\overrightarrow{GRF}(t)$ components from the auditory signal to the hands-off instant.

Conclusions

The current study revealed through inertial and effective force components assessment that, even with the new wedge authorization, the backstroke start might be considered a complex task. Set positioning constrains evidenced when performed starts in-water implied that slight $\vec{R}_{h\_Passive}(t)$ and $\vec{R}_{v\_Passive}(t)$ contribution was observed during a short period just after the hands-off. The $\vec{R}_{Passive}(t)$ influence was sharply replaced by $\vec{R}_{h\_Active}(t)$ and $\vec{R}_{v\_Active}(t)$ components, revealing that most of the backstroke start movement during the take-off phase is dependent upon swimmers effective muscular actions. These findings might be helpful for coaches to implement accurate resistance-training programs for successful backstroke start performance.

Acknowledgments

The authors acknowledge Engº Nuno Viriato of Institute of Mechanical Engineering and Industrial Management (INEGI) for his invaluable service in SolidWorks and with inertia tensor components and Engº Pedro Gonçalves of Biomechanics Laboratory of Faculty of Sport of University of Porto for his assistance with Matlab routine. This work was supported by the Coordination for the Improvement of Higher Personnel, Ministry of Education of Brazil under grant (0761/12-5/2012-2015) and the Foundation for Science and Technology under grant (EXPL/DTP-DES/2481/2013- FCOMP-01-0124-FEDER-041981).

References

Barlow, H,. Halaki, M., Stuelcken, M., Greene, A., & Sinclair, P.J. (2014). The effect of different kick start positions on OMEGA OSB11 blocks on free swimming time to 15 m in developmental level swimmers. *Human Movement Science, 34*, 178-186.

Bartlett R. (2007). Introduction to sports biomechanics. 2nd ed. New York: Routlegde.

Breed, R.V.P., & Young, W.B. (2003). The effect of a resistance-training program on the grab, track and swing starts in swimming. *Journal of Sports Sciences, 21*(3), 213-220.

Chang, Y-T., Chang, J-H., Huang, C-F. (2014). Ground reaction force characteristics of Tai Chi push hand. *Journal of Sports Sciences, 32*(18), 1698-1703..

de Jesus, K., de Jesus, K., Figueiredo, P., Gonçalves, P., Pereira, S., Vilas-Boas, J.P., Fernandes, R.J. (2011). Biomechanical analysis of two backstroke starts. *International Journal of Sports Medicine, 32*(7), 546-551.

de Jesus, K., de Jesus, K., Figueiredo, P., Gonçalves, P., Pereira, S., Vilas-Boas, J.P., Fernandes, R.J. (2013). Backstroke start kinematic and kinetic changes due to different feet positioning. *Journal of Sports Sciences, 31*(15), 1665-1675.

de Jesus, K., de Jesus, K., Abraldes, J.A., Medeiros, A.I.A., Fernandes, R.J., Vilas-Boas, J.P. Are the new starting block facilities beneficial for backstroke start performance? *Journal of Sports Sciences*, doi.org/10.1080/02640414.2015.1076166.

Guimarães, A.C.S., & Hay, J.G. (1985). A mechanical analysis of the grab starting technique in swimming. *International Journal of Sport Biomechanics, 1,* 25-35.

Hay, J.G., & Guimarães, A.C.S. (1983). A quantitative look at swimming biomechanics. In J.G. Hay (ed).. Starting, stroking and turning: a compilation of research on the biomechanics of swimming: University of Iowa,.76-82.

Hohmann, A., Fehr, U., Kirsten, R., & Krueger, T. (2008). Biomechanical analysis of the backstroke start technique in swimming. *E-Journal Bewegung und Training, 2*, 28-33.

Mourão, L., de Jesus, K., Roesler, H,, Machado, L., Fernandes, R.J., Vilas-Boas, J.P., & Vaz, M.A.P. (2015). Effective swimmer's action during the grab start technique. *PLoS ONE,10*: e0123001.

Murrel, D., & Dragunas, A. (2014), A comparison of two swimming start techniques from the Omega OSB11 starting block. *WURJ Health and Natural Sciences, 18*, 1-6.

NASA. (1978). Anthropometric source book. Volume I: Anthropometry for designers. Ohio: Yellow Springs..

Nguyen, C., Bradshaw, E., Pease, & D., Wilson, C. (2014). Is starting with the feet out of the water faster in backstroke swimming? *Sports Biomechanics, 13*(2), 154-165.

Rebutini, V.Z., Pereira, G., Bohrer, R.C., Ugrinowitsch, C., & Rodacki, A.L. (2014). Plyometric long jump training with progressive loading improves kinetic and kinematic swimming start parameters. *Journal of Strength and Conditioning Research,* in press.

Roesler, H., Haupenthak, A., Schütz, G.R., & de Souza, P.V. (2006). Dynamometric analysis of the maximum force applied in aquatic human. *Gait & Posture, 24*(4)*,* 412-417.

Sinistaj, S., Burkhadrt, D., Carradori, S., Taylor, W.R., & Lorenzetti. S. (2015). Kinetic and kinematic analysis of the backstroke start. In Colloud F, Noel H, Monnet T, (eds.) XXXIII International Symposium on Biomechanics in Sports, 257-260.

Slawson, S.E., Conway, P.P., Cossor, J., Chakravorti, N., & West, A.A. (2013). The categorisation of swimming start performance with reference to force generation on the main block and footrest components of the Omega OSB11 start blocks. *Journal of Sports Sciences, 31*(5), 468-478.

Takeda, T., Takagi, H., & Tsubakimoto, S. (2012). Effect of inclination and position of new swimming starting block's back plate on track-start performance. *Sports Biomechanics, 11*(3), 370-381.

Takeda, T., Itoi, O., Takagi, H., & Tsubakimoto, S. (2014). Kinematic analysis of the backstroke start: differences between backstroke specialists and non-specialists. *Journal of Sports Sciences, 32*(7), 635-641.

Tor, E., Pease, D., & Ball, K.A. (2015). The reliability of an instrumented start block analysis system. *Journal of Applied Biomechanics, 31*(1), 62-67.

Vantorre, J., Seifert, L., Fernandes, R.J., Vilas-Boas, J.P., & Chollet, D. (2010). Comparison of grab start between elite and trained swimmers. *International Journal of Sports Medicine, 31*(12), 887-893.

Chapter 11 General Discussion

Since 1950s with Heusner (1959), researches have been interested in swim start analysis, using diverse technologies and methods that have revealed how the initial race component could be optimized for better overall event results. The main efforts have been centred on ventral start improvements (e.g. Vantorre et al., 2014), probably due to the greater number of official events in which swimmers start over platforms (Theut & Jensen, 2006; Vilas-Boas & Fernandes, 2003). The backstroke start was firstly studied in 1960s and authors used cinematography to compare start performed at FINA and NCAA events (Rea & Soth, 1967). Following the main significant FINA rule changes in mid 2005, researchers have begun to analyse the backstroke start technique using detailed biomechanical tools (e.g. electromyography). Nevertheless, those studies have not admitted the entire backstroke start technique evolution, being the general purpose of this Thesis to update the backstroke start knowledge and technologies considering both, the current FINA starting (SW 6.1) and facility (FR 2.7 and FR 2.10) rules.

Main findings pointed out that: (i) backstroke start available literature have essentially used kinematics without a clear methodological consensus about start phases and parameters definition; (ii) most of elite swimmers have used start variants with feet partially emerged and hands on highest horizontal and vertical handgrip independent of competitive level, gender and backstroke event; (iii) only one research group have quantified backstroke start upper limbs kinetic profile; (iv) a new instrumented backstroke starting block provided accurate, reliable and valid 3D external ground reaction forces; (v) a large calibration volume depicted accurate 3D reconstruction for backstroke start analysis; (vi) Mocap system provided 3D tracking of the backstroke start movements from the full immersion until the 15 m mark; (vii) start variants performed with feet partially or entirely above water level with hands on highest horizontal and vertical handgrip depicted biomechanical advantages during wall contact phases compared to start variants performed with feet utterly immersed; (viii) start variants performed with feet

partially emerged and hands on highest horizontal and vertical handgrip displayed similar muscular activation responses, but these muscles registered different contribution in each starting phase; (ix) wedge use did not affect linear and angular kinematics and overall backstroke start performance, although performing start variant with hands on vertical handgrip with wedge indicates biomechanical advantages rather than without wedge use; (x) preferred and non-preferred upper and lower limbs differed considering kinetics at start variants performed with feet over the wedge and hands on highest horizontal and vertical handgrip; (xi) artificial neural network modelled backstroke start performance with greater accuracy compared to linear approach using kinetimatics and kinetics; (xii) algorithm to split passive from active forces was successfully implemented in symmetric ventral start; and (xiii) horizontal and vertical passive components contributed to raw forces just before the hands-off, showing a decrease just before the take-off.

Understanding and critically analysing the background research in backstroke start allowed filling the gaps, overcoming limitations on existing literature and improving future knowledge. In Chapter II it was used the narrative method to review the backstroke start literature due to the limited number of studies available complying with inclusion criteria (Pautasso, 2003). From this literature compilation, many controversies were noticed concerning study's aim, sample size and competitive level, data collection and treatment methods and further conclusions, agreeing with our previous assumptions. Those controversies have not been observed among ventral start studies (Vantorre et al., 2014; Vilas-Boas & Fernandes, 2003), which can be justified by the greater interest in starts performed over the block rather than in-water (Theut & Jensen, 2006). The noticeable interest in ventral start studies implied that scientific and coaching community assumed consistent data collection, treatment and analysis methods to facilitate comparisons in-between researchers (McDonnell et al., 2012). In backstroke start studies most authors had not clearly identified start variants, which should be a first attempt for methodology standardization (McDonnell et al., 2012). Moreover start phases definition and biomechanical parameters

studied had registered great variability among studies, mainly because part of them was conducted in competitive and another part in laboratory scenario. Studies conducted in elite competitions can guarantee the highest level of validity; however, data reliability, accuracy and reproducibility are compromised. Nevertheless, neither in competitive, nor in lab conditions, researchers have attempted to consider backstroke start analysis based on the combination of current swimming (SW 6.1) and facility rules (FR 2.7 and 2.10).

With the current FINA swimming and facility backstroke start rules, swimmers have been authorized to position their feet entirely immersed or emerged or partially emerged with hands on lowest, highest horizontal or vertical handgrip. To date, researchers had considered only the effects of different feet positioning on backstroke start performance, establishing two variants, namely feet parallel and entirely immersed and emerged (de Jesus et al., 2011, 2013; Nguyen et al., 2014). Thus, in Chapter III it was conducted a qualitative analysis that revealed the start variants that have been used during high calibre swimming events and their distribution by gender, event and competitive level. Considering all 100 and 200 m 2012 Olympic Games and 2013 Swimming World Championships heats, semi-finals and finals it was noticed that female backstrokers used more start variants than males in both events. When analysed 50, 100 and 200 m semi-finalists and finalists it was observed that independently of gender, competitive level and event, swimmers often adopted two start variants, both with feet partially emerged, but with hands on highest horizontal and vertical handgrip. These findings partially agreed our previously established hypothesis, that swimmers would select start variants that allowed them to increase their centre of mass positioning and to provide clean flight, once the hydrodynamic resistance is approximately 800 times greater than in air (Takeda et al., 2009). In fact, it was already pointed out that proficient backstrokers have progressively adopting feet out of the water level, which has shown some evidence of better overall start performance (Nguyen et al., 2014; Takeda et al., 2014).

Chapter II and III findings reinforced the need for methodological updating that would allow improving understanding about each current backstroke start variant, being a first objective attempt to help coaches and swimmers' decision. As the starting wall movements anticipate flight and underwater phases, the forces generated should be properly and detailed measured, being Appendix I an attempt to complement Chapter I findings. In fact, both studies allowed better understanding of the current backstroke start kinetics state of the art, identifying gaps and limitations of the existent literature. It was revealed that studies are limited to measure lower limbs reaction forces using commercial or homemade extensometric or piezoelectric force plates, corroborating our previous assumptions. Data about vertical upper and lower limbs reaction forces are still lacking and none research had attempted to provide each body side kinetic profile. The vertical ground reaction force can be considered decisive in backstroke start since swimmers have to organize their flight at almost the same water level (Takeda et al., 2014) and to strive for reduced kinetics asymmetry for steering goal achievement. Therefore, based on Chapter II, III and Appendix I findings, it was developed and validated an instrumented starting block (Chapter IV) composed of four triaxial extensometric waterproof force plates capable to cover all current backstroke start variants kinetics. Despite being a prototype, the instrumented starting block supplied accurate, reliable, reproducible and valid 3D (6DoF) ground reaction force data for integral backstroke start variants analysis, as previously done in ventral start studies (Tor et al., 2015a).

A combined kinematic and kinetic analysis during backstroke start wall contact phases can reveal in detail swimmers' strategies to achieve most adequate take-off for longer flight and less resistant water immersion at each start variant (Guimarães & Hay, 1985). Clean flight path and less resistant water entry would allow shorter swimmers' deceleration at underwater phases, since their best performance also depends upon horizontal velocity at entry (Tor et al., 2015b). Appendix II and III focused on kinematical methodology improvements to cover backstroke start movement analysis from acoustic signal to 15 m mark, using a 3D perspective. Appendix II depicted the development of a new calibration frame,

which was considered suitable to cover 3D backstroke start movements reconstructed from the auditory signal to full body immersion. Reconstruction errors were ~ 0.007 m for surface and underwater cameras, which can be considered acceptable taking into account errors reported in previous studies using shorter calibration volumes (e.g. Figueiredo et al., 2011; Gourgoulis et al., 2008). The 3D approach can provide accurate, reliable and reproducible data, however it is a time-consuming method (Barbosa et al., 2015). Therefore, in Appendix III it was tested a new method for backstroke kinematic analysis based on automatic tracking Mocap system and it was noticed that improvements in the system should be done before assessing 3D kinematics considering surface and underwater environment merged. To merge surface and underwater media in high velocity movement analysis evidenced method limitations, as previously mentioned (Kwon & Casebolt, 2006). Therefore, automatic tracking method can be used as an accurate tool for underwater backstroke start analysis, revealing that swimmers seem not to prioritize a glide phase performance, as described in ventral starts (Houel et al., 2009).

The methodology improvements allowed detailed biomechanical evaluation of backstroke start (Chapter V) considering variants depicted in Chapter III, after a one-month recommended familiarization period to reduce variant bias (e.g. Blanksby et al., 2002). Established hypotheses were partially confirmed, since swimmers using start variants with feet entirely emerged and hands on highest horizontal and vertical handgrips displayed 0.16 m greater vertical centre of mass set positioning, 0.28, 0.41 and 0.16 ([(N/BW).s]) vertical upper limbs impulse and horizontal and vertical lower limbs impulse (respectively) than variants with feet immersed. Positioning centre of mass higher than water level seem to imply greater vertical upper limbs impulse to lift swimmers' body out of the water, but can be advantageous since swimmers can improve flight distance (Nguyen et al., 2014), which is considered a very important variable due to the fact that swimmers can travel considerably faster through the air rather than in-water (Breed & Young, 2003; Takeda et al., 2009). Greater horizontal and vertical lower limbs impulse can reveal compromise between a pike and flat flight path (Seifert

et al., 2010), which is essential in backstroke start where swimmers should increase their vertical centre of mass trajectory for proper back arc angle (Takeda et al., 2014) without neglecting a longer flight distance. Most of differences among start variants were observed during the wall contact phases and swimmers did not transferred these biomechanical advantages throughout flight and underwater phases, and consequently, 15 m start time was invariable. Previous swimming ventral start (Vantorre et al., 2010) and long jump studies (Arampatzis et al., 1998) indicated that different motor profiles might lead to similar successful performance. Furthermore, it has been reported that underwater phases can compensate all differences produced during impulse and aerial trajectory (Vilas-Boas et al., 2003). Based on these findings, coaches should select the start variant that best fits swimmers' strength profile to take the most of each variant biomechanical advantage (Thanopoulos et al., 2012), instead of mimicking the most often used by elite swimmers (Chapter III).

It has been well emphasized that one of the requirements for proficient start is the generation of maximal and coordinated efforts in a short amount of time (Hohmann et al., 2008; Ball & Scurr, 2013). The most common non-invasive method for directly assessing neuromuscular contribution to any task is through surface EMG. The majority of studies published in swimming have used amplitude analysis methods (e.g. integrating raw signal, iEMG; Martens et al., 2015), which reflects muscle activation from both, motor unit recruitment and firing rate (Blasser et al., 2014). Despite EMG can provide relevant information for efficient coaching, this is a time-consuming method, thus, it was selected only two start variants (i.e. the commonly used in elite competitions, Chapter III) to compare the iEMG and relative activation time in-between them and between respective start phases of each start variant (Chapter VI). Findings partially agreed with established assumptions, revealing that upper and lower limbs iEMG were similar between hands on horizontal and vertical positioning from acoustic signal to 15 m. This result allows suggesting that, as in rebound jumping, muscles react according to a learned coordination program that guides execution of the jump irrespective of temporary voluntary orders from the central nervous system

(Rodacki & Fowler, 2001). Moreover, only Biceps Femoris depicted similar activation time throughout starting phases of both variants, also partially agreeing already established assumptions. This result corroborates a previous study that showed the continuous and progressive hip extension from the hands-off to the water immersion (Takeda et al., 2014). In the light of the observed results, coaches do not need to differentiate resistance-training programs between start variants adopted, but should pay attention on specific exercises to stimulate each upper and lower limb muscle role during the start.

Nowadays, the new wedge has been used in international events, and researchers should focus on helping coaches and swimmers about how to perform the backstroke start to obtain biomechanical advantages using this new facility. The authorization of a new wedge by FINA (FR 2.10) was probably based on the biomechanical advantages demonstrated when backstrokers used the wall gutter under NCAA rules (Chapter II). In Chapter VII it was tested the new wedge in its highest vertical positioning (i.e. 0.04 m above water level) considering that most swimmers prefer to use feet positioning above water level (Chapter III). In fact, it was already reported that elite swimmers have chosen to position their feet partially or entirely above water level (Nguyen et al., 2014; Takeda et al., 2014). Findings partially corroborate our previous assumptions, highlighting some biomechanical advantages when swimmers using the wedge in the start variant performed with hands vertically positioned, namely a greater take-off angle, centre of mass vertical positioning at flight and centre of mass vertical velocity at water immersion. These advantages did not allow a better 5 m start time than without wedge use, which might be explained by inappropriate lower limb water immersion strategy, hampering a small entry-hole (Seifert et al., 2010; Takeda et al., 2014). In addition, results also corroborate Chapter V and VI findings that the hands positioned on the highest horizontal or vertical grip with and without wedge use did not affect the backstroke start performance and swimmers' coordination to extend lower limbs joint. It seems that starting performance might be successful as long as initial set positioning is sufficient close to the preferred backstroke start variant, as also noticed for vertical jump performed at different

initial positions (Van Soest et al., 1994). Being the new wedge recently authorized, it is expected that further studies should consider analysing different heights combinations and handgrips configurations in a larger sample size with longer familiarisation period.

The backstroke start is a complex multi joint movement, such as gymnastic backward somersaults (e.g. Mathiyakom et al., 2006), and the swimmers' mechanical aim is to perform the greatest possible impulse in the shortest time with a proper steering goal (de Jesus et al., 2011). Meaningful kinetic differences between preferred and non-preferred upper and lower limbs do not seem advantageous, since it has direct implications on proper steering goal achievement, and consequently, overall start performance. Differences between preferred and non-preferred upper and lower limbs proficiency have been reported in several bilateral sports (e.g. basketball; Stockel & Valter, 2014), which were also confirmed in Chapter VIII. In fact, it was noticed that regardless start variant used (Chapter VI and VII), non-preferred upper and preferred lower limb depicted greater horizontal force at auditory signal and peak value before hands-off and take-off, respectively. Moreover, similarities between start variants were also confirmed when considering upper and lower limb kinetic asymmetries, with exception of the horizontal impulse that was greater for start variant with hands vertically positioned. It was hypothesized that those two start variants would be similar in asymmetry for most of kinetic parameters due to proximity in set positioning verified in Chapters III, V, VI and VII. It was recommended that researchers should evaluate and control preferred and non-preferred limb proficiency, as previously done (Luk et al., 2014), especially in start variant with hands horizontally positioned, where 82% of performance variance was attributed to high asymmetry at horizontal lower limbs peak force before hands-off.

Following the understanding about how the handgrips configuration and wedge use can affect kinematics and kinetics, it was conducted a study using non-linear and linear tools to model the most common backstroke start variants performance (Chapter IX). Researchers have used linear regression models to predict

swimming start performance in ventral (e.g. Vantorre et al., 2014) and backstroke events (e.g. Nguyen et al., 2014), however, the limitations of this method are well known and were tested in backstroke start. It was observed that non-linear (i.e. artificial neural network) and linear (i.e. over determined system) tools used with kinematic from acoustic signal until 5 m mark and upper and lower limb kinetic parameters as input variables were able to model the backstroke start performance of two current used variants (Chapter III, V, VI, VII and VIII). Nevertheless, the artificial neural network depicted more robust results with smaller values for the mean absolute percentage error than the linear model, agreeing with previous studies (Hahn, 2007; Pfeiffer & Hohmann et al., 2012; Silva et al., 2007). Despite the underwater phases can account for 80 to 90% of the start time variance, the interdependency among start phases has been well reported (e.g. Tor et al., 2015c), being needed focusing on movements strategy that might reduce deceleration during entry phases and consequently, posterior underwater trajectory. In Chapter IX, 26 variables, namely linear and angular kinematics and linear kinetics were selected as input for both models. From these variables, the 2nd lower limb horizontal peak force value, the total horizontal lower limbs impulse, the resultant take-off and entry velocity and the back arc angle during flight were already reported as relevant parameters to achieve shorter backstroke start time (de Jesus et al., 2011; Nguyen et al., 2014; Takeda et al., 2014). Therefore, to perform shorter 5 m start time using variant with hands on highest horizontal or vertical handgrip and the wedge, coaches and swimmers should focus on proper forces generation to improve take-off velocity and back arc angle reducing water entry deceleration.

Ground reaction forces have been often included in different starting technique prediction models (e.g. Nguyen et al., 2014), being needed to distinguish the effective forces produced by swimmers from inertia effects. Therefore, based on fundamental mechanics, it was firstly developed an algorithm to be applied in raw horizontal and vertical ground reaction forces during the grab start, since it is considered a suitable technique to simulate the rigid body falling experiments (Appendix IV). In fact, before the wedge authorization, it would be more complex

to evidence a vertical reaction component. It was hypothesized that previous ventral and also backstroke start kinetics findings (Appendix I) were being transmitted in an unclear way for coaching and scientific community. The grab start depicted considerable passive force contribution in the two most propulsive components (i.e. horizontal and vertical, Appendix IV), due to the similarity of the rigid body falling angles from the acoustic signal to take-off instant. The algorithm implemented during backstroke start force analysis (Chapter X) revealed that horizontal and vertical ground reaction forces are most dependent upon effective swimmers action; however passive horizontal and vertical components showed slightly contribution during a short period before the hands-off. These results agreed previous established hypothesis that swimmers holding themselves on the wedge would be able to apply horizontal and vertical ground reaction force dependent upon inertia and muscular effects. In backstroke start the angles formed between the centre of mass – centre of pressure and horizontal axis were predominantly below the 45º recommended to take the most of steering advantages, being the rigid body falling simulated with a shorter initial angle compared to the grab start condition. The values obtained in Chapters V and VII revealed that with and without the new wedge, take-off angles ranged from 20 to 30º. Findings obtained in Chapter X reinforces previous statements about the backstroke start complexity in achieving clear flight and entry phases through a take-off angle closer to the water level (Takeda et al., 2014) and the need to emphasize effective lower limb actions for vertical and horizontal propulsion.

Chapter 12 Conclusions

After the findings obtained in the collection of studies presented in this Thesis, it is pertinent to stress out the following conclusions:

(i) Research in backstroke start emerges in 1960s and actual handgrips configurations had not been considered until the implementation of the new wedge;

(ii) There are inconsistencies among studies regarding start phases and biomechanical parameters with most of studies not including the underwater phase to characterize backstroke start;

(iii) Several start variants have been chosen by elite backstrokers, being the start variants with feet partially emerged and hands on highest horizontal and vertical handgrip the most used;

(iv) The developed instrumented starting block for backstroke external kinetics assessment had not considered actual FINA facility rules and none research had measured separately preferred and non-preferred limb proficiency;

(v) The new instrumented starting block allowed accurate, reliable, reproducible and valid backstroke start kinetics data, being versatile to evaluate the different upper and lower limbs set configurations, independently;

(vi) Four independent 3D - 6DoF waterproof force plates, a handgrips pair and a new adjustable wedge pair allowed right and left upper and lower limbs analysis;

(vii) A new calibration volume (6.0 m length x 2.0 m height x 2.5 m width) allowed accurate surface and underwater 3D reconstruction for backstroke start kinematics;

(viii) The MoCap system allowed 3D backstroke start underwater phase analysis from full immersion until 15 m mark and revealed the inexistence of a well defined gliding phase;

(ix) The different feet and hands combinations used at set positioning revealed biomechanical advantages when swimmers positioned feet partially or entirely emerged and hands on highest horizontal and vertical handgrip;

(x) To position feet partially or entirely emerged and hands on highest horizontal and vertical handgrips did not guarantee shorter 15 m start time;

(xi) Different handgrips positioning (i.e. highest horizontal or vertical) did not affect upper and lower limbs electromyographic activation;

(xii) Upper and lower limb biarticular muscles activation depicted similarly between two start variants in the hands-off, take-off, flight and entry start phases;

(xiii) As in the electromyographic parameters, the handgrips did not affect linear and angular kinematics when performed with and without the new wedge;

(xiv) The new wedge did not affect, linear and angular kinematics when backstroke start was performed with horizontal or vertical handgrips;

(xv) Upper and lower limb preference did not determine backstroke start kinetics performance when swimmers using hands horizontal and vertically positioned;

(xvi) Upper and lower limb kinetics asymmetry was often similar between start variants and lower limb asymmetry influenced start performance when swimmers using variant with hands horizontally positioned;

(xvii) Non-linear modelling tool predicted backstroke start performance with smaller errors than linear tool using kinematic and kinetic parameters from the acoustic signal to the water immersion as input variables;

(xviii) An algorithm to determine passive and active force contribution from grab start raw force-time curves was successfully implemented in backstroke start;

(xix) Horizontal and vertical ground reaction backstroke start forces are dependent upon inertial effects and swimmers' muscular actions.

Chapter 13 Suggestions for Future Research

This Thesis considered technological and methodological improvements to provide coaches with some initial objective evidence that allow understanding biomechanics of different backstroke start variants performed under current FINA rules. Notwithstanding the Thesis relevancy for contribution of backstroke start state of the art, some gaps and limitations still remains, being our purpose to examine them in further studies, namely:

(i) Design optimization of the instrumented starting block prototype to spread installation and use in different swimming pool configurations;

(ii) Development of a dedicated and user-friendly external kinetics acquisition software;

(iii) Integration of the Mocap system to the instrumented starting block for backstroke start automatic tracking that covers full-body from acoustic signal to 15 m mark;

(iv) Determination of normative kinematics and external kinetics reference values for backstroke start performance in both genders and in different competitive levels;

(v) Implementation of computer simulation method considering different anthropometric database to model backstroke start performed with different handgrips and wedge positioning combinations;

(vi) Implementation of neural networks combined to other artificial intelligent techniques (as fuzzy logic) to model and predict 5 to 10 m backstroke start time;

(vii) Development and implementation of a resistance-training program based on anatomical principles, reaction forces and EMG findings to its effectiveness on backstroke start performance and technique.

Chapter 14 References

Chapter 1

Cossor, J., & Mason, B. (2001). Swim start performances at the Sydney 2000 Olympic Games. In: J.R. Blackwell, & R.H. Sanders (eds.), XIX International Symposium on Biomechanics in Sports: University of San Francisco, 70-74.

Ball, N., & Scurr, J. (2013). Electromyography normalization methods for high-velocity muscle actions: review and recommendations. *Journal of Applied Biomechanics, 29*(5), 600-608.

Barlow, H., Halaki, M., Stuelcken, M., Greene, A., & Sinclair, P.J. (2014). The effect of different kick start positions on OMEGA OSB11 blocks on free swimming time to 15 m in developmental level swimmers. *Human Movement Science, 34*, 178-186.

Bartlet, R. (2007). Introduction to sports biomechanics: analysing human movement patterns. Routledge (2nd edition), New York.

de Jesus, K., de Jesus, K., Figueiredo, P., Gonçalves, P., Pereira, S., Vilas-Boas, J.P., & Fernandes, R.J. (2011). Biomechanical analysis of backstroke swimming starts. *International Journal of Sports Medicine, 32*(7), 546-551.

de Jesus, K., de Jesus, K., Figueiredo, P., Gonçalves, P., Pereira, S., Vilas-Boas, J.P., & Fernandes, R.J. (2013). Backstroke start kinematic and kinetic changes due to different feet positioning. *Journal of Sports Sciences, 31*(15),1665-1675.

dos Santos, K.B., Pereira, G., Papoti, M., Bento, P.C., & Rodacki, A. (2013). Propulsive force asymmetry during tethered-swimming. *International Journal of Sports Medicine, 34*(7), 606-611.

Escamilla, R.F., & Andrews, J.R. (2009). Shoulder muscle recruitment patterns and related biomechanics during upper extremity sports. *Sports Medicine, 39*(7), 569-590.

Edelmann-Nusser, J., Hohmann, A., & Henneberg, B. (2002). Modeling and prediction of competitive performance in swimming upon neural networks. *European Journal of Sport Science, 2*(2), 1-10.

Galbraith, H., Scurr, J., Hencken, C., Wood, L., & Graham.Smith, P. (2008). Biomechanical comparions of the track start and the modified one-handed track start in competitive swimming: an intervention study. *Journal of Applied Biomechanics, 24*(4), 307-315.

Green, R.C., Cryer, W., Bangerter, B., Lewis, K., & Walker, J. (1987). Comparative analyses of two methods of backstroke starting: conventional and whip. In L. Tsarouchas, J., Terauds, B.A. Gowitzke, L.E. Holt (eds.), V International Symposium on Biomechanics in Sports: University of Greece, 281-292.

Guimarães, A.C.S., & Hay, J.G. (1985). A mechanical analysis of the grab starting technique in swimming. I*nternational Journal of Sport Biomechanics, 1*, 25-35.

Hay, J.G., & Guimarães, A.C.S. (1983). A quantitative look at swimming biomechanics. *Swimming Technique, 20(2)*, 11-17.

Hanin, Y., Malvela, M., & Hanina, M. (2004). Rapid correction of start technique in an Olympic-level swimmer: a case study using old way/new way. *Journal of Swimming Research, 16*, 11-17.

Hahn, M.E. (2007). Feasibility of estimating isokinetic knee torque using a neural network model. *Journal of Biomechanics, 40*(5), 1107-1114.

Hart, S., & Gabbard, C. (1997). Examining the stabilizing characteristics of footedness. *Laterality: asymmetries of body brain and cognition, 2*(1), 17-26.

Heusner, W.W. (1959). Theoretical specifications for the racing dive: optimum angle of take-off. *Research Quarterly, 30*(1), 25-37.

Hohmann, A., Fehr, U., Kirsten, R., & Krueger, T. (2008). Biomechanical analysis of the backstroke start technique in swimming. *E-Journal Bewegung und Training, 2*, 28-33.

Kudo, S. & Lee, M.K. (2010). Prediction of propulsive force exerted by the hand in swimming. In. P-L Kjendlie, R.K. Stallmann, & J Cabri (eds.), XI International Symposium on Biomechanics and Medicine in Swimming: Norwegian School of Sport Science, 112-115.

Larsen, O.W., Yancher, R.P., & Baer, C.L.H. (1981). Boat design and swimming performance. *Swimming Technique, 18*(2), 38-44.

Mason, B., Alcock, A., & Fowlie, J. (2007). A kinetic analysis and recommendations for elite swimmers performing the sprint start. In: H.J. Menzel, & M.H. Chagas (eds.), XXV International Symposium on Biomechanics in Sports: Federal University of the State of Minas Gerais, 192-195.

Martens, J., Figueiredo, P., & Daly, D. (2015). Electromyography in the four competitive swimming strokes: A systematic review. *Journal of Electromyography and Kinesiology, 25*(2), 273-291.

Mason, B., Mackintosh, C. Pease, D. (2012). The development of an analysis system to assist in the correction of inefficiencies in starts and turns for elite competitive swimming. In E.J. Bradshaw, A. Burnett, P.A. Hume (eds.), XXXth International Symposium on Biomechanics in Sports. Australian Catholic University, 249-252.

McLean, S.P., Holthe, M.J., Vint, P.F., Beckett, K.D., & Hinrichs, R.N. (2000). Addition of an approach to a swimming relay start. *Journal of Applied Biomechanics, 16*(4), 342-255.

Nguyen, C., Bradshaw, E., Pease, D., & Wilson, C. (2014). Is starting with the feet out of the water faster in backstroke swimming? *Sports Biomechanics, 13*(2), 154-165.

Olstad, B.H., Zinner, C., Haakonsen, D., Cabri, J., & Kjendlie, P-L. (2014). A new approach for identifying phases of the breastroke wave kick and calculation of feet slip using 3D automatic motion tracking. 195-199. In: B. Mason (ed.), XII International Symposium for Biomechanics and Medicine in Swimming. Australian Institute of Sports, 112-117.

Pautasso, M. (2013). Ten simple rules for writing a literature review. *Plos Computational Biology, 9*(7), e1003149.

Pfeiffer, M., & Hohmann, A. (2012). Applications of neural networks in training science. *Human Movement Science, 31*(2), 344-359.

Psycharakis, S., Sanders, R., & Mill, F. (2005). A calibration frame for 3D swimming analysis. In. Q. Wang (ed.), XXIII International Symposium on Biomechanics in Sports: University of Beijing, 901-904.

Rea, W.M., & Soth, S. (1967). Revolutionary backstroke start. *Swimming Technique, 3*, 94-95.

Ribeiro, J., Morais, S.T., Figueiredo, P., de Jesus, K., Vilas-Boas, J.P., & Fernandes, R.J. (2014). Effect of fatigue in spatiotemporal parameters during 100 m front-crawl event monitored through 3D dual-media automatic tracking. In. B. Mason (ed.), XII International Symposium for Biomechanics and Medicine in Swimming: Australian Institute of Sports, 136-140.

Sanders, R. H. (2002). New analysis procedures for giving feedback to swimming coaches and swimmers. In K. Gianikelis, B.R. Mason, H. M. Toussaint, R. Arellano, R.H. Sanders (eds.), XX International Symposium on Biomechanics in Sports: University of Extremadura, 1-14.

Sanders, R., Psycharakis, S., McCabe, C., Naemi, R., Connaboy, C., Shuping, L., Scott, G., & Spence, A. (2006). Analysis of swimming technique: state of the art applications and implications. In J.P. Vilas-Boas, F. Alves, & A. Marques (eds.), X International Symposium on Biomechanics and Medicine in Swimming: University of Porto, 20-24.

Sanders, R.H., Thow, J., Alcock, A., Fairweather, M., Riach, I., & Mather, F. (2012). How can asymmetries in swimming be identified and measured? *Journal of Swimming Research, 19(1)*, 1-15.

Seifert, L., Vantorre, J., Lemaitre, F., Chollet, D., Toussaint, H.M., & Vilas-Boas, J.P. (2010). Different profiles of the aerial start phase in front crawl. *Journal of Strength and Conditioning Research, 24*(4), 507-516.

Stockel, T. & Valter, C. (2014). Hand preference patterns in expert basketball players: interrelations between basketball-specific and everyday life behaviour. *Human Movement Science, 38*, 143-151.

Stratten, G. (1970). A comparison of three backstroke starts. *Swimming Technique, 7*, 55-60.

Takeda, T., Itoi, O., Takagi, H., & Tsubakimoto, S. (2014). Kinematic analysis of the backstroke start: differences between backstroke specialists and non-specialists. *Journal of Sports Sciences, 32*(7), 635-641.

Theut, K.M., & Jensen, R.L. (2006). A comparison of two backstroke starts. In H. Schwameder, G. Strutzenberger, V. Fastenbauer, S. Lindinger, & E. Muller (eds.), XXIV International Symposium on Biomechanics in Sports: University of Salzburg, 1-5.

Thow, J.L., Naemi, R., & Sanders, R.H. (2012). Comparison of modes of feedback on performance in swimming. *Journal of Sports Sciences, 30*(1), 43-52.

Tor, E., Pease, D.L., & Ball, K.A. (2015a). The reliability of an instrumented starting block analysis system. *Journal of Applied Biomechanics, 31*(1), 62-67.

Tor, E., Pease, D.L., & Ball, K.A. (2015b). Key parameters of the swimming start and their relationship to start performance. *Journal of Sports Sciences, 33*(13), 1313-1321.
Vilas-Boas, J.P., & Fernandes, R.J. (2003). Swimming starts and turns: determinant factors of swimming performance In P. Pelayo (ed.), Actes des 3èmes journées spécialisées de natation. University of Lille, 84-95.
Vantorre, J., Seifert, L., Fernandes, R.J., Vilas-Boas, J.P., & Chollet, D. (2010). Comparison of grab start between elite and trained swimmers. *International Journal of Sports Medicine, 31*(12), 887-893.
Vantorre, J., Chollet, D., & Seifert, L. (2014). Biomechanical analysis of the swim-start: a review. *Journal of Sports Science and Medicine, 13*(2) 223-231.
Van Soest, A.J., Bobbert, M.F., & Van Ingen Schenau, G.J. (1994). A control strategy for the execution of explosive movements from varying starting positions. *Journal of Neurophysiology, 71*(4), 1390-1402.
Wilson, B.D., & Howard, A. (1983). The use of cluster analysis in movement descripion and classification of the backstroke swim start. In B. Matsui and K. Kobayashi (eds.), Bioemchanics VIII-B: Human Kinetics Publisher, 1223-1230.
Wright, D.A. (2011). Development of a waterproof force plate for pool applications. Master's thesis of Science in the Graduate School of the Ohio State University.
Yoshioka, S., Nagano, A., Hay, D.C., & Fukashiro, S. (2010). The effect of bilateral asymmetry of muscle strength on jumping height of the countermovement jump: a computer simulation study. *Journal of Sports Sciences, 28*(2), 209-218.
Yoshioka, S., Nagano, A., Hay, D.C., & Fukashiro, S. (2011). The effect of bilateral asymmetry of muscle strength on the height of a squat jump: a computer simulation study. *Journal of Sports Sciences, 29*(8), 867-877.
Zehr, E.P. (2005). Neural control of rhytmic human movement: the common core hyphotesis. *Exercise and Sport Sciences Reviews, 33*(1), 54-60.

Chapter 11

Aramptazis, A., Walsh, M., & Bruggemann, G-P. (1998). Biomechanical analysis of the long jump at the VIth world championships in athletics. In H.J. Riehle, & M.M., Vieten (eds.) XVI International Symposium on Biomechanics in Sports: University of Konstanz, 108-111,.
Ball, N., & Scurr, J. (2013). Electromyography normalization methods for high-velocity muscle actions: review and recommendations. *Journal of Applied Biomechanics, 29*(5), 600-608.
Barbosa, T.M., de Jesus, K., Abraldes, J.A., Ribeiro, J., Figueiredo, P., Vilas-Boas, J.P., & Fernandes, R.J. (2015). Effects of protocol step length on biomechanical measures in swimming. *International Journal of Sports Physiology and Performance, 10*(2), 211-218.
Blanksby, B., Nicholson, L., & Elliot, B. (2002). Biomechanical analysis of the grab, track and handle swimming starts: an intervention study. *Sports Biomechanics, 1*(1), 11-24.
Blasser, R.J., Couls, L.M., Lee, C.F:, Zuniga, J.M., & Malek, M.H. (2014). Comparing EMG amplitude patterns of responses during dynamic exercise: polynomial vs log-transformed regresssion. *Scandinavian Journal of Medicine and Science in Sports, 25*(2), 159-165.
Breed, Young, R.V.P., & Young, W.B. (2003). The effect of resistance training progamme on the grab, track and swing starts in swimming. *Journal of Sports Sciences, 21*(3), 213-220.
de Jesus, K., de Jesus, K., Figueiredo, P., Gonçalves, P., Pereira, S., Vilas-Boas, J.P., & Fernandes, R.J. (2011). Biomechanical analysis of backstroke start swimming starts. *International Journal of Sports Medicine, 32*(7), 546-551.
de Jesus, K., de Jesusk K., Figueiredo, P., Gonçalves, P., Pereira, S., Vilas-Boas, J.P., & Fernandes, R.J. (2013). Backstroke start kinematic and kinetic changes due to different feet positioning. *Journal of Sports Sciences, 31*(15), 1665-1675.
Figueiredo, P., Machado, L., Vilas-Boas, J.P., & Fernandes, R.J. (2011). Reconstruction error of calibration voume's coordinates for 3D swimming kinematics. *Journal of Human Kinetics, 29*, 35-40.
Guimarães, A.C.S., & Hay, J.G. (1985). A mechanical analysis of the grab starting technique in swimming. *International Journal of Sport Biomechanics, 1*, 25-35

Gourgoulis, V., Aggeloussis, N., Kasimatis, P., Vezos, N., Boli, A. & Mavromatis, G. (2008). Reconstruction accuracy in underwater three-dimensional kinematics. *Journal of Science and Medicine in Sport, 11*(2), 90-95.

Hahn, M.E. (2007). Feasibility of estimating isokinetic knee torque using a neural network model. *Journal of Biomechanics, 40*(5), 1107-114.

Heusner, W.W. (1959). Theoretical specifications for the racing dive: optimum angle of take-off. *Research Quarterly, 30*(1), 25-37.

Hohmann, A., Fehr, U., Kirsten, R., & Krueger, T. (2008). Biomechanical analysis of the backstroke start technique in swimming. *E-Journal Bewegung Training, 2*, 28-33.

Houel, N., Elipot, M., André, F., & Hellard, P. (2009). Influences of angles of attack, frequency and kick amplitude on swimmer's horizontal velocity during underwater phase of a grab start. *Journal of Applied Biomechanics, 29*(1), 49-54.

Kwon, Y.H, & Casebolt, J.B. (2006). Effects of light refraction on the accuracy of camera calibration and reconstruction in underwater motion analysis. *Sports Biomechanics, 5*(2), 315-340.

Luk, H.Y., Winter, C., O'Neil, E., & Thompson, B.A. (2014). Comparison of muscle strength imbalance in powerlifter and jumpers. *Journal of Strength and Conditioning Research, 28*(1), 23-27.

Mathiyakom, W., NcNitt-Gray, J.L., & Wilcox, R. (2006). Lower extremity control and dynamics during backward angular impulse generation in backward translationg tasks. *Experimental Brain Research, 169*(3), 377-88.

McDonnell, L.K., Hume, P.A., & Nolte, V. (2012). An observational model for biomechanical assessment of sprint kayaking technique. *Sports Biomechanics, 11*(4), 507-523.

Nguyen, C., Bradshaw, E.J., Pease, D., & Wilson, C. (2014). Is starting with the feet out of the water faster in backstroke swmming? *Sports Biomechanics, 13*(2), 154-165.

Pautasso, M. (2013). Ten simple rules for writing a literature review. *Plos Computational Biology, 9*(7), e1003149.

Pfeiffer, M. & Hohmann, A. (2012). Applications of neural networks in training science. *Human Movement Science, 31*(2), 344-359.

Rea, W.M., & Soth, S. (1967). Revolutionary backstroke start. *Swimming Technique, 3*, 94-95.

Rodacki, A.L., & Fowler, N.E. (2001). Intermuscular coordination during pendulum rebound exercises. *Journal of Sports Sciences, 19*(6), 411-425.

Seifert, L., Vantorre, J., Lemaitre, F., Chollet, D., Toussaint, & Vilas-Boas, J.P. (2010). Different profiles of the aerial start phase in front crawl. *Journal of Strength and Conditioning Research, 24*(2), 507-516.

Stockel, T., & Valter, C. (2014). Hand preference patterns in expert basketball players: interrelations between basketball-specific and everyday life behavior. *Human Movement Science, 38*, 143-151.

Takeda, T., Ichikawa, H., Takagi, H., & Tsubakimoto, S. (2009). Do differences in initial speed persist to the stroke phase in front-crawl swimming? *Journal of Sports Sciences, 27*(13), 1449-1454.

Takeda, T., Itoi, O., Takagi, H., & Tsubakimoto, S. (2014). Kinematic analysis of the backstroke start: differences between backstroke specialists and non-specialists. *Journal of Sports Sciences, 32*(7), 635-641.

Theut, K.M., & Jensen, R.L. (2006). A comparison of two backstroke starts. In: H. Schwameder, G. Strutzenberger, V. Fastenbauer, S. Lindinger, & E. Muller (eds.) ,XXIV International Symposium on Biomechanics in Sports: University of Salzburg, 1-5.

Thanopoulos, V., Rozi, G., Okicic, T., Dopsaj, M., Jorgic, B., Madic, D., Velixkovic, S., Milanovic, Z., Spanou, F., & Batis, E. (2012). Differences in the effciency between the grab and track starts for both genders in greek young swimmers. *Journal of Human Kinetics,* 23, 43-51.

Tor, E., Pease, D.L., & Ball, K.A. (2015a). The reliability of an instrumented start block analysis system. *Journal of Applied Biomechanics, 31*(1), 62-67.

Tor, E., Pease, D.L., & Ball, K.A. (2015b). Comparing three underwater trajectories of the swimming start. *Journal of Science and Medicine in Sport*, pii S1440-2440(14)00205-9. Doi: 10.1016/j.sams.2014.10.005.

Tor, E., Pease, D.L., & Ball, K.A. (2015c). Key parameters of the swimming start and their relationship to start performance. *Journal of Sports Sciences, 33*(13), 1313-1321.

Van Soest, A.J., Bobbert, M.F., & Van Ingen Schenau, G.J. (1994). A control startegy for the execution of explosive movements from varying starting positions. *Journal of Neurophysiology, 71*(4), 1390-1402.

Vantorre, J., Seifert, L., Fernandes, R.J., Vilas-Boas, J.P., & Chollet, D. (2010). Comparison of grab start between elite and trained swimmers. *International Journal of Sports Medicine, 31*(12) 887-893.

Vantorre, J., Chollet, D., & Seifert, L. (2014). Biomechanical analysis of the swim-start: a review. *Journal of Sports Science and Medicine, 13*(2), 223-231.

Vilas-Boas, J.P., & Fernandes, R.J. (2003). Swimming starts and turns: determinant factors of swimming performance. Actes des 3èmes journées spécialisées de natation: University of Lille, 84-95

Vilas-Boas, J.P., Cruz, J., Sousa, F., Conceição, F., Fernandes, R., & Carvalho (2003). Biomechanical analysis of ventral swimming starts: comparison of the grab with two track-start techniques. In: J-C- Chatard (ed.), IX International Symposium on Biomechanics and Medicine in Swimming, University of Saint Etienne, France, 249-253,.

Zehr, E. P. (2005). Neural control of rhytmic human movement: the commin core hypothesis. *Exercise and Sport Sciences Reviews, 33*(1), 54-60.

Appendix I

External kinetics in individual and relay swimming starts: A review.

Luis Mourão[1,2], Karla de Jesus[2], Kelly de Jesus[2], Ricardo J. Fernandes[2,3], Mário A. P. Vaz[3,4], João Paulo Vilas-Boas[2,3].

[1] Superior School of Industrial Studies and Management, Porto Polytechnic Institute, Vila do Conde, Portugal

[2] Centre of Research, Education, Innovation and Intervention in Sport, Faculty of Sport, University of Porto, Porto, Portugal

[3] Porto Biomechanics Laboratory (LABIOMEP), Porto, Portugal

[4] Institute of Mechanical Engineering and Industrial Management, Faculty of Engineering, University of Porto, Porto, Portugal

Published on XII International Symposium for Biomechanics and Medicine in Swimming (2014): 179-184.

Abstract

This study aimed to present a literature review on the external kinetics of swimming starts for the purposes of summarising and highlighting existing knowledge, identifying gaps and limitations and challenging new researchers for future projects. A preliminary literature search was performed using relevant electronic databases, only for English written documents published before September 2013. Keywords including “swimming” and “start” were used to locate documents. Proceedings of the scientific conferences of Biomechanics and Medicine in Swimming (BMS) and the International Society of Biomechanics in Sports (ISBS) from 1970 and 1983, respectively, to 2013 were examined. Included studies were experimental biomechanical approaches in laboratory setting relating to external kinetics assessments on swimming starts. Twenty-eight studies were included in this review, of which 10 are peer-review journal articles and 18 are proceedings from the BMS and ISBS Congress series. From the overall included studies, 82.14% analysed the individual ventral starts, followed by 14.28% at backstroke and only 3.57% at relay starts. Twenty-five per cent from the overall ventral starting studies measured the external horizontal and vertical forces acting on the swimmer’s hands and only one research group has yet published about the upper limbs horizontal force on the backstroke start. Previous studies have presented unique contribution in swimming start kinetics; however, future researches should focus on devices capabilities improvements based on the current starting block configuration, mainly for dorsal and relay starting kinetics analysis purposes, and considering 3D-6DoF analysis of the forces exerted by each of the four limbs.

Key words: biomechanics, forces, moments, swimming analysis, starting techniques

Introduction

The swimming start, defined by the time period between the starting signal until the swimmer's head achieve 15 m (e.g. Vantorre et al., 2010), is an important part of short and middle distance swimming events. For example, 15 m after the start, the second-placed at men's 100 m freestyle at Barcelona 2013 Swimming World Championships was 0.08 s slower than the winner, and the final race time difference was only 0.11 s. The importance of the start is emphasized further in middle distance events, since, in the same swimming competition, the winner at men's 200 m freestyle performed the fastest 15m starting time during the final. In fact, at the recent elite level swimming competitions it is not the swimming speed that wins races but rather the better technicians in starts and also turns (Mason et al., 2012).

The swimming start is composed of several phases: block/wall, flight, entry, glide, leg kicking and swimming (Slawson et al., 2013; Vantorre et al., 2010), which are interdependent (Vantorre et al., 2010). According to Guimarães and Hay (1985) and Mason et al. (2007), the block phase determines what happens in flight and subsequently the underwater phase, respectively. Vantorre et al. (2010) have verified that the block phase negatively correlated with the starting time and advised swimmers to perform a rapid reaction to the starting signal and impulse over the starting block. In fact, the study of the ground reaction forces, which generate the swimmers' movements that attend such above-mentioned requirements have been conducted since the 1970s. To date, Elliot and Sinclair (1971) were the pioneer on the starting block instrumentation for direct force measurements.

Despite the well-accepted relevance of the external kinetics assessment and understanding at swimming starts, no former review was found in the literature about the different dynamometric devices and respective parameters assessed. It would be interesting to find scientific evidence and report the advancements pertaining to the direct forces measurement in individual and relay swimming

starts. Considering that the international swimming rules for individual and relay starting recommendations have changed, and the starting block has undergone many adaptations, it is crucial to gather the most relevant studies in a synthesised critical review. This study reviewed the swimming literature on starting external kinetics for the purposes of summarising and highlighting existing knowledge, identifying gaps and limitations and challenging new researchers for future projects.

Methods

A preliminary literature search was performed using PubMed, SportDiscus, Scopus and ISI Web of Knowledge electronic databases, only for English written documents published before September 2013. Keywords including “swimming” and “start” were initially used to locate documents. Proceedings of the scientific conferences of Biomechanics and Medicine in Swimming (BMS) and the International Society of Biomechanics in Sports (ISBS) from 1970 and 1983, respectively, to 2013 were examined. Included studies were experimental biomechanical approaches in laboratory setting relating to external kinetics assessments on swimming starts. The documents that were available only as abstracts and duplicated studies were excluded.

Results

Table 1 display the ultimately 28 studies included in this review, 10 of which are peer-review journal articles and 18 are proceedings from the BMS and ISBS Congress series. Twenty-five and 46.42% from the overall starting studies applied the strain gauges and piezoelectric crystals technology, respectively. From the overall included studies, 82.14% analysed the individual ventral starts, followed by 14.28% at backstroke and only 3.57% at relay starts. Twenty-five per cent from the overall ventral starting studies measured the external horizontal

and vertical forces acting on the swimmer's hands. Only one research group (Swimming Science, 2014) has yet published about the upper limbs horizontal force on the backstroke start. Researchers have instrumented the handgrips with load cells or bonded strain gauges directly to the hands bar to measure the overall upper limbs force. To measure the horizontal and resultant lower limbs external kinetics at backstroke starting, researchers have used one force plate, while for ventral starts one and two force plates have been mounted over the starting block to measure mainly the horizontal and vertical reaction force components. Despite most of the research groups have used three-dimensional sensors, only two have studied the lateral force component action on the swimmers' lower limbs. Moments of force and centre of pressure were assessed once at individual ventral start.

Table 1. The 28 studies that assessed the external forces in individual ventral and dorsal and relay starts, and the corresponding general description.

Authors	Start technique	Forces assessed
Elliot and Sinclair (1971)	Ventral	Horizontal lower limbs
Cavanagh et al. (1975)	Grab	Horizontal and vertical upper limbs
Stevenson and Morehouse (1978)	Grab	Horizontal and vertical upper limbs
Shierman (1978)	Grab	Horizontal and vertical lower limbs
Zatsiorsky et al. (1979)	Arm swing, grab and track	Horizontal and vertical lower limbs
Hay and Guimarães (1983)	Grab	Horizontal upper and lower limbs
Vilas-Boas et al. (2000)	Track	Horizontal, vertical and resultant
Naemi et al. (2000)	Grab	Horizontal and vertical lower limbs
Krueger et al. (2003)	Grab and track	Horizontal and resultant lower limbs
Breed and Young (2003)	Grab, track, swing	Horizontal upper and lower limbs
Vilas-Boas et al. (2003)	Grab and track	Horizontal, vertical lower limbs
Benjanuvatra et al. (2004)	Grab and track	Horizontal and vertical lower limbs
Kibele et al. (2005)	Ventral	Horizontal, vertical and resultant
Arellano et al. (2005)	Grab	Horizontal and vertical lower limbs
Mason et al. (2007)	Grab	Horizontal lower limbs
Hohmann et al. (2008)	Backstroke	Horizontal and vertical lower limbs
Galbraith et al. (2008)	Track and one handed track	Horizontal lower and vertical upper and lower limbs
Vint et al. (2009)	Track	Horizontal upper limbs
de Jesus et al. (2010)	Backstroke	Horizontal lower limbs
Vantorre et al. (2010)	Grab	Horizontal and vertical lower limbs
Takeda et al. (2010)	Relay	Horizontal lower limbs
Cossor et al. (2011)	Track	Horizontal and vertical lower limbs
de Jesus et al. (2011)	Backstroke	Horizontal lower and upper limbs
Kilduffi et al. (2011)	Ventral	Horizontal and vertical lower limbs
Slawson et al. (2011)	Track	Horizontal and vertical lower limbs
Honda et al. (2012)	Track and kick	Horizontal vertical and resultant, vertical upper limbs
de Jesus et al. (2013)	Backstroke	Horizontal lower and upper limbs
Slawson et al. (2013)	Kick	Horizontal and vertical lower limbs

Discussion

The external force assessments during swimming starts are considered of great value for coaches and swimmers, since they provide information about how swimmers' movements are generated to propel themselves out of the starting block. The findings of this study evidence that swimming researchers have been very concerned about the external kinetics assessment at individual ventral starts, and have optimized the devices according to the starting rule changes for block configuration (FINA, FR 2.7). However, much effort should be invested to the study of the upper limbs dynamometry, mainly considering all the possibilities allowed by the FINA regulations, as performed by Vint et al. (2009) with instrumented front and side handgrips. Researchers should also consider the implementation of force sensors in lateral handgrips to knowledge about the dynamometric profile used at the tuck starting technique.

In contrast to the substantial quantity of studies which approach kinetics at individual ventral starts, there is a paucity of backstroke start kinetic data, mainly due to the technical difficulties associated with the adaptation of the kinetic devices to the starting block and pool wall (cf. de Jesus et al., 2011, 2013). Despite the considerable contribution provided by the previous studies, a large effort should be invested to adapt the kinetic devices according to the actual starting block configuration, as implementing the two horizontal and lateral backstroke start handgrips. Considering the individual ventral and dorsal starts, the relay techniques have received much less attention, since only one research group has attempted to analyze the horizontal ground reaction force component in three different techniques (cf. Takeda et al., 2010). Further research should be conducted including the rear back plate to verify if swimmers change the respective force profiles when performing relay starts using this recent authorized device.

The consistent use of three dimensional force sensors has been implemented mainly to study the horizontal (antero-posterior) and vertical upper and lower

limbs force components. In fact, the major and relevant components are the forces applied in the vertical and antero-posterior axes (Slawson et al., 2013); however, the medio-lateral axis was studied by Vantorre et al. (2010) in elite and trained swimmers, and might be considered an important feedback to improve technique and performance of young swimmers.

Conclusion

The external forces assessment during starts is an important concern of the swimming research community. Researchers have continually adapted the instrumented starting block to measure upper and lower limbs forces, mainly at individual ventral starts. However, sports biomechanics and engineers should invest effort to develop a 3D kinetic system based on the actual block configuration capable to identify the upper and lower limbs contribution to propel starters out of the block/wall at different starting techniques.

Acknowledgments

This research was supported by CAPES (BEX 0761/12-5/2012-2014), Santander Totta Bank (PP-IJUP2011-123) and FCT (EXPL/DTP-DES/2481/2013- FCOMP-01-0124-FEDER-041981).

References

Arellano, R., Liana, S., Tella, V., Morales, E., & Mercadé, J. (2005). A comparison CMJ, simulated and swimming grab-start force recordings and their relationships with the start performance. In Q. Wang (ed.), XXIII International Symposium on Biomechanics in Sports: University of Beijing, 923-926.

Benjanuvatra, N., Lyttle, A., Blanksby, B., & Larkin, D. (2004). Force development profile of the lower limbs in the grab and track start in swimming. In M. Lamontagne, D. Gordon, E. Robertson, & H. Sveistrup (eds.), XXII International Symposium on Biomechanics in Sports, 399-402.

Breed, R.V.P., & Young, W.B. (2003). The effect of a resistance training programme on the grab, track and swing starts in swimming. *Journal of Sports Sciences, 21*(3), 213-220.

Cavanagh, P.R., Palmgren, J.V., & Kerr, B.A. (1975). A device to measure forces at the hands during the grab start. In L. Lewillie, & J.P. Clarys (eds.), II International Symposium on Biomechanics and Medicine in Swimming: University Park Press, 43-50.

Cossor, J., Slawson, S., Shillabeer, B., Conway, P., & West, A. (2011). Are land tests a good predictor of swim start performance? In J.P., Vilas-Boas, L. Machado, K. Veloso (eds.), XXIX International Symposium on Biomechanics in Sports: University of Porto, 183-186.

de Jesus, K., de Jesus, K., Figueiredo, P., Gonçalves, P., Pereira, S. M., Vilas-Boas, J.P., & Fernandes, R.J. (2010). In P-L. Kjendlie, R.K. Stallman, & J. Cabri (eds.), XI International Symposium on Biomechanics and Medicine in Swimming: Norwegian School of Sport Science, 64-66.

de Jesus, K., de Jesus, K., Figueiredo, P., Gonçalves, P., Pereira, S., Vilas-Boas, J.P., & Fernandes, R.J. (2011). Biomechanical analysis of backstroke swimming starts. *Internation Journal of Sports Medicine, 32*(7), 546-551.

de Jesus, K., de Jesus, K., Figueiredo, P., Gonçalves, P., Pereira, S., Vilas-Boas, J.P., & Fernandes, R.J. (2013). Backstroke start kinematic and kinetic changes due to different feet positioning. *Journal of Sports Sciences, 31*(15),1665-1675.

Elliott, G. M., & Sinclair, H. (1971). The influence of block angle on swimming sprint starts. In L. Lewillie, & J.P. Clarys (eds.), I International Symposium on Biomechanics and Medicine in Swimming: University of Brussels, 183-189.

Galbraith, H., Scurr, J., Hencken, C., Wood, L., & Graham-Smith, P. (2008). Biomechanical comparison of the track start and the modified one-handed track start in competitive swimming: an intervention study. *Journal of Applied Biomechanics, 24*(4), 307-315.

Guimarães, A., & Hay, J. (1985). A mechanical analysis of the grab starting technique in swimming. *International Journal of Sports Biomechanics,* 1, 25-35.

Hay, J.G., Guimarães, A.C.S., & Grimstron, S.K. (1983). A quantitative look at swimming biomechanics. *Swimming Technique, 20*, 11–17.

Honda, K., Sinclair,Mason, B., & Pease, D. (2012). The effect of starting position on elite swim start performance using an angled kick plate. In E.J.Bradshaw, A. Burnett, & P.A. Hume (eds.), XXXI International Symposium on Biomechanics in Sports: Australian Catholic University, 249-252.

Hohmann, A., Fehr, U., Kirsten, R., & Krueger, T. (2008). Biomechanical analysis of the backstroke start technique in swimming. *E-Journal Bewegung und Training, 2*, 28-33.

Kibele, A., Siekmann, T., & Ungerechts, B. (2005). A biomechanical evaluation of dive start performance in swimming-force development characteristics and angular momentum. In Q. Wang (ed.), XXIII International Symposium on Biomechanics in Sports: University of Beijing, 890.

Kilduff, L.P., Cunningham, D. J., Owen. N.J., West, D. J., Bracken, R. M., & Cook, C.J. (2011). Effect of postactivation potentiation on swimming starts in international sprint swimmers. *Journal of Strength and Conditioning Research, 25*, 2418-2423.

Kruger T., Wick D., Hohmann A., El-Bahrawi M., & Koth A. (2003). Biomechanics of the Grab and Track Start Technique. In J.-C. Chatard (ed.), IX International Symposium on Biomechanics and Medicine in Swimming: University of Saint Etienne, 229-223.

Mason, B., Alcock, A., & Fowlie, J. (2007). A kinetic analysis and recommendations for elite swimmers performing the sprint start. In H.J. Menzel, & M.H. Chagas (eds.), XXV International Symposium on Biomechanics in Sports: Federal University of the State of Minas Gerais, 192-195.

Mason, B., Mackintosh, C., & Pease, D. (2012). The development of an analysis system to assist in the correction inefficiencies in starts and turns for elite competitive swimming. In E.J.Bradshaw, A. Burnett, & P.A. Hume (eds.). Proceedings of the XXX International Symposium on Biomechanics in Sports: Australian Catholic University, 249-252.

Naemi, R., Arshi, A.R., Ahadian, A., & Barjasteh, B. (2001). 3D kinematic and kinetic analyses of two methods for grab start technique. In J. Blackwell, & R.H. Sanders (eds.), XIX International Symposium on Biomechanics in Sports: University of San Francisco, 96-99.

Slawson, S.E., Conway, P.P., Cossor, J., Chakravorti, N., Le-Sage, T., & West, A.A. (2011). The effect of start block configuration and swimmer kinematics on starting performance in elite swimmers using the Omega OSB11 block. *Proceeded Engineering, 13*, 141-147.

Slawson, S.E., Conway, P.P., Cossor, J., Chakravorti, N., & West, A.A. (2013). The cathegorisation of swimming start performance with reference to force generation on the main block and footrest components of the Omega OSB11 start blocks. *Journal of Sports Sciences, 31*(5), 468-478.

Stevenson J.R., & Morehouse C.A. (1979). Influence of Starting-Block Angle on the Grab Start in Competitive Swimming. In J. Terauds, & E.W. Bedingfield (eds.), III International Symposium on Biomechanics and Medicine in Swimming: University Park Press, 207-214.

Shierman, G. (1978). Stability in competitive swimming starts*. Swimming Technique, 14*, 117-118.

Swimming Science (2014). 'Friday Interview Ricardo Jorge Pinto Fernandes, PhD Discusses Backstroke Starts' (2014), Retrieved 12 January, 2014, from http://www.swimmingscience.net/2014/01/friday-interview-ricardo-jorge-pinto.html

Takeda, T., Takagi, H., & Tsubakimoto, S. (2010). Comparison among three types of relay starts in competitive swimming. In P-L. Kjendlie, R.K. Stallman, & J. Cabri (eds.), XI International Symposium on Biomechanics and Medicine in Swimming: Norwegian School of Sport Science, 170-172.

Zatsiorsky, V.M., Bulgakova, N.Z., & Chaplinsky, N.M. (1979). Biomechanical analysis of starting techniques in swimming. In J. Terauds, & E.W. Bedingfield (eds.), III International Symposium on Biomechanics and Medicine in Swimming: University Park Press, 199-206.

Vantorre, J., Seifert, L., Fernandes, R.J., Vilas-Boas, J.P., & Chollet, D. (2010). Comparison of grab start between elite and trained swimmers. *International Journal of Sports Medicine, 31*(12), 887-893.

Vilas-Boas, J.P., Cruz, M.J., Sousa, F., Conceição, F., & Carvalho, J.M. (2000). Integrated kinematic and dynamic analysis of two track-start techniques. In Y. Hong, D.P. Johns, R. Sanders (eds.), XVIII International Symposium on Biomechanics in Sports: University of Hong Kong, 113–117.

Vilas-Boas, J.P., Cruz, M., Sousa, F., Conceição, F., Fernandes, R., & Carvalho, J. (2003). Biomechanical analysis of ventral swimming starts: comparison of the grab start with two track-start techniques. In J.-C. Chatard (ed.), IX International Symposium on Biomechanics and Medicine in Swimming: University of Saint Etienne, 249-253.

Vint, P.F., Hinrichs, R.N., Riewald, S.K., Mason, R.A., & McLean, S.P. (2009). Effects of handle and block configuration on swim start performance. In A.J. Harrison, R. Anderson, & I. Kenny (eds.), XXVII International Symposium on Biomechanics in Sports: University of Limerick, 102-105.

Appendix II

Reconstruction accuracy assessment of surface and underwater 3D motion analysis: a new approach

Kelly de Jesus[1], Karla de Jesus[1], Pedro Figueiredo[1,2], João Paulo Vilas-Boas[1,3], Ricardo J. Fernandes[1,3], Leandro J. Machado [1,3].

[1] Centre of Research, Education, Innovation and Intervention in Sport, Faculty of Sport, University of Porto, Porto, Portugal
[2] School of Physical Education, Federal University of Rio Grande do Sul, Brazil
[3] Porto Biomechanics Laboratory (LABIOMEP), Porto, Portugal

Accepted for publication on Computational and Mathematical Methods in Medicine (2015).

Abstract

This study assessed accuracy of surface and underwater 3D reconstruction of a calibration volume with and without homography. A calibration volume (6000 x 2000 x 2500 mm) with 236 markers (64 above and 88 underwater control points – with 8 common points at water surface – and 92 validation points) was positioned on a 25 m swimming pool and recorded with two surface and four underwater cameras. Planar homography estimation for each calibration plane was computed to perform image rectification. Direct linear transformation algorithm for 3D reconstruction was applied, using 1600000 different combinations of 32 and 44 points out of the 64 and 88 control points for surface and underwater markers (respectively). Root Mean Square (RMS) error with homography of control and validations points was lower than without it for surface and underwater cameras ($P \leq 0.03$). With homography, RMS errors of control and validation points were similar between surface and underwater cameras ($P \geq 0.47$). Without homography, RMS error of control points was greater for underwater than surface cameras ($P \leq 0.04$) and the opposite was observed for validation points ($P \leq 0.04$). It is recommended that future studies using 3D reconstruction should include homography to improve swimming movement analysis accuracy.

Key words: biomechanics, kinematics, planar homography, 3D dual media reconstruction

Introduction

The application of a multi digital camera set up for three-dimensional (3D) analysis is frequently implemented in controlled indoor or laboratory settings (Bartlett, 2007; Silvatti et al., 2012a). However, its use outdoors or in constrained environments for specific sport applications is very limited (Silvatti et al., 2012b). Furthermore, in specific underwater conditions there are a number of technical issues (e.g. camera arrangement, calibration and protocol methodology, and motion data collection) that lead to a preference of a two-dimensional (2D) data collection (on one side of the body, assuming the existence of a bilateral symmetry; Psycharakis et al., 2005). This 2D approach might be less complex to use in traditional aquatic settings, but it implies a higher occurrence of errors by disregarding the multi-planar nature of the swimmers' movement characteristics (Figueiredo et al., 2011).

Complementarily, manual tracking is the most used method to detect and follow the trajectory of body anatomical landmarks and calibration points (often attached to a custom static support recorded by each video camera field of view) during underwater movement quantitative analysis (e.g. de Jesus et al., 2012). With this process, the coordinates of the calibration points are registered in each camera 2D field of view, allowing a 3D movement reconstruction through the use of the direct linear transformation algorithm (DLT) (Chen et al., 1994). Previous findings revealed that the increase in number (e.g. from 8 to 20-24; Chen et al., 1994; Figueiredo et al., 2011; Psycharakis et al., 2005) and wider distribution (Chen et al., 1994, Challis, 2005) of the control points as well as the decrease in the calibration volume size (Gourgoulis et al., 2008; Lan et al., 1992) had improved the 3D reconstruction accuracy for surface and/or underwater cameras. Nevertheless, large calibration volumes are needed in swimming analysis since they minimize data extrapolation beyond the calibrated space, increasing further measurements accuracy (Psycharakis et al., 2010). Moreover studies have often reported larger errors for underwater camera views and have justified them

through light refraction (water has higher refraction index than air) and consequently image deformation.

In addition, for a more accurate 3D reconstruction, the displacement of each pixel across the images (induced by camera, scene position and/or independent object-motion) should also be controlled (Alvarez et al., 2012; Chen and Chen, 2013; Lingaiah & Suryanarayana, 1991; Nejadasl & Lindenbergh, 2014). For this purpose, homography is considered as a key step to obtain mappings between scene images, since computing homographies are faster and less erroneous than the motion process structure. This is justified by the fact that, the homography parameters are determined by few corresponding points (Alvarez et al., 2012; Nejadasl & Linderbergh, 2014), being typically estimated between images by finding feature correspondence. To the best of our knowledge, no research in swimming kinematics has considered the homography as a transformation method for 3D image rectification; we aimed to compare the 3D reconstruction accuracy in a large and static calibration volume (for surface and underwater digital video) using different calibration point sequences. The homography technique was applied to correct control points in each camera field of view and compared with the non-homography implementation. Following Nejadasl and Lindenbergh (2014), it was hypothesised that implementing homography technology would improve 3D reconstruction accuracy. Moreover, it is expected that using or not homography, underwater cameras would display greater 3D reconstruction errors than surface cameras.

Material and methods

Static calibration volume

A 3D calibration volume was designed using the software Solid Works 2013 (3D CAD Premium, Dassault Systèmes SolidWorks Corporation, USA; Figure 1), being based on rigid structures used in previous swimming related studies (Figueiredo et al., 2011; Gourgoulis et al., 2008; Psycharakis et al., 2005).

Afterwards, it was built using a computer numerical control machine and was comprised of three blocks, each one with the following dimensions: (i) 2000 mm length, 2500 mm height and 2000 mm width. These parts were framed and joined to form a rectangular prism of 6000 x 2500 x 2000 mm^3 (with a total calibration space of 30 x 109 mm^3), enabling the record of at least two complete consecutive swimming cycles. The 3D coordinate accuracy of the calibration volume was 1.2 mm for horizontal (x) and vertical (y) and 1.4 mm for lateral axis (z).

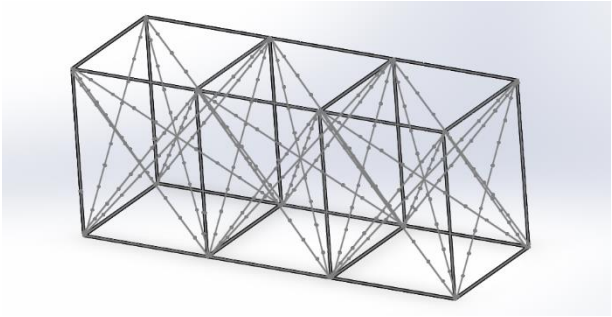

Figure 1. The rectangular prism used as the static calibration volume.

The calibration volume structure was manufactured in anodised aluminium with 25 mm diameter, selected on the basis of its high flexural stiffness relative to its weight, allowing reduced distortions due to frequent research use or/and to the swimming pool environment (Lingaiah & Suryanarayana, 1991). Stainless steel cables (5 mm) were used to triangulate each frame part, ensuring that the adjoining sides of the frame followed orthogonality. Two hundred and thirty-six black tape markers (15 mm width each) were attached with 250 mm separation on the aluminium tubes in the x-, y- and z-axes. A laser device was used to improve the accuracy of markers placing (Nano, Wicked Lasers©, Hong Kong). The 3D coordinate's accuracy of the markers were 0.5 mm for x and y and 0.9 mm for z.

Data collection

The 236 calibration points distribution in the calibration volume was registered simultaneously by four under and two surface water stationary video cameras (HDR CX160E, Sony Electronics Inc., Tokyo, Japan) recording at 50 Hz. The

calibration volume was positioned in the centre of a 25 m swimming pool (1900 mm depth) and its longitudinal axis was aligned with the lateral wall of the swimming pool. Figure 2 shows the calibration volume and the 3D camera set-up: the surface and underwater cameras were placed at an equal distance from the respective centre, forming an angle of 100° between the axes of the two surface water cameras while the angle established by the underwater cameras varied between 75 and 110° (Figueiredo et al., 2011).

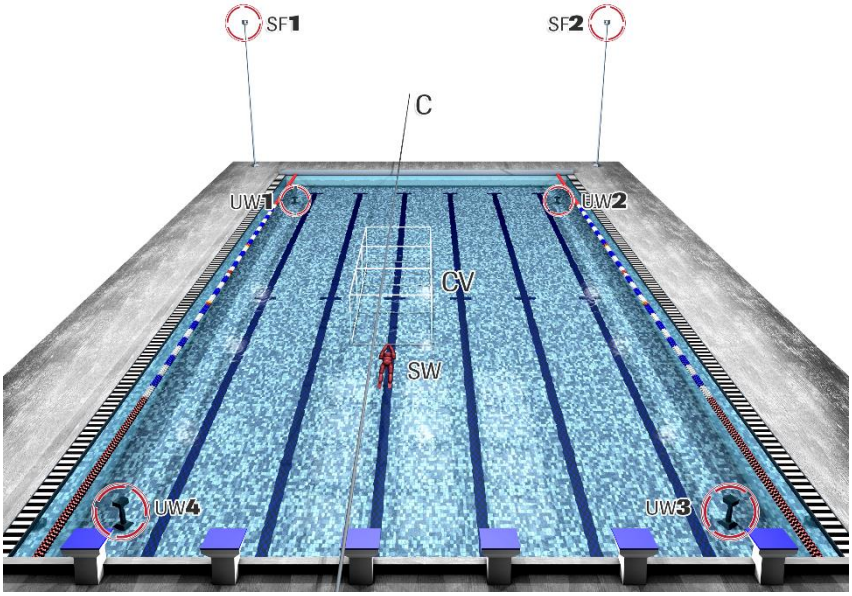

Figure 2. Experimental 3D cameras setup. Cameras UW1, UW2, UW3 and UW4: - 1st, 2nd, 3rd and 4th underwater cameras. Cameras SF1 and SF2: 1st and 2nd surface cameras. Calibration volume - CV. Swimmer – SW.

The surface cameras were positioned in tripods (Hamma Ltd., Hampshire, UK) at 3.5 m (height) and the underwater were maintained in a waterproof housing (SPK-HCH, Sony Electronics Inc., Tokyo, Japan) and fixed on tripods at 1.0 to 1.5 m (depth). A LED system visible in each video camera field of view was used for image synchronisation.

Data Analysis

The 236 points on the calibration volume with known coordinates were manually digitised (Matlab version R2012a, The Mathworks, Inc., USA) to obtain their

coordinates and the DLT method was applied for 3D reconstruction according to Equation 1 (Abdel-Aziz & Karara, 1971).

$$u = \frac{L_1 x + L_2 y + L_3 z + L_4}{L_9 x + L_{10} y + L_{11} z + 1}$$
$$v = \frac{L_5 x + L_6 y + L_7 z + L_8}{L_9 x + L_{10} y + L_{11} z + 1} \quad (1)$$

To evaluate the quality of manual digitization procedure, a specific routine in the Matlab software was developed to identify the difference between real and estimated coordinate values. The routine consisted in classifying the digitized points into large, medium and small errors, being: (i) large error, represented by red color (error > 25 mm), (ii) medium error, represented by orange color (15 mm < error < 25 mm) and (iii) small error, represented by green and blue colors (error ≤ 15mm). After this analysis, depending on the results obtained, the points were re-digitized until optimal value achievement. A limit of 25 mm for the difference between the real and estimated coordinates was imposed for each camera view and several points have shown errors in the range of 25 and 33 mm, which was a hint to the use of manual homography transformation to assign the real coordinates to each projected point, and to avoid possible mistakes.

Under linear projection, the mapping from a pixel (u,v) to a control point (x,y,0) on the calibration plane is encapsulated by a homography matrix H as:

$$\begin{pmatrix} x \\ y \\ 1 \end{pmatrix} = H_{3x3} \begin{pmatrix} u \\ v \\ 1 \end{pmatrix} = \begin{pmatrix} h_{11} & h_{12} & h_{13} \\ h_{21} & h_{22} & h_{23} \\ h_{31} & h_{32} & h_{33} \end{pmatrix} . \begin{pmatrix} u \\ v \\ 1 \end{pmatrix} \quad (2)$$

Given at least four point correspondences, $(ui, vi) \rightarrow (xi, yi, 0)$, the homography can be estimated by solving the over-determined homogeneous linear system.

$$\begin{pmatrix} u_1 & v_1 & 1 & 0 & 0 & 0 & -x_1u_1 & -x_1v_1 & -x_1 \\ 0 & 0 & 0 & -u_1 & -v_1 & -1 & y_1u_1 & y_1v_1 & y_1 \\ u_2 & v_2 & 1 & 0 & 0 & 0 & -x_2u_2 & -x_2v_2 & -x_2 \\ 0 & 0 & 0 & -u_2 & -v_2 & -1 & y_2u_2 & y_2v_2 & y_2 \\ u_3 & v_3 & 1 & 0 & 0 & 0 & -x_3u_3 & -x_3v_3 & -x_3 \\ 0 & 0 & 0 & -u_3 & -v_3 & -1 & y_3u_3 & y_3v_3 & y_3 \\ u_4 & v_4 & 1 & 0 & 0 & 0 & -x_4u_4 & -x_4v_4 & -x_4 \\ 0 & 0 & 0 & -u_4 & -v_4 & -1 & y_4u_4 & y_4v_4 & y_4 \end{pmatrix} . \begin{pmatrix} h_{11} \\ h_{12} \\ h_{13} \\ h_{21} \\ h_{22} \\ h_{23} \\ h_{31} \\ h_{32} \\ h_{33} \end{pmatrix} = 0 \qquad (3)$$

The point correspondences are derived from the manually digitized calibration points and their real coordinates. Once the homography is estimated, a projected feature point detected at pixel (u_p, v_p) can be associated to its world coordinates according to Equation 2.

During the manual homography analysis the two camera sets (i.e. surface and underwater) were independent in-between, as shown in Figure 3.
Of the 236 points on the calibration volume with known coordinates located at the horizontal and vertical rods making the calibration volume, a total of 64 surface and 88 underwater markers near the frame inner and outer corners and at the water line were selected to be the control points (circles and diamonds in Figure 4). The points at the water line were common to both surface and underwater control points. The remaining 92 points (38 surface and 54 underwater) were used as the validation points.

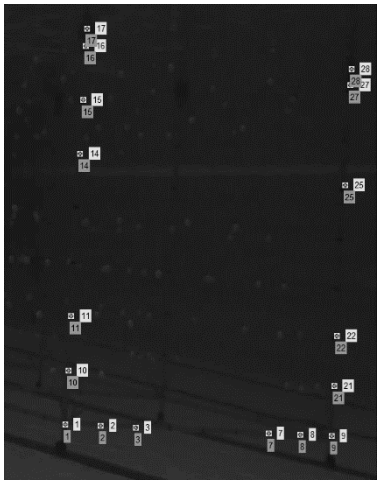

Figure 3. Visual comparison of 3D reconstruction for the homographic transform of a calibration volume plane. Unnumbered squares: original points from digitizing, cross on the unnumbered squares: point after homographic transform.

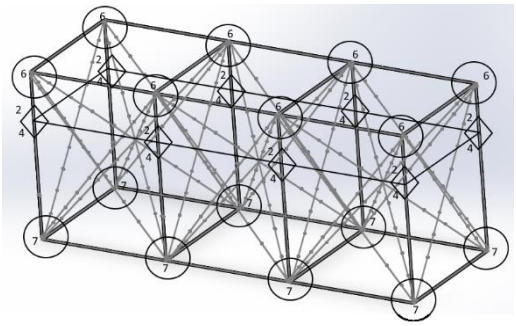

Figure 4. Location of the control points on the static calibration volume.

From each of those areas referred to above, points were systematically combined in sets of 3 per corner (whenever possible), resulting in sets of 40 and 48 calibration points for surface and underwater, respectively. From these calibration points, the DLT transform was performed and applied to the remaining control points and separately for the validation points.

Then, a new combination of calibration points from the control points was selected and a new DLT transform was again performed and applied to the remaining points. This systematic selection procedure resulted in over 1.5 million different combinations for the underwater control points and over 1000 combinations for the surface control points.

When the homography transformation was used to smooth the digitizing errors, it was applied only to the control points and then the above-referred systematic selection procedure was used. To simplify, the homography transformation was applied to a plane defined by a given set of rods, for each camera separately, with the process being applied three times to each camera to account for the rods that are common to two planes. Validation points were not smoothed by the homography transformation; however these points will not be digitized in future uses of the calibration volume.

Accuracy

All reconstruction errors were calculated from the raw coordinate data, without any smoothing procedure (Scheirman et al., 1998), and determined by the Root Mean Square (RMS) error of the 92 validation points (for the total calibration volume), using the following equations:

$$X_r = \sqrt{\frac{1}{N}\sum_{i=1}^{N}\left(x_{ni} - x_i\right)^2} \quad (4)$$

$$Y_r = \sqrt{\frac{1}{N}\sum_{i=1}^{N}\left(y_{ni} - y_i\right)^2} \quad (5)$$

$$Z_r = \sqrt{\frac{1}{N}\sum_{i=1}^{N}\left(z_{ni} - z_i\right)^2} \quad (6)$$

$$R = \sqrt{\frac{1}{N}\sum_{i=1}^{N}\left[\left(x_{ni} - x_i\right)^2 + \left(y_{ni} - y_i\right)^2 + \left(z_{ni} - z_i\right)^2\right]} \quad (7)$$

Where, X_r, Y_r, Z_r and R were the RMS errors for each axis and for the resultant error (respectively), x_{ni}, y_{ni} and z_{ni} were the real coordinates, x_i, y_i and z_i were the reconstructed coordinates and N was the number of points used.

Statistical analysis

Data are reported as mean and standard deviations (±SD). The normality distribution was checked and confirmed with Shapiro-Wilk's test. A two-way repeated measures ANOVA (homography x cameras) on control and validation

points was performed after verifying sphericity (Mauchly's test). Pairwise multiple post hoc comparisons were conducted with Bonferroni's correction. The level of significance was set at α = 0.05 (2-tailed). All data were analyzed using the IBM® Statistical Package for Social Sciences (SPSS) 20.0.

Results and Discussion

Figure 5 (panel a and b) depicts the mean and SD values of the RMS errors (mm) for the 3D reconstruction of surface (over 1000 combinations of trial subsets of 40 points each from the set of 64 control points near the corners) and underwater cameras (over 1600000 combinations of trial subsets of 48 points each from the set of 88 control points near the corners) cameras with and without homography transformation. Considering reconstruction through control point sets, homography use has revealed lower RMS errors for surface and underwater cameras rather than without it, being 7.3 ± 4.5 vs. 10.5 ± 4.8 for surface ($P < 0.01$) and 7.7 ± 3.8 vs. 12.1 ± 5.1 for underwater views ($P < 0.01$). Surface and underwater cameras have shown similar RMS error with homography ($P = 0.47$), although, without it, RMS error was greater for underwater than for surface cameras ($P < 0.04$).

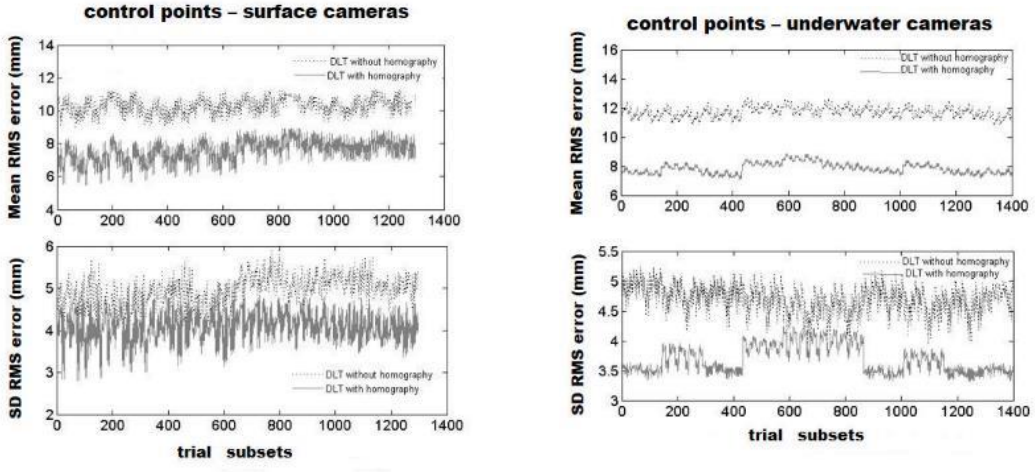

Panel a Panel b

Figure 5. Panel a. RMS errors for the 3D reconstruction of surface cameras without (dotted line) and with homography (continuous grey line) transformation obtained from subsets of 40/64 control points positioned on the horizontal and vertical corner rods. Trial subsets in the x axis

represents the (arbitrary) ID of the simulation case with different subsets of control point. Panel b. RMS errors for the 3D reconstruction of underwater cameras without (dotted line) and with homography (continuous grey line) transformation obtained from subsets of 48/88 control points positioned on the horizontal and vertical corner rods. Trial subsets in the x axis represents the (arbitrary) ID of the simulation case with different subsets of control points.

Figure 6 (panel a and b) depict the mean and SD values of the RMS errors (mm) for 3D reconstruction of surface (38 validation points) and underwater (54 validation points) cameras with and without homography transformation. Regarding reconstruction through validation point sets, RMS error was lower with homography than without it for both cameras sets, being 12.1 ± 6.5 vs. 15.9 ± 6.6 for surface ($P < 0.01$) and 10.8 ± 5.3 vs. 13.3 ± 6.7 for underwater views ($P < 0.03$). Surface and underwater câmeras evidenced similar RMS errors with homography ($P = 0.49$), but, without it, RMS reconstruction errors of surface were greater than underwater points ($P < 0.04$).

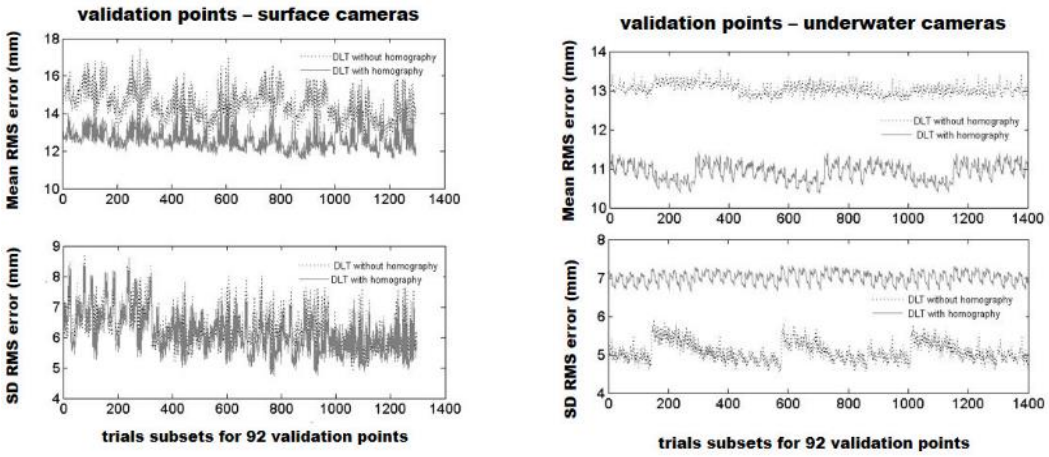

Panel a Panel b

Figure 6. Panel a. RMS errors for 3D reconstruction with 92 validation points of the horizontal facets of surface (38 points) camera without (dotted line) and with homography (continuous grey line) transformation. Trial subsets in the x axis represents the (arbitrary) ID of the simulation case with different subsets of control points. Panel b. RMS errors for 3D reconstruction with 92 validation points of the horizontal facets of underwater (54 points) camera without (dotted line) and with homography (continuous grey line) transformation. Trial subsets in the x axis represents the (arbitrary) ID of the simulation case with different subsets of control points.

Discussion

The kinematic analysis in swimming imposes obstacles to data acquisition, particularly by the existence of errors associated to image distortion, digitalization and 3D reconstruction (Bartlett, 2007; Kwon & Casebolt, 2006). Thus, it is crucial to observe its influence on the final results, analysing validity, reliability and accuracy (Scheirman et al., 1998). To the best of our best knowledge, the current study is the first that analysed the effects of homography and cameras positioning (surface/underwater) on 3D RMS reconstruction errors in swimming. Main findings were as follows: 1) using homography, RMS errors of control and validation points were smaller than without homography use and remained similar between surface and underwater cameras and; 2) without homography, RMS errors of control points were greater for underwater rather than for surface cameras and, in opposition, RMS errors of validation points were greater for surface than for underwater cameras. These current findings partially confirm the already established hypotheses and suggested that homography method applied for surface and underwater cameras is suitable to minimize the error magnitude provided by large calibration volume dimensions.

Literature pointed out that the number of control points and its respective distribution on calibration volume is determinant for 3D reconstruction accuracy of surface and underwater cameras (Challis, 2005; Chen, 1994; Figueiredo et al., 2011; Gourgoulis et al., 2008; Kwon & Casebolt, 2006; Psycharakis et al., 2005). In the current study, the number of control points distributed on the corners and facets for surface and underwater cameras were quite larger than those usually reported in swimming related studies (de Jesus et al., 2012; Figueiredo et al., 2011; Gourgoulis et al., 2008; Psycharakis et al., 2005; Psycharakis et al., 2010). The use of 8 to 30 control points distributed at the horizontal and vertical rods is often used for swimming 3D reconstruction with shorter calibration volume dimensions (Figueiredo et al., 2011; Psycharakis et al., 2005) than those applied in the current study. Figure 4 revealed that the best set of control points was

located on the corner and facets agreeing with previous study suggestions (e.g. Figueiredo et al., 2011). As calibration volume size increases, it has been recommended to increase the number of control points with proper distribution to ensure accuracy augmentation (Chen et al., 1994; Lauder et al., 1998; Psycharakis et al., 2005). Hence, researchers using static calibration structures with similar dimensions than those used in the current study should prioritize those criteria. Notwithstanding the number and location of control points as well as the calibration volume size relevance for better 3D reconstruction accuracy, (Chen et al., 1994; Lam et al., 1992), the effects of displacement of each pixel across the images induced by camera, scene position and/or independent object-motion should also be considered in swimming analysis, since they have greatly affected reconstruction in other sport scenarios (Alvarez et al., 2011; Alvarez et al., 2012; Nejadasl & Lindenbergh, 2014). These drawbacks have been minimized through the use of different methods (Wang et al., 2005) being homography estimation well accepted as a key step to obtain mappings between scene images providing less erroneous 3D reconstruction (Nejadasl & Lindenbergh, 2014).

In the light of those benefits provided by homography technique, its use was tested in swimming and has revealed a decrease in RMS errors of control and validation points for surface and underwater cameras, corroborating previous findings considering reconstruction from multiple perspective views (Alvarez et al., 2011; Alvarez et al., 2012). For example, Alvarez et al. (2011) analysing competitive tennis observed a reduction of ≥ 10 mm on RMS error of control points when using homography estimation, which was higher than the current findings. In the present study, a reduction of 3 to 5 mm on RMS errors for both control and validation points in surface and underwater views was considered quite relevant due, especially for underwater cameras, to video recordings complexity in aquatic scenarios (Kwon & Casebolt, 2006). Differences between Alvarez et al. (2011) study and the present study findings for surface RMS errors can be attributed to the greater incidence of light refraction and the smaller number of cameras used to record video images in swimming pool environment.

Despite several previous findings considering underwater and surface 3D reconstruction analysis, the current study evidenced that swimming researchers should focus on homography implementation to test present results replication on their specific 3D cameras arrangements.

The control points and calibration volume sizes have not been an exclusive research topic in swimming 3D reconstruction studies, being researchers also interested in comparing RMS errors between underwater and surface cameras (Figueiredo et al., 2011; Gourgoulis et al., 2008; Psycharakis et al., 2005). However, this problematic should not be considered as the major research concern, since specialized literature has evidenced greater underwater RMS errors rather than surface cameras prior to 1990s (e.g. Hay & Guimarães, 1983). Researchers should focus on methods that allow minimizing errors from estimated to real coordinates of each camera, as homography has demonstrated. Implementation of homography has provided similar RMS errors for surface and underwater cameras, and these findings suggest for these sets of points that homography can be considered more advantageous for underwater reconstruction. Without homography, surface reported lower RMS errors of control points than underwater cameras, as currently shown in literature (Figueiredo et al., 2011; Gourgoulis et al., 2008; Psycharakis et al., 2005). These authors displayed RMS errors ranging from 4.06 to 6.16 mm for surface and 4.04 to 7.38 mm for underwater cameras, which were lower than the current results and that can be explained by differences in calibration volume sizes. Despite these differences, the large calibration volume used in the current study presented acceptable RMS errors of control points for surface and underwater cameras, avoiding the need of extrapolation beyond the calibrated space (e.g. Gourgoulis et al., 2008). The greater RMS error for surface than underwater cameras when considering validation points, suggesting that, when homography is not used in large calibration volume dimensions, researchers should choose control instead validation points for surface reconstruction.

Further considerations

Notwithstanding the originality and relevance of the current data, some considerations should be taken into account. First, static calibration volumes remain by far the most widely used for swimming 3D reconstruction, although promising alternative calibration methods as chessboard and moving wand, have shown interesting results (SIlvatti et al., 2012a; Silvatti et al., 2012b). Nevertheless, these methods do not minimize extrapolation occurrence beyond the calibrated space, increasing measurements inaccuracy. The large calibration volume used in this study registered low and acceptable reconstruction accuracy errors to record at least two swimming cycles, but researchers are advised to take some cautions during video recording data collections. Second, manual digitization process implies systematic and random errors (Bartlett, 2007); however, in the current study they were kept in an acceptable level (≤ 8 mm) (Lam et al., 1992). Third, the large number of control points used in the present study for surface and underwater reconstruction allowed obtaining low RMS error for a large calibration structure, although it is acknowledged that a minimum of six non-coplanar control points well distributed over the calibration volume can preserve adequate accuracy. Six control points recommendation can simplify digitization process; however those points seem not enough to supply reliable reconstruction of large calibration volumes.

Conclusions

In the current study, the implementation of planar projective transformation through homography indicated that the RMS reconstruction errors of a set of 40/64 (surface) and 48/88 (underwater) control points positioned on the orthogonal corners and facets of a calibration volume with 6000 x 2500 x 2000 mm were similar and acceptable for surface and underwater views. Based on these findings, future studies using large calibration volumes able to record at

least two cycles of a given swimming technique should consider homography transformation to smooth the digitized control points and improve the DLT reconstruction accuracy.

Acknowledgments

This study was supported by grants: CAPES/543110-7/2011-2015 Brazil, PTDC/DES/101224/2008 (FCOMP-01-0124-FEDER-009577). The authors acknowledge Pedro Sousa for the experimental setup drawings, M.Sc. António José Ramos Silva of the Faculty of Engineering of University of Porto for his invaluable service in SolidWorks and M.Sc. Lígia Costa of Faculty of Sport of University of Porto for her involvement in the data collection.

References

Abdel-Aziz, Y., & Karara, H. (1971). Direct linear transformation: from comparator coordinates into object coordinates in close range photogrammetry". In Symposium on close-range photogrammetry, Falls Church: American Society of Photogrammetry, 1-18.

Alvarez L., Gómez L., & Sendra J.R. (2011). Accurate depth dependent lens distortions models: an applications to planar view scenarios. *Journal Mathematical Imaging and Vison, 39*(1), 75-85.

Alvarez, L., Gomez, L., Pedro, H., & Mazorra L. (2012). Automatic camera pose recognition in planar view scenarios," progress in pattern recognition, image analysis, computer vision, and application: Lecture notes in computer science, 7441, 46-413.

Bartlett, R. (2007). Introduction to sports biomechanics: analysing human movement patterns. 2nd edition, Routledge London.

Challis, J.H. (1995). A multiphase calibration procedure for the direct linear transformation. *Journal of Applied Biomechanics, 11*(3), 351-358.

Chen, L., Armstrong, C.W., & Raftopoulos D.D. (1994). An investigation on the accuracy of three-dimensional space reconstruction using the direct linear transformation technique. *Journal of Biomechanics, 27*(4), 493-500.

Chen, C.Y., & Chen, H.J. (2013). An incremental target-adapted strategy for active geometric calibration of projector-camera systems. *Sensors, 13*(2), 2664-2681.

de Jesus, K., Figueiredo, P., de Jesus, K., Pereira, F. Vilas-Boas, J. P., Machado, L.R., & Fernandes, R.J. (2012). Kinematic analysis of three water polo front crawl styles. *Journal of Sports Sciences, 30*(7), 715-723.

Figueiredo, P. Machado, L., Vilas-Boas, J.P., & Fernandes, R.J. (2011). Reconstruction error of calibration volume's coordinates for 3D swimming kinematics. *Journal of Human Kinetics, 29*, 35-40.

Gourgoulis V., Aggeloussis, N., Kasimatis, P., Vezos, N., Boli, A., & Mavromatis, G. (2008). Reconstruction accuracy in underwater three-dimensional kinematic analysis. *Journal of Science and Medicine in Sport, 11*(2), 90-95.

Hay, J.G., & Guimarães, A.C.S. (1983). A quantitative look at swimming biomechanics.. *Swimming Technique, 20*, 11-17.

Kwon, Y.H., & Casebolt, J.B. (2006). Effects of light refraction on the accuracy of camera calibration and reconstruction in underwater motion analysis. *Sports Biomechanics, 5 (2)*, 315-340.

Lam, T.C., Frank, C.B., & Shrive N.G. (1992). Calibrations characteristics of a video dimension analyser (VDA) system. *Journal of Biomechanics, 25*(10), 1227-1231.

Lauder, M.A., Dabnichki, P., & Bartlett, R.M. (1998). Three-dimensional reconstruction accuracy within a calibrated volume. In I. Shake (ed.), The engineering of sport: design and development. United Kingdom: Blackwell Science, 441-448.

Lingaiah K., & Suryanarayana B.G. (1991). Strength and stiffness of sandwich beams in bending. *Experimental Mechanics, 31*(1), 1-7.

Nejadasl, F.K., & Lindenbergh, R. (2014). Sequential and automatic image-sequence registration of rods areas monitored from a hovering helicopter. *Sensors, 14*(9), 16630-16650.

Psycharakis S., Sanders, R., & Mill, F. (2005). A calibration frame for 3D swimming analysis. In Q. Wang (ed.), XXIII International Symposium on Biomechanics in Sports: University of Beijing,, 901-904.

Psycharakis, S.G., Naemi, R., Connaboy, C., McCabe, C., & Sanders, R.H. (2010). Three-dimensional analysis of intracycle velocity fluctuations in front crawl swimming. *Scandinavian Journal of Medicine & Science in Sports, 20*(1), 128-135.

Scheirman, G., Porter, J., Leigh, M., & Musick, M. (1998). An integrated method to obtain three-dimensional coordinates using panning and tilting video cameras. In H.J Riehle, & M.M Viete (eds.), XVI International Symposium on Biomechanics in Sports: University of Konstanz, 567-569.

Silvatti, A.P., Dias, F.A.S., Cerveri, P., Barros, R.M.L. (2012a). Comparison of different camera calibration approaches for underwater applications. *Journal of Biomechanics, 45*(6), 1112-1116.

Silvatti A.P., Cerveri P., Thelles T., Dias F.A.S., Baroni, G. & Barros, R.M.L. (2012b). Quantitative underwater 3D motion analysis using submerged video cameras: accuracy analysis and trajectory reconstruction. *Computer Methods in Biomechanics and Biomedical and Engineering, 16*(11), 1240-1248.

Appendix III

Should the gliding phase be included in the backstroke starting analysis?

Karla de Jesus[1], Kelly de Jesus[1], Sara T. Morais[1,2], João Ribeiro[1], Ricardo J. Fernandes[1,2], João Paulo Vilas-Boas[1,2].

[1] Centre of Research, Education, Innovation and Intervention in Sport, Faculty of Sport, University of Porto, Porto, Portugal
[2] Porto Biomechanics Laboratory (LABIOMEP), Porto, Portugal

Published on XII International Symposium on Biomechanics and Medicine in Swimming (2014): 112-117.

Abstract

This study aimed to characterise the underwater phase at backstroke start. Nine highly trained backstroke swimmers performed a maximal 3x15 m of the starting variant with feet parallel and partially emerged and the highest horizontal handgrip. The best 15 m trial was selected for each swimmer. Motion capture system tracked right side markers. Each individual velocity curve was normalized from the immersion until the beginning of the upper limbs propulsion. The velocity at full immersion and at five critical instants of the 1st undulatory underwater cycle was assessed. After the full immersion, swimmers performed a downward kick with lower horizontal and resultant velocity than those displayed at full immersion (1.15±0.18 vs. 2.09±0.26 and 1.62±0.36 vs. 2.39±0.33 m/s, respectively). The transition to the 1st upward kick generated greater horizontal, vertical and resultant velocity than those noted at 1st downward kick (1.79±0.18 vs. 1.15±0.18, -1.23±0.51 vs. -1.0±0.34, 2.14±0.23 vs. 1.62±0.36 m/s, respectively). Compared to the 1st upward kick, swimmers displayed lower horizontal, vertical and resultant velocity at the 1st part of the transition from the 1st up to the 2nd downward kick (1.67±0.15 vs. 1.79±0.18, -0.29±0.21 vs. -1.23±0.51, 1.73±0.13 vs. 2.14±0.23 m/s, respectively). Lower horizontal and resultant velocity was observed at the 2nd downward kick compared to the 2nd part of the transition from the 1st up to 2nd downward kick (0.96±0.22 vs. 1.68±0.14, 1.14±0.30 vs. 1.70±0.15 m/s, respectively). Subsequently to the full immersion, a downward kick was performed implying the swimmers' deceleration, which was minimized by continued undulatory underwater cycles. These findings highlighted the absence of the gliding phase at backstroke start.

Key words: biomechanics, kinematics, hip velocity-time curve, swimming, dorsal start, starting variants

Introduction

The swimming start is accepted as an important part of short and middle distance swimming events, and, if performed effectively, might decide the swimmer's classification (de Jesus et al., 2011). For instance, 15 m after the start, the second-placed at men's 100 m backstroke at Barcelona 2013 Swimming World Championships was 0.20 s slower than the winner, and the final race time difference was 0.19 s. The importance of the start is emphasized further by the observation that the differences between the individual 15 m performances of international level swimmers might correspond to 0.30 s (cf. Vantorre et al., 2010).

The starting performance is usually defined by the period between the starting signal until the swimmer's head achieve 15 m (e.g. Vantorre et al., 2010), and it is composed of several phases, namely block/wall, flight, entry, underwater and swimming phases (Vantorre et al., 2010). The underwater phase of the start is divided into the glide and underwater undulatory swimming (Maglischo, 2003; Vantorre et al., 2010). The glide corresponds to the period between swimmer's full immersion and beginning of lower limbs propulsion (Vantorre et al., 2010), and the undulatory underwater swimming is defined between gliding ending and beginning of upper limbs propulsion (de Jesus et al., 2012; Vantorre et al., 2010). Several authors studied in detail the underwater phase at ventral starts (e.g. Vantorre et al., 2010), while minor attention has been paid to the backstroke starting technique. Cohen et al. (2011) studied one dorsal undulatory underwater swimming cycle using numerical method, while de Jesus et al. (2012) analysed kinematics of the four initial and last four undulatory cycles at different backstroke starting variants. In both studies, authors have not attempted to analyse the underwater phase movements performed after full immersion. According to Maglischo (2003), the underwater phase of backstroke start displays a well-defined gliding period, although it was described after descendent swimmer's actions. Hohmann et al. (2008) described undulatory underwater kicking movements immediately after swimmer's immersion. In fact, since backstroke

swimmers have to perform upper, trunk and lower limbs movements to decrease the vertical displacement after backstroke start full immersion (Green et al., 1987), it might be speculated that propulsive actions occur as soon as swimmers entering the water, evidencing the inexistence of a conventional gliding phase at backstroke start. This study aimed to characterise the underwater phase kinematics at one of the most used backstroke starting variants.

Methods

After a month of backstroke starting training period, 9 highly trained backstroke swimmers (22.22 ± 6.37 yrs, 1.78 ± 0.04 m, 72.67 ± 10.85 kg) performed three 15 m maximal trials of the backstroke starting variant with feet parallel and partially emerged and the highest horizontal handgrip with 3 min resting. Starting signals were produced through a starter device (ProStart, Colorado Time System, USA). The best trial in terms of 15 m performance of each swimmer was selected for analysis.

Synchronized to the starting device, an optical motion capture system was used with six underwater cameras (Oqus, Qualisys AB, Sweden), five lateral and one obliquely positioned regarding to the swimmer's plane of movement. Lateral cameras were alternatively placed at 0.10 m below the water surface and at the swimming pool bottom and were 0.5, 5, 10, 15 and 20 m away from the starting wall. The oblique camera was positioned 20 and 5 m away from the frontal and lateral pool wall, respectively. The camera lenses were targeted to the swimmer's trajectory and registered the swimmers' movements from the full body immersion until the beginning of the upper limbs propulsion.

The underwater calibration was performed with a static calibration frame (positioned 5 m further from the pool wall) to create the virtual origin in the 3D environment and a wand calibration was used to perform the dynamic calibration,

which covered the expected performance volume. Figure 1 shows the six cameras positioning and the covered calibration volume.

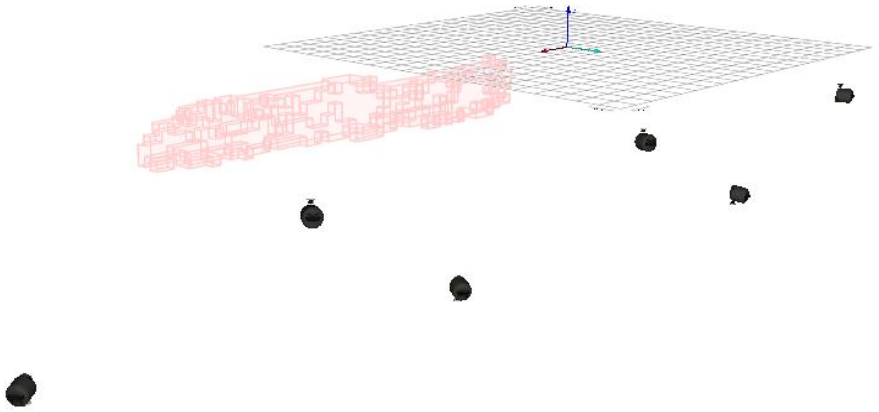

Figure 1. The six cameras positioning

A short data acquisition was performed prior to the backstroke start recordings, to determine the water surface position and orientation relative to the origin of the calibration frame. As the underwater motion analysis imposes several unique obstacles such as insufficient illumination and reflex, and these adversities reduce the calibration accuracy, markers exposure time and threshold were adjusted according to the different environmental conditions.

The cameras tracked the swimmers' right hip reflective marker, and the horizontal, vertical and resultant hip velocity-time curves were processed using Qualisys Track Manager (Qualisys AB, Sweden). A referential transformation was applied to the original calibration referential in order to align it with the water level at the starting block, setting this point as the new referential origin. Each individual velocity time-curve was smoothed using a low pass digital filter, and subsequently normalized in time from the hallux immersion until the beginning of the upper limbs propulsion using a custom-designed software program (MatLab, 7.11.0 R2010b, The MathWorks Inc., USA). The velocity at full immersion and at five critical instants of the 1st undulatory underwater kicking cycle was assessed at each normalised individual curve. These velocity-time curve instants

corresponded to the minimum velocity achieved during the 1st downward kicking, the maximal velocity during the 1st upward kicking, the minimum velocity during the 1st part of the transition from the 1st upward to the 2nd downward kicking, the maximal velocity during the 2nd part of the transition from the 1st upward to the 2nd downward kicking, and the minimum velocity achieved during the 2nd downward kicking. Figure 2 presents the respective critical instants studied, which are represented by stick figures on the mean resultant hip-velocity to time curve of the nine swimmers.

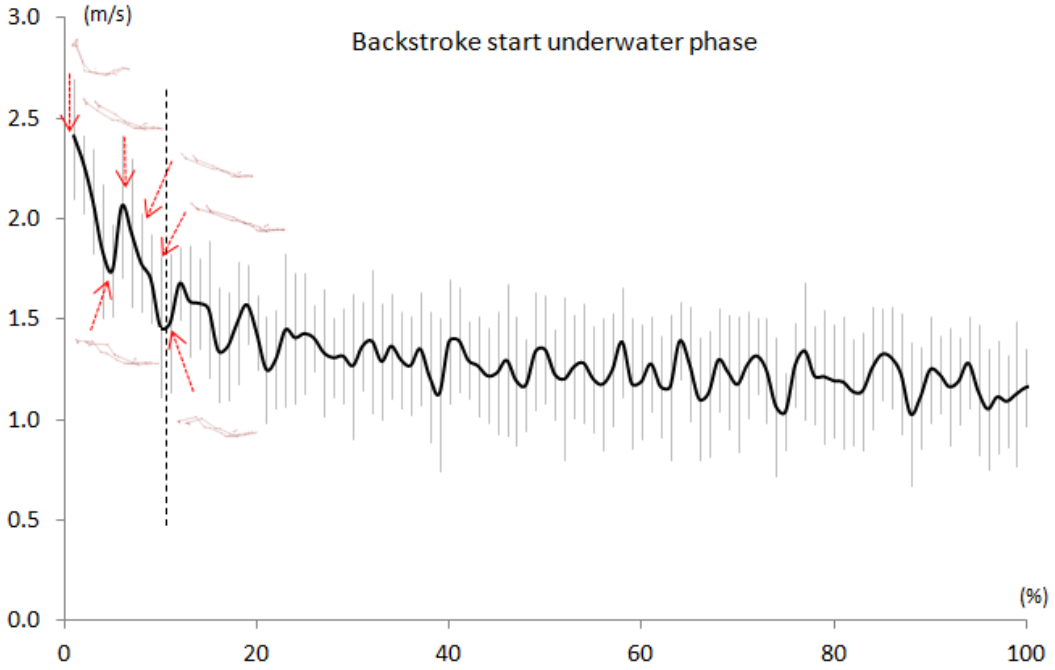

Figure 2. Mean resultant hip-velocity to time curve of the nine swimmers (continuous line) expressed as a percentage of the full swimmer's immersion until the beginning of the upper limbs propulsion. The vertical shaded lines denote the standard deviations. The six critical instants are represented and illustrated with stick figures.

Paired sample t-test was used to determine the effects caused by the critical instant on the velocity time-curve profile (*P*-value ≤ .05). The effect size was calculated based on Cohen's (1988) criteria. It was considered small if $0 \leq |d| \leq 0.2$, medium if $0.2 \leq |d| \leq 0.5$, and large if $|d| > 0.5$.

Results

Table 1 displays the mean (± s) values of horizontal, vertical and resultant swimmers' hip velocity at each critical instant analysed, with P-value and effect size (d) reported for the comparisons between the respective critical instants. Compared to the full immersion, swimmers displayed shorter horizontal and resultant velocity with a large magnitude effect size; however, non-difference was observed for the vertical component, with moderate effect size. During the 1st upward kicking, greater horizontal, vertical and resultant velocity was generated than those noted during the 1st downward kicking, with large effect size. Compared to the 1st upward kick, swimmers displayed lower horizontal, vertical and resultant velocity during the 1st part of the transition from the 1st up to the 2nd downward kick, with large effect size. Difference was not noted between the 1st and 2nd part of the transition from the upward to the downward kicking for the horizontal, vertical and resultant velocity, with small, large and medium effect size, respectively. Lower horizontal and resultant velocity was observed during the 2nd downward kick compared to the 2nd part of the transition from 1st up to 2nd downward kick, with large effect size. Greater downward vertical velocity was displayed during the 2nd downward kick compared to 2nd part of the transition from 1st up to 2nd downward kick, with large effect size.

Table 1. Mean (± sd) of horizontal, vertical and resultant swimmers' hip velocity at each critical instant analysed, with P-value and effect size (d) reported for each comparison between critical instants.

Velocity ($m \cdot s^{-1}$)	Critical instants	Mean (± *sd*)	*P*-value	Effect size (*d*)
Horizontal	SFIM	2.09±0.26	0.012	5.49
	1st DWN KICK	1.15±0.18		
	1st DWN KICK	1.15±0.18	0.008	-3.31
	UPW KICK	1.79 ±0.18		
	UPW KICK	1.79 ±0.18	0.012	1.19
	1st UP to DWN KICK	1.67 ± 0.15		
	1st UP to DWN KICK	1.67 ±0.15	0.513	-0.04
	2nd UP to DWN KICK	1.68 ±0.14		
	2nd UP to DWN KICK	1.68 ±0.14	0.008	4.40
	2nd DWN KICK	0.96 ±0.22		
Vertical	SFIM	-1.16±0.30	0.77	-0.35
	1st DWN KICK	-1.00±0.34		
	1st DWN KICK	-1.00±0.34	0.05	0.81
	UPW KICK	-1.23±0.51		
	UPW KICK	-1.23±0.51	0.01	-2.20
	1st UP to DWN KICK	-0.29±0.21		
	1st UP to DWN KICK	-0.29±0.21	0.09	-0.77
	2nd UP to DWN KICK	-0.01±0.43		
	2nd UP to DWN KICK	-0.01±0.43	0.01	1.38
	2nd DWN KICK	-0.56±0.21		
Resultant	SFIM	2.39±0.33	0.01	3.40
	1st DWN KICK	1.62±0.36		
	1st DWN KICK	1.62±0.36	0.01	-1.78
	UPW KICK	2.14±0.23		
	UPW KICK	2.14±0.23	0.008	2.42
	1st UP to DWN KICK	1.73±0.13		
	1st UP to DWN KICK	1.73±0.13	0.51	0.35
	2nd UP to DWN KICK	1.70±0.15		
	2nd UP to DWN KICK	1.70±0.15	0.008	3.06
	2nd DWN KICK	1.14±0.39		

Note: SFIM (swimmer's full immersion), 1st DWN KICK (first downward kicking); UPW KICK (upward kicking); 1st UP to DWN KICK (first part of the transition from the 1st upward to the 2nd downward kicking); 2nd UP to DWN KICK (second part of the transition from the 1st upward to the 2nd downward kicking); 2nd DWN KICK (second downward kicking).

Discussion

According to some previous reports considering the ventral (Vantorre et al., 2010) and backstroke starting technique (Maglischo, 2003), the underwater phase has been divided into gliding and underwater undulatory swimming. Swimmers have been recommended to spend ~1s gliding in a hydrodynamic body position before the beginning of the lower limbs propulsion (Maglischo, 2003; Vantorre et al.,

2010). Contradictorily, Hohmann et al. (2008) described the entry and gliding phases at backstroke starting technique including downward and upward lower limbs movements. In accordance to Green et al. (1987), after the backstroke starting entry phase, swimmers have to perform trunk, upper and lower limbs movements to alter the vertical downward displacement. These unclear starting phases' definitions hamper an effective communication among biomechanists, coaches and swimmers, implying failure to apply research findings. Therefore, this study proposed to analyze the underwater phase kinematics of a commonly used backstroke starting variant, providing further insights into the underwater phases' definition used for research and practical applications. The current findings indicated that subsequently to the full immersion, a downward kicking is performed implying a swimmers' deceleration magnitude reduction, and specially an antero-posterior deceleration reduction, which is further minimized by immediately continued undulatory underwater swimming cycles (Figure 2). Thus, these results newly evidenced the absence of the gliding phase during the backstroke start, as we have previously hypothesized.

Despite the high horizontal and resultant velocity achieved immediately after the starting entry phase (Figure 2), the backstroke swimmers were unable to sustain such velocities in a hydrodynamic position due to the pronounced vertical displacement occurring during immersion. The swimmers generate a high tendency toward rotation during the flight for the backward swing movement and subsequently hole water entry (Maglischo, 2003), which must be controlled as soon as the swimmer's hip immerge (Green et al., 1987). Since the resultant velocity achieved immediately after the water immersion have been considered a determinant factor to reduce the backstroke starting time (de Jesus et al., 2011), coaches and swimmers should pay attention to minimise this velocity loss at the end of the downward and beginning of the upward kicking cycle. According to Maglischo (2003), swimmers who intend to perform longest undulatory underwater swimming phase should allow the body to travel deeper into the water by gliding for a short time before the beginning of kicking movements. In opposition, swimmers performing shortest undulatory underwater swimming

phase lift the upper limbs sharply and bring the lower limbs down in preparation for the kicking movements almost immediately after the full immersion (Maglischo, 2003). Based on these statements it has been suggested that backstroke swimmers may adopt different underwater starting phase profiles; however, in the present study and for the analysed starting variant, all swimmers performed a downward undulatory kicking after the full immersion, and continue the undulatory movement afterword, evidencing no gliding phase at all.

During the 1st downward undulatory underwater kicking, the vertical downward path is changed (Green et al., 1987; Maglischo, 2003), but at the respective kick ending, and begging of the upward kicking, the horizontal and resultant velocity achieved the minimum value. The largest projected frontal area (and consequently net drag force) when the knee attains maximum flexion were pointed out to create a large negative swimmers' acceleration (Cohen et al., 2012). The negative acceleration in the resultant (Figure 2) and horizontal velocity components due to the 1st downward kicking was suddenly minimized by an upward undulatory swimming movement. In fact, stronger vortex rings and consequently greater trust generation were observed in the extension compared to the flexion kicking (Cohen et al., 2012). According to de Jesus et al. (2012), the 1st undulatory underwater swimming cycles displayed greater horizontal velocity than the last cycles. The downward vertical velocity during the 1st upward kicking was also greater than during the 1st downward kicking, which is due to the hip downward reaction to the torque produced by the lower limbs during upward movement.

The first part of the transition from the 1st upward to the 2nd downward kicking generated shorter horizontal, vertical and resultant velocity. Indeed, subsequently to the end of the 1st upward kicking, swimmers increase the respective frontal area and consequently the pressure drag (Cohen et al., 2012), hampering the forward displacement. In addition, vertical downward displacement is reduced since the greater torque seems to be generated previously to the first part of the transition from the upward to the downward kicking. The first and second part of

the transition from the 1st upward to the 2nd downward kicking did not differ for horizontal, vertical and resultant velocity components, indicating that the stream wise forces are constant and close to neutral, meaning this is a recovery phase of the kicking cycle and has a minor effect on the velocity of the swimmer (Cohen et al., 2012). As the knee flexion continues until the maximum value, the frontal area increases (Cohen et al., 2012) and negative acceleration is observed at the end of the undulatory underwater swimming cycle. In the present study, the three velocity components analyzed presented shorter values than the 2nd part of the transition from the 1st to the 2nd downward kicking.

Conclusion

This is the first attempt to describe the underwater phase kinematics subsequent to a commonly used backstroke starting variant. The studies conducted in this starting phase are obsolete and scarce, and have not explained consistently the underwater sub phase's definition. In the present study, after the full immersion, a downward kick was performed implying the swimmers' negative acceleration. This detrimental effect on horizontal and resultant velocity components were minimized by continued undulatory underwater cycles, evidencing the absence of the gliding phase at backstroke start. Further biomechanical studies are required to detailed analyze the underwater starting phase when backstroke swimmers performing different starting variants. Based on the current findings, coaches and swimmers should minimize the maximal knee flexion at the 1st downward kicking, which reduces the projected frontal area and resistive drag.

Acknowledgments

This research was supported by Coordination for the Improvement of Higher Education Personnel Foundation (BEX 0761/12-5/2012-2014), Santander Totta

Bank (PP-IJUP2011-123) and Science and Technology and Foundation (EXPL/DTP-DES/2481/2013).

References

Cohen, J. (1988). Statistical power analysis for the behavioral sciences. Hillsdale, New Jersey: Lawrence Erlbaum Associates.

Cohen, R.C.Z., Cleary, P.W., & Mason, B.R. (2012). Simulations of dolphin kick swimming using smoothed particle hydrodynamics. *Human Movement Science, 31*(3), 604-619.

de Jesus, K., de Jesus, K., Figueiredo, P., Gonçalves, P., Vilas-Boas, J.P., & Fernandes, R.J. (2011). Biomechanical analysis of backstroke swimming starts. *International Journal of Sports Medicine, 32*(7), 546-551.

de Jesus, K., de Jesus, K., Machado, L., Fernandes, R.J., & Vilas-Boas, J.P. (2012). Linear kinematics of the underwater undulatory swimming phase performed after two backstroke starting techniques. In E.J.Bradshaw, A. Burnett, & P.A. Hume (eds.), XXX International Symposium on Biomechanics in Sports: Australian Catholic University, 371-373.

Green, R., Cryer, W., Bangerter, B., Lewis, K., & Walker, J. (1987). Comparative analyses of two methods of backstroke starting: conventional and whip. In L. Tsarouchas, J. Terauds, B.A. Gowitzke, & L.E. Holt (eds.), V International Symposium on Biomechanics in Sports: University of Greece, 281-292.

Hohmann, A., Fehr, U., Kirsten, & R., Krueger, T. (2008). Biomechanical analysis of the backstroke start technique in swimming. *E-Journal Bewegung und Training, 2*, 28-33.

Maglischo, E.W. (2003). Swimming fastest: the essential reference on technique, training, and program design. Champaign, Illinois: Human Kinetics.

Vantorre, J., Seifert, L., Fernandes, R.J., Vilas-Boas, J.P., & Chollet, D. (2010). Kinematical profiling of the front crawl start. *International Journal of Sports Medicine, 31*(1), 16-21.

Appendix IV

Effective swimmer's action during the grab start technique

Luís Mourão[1,2], Karla de Jesus[2*], Hélio Roesler[2,3], Leandro J. Machado[2,4], Ricardo J. Fernandes[2,4], João Paulo Vilas-Boas[2,4], Mário A.P. Vaz[4,5].

[1] Superior School of Industrial Studies and Management, Porto Polytechnic Institute, Vila do Conde, Portugal

[2] Centre of Research, Education, Innovation and Intervention in Sport, Faculty of Sport, University of Porto, Porto, Portugal

[3] Aquatic Biomechanics Research Laboratory, Health and Sports Science Centre University of the State of Santa Catarina, Florianópolis, Santa Catarina, Brazil.

[4] Porto Biomechanics Laboratory, University of Porto, Porto, Portugal

[5] Institute of Mechanical Engineering and Industrial Management, Faculty of Engineering, University of Porto, Porto, Portugal

Published on PlosONE (2015), 10(5), e0123001.

Abstract

The external forces applied in swimming starts have been often studied, but using direct analysis and simple interpretation data processes. This study aimed to develop a tool for vertical and horizontal force assessment based on the swimmers' propulsive and structural forces (passive forces due to dead weight) applied during the block phase. Four methodological pathways were followed: the experimented fall of a rigid body, the swimmers' inertia effect, the development of a mathematical model to describe the outcome of the rigid body fall and its generalization to include the effects of the inertia, and the experimental swimmers' starting protocol analysed with the inclusion of the developed mathematical tool. The first three methodological steps resulted in the description and computation of the passive force components. At the fourth step, six well-trained swimmers performed three 15 m maximal grab start trials and three-dimensional (3D) kinetic data were obtained using six degrees of freedom force plate. The passive force contribution to the start performance obtained from the model was subtracted from the experimental force due to the swimmers resulting in the swimmers' active forces. As expected, the swimmers' vertical and horizontal active forces accounted for the maximum variability contribution of the experimental forces. It was found that the active force profile for the vertical and horizontal components resembled one another. These findings should be considered in clarifying the active swimmers' force variability and the respective geometrical profile as indicators to redefine steering strategies.

Key words: biomechanics, ground reaction forces, swimming, swimming starts

Introduction

It is known that the 15 m starting performance can differ amongst elite swimmers by only ~0.40 s (Mason et al., 2012; Seifert et al., 2010), with a decisive effect on the final result in several competitive events. The grab and track starts used in ventral events are the most extensively studied techniques (Vantorre et al., 2010a) in the grab start, the swimmers' hands grasp the front edge of the block (either between or at the outer edge of the feet) and in the track start swimmers position one foot on the front edge of the starting block and the other foot behind, with the possibility of placing the body weight toward the front edge or toward the rear of the block (Seifert et al., 2010; Vilas-Boas et al., 2003).

Some authors have studied the external forces that affect the swimmers' movement on the starting block during the grab and/or track start techniques (Breed & Young, 2003; Galbraith et al., 2008; Guimarães & Hay, 1985; Slawson et al., 2013; Vantorre et al., 2010b; Vilas-Boas et al., 2003) by measuring the total anterior-posterior (Breed & Young, 2003; Galbraith et al., 2008; Guimarães & Hay, 1985; Slawson et al., 2013; Vantorre et al., 2010; Vilas-Boas et al., 2003), vertical (Slawson et al., 2013; Vantorre et al., 2010; Vilas-Boas et al., 2003) and lateral reaction forces (Vantorre et al., 2010b). The vertical force applied into the block accelerates the swimmer's centre of mass (CM) in the upward/downward direction, the anterior-posterior force generates propulsion mainly in the forward direction and the lateral force is essentially a controlling movement (Lyttle & Benjanuvatra, 2005).

Despite the essential contribution of previous research regarding the external kinetics involved during ventral swimming starts, the process of interpreting and analysing data is still not as effective as it should be (Slawson et al., 2013). Based on fundamental mechanics, the forces applied on the starting block may be interpreted as being dependent upon the active forces and the body weight dynamical effects in each successive body position enabling to provide more accurate information about performance diagnosis (Hoelfelder et al., 2013).

Using Newton's 3rd law, the total ground reaction force exerted by the starting block on the swimmer $\left(\overrightarrow{GRF}(t)=\left(GRF_h(t),GRF_v(t)\right)\right)$, where it has been separated into its most relevant components accordingly to Lyttle and Banjanuvatra (2005), is the opposite of the action force applied on the block surface, and it involves the swimmer's muscular action and postural effect while moving (changing multi-segment configuration and CM position). Sometimes the vertical component of GRF is termed $\overrightarrow{N}$, the normal reaction, and the horizontal component is termed $\overrightarrow{F}_s$, the static friction. Returning to the swimming start block, the swimmer's acceleration is defined through Newton's 2nd law as:

$$\overrightarrow{GRF}(\mathrm{t})+\vec{W}=\mathrm{m}\cdot\vec{a}_{\mathrm{swimmer}}(\mathrm{t}) \tag{1}$$

Where $\vec{W}$, m and $\vec{a}_{swimmer}(t)$ are the swimmer's weight, mass and acceleration, respectively, being $\overrightarrow{GRF}$ applied at the halluces (feet) and $\vec{W}$ at the center of mass. In accordance, the total impulse or linear momentum increment $\left(\Delta\vec{p}\right)$, leading to CM kinematics classical description is defined as the time integral:

$$\int_0^{\tau}\left(\overrightarrow{GRF}(\mathrm{t})+\vec{W}\right)\cdot\mathrm{dt}=\ \Delta\vec{\mathrm{p}} \tag{2}$$

However, even in the absence of a swimmer's active starting effort, impulse generation remains, which can be evidenced by considering the fall of a similar passive rigid body. Therefore, in this particular case, the $\overrightarrow{GRF}$ is simply a passive force, that is:

$$\overrightarrow{GRF}(t)=\vec{R}_{Passive}(t) \tag{3}$$

The $\vec{R}_{Passive}(t)$ (the $\overrightarrow{GRF}(t)$ applied to the inertial structure of the swimmer's body) should be considered in this formalism as the one generated by a falling inert rigid

body. Keeping in mind these ideas, it is suggested to decompose $\overrightarrow{GRF}(t)$ in the general (and real) case into passive and active components, as:

$$\overrightarrow{GRF}(t) = \vec{R}_{Passive}(t) + \vec{R}_{Active}(t) \quad (4)$$

where $\vec{R}_{Active}(t)$ is in the opposite direction to that of the propulsive force vector applied to the block by the swimmer's muscular actions and $\vec{R}_{Passive}(t)$ is the same as in equation 3.

The aim of this research is to decompose the $\overrightarrow{GRF}(t)$ into $\vec{R}_{Active}(t)$ and $\vec{R}_{Passive}(t)$ in the grab start, which is one of the most used ventral starting techniques (Elipot et al., 2009; Seifert et al., 2010; Vantorre et al., 2010a, b). This start technique is the most suitable to apply the force splitting formalism, since the swimmer's body is in contact with the platform by means of the halluces-platform alignment whose centre should be the centre of pressure (COP). In fact, this particular geometry may be described as the CM rotation around the halluces lateral-medial axis, combined with the CM displacement along the anterior-posterior CM-COP direction. As this geometry is partly shared with the track start, a similar approach can be applied when the swimmer's rear lower limb leaves the block. It is hypothesised that it is possible to decompose $\overrightarrow{GRF}(t)$ into its $\vec{R}_{Passive}(t)$ and $\vec{R}_{Active}(t)$ components, allowing researchers and coaches to better understand the real swimmer's force generation contribution during the block phase.

Material and Methods

General description

Four working pathways were followed: (i) the experimented fall of a simple rigid body; (ii) the swimmers' matrix of inertia determination; (iii) the development of a mathematical model to describe the outcomes of the rigid body fall experiment

and its generalization to provide replacement of the calculated inertia; and (iv) the experimental start protocol and data analysis including the developed mathematical model. The first three steps were defined to achieve the transient swimmer's angular positions during the starting movement in order to better understand the influence of the passive forces on start performance.

Physical rigid body falling

A rigid rectangular stainless steel structure (1.80 m in height, 0.30 m in width and 27 kg total mass) was used. The structure CM was located at 0.9 m height and two stainless steel masses (10 kg each) were fixed at that height in each structure side. The lower extremity structure's was rectangular and divided into two contact surfaces (0.044 m x 0.037 m) (Figure 1A). To simulate the support of the swimmer's feet, the structure was balanced at the front edge of a 3D force plate horizontally positioned (Bertec FP 4060-15, Bertec Corp., USA) operating at 1000 Hz sample rate. From this initial position ($90^o > \theta(0) > 85^o$, measured to the horizontal plane) the rigid body was allowed to drop (Figure 1B) and the vertical and anterior-posterior $\overrightarrow{GRF}(t)$ components were recorded. Six successive trials were conducted to verify the force profile's repeatability. Data were collected using a 16 bit analogue-to-digital converter (Biopac MP 150, Biopac Systems, Inc., USA) and graphically expressed as function of time.

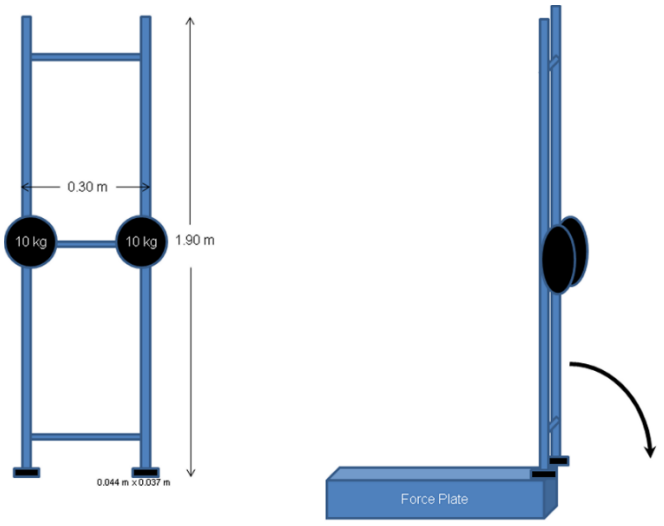

A) B)

Figure 1. Scheme of a rigid body balanced at the force plate border: frontal view (A) and isometric falling rotation around the medial-lateral axis that contains the centre of pressure (B).

Minimum and maximal values of inertia

Starting with a swimmer model, the minimum and maximum values of the moment of inertia around halluces (I_{zz}), defined by the last component of the inertia tensor matrix, were calculated and are presented below (Table 1). These values were assessed using a model of a rigid articulated body with mass 86.7 kg, volume 90.5 dm^3 and area of 3.28 m^2 compatible with two transient swimmer's inter-segmental realistic body positions assumed during the grab start: the most contracted (Figure 2A) and the most extended (Figure 2B) with CM-COP of 0.67 m and 1.15 m, respectively. The expression "articulated" refers to the reality-based effective transition from the 1st to the 2nd grab start positions. The NASA [13] human body anthropometrical inertial model was used to calculate the I_{zz} values around halluces in both positions (considering the sagittal symmetry) using SolidWorks (3D CAD, DS Solidworks, Dassault Systèmes S.A., USA).

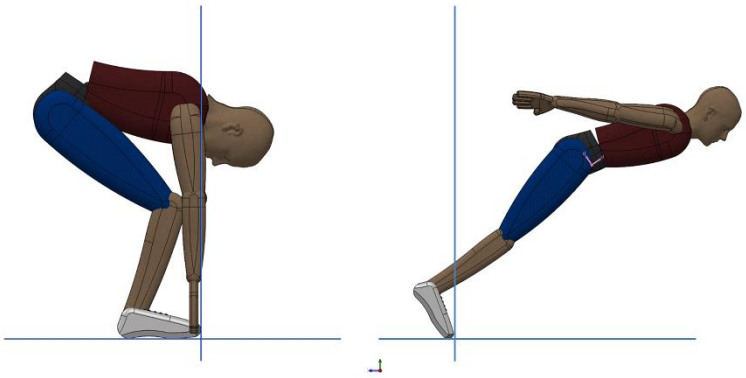

A) B)

Figure 2. Two rigid articulated body positions mimicking two limit transient body positions: the most contracted (A) and the most extended (B).

Mathematical model of rigid body fall

The simple rigid body falling mathematical description was conducted using the previously calculated I_{zz} and the CM locus modelling. Since the motion of the rigid body is a rotation about the contact point on the starting block it is preferable to use polar coordinates. The forces acting on the radial direction are the

projection of the weight $\left(\left\|\overrightarrow{\text{Proj}_{\vec{W}}}\right\| = m \cdot g \cdot \sin\theta\right)$ and the GRF, which in this work is assumed to have only a radial component. Since this force will be called the passive component, to avoid confusion with the measured GRF from the swimmer, it will be termed $R_{Passive} = \left\|\vec{R}_{Passive}\right\|$. The vectorial sum of the three forces, the centrifugal force $\overrightarrow{F}_{co}\left(\left\|\overrightarrow{F}_{co}\right\| = m \cdot \frac{v^2}{r_{CM}} = m \cdot r_{CM} \cdot \omega^2\right)$, the centripetal force $\left(\left\|\overrightarrow{\text{Proj}_{\vec{W}}}\right\|\right)$ and $R_{Passive}$ are in equilibrium along radial position, while in contact, whose effects may also be accounted for by the use of an accelerated referential (Figure 3), that is $R_{Passive} - m \cdot g \cdot \sin\theta + m \cdot r_{CM} \cdot \omega^2 = 0$ or, equivalently, the following statement:

$$R_{Passive} = m \cdot g \cdot \sin\theta - m \cdot r_{CM} \cdot \omega^2 \tag{5}$$

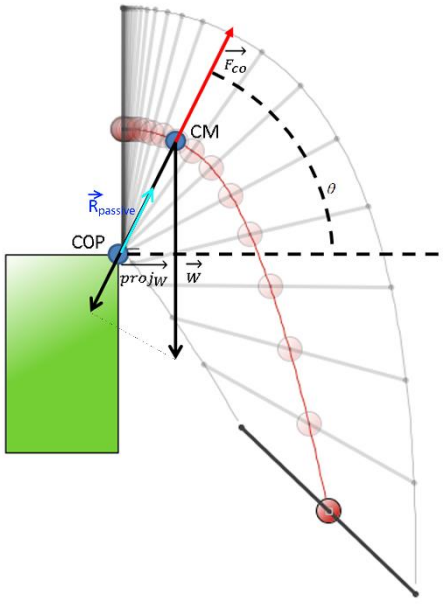

Figure 3. Simulation of the fall of rigid body, representing θ the angle to the horizontal, COP the Centre of Pressure, CM the Centre of Mass locus, the $\overrightarrow{proj_{\vec{W}}}$ is the weight projection to the CM-COP direction, $\vec{W}$ is the rigid body weight, $\vec{R}_{Passive}$ is the ground reaction force, and $\overrightarrow{F_{co}}$ is the centrifugal force.

For the tangential direction, the motion is better described by Newton's 2nd law in rotation form, that is $\vec{\tau} = [I] \cdot \vec{\alpha}$, where $\vec{\tau}$ is the sum of the moments of force about the rotational axis, $[I]$ is the nine components moment of inertial tensor and $\vec{\alpha}$ is the angular acceleration. In the present case the ground reaction force $\left(\vec{R}_{Passive}\right)$ produces no moment, as it acts on the rotation axis (COP), and the moment of the weight is due to its tangential component, that is $\left\|\vec{\tau}\right\| = \left\|\vec{r}_{CM} \times \vec{W}\right\| = r_{CM} \cdot m \cdot g \cdot \cos\left(\theta(t)\right) = \left\|[I] \cdot \vec{\alpha}\right\|$. Halluces axis shares the direction with the angular velocity $\left(\vec{\omega}\right)$ and angular acceleration $\left(\vec{\alpha} = \frac{d\vec{\omega}}{dt}\right)$ vector (i.e. direction *z*, medio-lateral), whose expression in *xyz* reference axis is $\vec{\omega} = \begin{pmatrix} 0 \\ 0 \\ \omega \end{pmatrix}$ and $\vec{\alpha} = \begin{pmatrix} 0 \\ 0 \\ \alpha \end{pmatrix}$, respectively. In the grab start case, the moment of inertial tensor is practically reduced to I_{zz}, since the modulus of tensor product gives $\left\|[I] \cdot \vec{\alpha}\right\| = \left\| \begin{pmatrix} I_{xz} \\ I_{yz} \\ I_{zz} \end{pmatrix} \cdot \alpha \right\| \approx I_{zz} \cdot \alpha$. Since $\left\|\vec{\alpha}\right\| = \frac{d^2\theta}{dt^2} = \frac{d\omega}{dt}$ the differential equation to be solved is $\frac{d^2(\theta)}{dt^2} = -r_{CM} \cdot m \cdot g \cdot \frac{\cos\left(\theta(t)\right)}{I_{zz}}$. To numerically solve this equation it is converted into two coupled nonlinear differential equations:

$$\begin{cases} \frac{d\left(\omega(t)\right)}{dt} = -r_{CM} \cdot m \cdot g \cdot \frac{\cos\left(\theta(t)\right)}{I_{zz}} \\ \frac{d\left(\theta(t)\right)}{dt} = \omega(t) \end{cases} \tag{6}$$

Where $\theta(t)$ and $\omega(t)$ are unknown functions of time, I_{zz} is the moment of inertia

around COP and one can identify the swimmers main anthropometric parameters, namely m, r_{CM} and I_{zz}. One used a Runge-Kutta method (function ode45, The MathWorks Inc, Matlab R2014b) to numerically solve the equations, with initial conditions that were defined as $\omega(0) = 0\ rad \cdot s^{-1}$; $\theta(0) = \frac{\pi}{2} - 0.001\ rad$ using a modelling software (Modellus 4.01, Modellus, Portugal).

The halluces contact line was considered as the contact locus with the starting block and deformations of the contact areas and tiny COP displacements were discarded.

The two previously obtained rigid articulated body configurations of the inertial tensor and CM position were used to assess the weight torque in the two limiting swimmer configuration (most contracted and most extended) that leads to angular position, angular velocity, angular acceleration (equations 6). However, contact forces and linear velocity are the observable parameters. It is possible to associate the $\vec{R}_{Passive}$ components with $\theta(t)$ and $\omega(t)$. These components are the observable (and therefore, measured) forces while in contact to ground. Equations (7) state force association while equations (8) state position-velocity $(\vec{r}_{\mathrm{CM}}, \vec{v}_{\mathrm{CM}})$ respectively, vectorial association.

$$\begin{cases} R_{\mathrm{v\_passive}} = m \cdot \left(g \cdot sin\theta - r_{CM} \cdot \omega^2 \right) \cdot sin\theta \\ R_{\mathrm{h\_passive}} = m \cdot \left(g \cdot sin\theta - r_{CM} \cdot \omega^2 \right) \cdot cos\theta \end{cases} \tag{7}$$

$$\begin{cases} \vec{r}_{\mathrm{CM}} = r_{CM} \cdot (cos\theta, sin\theta) \\ \vec{v}_{\mathrm{CM}} = r_{CM} \cdot \omega \cdot (sin\theta, -cos\theta) \end{cases} \tag{8}$$

Equations (7) and (8) state for the CM kinetics and for the CM kinematics description while in contact to ground with COP as origin of the Cartesian referential frame. The resulting movement should be a pure rotation around the COP.

Knowing that the grab start was selected due to rotations around both halluces axis, any difference of the measured contact force-time curves (incremental or decremental) during the movement compared to the passive force (equations 7) should be interpreted as the swimmer's active force effect.

An evidence of this model is that, as it is a pure rotation around COP, the swimmer is only able to perform forces parallel to the CM-COP segment.

Experimental protocol

Ethics statement

The present study was approved by the Ethics Committee of Faculty of Sport from the University of Porto. All participants provided informed written consent before data collection. The procedures were performed according to the Declaration of Helsinki.

Experimental measures and analyses

Six well-trained swimmers (24.25 $\pm$ 3.61 years of age; 1.73 $\pm$ 0.08 m of height, and 68.19 $\pm$ 10.78 kg of body mass), were made fully conversant with the protocol. After a standardized warm-up, participants performed three 15 m maximal grab start repetitions (3 min resting) over a 3D force plate (Bertec FP 4060-15, Bertec Corp., USA) sampling at 1000 Hz and mounted on a special support designed to replicate a starting block used in international level competitions. A starter device (Omega StartTime IV, Swiss Timing Ltd., Switzerland) was instrumented to simultaneously produce the starting signal and export a trigger signal allowing data synchronization with the acquired $\overrightarrow{GRF}(t)$ curves and analogue-to-digital converted by a 16 bit A/D converter (Biopac MP 150, Biopac Systems, Inc., USA). The block surface angle to the horizontal reference plane (10º) was corrected by applying a suitable rotation matrix and, therefore, vertical vs. horizontal forces were assumed rather than perpendicular vs. anterior-posterior forces.

In order to allow the comparison of the forces produced by swimmers of different masses, the forces (both the passive obtained from the model and the measured GRF from the swimmer starting motion) were divided by the respective weight. Following the experimental protocol the active and passive from raw force splitting tool was applied. The algorithm assumes the perpendicular to CM-COP segment active force unavailability, which means that raw force leads also to a raw θ estimator. In first step, we calculate $\theta_{Raw}(t) = \text{atan}\left(\frac{GRF_v(t)}{GRF_h(t)}\right)$, where $GRF_h(t)$ and $GRF_v(t)$ are the horizontal and vertical $\overrightarrow{GRF}(t)$ components, respectively. Simultaneously, it is built the intermediate force-time variables of equations (9).

$$\begin{cases} R_{h\_Passive\_i}(t_1) = \frac{m_{swimmer}}{m_{Model}} R_{h\_Passive\_Model}(t_1) \\ R_{v\_Passive\_i}(t_1) = \frac{m_{swimmer}}{m_{Model}} R_{v\_Passive\_Model}(t_1) \\ \theta_{Passive\_i}(t_1) = \text{atan}\left(\frac{R_{v\_Passive\_i}(t_1)}{R_{h\_Passive\_i}(t_1)}\right) \end{cases} \quad (9)$$

where $R_{h\_Passive\_i}(t_1)$ and $R_{v\_Passive\_i}(t_1)$ are the passive reaction horizontal and vertical and $\theta_{Passive\_i}(t_1)$ is the angle to the vertical. These force values are adjusted, therefore, to the mass of the swimmer but are expressed in the dependency of the unknown time t_1. The $\theta_{Passive\_i}(t_1)$ angle provides t_1 determination so that minimum of $\left|\theta_{Passive\_i}(t_1) - \theta_{Raw}(t)\right|$ at instant t is reached. Figure 4A S1 Files represents the stepwise algorithm for t_1 finding. From t_1 it is built $R_{h\_Passive}(t) = R_{h\_Passive\_i}(t_1)$ and $R_{v\_Passive}(t) = R_{v\_Passive\_i}(t_1)$. In the last step, $\vec{R}_{Active}(t)$ is calculated with equations (10).

$$\begin{cases} R_{h\_Active}(t) = GRF_h(t) - R_{h\_Passive}(t) \\ R_{v\_Active}(t) = GRF_v(t) - R_{v\_Passive}(t) \end{cases} \quad (10)$$

Figure 4B diagram depicts the general operations done to split the active S1 Files and passive from the raw force.

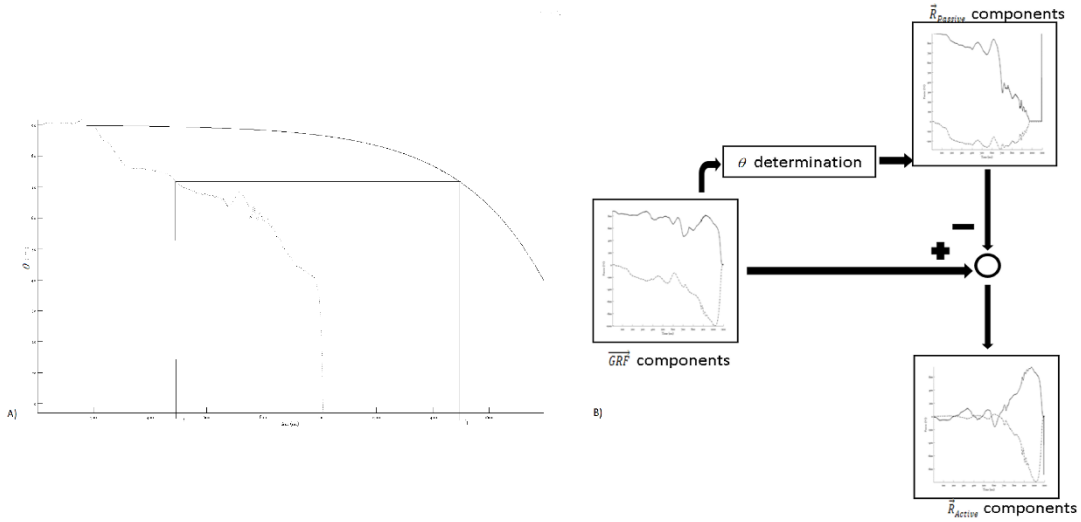

Figure 4. $\theta(t_1)$ determination to process the $\overrightarrow{GRF}(t)$ components to split it in $\vec{R}_{Passive}$ and the $\overrightarrow{R_{Active}}$ algorithm: graphical description with θ generated by the swimmer in dashed-dotted curve and rigid articulated body in continuous curve (panel A) and raw algorithm flowchart (panel B).

Statistical procedures

Pearson correlation coefficient between experimental rigid body fall and simulated were used in the vertical and horizontal force components. The three force-time curves (raw, active and passive) of each swimmer (i.e., 18 force-time curves for each pair of forces studied) were reported as mean (±s) and the variability displayed in each mean curve was assessed by the coefficient of variation.

Results

Physical rigid body falling and simulations

Figure 5 displays the vertical and horizontal components of the $\overrightarrow{GRF}(t)$ measured during the experimental rotating fall of the rigid body, and the respective simulation. For the experimental rotating fall, there was a quasi-stable

vertical force-time curve profile up to ~650 ms and, subsequently, a monotonic force reduction until the take-off. The horizontal component displayed a stable zero value up to ~150 ms and a monotonic increase until ~1150 ms, which characterizes a peak of -74 N (i.e., ~30% of the body weight considered) before the take-off. Even in the absence of any active propulsion effort, real propulsion can be observed. The force-time curves processed by means of the simulation was similar to the profile observed during the rigid body fall experiment. It was noted a quasi-stable vertical force-time curve profile up to ~1300 ms and, subsequently, a monotonic force reduction until the take-off. From the horizontal component, a stable value was displayed up to ~750 ms and a monotonic increase until ~1800 ms that characterizes a peak of -80 N (i.e., 30% of the body weight considered) before the take-off. Correlation for the vertical and horizontal components between experimental and simulated was 0.905 and 0.999 respectively.

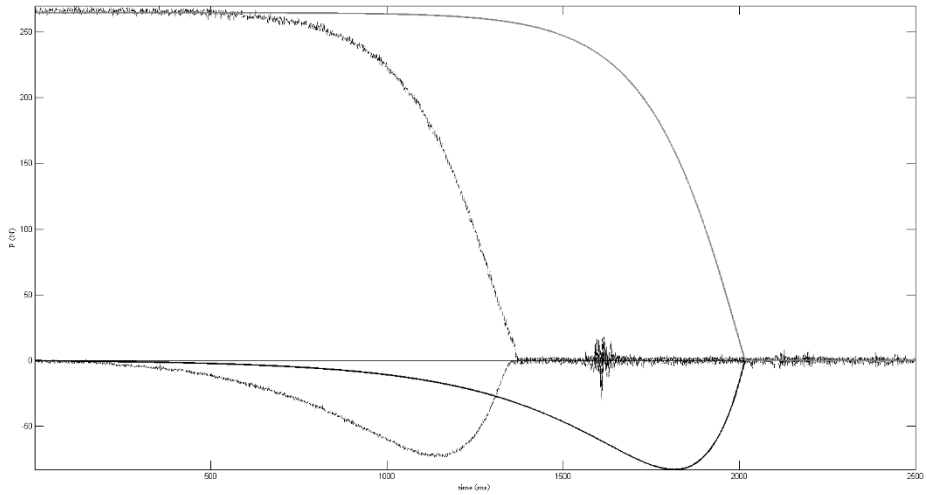

Figure 5. Experimental rigid body falling pattern (discretized lines) and force obtained from the mathematical model of $\overrightarrow{R}_{Passive}$ (continuous line) pattern. The vertical and horizontal force components, in both cases, are represented. For clarity of representation the horizontal component has been multiplied by -1.

The minimum and maximum inertia matrix component I_{zz} obtained in the respective most contracted and extended rigid articulated body positions (Figure 2) is used to provide correction to the model considered in the rigid body fall

simulation. Complete matrix components are presented in Table 1. The $I_{zz} >> I_{yz}, I_{xz}$ justifies the non-meaningfulness of differences of I_{yz}, I_{xz} values between both rigid articulated body positions. Inertia I_{zz} value almost doubles from the most contracted to the most extended rigid articulated body positions.

Table 1. Inertia Tensors ($kg \cdot m^2$) calculated to hallux rotation point in the two rigid articulated body positions.

Rigid articulated body positions	Moment of Inertia matricial components
Most contracted	$\begin{bmatrix} I_{xx} & I_{xy} & I_{xz} \\ I_{yx} & I_{yy} & I_{yz} \\ I_{zx} & I_{zy} & I_{zz} \end{bmatrix} = \begin{bmatrix} +44.6929 & -14.1389 & +0.0007 \\ -14.1389 & +8.1041 & -0.0018 \\ +0.0007 & -0.0018 & +50.8178 \end{bmatrix}$
Most extended	$\begin{bmatrix} I_{xx} & I_{xy} & I_{xz} \\ I_{yx} & I_{yy} & I_{yz} \\ I_{zx} & I_{zy} & I_{zz} \end{bmatrix} = \begin{bmatrix} +59.6219 & +54.1270 & -0.0000 \\ +54.1270 & +55.9084 & -0.0000 \\ -0.0000 & -0.0000 & +113.2425 \end{bmatrix}$

Figure 6A displays the different simulations for the mathematical model for the angle θ, the blue and cyan lines for a model with 90 kg and the red and magenta for a model with 60 kg. In this panel it is obvious that the time to take-off varies with the inertial properties of the model and the starting conditions. However if we plot in the horizontal axis the time to take-off, then the models all converge to a common area, as depicted in Figure 6B.

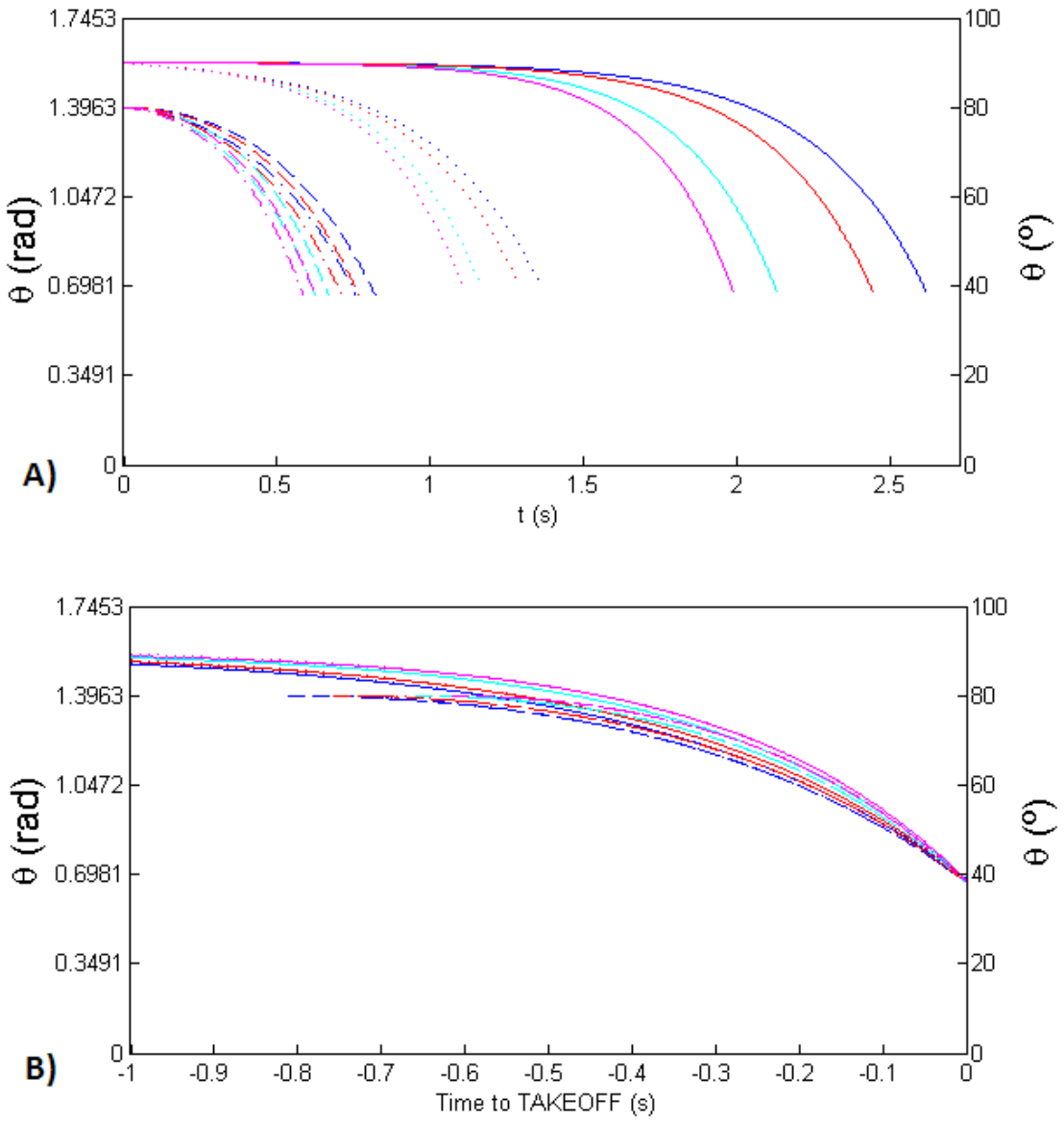

Figure 6. Angle to the horizontal for the mathematical model of rigid body free rotating fall. In both panels the blue and cyan lines for a model with 90 kg and the red and magenta for a model with 60 kg. The initial conditions are: solid lines: θ(0)=89.9º;ω(0)=0 $rad.s-1$; dashed lines: θ(0)=80º; ω(0)=0 $rad.s-1$; dotted lines: θ(0)=90º; ω(0)=-0.1 $rad.s-1$; dash-dotted lines: θ(0)=89.9º; ω(0)=-0.1 $rad.s-1$. In panel A the angles generated have the same initial origin time and in panel B have the same take-off instant.

The same is true for the force, both the horizontal and the vertical, as displayed in Figure 7.

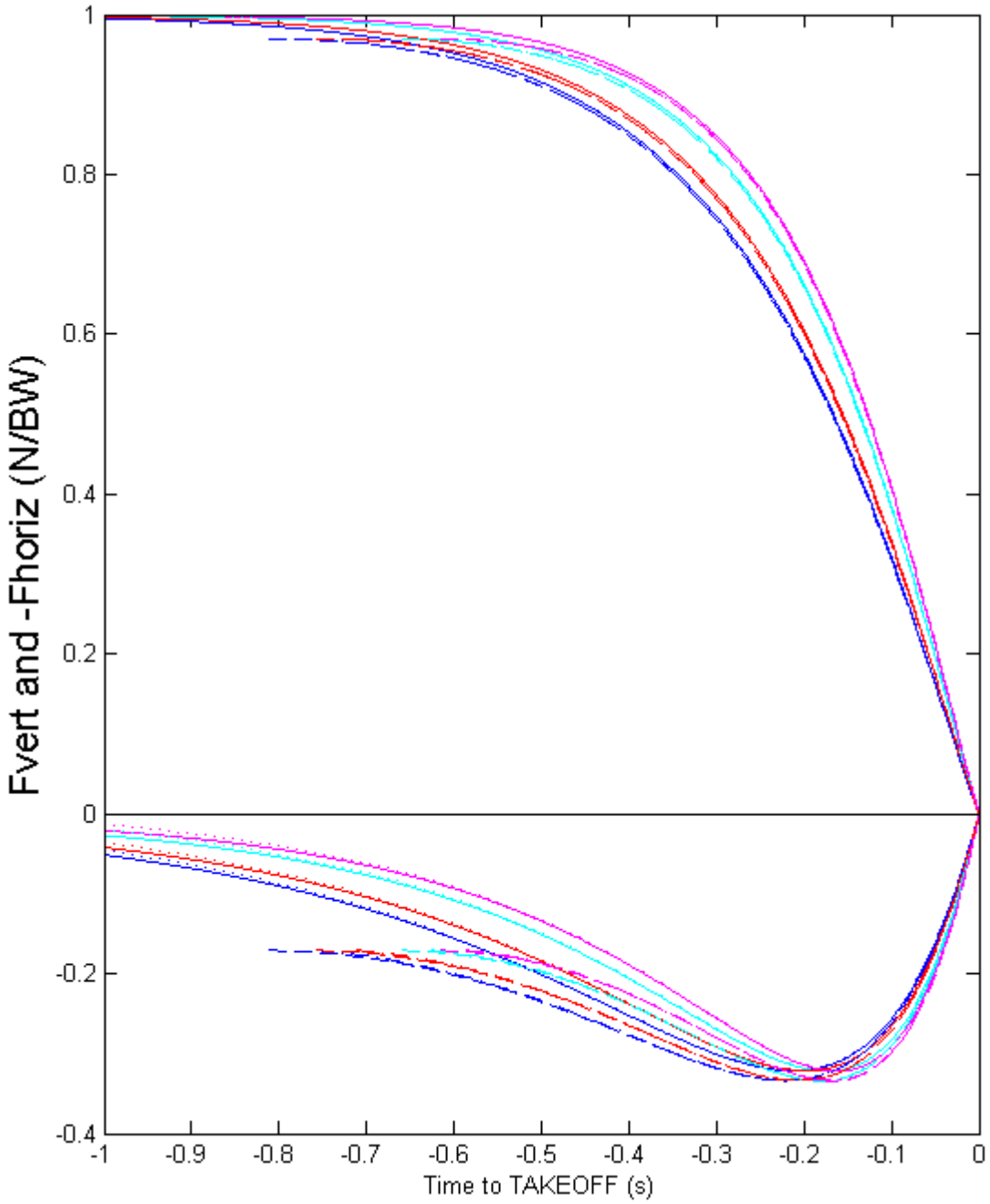

Figure 7. Horizontal and vertical components of the force for the mathematical model of rigid body free rotating fall. In both panels the blue and cyan lines stand for a model with 90 kg and the red and magenta for a model with 60 kg. The initial conditions are: solid lines: $\theta(0)=89.9^{o}$;$\omega(0)=0\ rad\cdot s^{-1}$; dashed lines: $\theta(0)=80^{o}$; $\omega(0)=0\ rad\cdot s^{-1}$; dotted lines: $\theta(0)=90^{o}$; $\omega(0)=-0.1\ rad\cdot s^{-1}$; dash-dotted lines: $\theta(0)=89.9^{o}$; $\omega(0)=-0.1\ rad\cdot s^{-1}$. For clarity of representation, the horizontal component has been multiplied by -1.

Experimental starting protocol

Figure 8 S1 Files exhibits the angles (θ) generated by the swimmer $\overrightarrow{GRF}(t)$, by the most contracted and by the most extended rigid articulated body falling $\vec{R}_{Passive}(t)$ curves for the equal conditions presented in Figure 6 and 7. The non-smooth swimmer's θ curve exhibits extension values down to ~0º, but only for short time period. The unanimated bodies presented similar θ values for take-off and pattern smoothness, and generate a range of values that does not include the swimmer θ generated, particularly in the latest values.

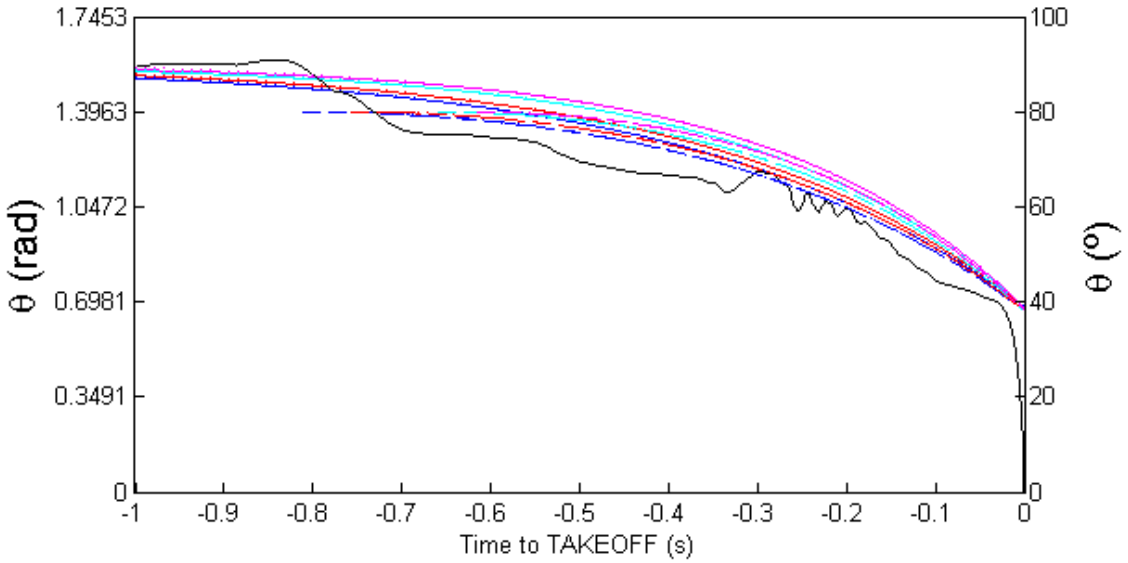

Figure 8. Angle to the horizontal produced by the swimmer, while in contact to block (continuous black line) and angle to the horizontal for the mathematical model of rigid body free rotating fall. The blue and cyan lines stand for a model with 90 kg and the red and magenta for a model with 60 kg. The initial conditions are: solid lines: θ(0)=89.9º;ω(0)=0 $rad \cdot s^{-1}$; dashed lines: θ(0)=80º; ω(0)=0 $rad \cdot s^{-1}$; dotted lines: θ(0)=90º; ω(0)=-0.1 $rad \cdot s^{-1}$; dash-dotted lines: θ(0)=89.9º; ω(0)=-0.1 $rad \cdot s^{-1}$. The angles generated have the same take-off instant.

The application of the previously mentioned θ mapping and determination in each of the 18 individual curves S1 Files lead to the mean raw, passive and active force-time curves and respective (±*sd*) (Figure 9A, B and C, respectively). Regarding the vertical and horizontal raw force components (Figure 9A), a progressive variability was observed from ~50 to 100% of block time and force values CV of 25.4 and 37.8%, respectively. Concerning both $\vec{R}_{Passive}(t)$

components (Figure 9B), the vertical force showed a progressive variability from ~25 to 100% of block time and force values CV of 16.9%, whereas the horizontal force registered a more restrictive variability (between ~50 to 70% of block time and force values CV of 16.9%). Considering both $\vec{R}_{Active}(t)$ components (Figure 9C), it is verified an abrupt increase in variance from 40% to 100% of block time and force values CV of 67.9% and 66.2%, respectively. An evident symmetry between vertical and horizontal active force mean profiles is noted from the starting signal to the take-off instant (Figure 9C).

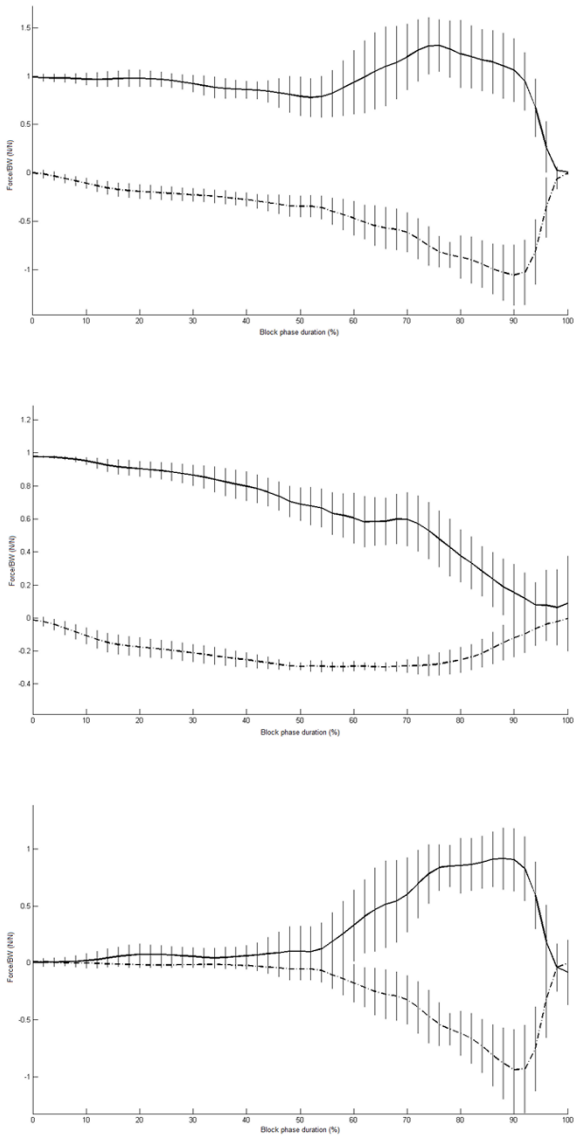

(a)

(b)

(c)

Figure 9. Mean horizontal and vertical (dash-dotted line and continuous line, respectively) force-time curves for the grab start technique, expressed as a percentage of the time period between

starting signal and the take-off instant: Raw mean forces (A), passive mean forces (B) and active mean forces (C). The vertical continuous bars denote the local standard variations for each force component. Force data are presented as a fraction of the swimmers' body weight (BW). For clarity of representation the horizontal component has been multiplied by -1.

Discussion

In swimming, the start phase is typically divided into the block, flight and underwater sub phases (Elipot et al., 2009; Slawson et al., 2013; Vilas-Boas et al., 2003), with the former considered determinant since it initiates the starting action and prepares the following phases (Vantorre et al., 2010a). In fact, the study of the force behaviour during the block phase has received considerable attention (Breed & Young, 2003; Galbraith et al., 2008; Guimarães & Hay, 1985; Lyttle & Benjanuvatra, 2005; Slawson et al., 2013; Vantorre et al., 2010b; Vilas-Boas et al., 2003), but researchers have not yet considered the study of dynamometric data based on the physics of the superposition principles, limiting its applicability to regular performance diagnosis (Holfelder et al., 2013). Therefore, we aimed to implement a tool to study the $\overrightarrow{GRF}(t)$ applied on the swimmers during the block phase, splitting $\vec{R}_{Active}(t)$ from $\vec{R}_{Passive}(t)$. The pathways used allowed an appropriate description of both force contributions from the raw data, confirming the hypothesis that swimmer's forces applied on the starting block are dependent on muscular based biomechanical actions and on the body weight dynamical effects. The application of the splitting algorithm led to a noticeable force variability dependence on $\vec{R}_{Active}(t)$, highlighting that swimmers' voluntary propulsion is more evident in raw $\overrightarrow{GRF}(t)$ variability than $\vec{R}_{Passive}(t)$.

The current study was conducted with three stepwise determinations with the first two (defined by the force patterns assessment during the falling rigid body) leading to model forces and variable dependencies that were achieved in the

following two steps. The force-time curves displayed during the rigid body experiment were similar to the maximum vertical and horizontal force profiles observed during the simulation of the respective phenomena (correlation values, time delays, and maxima/minima values), except the added contact time due to the initial angle (Figure 5). The correlation findings for the vertical force curves are less than 0.95 due to lack of initial data, probably on account of high θ accomplishment difficulties. The horizontal peak force observed before the take-off, noticed in the force-time curves of the rigid body experiment and simulation (Figure 5), has a similar profile to that displayed in a previous ventral start study (Slawson et al., 2013). Swimmers seem to generate the main take-off propulsion between the most contracted and the most extended postures. While mimicking the swimmer postural segment geometries, an unanimated articulated rigid body allows the determination of moment of inertia around COP and limits their respective I_{zz} values. The changes in inertia moments due to the two different inter-segmental positions (Figure 2) were used in simulations and have shown no effect in the force-time curve profiles allowing the use of $\theta = \arctan\left(GRF_v / GRF_h\right)$ as a parameter in the CM-COP direction, which was essential for the tool that separated $\vec{R}_{Active}(t)$ from $\vec{R}_{Passive}(t)$ S1 Files (Fig. 4). Unanimated θ curve exhibited similarity, while the swimmer's θ curve exhibits more irregularities, since the latter depends upon swimmer's muscular actions. The unanimated curves were similar because I_{zz} doubles (from 50.8 to 113 $kg \cdot m^2$, ratio of 2.22) while r_{CM} also almost doubles (from 0.67 to 1.15 m, ratio of 1.72) making equations (6) almost invariant. Another supplemental reasoning can generate another quasi-invariance on equations (6) taking account on the, supposedly, independent anthropometric variables. For instance, consider two ideal swimmers (or any two objects) with different body mass, ascribed m_1 and m_2 but with a similar volumetric mass and with a possible perfect 3D homothety between them. It is possible to perform a transformation between them that applies, as in equations (11).

$$\begin{cases} L_1 \to L_2 = \sqrt[3]{\frac{m_2}{m_1}} L_1 \\ V_1 \to V_2 = \frac{m_2}{m_1} V_1 \\ I_1 \to I_2 = \left(\sqrt[3]{\frac{m_2}{m_1}} \right)^2 \frac{m_2}{m_1} I_1 \end{cases} \quad (11)$$

Where L stands for any one-dimensional quantity like $r_{CM}(m)$, $V(m^3)$ for volume and $I(kg \cdot m^2)$ the inertia moment around COP. These transformations, taken simultaneously, leave the equations (6) with a $\cos(\theta)$ coefficient reduced to 79% if $\frac{m_2}{m_1} = 2$, which is not an usual ratio, while $\frac{m_2}{m_1} = 1.25$ reduces to 93% from the lighter (being the faster) to heavier (being the slower) value. Bigger limb dimensions in the heaviest swimmer could, however, enable contact during time enough to produce more impulse, compensating the loss above mentioned. Equations (7) and (8) that might differ as r_{CM} slightly changes, remain seemingly unchanged in function of θ. The results of the two mentioned quasi-invariances also motivate us to search what defines the anthropometric difference between swimmers (i.e., intersegment distances and distribution of masses, and specific mass strength or power).

The theta mapping methodology was implemented on a raw swimmer pattern S1 Files (Figure 8) where it is observed the theoretical take-off angle reached before the unanimated curves did. That precise instant should be the matching of the overall curves and posterior force is a pure voluntary force. If the matching of the take-off angles took place then the posterior force exerted should be voluntary force. Also the anterior angle pattern would belong to the neighbourhood of the swimmer's angle take-off instant the theta earlier values belong to the neighbourhood of the other unanimated curves presented. The theta mapping methodology was also applied on raw swimmers' force patterns (Figure 9A),

allowing the splitting of $\vec{R}_{Passive}(t)$ from $\vec{R}_{Active}(t)$ (Figure 9B and C) S1 Files. The raw force-time curves variability was comprised of the respective $\vec{R}_{Passive}(t)$ and $\vec{R}_{Active}(t)$ variability and it was most evidenced in the last 50% of the block time for vertical and horizontal components. This finding was expected since swimmers can effectively propel themselves out of the starting block after the hands leave the handgrips, generating greater resultant impulse with the lower than with the upper limbs (Breed & Young, 2003; de Jesus et al., 2011; Galbraith et al., 2008; Guimarães & Hay, 1985; Lyttle & Benjanvatra, 2005; Slawson et al., 2013). In fact, $\vec{R}_{Active}(t)$ components also displayed an increased variability from the 40% of the block time, seeming to be the major contributor to the raw variability. The main swimmer's task has environmental and organism constraints are faced during the most propulsive block instants and subtle differences may distinguish swimmers and swimmers' trials as a consequence of environmental changes, training procedures or learning phenomena (Preatoni et al., 2013). In contrast, the $\vec{R}_{Passive}(t)$ components are dependent on swimmers' structure and inertial components, reducing the degrees of freedom involved in swimming start movement and, the consequential variability.

Despite the noticeable contribution of the $\vec{R}_{Active}(t)$ components to the raw force-time curves variability, it should also be considered as their symmetric profile registered from the starting signal to the take-off (Figure 9C), which could indicate a ~45º declination body steering intention. In fact, since the starting signal, swimmers seem to compensate the vertical force reduction as a strategy to falling in a controlled vertical speed, allowing the best angular determination for explosive force during the take-off instants. Force-time curves observed in other swimming start techniques have already displayed qualitatively this symmetry in raw data (Slawon et al., 2013), but no further clarification was exhibited. Several previous raw $\overrightarrow{GRF}(t)$ research findings may lead to a misunderstanding of the real muscular action measurement. The current study evidences the need to

consider $\vec{R}_{Active}(t)$ and $\vec{R}_{Passive}(t)$ components to avoid the raw force-time curves masking effects.

Notwithstanding the study's originality and relevance, some limitations and future research directions should be considered. Firstly, the mathematical model applied still lacks a refined description of part of the rotational angular velocity impact, since the COP might have tiny anterior-posterior movements that were not considered; this indicates the need to include angular positioning and angular velocity mappings for the rigid articulated body passive reaction calculations, particularly knowing that slight angular changes in the beginning can substantially reduce block contact times. We should point out that ω cannot vary randomly and has peak values constraints (taking account of its influence in equations 7 and 8, which could limit its instantaneous variance, avoiding some of the noticed ringing in $\vec{R}_{Passive}(t)$. This might be an improvement in the development of future algorithms. Secondly, as the lateral responsiveness was not considered, its consistent assessment is recommended to provide detailed dynamometric information for proper forces direction achievement. Calculations could lead to inertial tensor components of mimicking rigid articulated body positions, considering a brand new segment arrangement compatible with the track start, which is also a very commonly used technique. This inertial tensor would lack the proposed grab start sagittal symmetry, and would have, theoretically, dependency on time, but further studies could reveal its minimum and maximum values and how rotation around the hallux would change its dynamical behaviour. The segment arrangement with its origin in the front limb (when rear lower limb takes off) combined with initial angular velocity could lead, once again, to separating assessment, since CM to COP segment and subsequent former grab start considerations could be applied. Future studies should include different intersegmental compatible rigid articulated body transient swimmer's inter-segmental in ventral and dorsal realistic start body positions to map more I_{zz} values.

Conclusions

This is the first study that has implemented a tool to analyse the active and passive vertical and horizontal reaction forces applied by the swimmers during the block phase of a grab start. Experimental events and simulations have confirmed the passive contribution on raw force data and have allowed the separating of the active force component from the swimmers' force-time curves. The active forces seem to strongly contribute to the raw force variability and denote a vertical and horizontal symmetric profile characteristic of the optimum projection angle to obtain a maximal horizontal displacement range. Future research should consider the active and passive force profiles in different starting techniques for performance advances and aid diagnostics for coaching.

Acknowledgements

The authors acknowledge Engº Nuno Viriato of Institute of Mechanical Engineering and Industrial Management (INEGI) for his invaluable service in SolidWorks and with inertia tensor components and M.Sc. Kelly de Jesus for her involvement in the data collection.

References

Breed, R.V.P.,& Young, W.B. (2003) The effect of a resistance training programme on the grab, track and swing starts in swimming. *Journal of Sports Sciences, 21*(3) 213-220.

de Jesus, K., de Jesus, K., Figueiredo, P., Gonçalves, P., Pereira, S., Vilas-Boas J.P., & Fernandes, R.J. (2011). Biomechanical analysis of backstroke swimming starts. *International Journal of Sports Medicine, 32*(7), 546-551.

Elipot, M., Hellard, P., Taïar, R., Boissière, E., Rey, J.L., Lecat, S., & Houel, N. (2009). Analysis of swimmers' velocity during the underwater gliding motion following grab start. *Journal of Biomechanics, 42*(9) 1367-1370.

Galbraith, H., Scurr, J., Hencken, C., Wood, L., & Graham-Smith, P. (2008). Biomechanical comparison of the track start and the modified one-handed track start in competitive swimming: an intervention study. *Journal of Applied Biomechanics, 24*(4), 307-315.

Guimarães, A.C.S., & Hay, J.G. (1985). A mechanical analysis of the grab starting technique in swimming. *International Journal of Sport Biomechanics, 1*, 25-35.

Holfelder, B., Brown, N., & Bubeck, D. (2013). The influence of sex, stroke and distance on the lactate characteristics in high performance swimming. *PLoS One,* 8(10), e77185.

Lyttle, A.D, & Benjanuvatra, N. (2005) Start right? A biomechanical review of dive start performance. Available: http://coachesinfo.com/category/swimming/321. Accessed 19 March 2014.

Mason, B., Mackintosh, C., & Pease, D. (2012). The development of an analysis system to assist in the correction of inefficiencies in stars and turns for elite competitive swimming. In E.J.Bradshaw, A. Burnett, & P.A. Hume (eds.), XXXI International Symposium on Biomechanics in Sports: Australian Catholic University, 249-252.

NASA, (1978). Anthropometric source book. Volume I: Anthropometry for designers. Ohio: Yellow Springs.

Preatoni, E., Hamill, J., Harrison, A.J., Hayes, K., Van Emmerik, R. E., Wilson, C., & Rodano, R. (2013). Movement variability and skills monitoring in sports. *Sports Biomechanics, 12*(2) 69-92.

Seifert, L., Vantorre, J., Lemaitre, F., Chollet, D., Toussaint, H.M., & Vilas-Boas J.P. (2010). Different profiles of the aerial start phase in front crawl. *Journal of Strength and Conditioning Research, 24*(2) 507-516.

Slawson, S.E., Conway, P.P., Cossor, J., Chakravorti, N., & West, A.A. (2013). The categorisation of swimming start performance with reference to force generation on the main block and footrest components of the Omega OSB11. start blocks. *Journal of Sports Sciences, 31*(5) 468-478.

Vantorre, J., Seifert, L., Fernandes, R. J., Vilas-Boas, J. P., & Chollet, D. (2010a). Kinematical profiling of the front crawl start. *International Journal of Sports Medicine, 31*(1), 16-21.

Vantorre, J., Seifert, L., Fernandes, R.J., Vilas-Boas, J.P., & Chollet, D. (2010b). Comparison of grab start between elite and trained swimmers. *International Journal of Sports Medicine, 31*(12), 887-893.

Vilas-Boas JP, Cruz J, Sousa F, Conceição F, Fernandes R, Carvalho, J. (2003). Biomechanical analysis of the ventral swimming starts: comparison of the grab start with two track-start techniques. In J.-C. Chatard (ed.), IX Symposium on Biomechanics and Medicine in Swimming: University of Saint Etienne, 249-253.